Scuola Internazionale Superiore di Studi Avanzati - Trieste

INTERNATIONAL CENTRE FOR THEORETICAL PHYSICS
INTERNATIONAL SCHOOL FOR ADVANCED STUDIES
Area of Physics
Astroparticle Physics Joint PhD Programme

Phenomenological Applications of Effective Field Theory: Neutrinos and LHC Physics

Candidate: **Yakefu Reyimuaji**

Supervisor: **Prof. Andrea Romanino**

Co-supervisor: **Dr. Aleksandr Azatov**

A Thesis Submitted for the Degree of Doctor of Philosophy

September 2018

SISSA - Via Bonomea 265 - 34136 TRIESTE - ITALY

Life is like riding a bicycle. To keep your balance, you must keep moving.

Albert Einstein

Abstract

The understanding of the principles underlying the structure of fermion masses and mixing is one of the important open problems in present day research in particle physics. One way to address this problem is by means of a symmetry principle, as it has been often the case in particle physics. Several efforts have been spent in particular to understand lepton masses and mixing by means of flavour symmetries. The first part of this thesis deals with the following problem: can an unbroken flavour symmetry provide an approximate description of lepton masses and mixing in the symmetric limit? Even though many models are available relying on specific flavour groups, a comprehensive analysis along the above direction is missing. We provide a complete answer to this question in two different cases of neutrino mass generation, from the Weinberg operator or from the seesaw mechanism. We allow the symmetry group to be as general as possible. We show that the pattern of lepton masses and mixing only depends on the dimension, type (real, pseudoreal and complex) and equivalence of the irreducible components ("irrep decompositions") of the flavour group representations. In other words, we will derive relations between irrep decompositions and lepton mass patterns, and also between irrep decompositions and possible structures of the PMNS matrix. As we will see, once the decomposition of flavour group representation into irreducible components is specified, one can write down the mass pattern and corresponding form of the mixing matrix without knowing the explicit mass matrix.

First we assume that the light neutrino masses are generated by the Weinberg operator, and that the flavour symmetry directly constrains their mass matrix. Under this assumption, we find that there are six viable cases which can account for the approximate description of lepton masses and mixing in the symmetric limit. In all of these cases the neutrino mass spectrum is either inverted hierarchical or the neutrino mass matrix is completely unconstrained (anarchy). In the context of $SU(5)$ unification, only the anarchical option is allowed. Therefore, if the present hint of a normal hierarchical spectrum were confirmed, we would conclude (under the above assumption) that symmetry breaking effects must play a primary role in the understanding of neutrino flavour observables.

Then, we consider the case in which light neutrino masses originate from the type I seesaw mechanism and take into account also the transformation properties of the singlet neutrinos under the flavour group. Such a "high-scale" is not always equivalent to the previous "low-scale" analysis. We recover the conditions under which the equivalence of the two analyses necessarily holds. When the two analyses are equivalent, the conclusions obtained in the low-scale analysis hold. Otherwise, the high-scale analysis may provide new results and a normal hierarchy of neutrino masses can be obtained in the symmetric limit.

The last part of the thesis is devoted to the new measurements of the anomalous triple gauge boson couplings in the electroweak sector. The goal is to find measurements leading

to a large increase of the interference between the SM amplitude and the contributions from CP-even dimension six operators in the effective field theory. In particular, in order to overcome non-interference, due to the helicity selection rule, between the amplitudes of the SM and the operator O_{3W} in the tree level process of $q\bar{q} \to V_T V_T$, in which V_T is transverse polarization state of weak gauge bosons, we propose two distributions that will lead to a better accuracy. The first one is the angular distribution of the interference cross section over the SM one, for the decay of two final state vector bosons. The second one considers a beyond leading order effect from adding one hard jet in the final state. Improvements compared to the traditional methods as well as LHC high luminosity prospects will also be discussed.

Acknowledgements

First and foremost, I would like to thank Prof. Andrea Romanino, who taught me two courses of the standard model as well as beyond standard model and supervised me during the PhD study at SISSA and ICTP. I was inspired from his excellent lectures and decided to work in physics beyond standard model as my future carrier. I want to express my sincere gratitude for his patient guidance, encouragement, understanding, constant support, countless discussions and invaluable advices throughout my time as his student. I greatly appreciate his suggestions and comments for the successful completion of this thesis.

I would like to express my special thanks to all the professors in astroparticle physics and theoretical particle physics groups of SISSA. I am very grateful for obtaining this precious opportunity to be one of the graduate student of SISSA. It is an unforgettable memory for me to study in the joint PhD program of SISSA and ICTP. I am in debt to ICTP director Prof. Fernando Quevedo, HECAP group researcher Prof. Kumar Narain and other staff members for giving me this opportunity to pursue my PhD in a such excellent scientific environment. It is my great honour to be a graduate student of these two international research centers.

I am grateful to A. Azatov, J. Elias-Miró and E. Venturini for the interactive discussions during our fruitful collaboration. It was a nice experience for me, I am glad to work with them.

Many thanks to students' secretaries, library staffs and administrators at ICTP and SISSA. A special thank goes to SISSA secretary Riccardo Iancer, I really appreciate his help in resolving the problems.

I also owe my sincere thanks to my friends, PhD colleagues and all the graduate students of astroparticle physics and theoretical particle physics groups in SISSA. I cannot forget those friends who helped me during the hard times, encouraged me, and celebrated my happiness together. I have a lifelong memory from living with them in the beautiful city Trieste, having fun and enjoyment from our so many indoor and outdoor activities like birthday parties, chats, picnics and hikings. Special thanks, in particular, to João and Sílvia, Vladimir and Tatyana, Matteo, Mengqi, Costantino, Vedran, Lorenzo, André, Francesca, Gabriele. I very much appreciate their support and help for me and for my family. I would like to express my deep gratitude to João and Sílvia, thank you again for your hospitality and kindness. Our friendship and everything you have done for my family will be remembered and cherished all the time.

I want to express my heartfelt thanks to Asiya, my wife, for her continuous support, encouragement and understanding. She has been living with me since last several years of my studying abroad, leaving very far away from her parents, relatives and friends. Thank you for accompanying with me in the very new environment in order not to make me feel lonely, for being my best friend and for filling our home with love and happiness.

Completing this thesis would not be possible without your support, your devotion to me and to our family, and your hard work for taking care of our little angel Nadire. I am beyond words in gratitude, thank you very much for everything. I dedicate this thesis to both of you.

I owe tons of gratitude to my parents, brothers and sisters, without their constant love and support I cannot imagine myself today. I would like to extend my sincere thanks to my wife's family, I very much appreciated their support and understanding. I miss and recall my loving mother, even though I cannot see her forever, she is always with me and she is in the every single line of my thesis.

Finally, I would like to thank all the people who helped me in the various aspects of my life and study, and sincere apologies for those to whom I couldn't thank by mentioning their names individually.

List of publications

This PhD thesis is based on the following publications listed in chronological order:

- A. Azatov, J. Elias-Miró, Y. Reyimuaji and E. Venturini, *Novel measurements of anomalous triple gauge couplings for the LHC*, *JHEP* **10** (2017) 027 [arXiv:1707.08060].
- Y. Reyimuaji and A. Romanino, *Can an unbroken flavour symmetry provide an approximate description of lepton masses and mixing?*, *JHEP* **03** (2018) 067 [arXiv:1801.10530].
- Y. Reyimuaji and A. Romanino, *Flavour symmetries in the context of the seesaw mechanism*, in preparation.

The research performed during the PhD study has been presented at international conferences and workshops, and contributed to the following conference proceeding co-authored by the thesis author:

- Y. Reyimuaji and A. Romanino, *General considerations on lepton mass matrices*, *PoS* **CORFU2017** (2018) 024.

Contents

List of figures

List of tables

Dedicated to my family

Chapter 1

General introduction

The past several decades have witnessed a tremendous success of the standard model (SM) of particle physics. With the discovery of the Higgs boson at LHC in 2012, the existence of the last missing building block of SM was confirmed: all SM predictions have been successfully tested by a vast variety of experiments, with good accuracy and agreement. Even though there is no doubt that the SM is one of the most successful and powerful theory ever built, there is a wide consensus that it is not the ultimate theory of everything for several reasons.

On the one hand, there are many experimental problems (hints), like neutrino mass, dark matter, gravity, baryon asymmetry in the Universe, (gauge couplings and quantum numbers unification, inflation), as well as some theoretical problems (puzzles), such as the hierarchy problem, the naturalness problem, the strong CP problem, the cosmological constant problem, (the flavour structure of the SM, the pattern of fermion masses and mixing, the quantization of the electric charge), that cannot be explained by the SM. As we know, the SM gauge principle governs all strong, weak and electromagnetic interactions in terms of just three parameters, but the SM contains several other parameters that still unexplained by the SM itself. This is particularly true in the Yukawa sector of the SM Lagrangian which determines all matter interactions which give rise to the fermion masses, mixing and their interactions with Higgs field. Can the Yukawa parameters be understood in terms of more fundamental physics? Why there are such a big hierarchy among fermion Yukawa couplings (more precisely fermion masses)? Why lepton mixing is so different from quark mixing? An honest answer, at the moment, is we don't know why they appear as they do, but there can be following two possible rough expectations to them:

- There might be undiscovered principle, like extension of the SM symmetries, that explains the origin of all these seemingly free parameters and determine most of them.
- Those free parameters are just accidental and Nature choose them as they are.

The first possibility is obviously more appealing. Part of this thesis is devoted to its study.

On the other hand, the SM is a low energy approximation of some UV theory. The SM is a quantum field theory respecting a specific gauge symmetry, allowing to have a spontaneous symmetry breaking, and satisfying the renormalizability condition. As an effective field theory (EFT), it holds up to certain energy scale Λ, above which new physics effects suppose to play a significant role. The null result from the new physics search in LHC so far indicates that if a new physics interacts strongly with matter then there is wide mass gap between the new physics scale and electroweak scale, which makes the treatment of the SM as an effective field theory more robust. The power counting analysis indicates that the effects of short distance physics is suppressed by the $(E/\Lambda)^{D-4}$ with $D > 4$ on the low energy observables, and our ignorance of new physics can be parameterized by the non-renormalizable operators of the EFT. If the scale is high enough $\Lambda \gg E$ then the renormalizable part of the Lagrangian is a good approximation. If a theory like SM written at the renormalizable level fails to explain a certain phenomenon, then we may learn about the scale, at which the SM stops being a valid theory, by considering non-renormalizable terms. A simple example of this is provided by neutrino masses, which are zero by construction of the SM and can be generated by a dimension five operator, the so called Weinberg operator [1], associated to the scale that can be as large as 10^{15} GeV.

1.1 The standard model in a nutshell

The SM is a theory that describes three out of the four forces known in Nature, namely it is the theory of strong, weak and electromagnetic interactions of all elementary particles known up-to-date, and it does not account for the gravity. The SM is defined by the following two ingredients:

(i) Symmetries and spontaneous symmetry breaking (SSB) :
The gauge group of the SM:

$$G_{\rm SM} = SU(3)_{\rm C} \times SU(2)_{\rm L} \times U(1)_{\rm Y}, \tag{1.1}$$

that is spontaneously broken to the subgroup

$$SU(3)_{\rm C} \times U(1)_{\rm EM}. \tag{1.2}$$

(ii) The representations of fermions and scalars under the gauge group:
In the SM, there are five types of fermions, which are the quark doublet, the up quark singlet, the down quark singlet, the lepton doublet and the lepton singlet, denoted by

$$q_i, \quad u_i^c, \quad d_i^c, \quad l_i, \quad e_i^c, \quad i = 1, 2, 3 \tag{1.3}$$

respectively, and there is one scalar doublet

$$h = (h^+, h^0)^T. \tag{1.4}$$

Here the "singlet" and the "doublet" refer to $SU(2)_{\rm L}$. Each of these fermions comes in three families and their transformation properties under the representations of $G_{\rm SM}$ are given in table 1.1. The local gauge symmetries determines which vector bosons exist in Nature and how they transform under the $G_{\rm SM}$. Note that we are using Weyl spinor notation, all fermions are left-handed, even though the subscripts are omitted, and their charge conjugated counterparts transform as a Dirac conjugate of Right-handed fields $\psi^c_{\rm L} \sim \overline{\psi_{\rm R}}$.

Fields	$(SU(3)_{\rm C}, SU(2)_{\rm L})_{\rm Y}$	Fields	$(SU(3)_{\rm C}, SU(2)_{\rm L})_{\rm Y}$
$q_i = (u_i, d_i)^T$	$(3,2)_{1/6}$	$l_i = (\nu_i, e_i)^T$	$(1,2)_{-1/2}$
u^c_i	$(\bar{3},1)_{-2/3}$	e^c_i	$(1,1)_1$
d^c_i	$(\bar{3},1)_{1/3}$	h	$(1,2)_{1/2}$
G_μ	$(8,1)_0$	W_μ	$(1,3)_0$
B_μ	$(1,1)_0$		

Table 1.1: The SM fields gauge quantum numbers.

Gauge invariance provides us with a set of constraints on the Lagrangian. Having a set of charge assignments of the SM fields in table 1.1, all possible gauge invariant, of course must first of all be Lorentz invariant, and the renormalizable terms in the Lagrangian consisting of the SM fields and their covariant derivatives can be grouped into three pieces

$$\mathcal{L}_{\rm SM} = \mathcal{L}_{\rm gauge} + \mathcal{L}_{\rm flavour} + \mathcal{L}_{\rm EWSB}\,. \tag{1.5}$$

Each of these parts are

$$\begin{aligned} \mathcal{L}_{\rm gauge} &= \sum_\psi \psi^\dagger i\sigma^\mu D_\mu \psi - \frac{1}{4}\sum_V V_{\mu\nu}V^{\mu\nu}\,, \\ -\mathcal{L}_{\rm flavour} &= y^U_{ij} u^c_i q_j h + y^D_{ij} d^c_i q_j h^c + y^E_{ij} e^c_i l_j h^c + h.c.\,, \\ \mathcal{L}_{\rm EWSB} &= (D_\mu h)^\dagger (D^\mu h) + \mu^2 (h^\dagger h) - \lambda (h^\dagger h)^2\,, \end{aligned} \tag{1.6}$$

where

$$\begin{aligned} \psi &= q_i, u^c_i, d^c_i, l_i, e^c_i\,, \quad V = G_a, W_i, B, \quad h^c = i\sigma_2 h^*\,, \\ D_\mu &= \partial_\mu + i g_s G^a_\mu T^{(3)}_a + i g W^i_\mu T^{(2)}_i + i g' B_\mu Y\,, \\ V_{\mu\nu} &= \partial_\mu V_\nu - \partial_\nu V_\mu + i g_{\rm v}[V_\mu, V_\nu]\,, \end{aligned} \tag{1.7}$$

and traces in the gauge kinetic terms of non-abelian gauge fields with proper normalization coefficients are understood. Even though all the $SU(2)_{\rm L}$ invariant contractions between

two doublets are not written explicitly, one can easily recover them in a similar way, for example, as the contraction between the q_j and h, which is given by $\varepsilon_{rs} q_{jr} h_s$ with r and s doublet indices. In this Lagrangian all gauge fixing terms, a topological term and ghost terms are omitted.

1.2 The effective approach

Searching for new physics in the past as well as present-day efforts to go Beyond Standard Model (BSM) basically relies on the two main techniques: the direct detection of new particles from the collider experiment, as in the latest example of Higgs boson discovery at the LHC; or the scrutiny of the deviations from the standard model predictions in some interaction channels, which is most often described by the EFT approach. The fact that no new particle has been discovered at the LHC so far is sending us a hint of the existence of a rather big mass gap between the electroweak scale and a new physics scale, if there is a strong interaction between the new particles and the SM particles. This suggests the EFT method is valid and very useful, at least, up to several TeV energy before a new particle is discovered, so one of the our goals will be concentrated on the path going beyond SM by EFT analysis. This is the model independent and very powerful way to describe the effect of high energy theory on low energy observables in terms of the low energy degrees of freedom only, even without knowing what are the new heavy fields and which is the details of full high energy Lagrangian, as long as one is focusing on low energy phenomena.

We will use the EFT method in two directions: on the one hand, the flavour structure of the SM and in particular in the lepton sector, by describing neutrino masses through the Weinberg effective operator. We will also discuss limits of this approach when applied to flavour symmetries. On the other hand, we will use EFT approach to parameterize possible deviations from the SM by focusing on the measurements of electroweak triple gauge boson couplings.

Let us now see greater detail the basics of the effective approach. Consider a fundamental theory, whose Lagrangian $\mathcal{L}(\varphi, \phi)$ depends on light and heavy degrees of freedom, φ and ϕ respectively. When we are working at low energy, $E \ll M_\phi \equiv \Lambda$, we can describe $\mathcal{L}(\varphi, \phi)$ by an effective Lagrangian $\mathcal{L}_{\mathrm{EFT}}(\varphi) = \mathcal{L}\left(\varphi, \phi(\varphi)\right)$, where $\phi(\varphi)$ is obtained by the heavy fields equations of motion. $\mathcal{L}_{\mathrm{EFT}}(\varphi)$ is highly non-renormalizable and can be expand in a series in the dimension of its operators:

$$\mathcal{L}_{\mathrm{EFT}}(\varphi) = \mathcal{L}_{\mathrm{ren}}(\varphi) + \sum_{d>4} \sum_{i} \frac{C_i^{(d)}}{\Lambda^{d-4}} O_i^{(d)}(\varphi), \tag{1.8}$$

where $\mathcal{L}_{\mathrm{ren}}(\varphi)$ is the renormalizable part of the Lagrangian and the dimensionless expansion parameters $C_i^{(d)}$ are called Wilson coefficients. They can be fixed, once the UV

theory is specified, by comparing a certain physical quantity computed in the UV theory with that obtained from the EFT calculation. In case the fundamental theory is not known, experimental identifications of $C_i^{(d)}$ gives a powerful hint about the physics that generates the expansion, as it happened for the electroweak interactions of the SM, hinted from the already known effective Fermi theory. The non-renormalizable part of the Lagrangian accounts for the virtual effects of the exchange of heavy fields ϕ. We can retain only the operators up to a certain dimension, depending on the accuracy we want to reach. From this Lagrangian one can see that the higher the dimension of an operator $O_i^{(d)}$, the more powerful the suppression of Λ in its coefficient. This means that lower dimensional non-renormalizable operators are less suppressed and they can play a more significant role in low energy phenomena than the higher dimensional ones.

What above can be applied to the SM, where the short distance physics effects on the SM processes associated to heavier new physics can be effectively parameterized by adding non-renormalizable operators, suppressed by the mass scales of new degrees of freedom, to the SM Lagrangian. Such operators must be invariant under the $SU(3)_{\rm C}\times SU(2)_{\rm L}\times U(1)_{\rm Y}$ gauge transformations. The idea is then to consider the SM Lagrangian, plus suitable non-renormalizable interactions, as the low energy limit of a theory assigned at some high-scale $\Lambda \gg v$

$$\mathcal{L}_{\rm SM}^{\rm eff} = \mathcal{L}_{\rm SM}^{\rm ren} + \mathcal{L}_{\rm SM}^{\rm NR}, \tag{1.9}$$

where $\mathcal{L}_{\rm SM}^{\rm ren}$ is the SM Lagrangian and $\mathcal{L}_{\rm SM}^{\rm NR}$ contains non-renormalizable operators involving the SM fields and invariants under the SM gauge transformations. The experimental constraints on the coefficients in $\mathcal{L}_{\rm SM}^{\rm NR}$ have to be taken into account when one tries to construct a fundamental theory.

In the next sections we will deal with effective operators that are particularly relevant experimentally, and so also for the construction of the theories beyond the SM.

Generally speaking , the efforts in this thesis attempt to address two broad questions related to the rather different areas of research. First of all, we will find a general argument to explain if lepton masses and mixing patterns can be approximately described in terms of a flavour symmetry (together with symmetry breaking effects in the context of the EFT description in terms of the Weinberg operator). We will provide a complete answer to the following question: what are the flavour symmetries and their representations that can give an approximate description of lepton masses and mixing? This question will be studied in two cases: in the first case we will do low-scale analysis by assuming neutrino masses are obtained from the Weinberg operator after electroweak symmetry breaking. In the second case, we will assume that neutrino masses are originated from the type I seesaw mechanism and take into account also the non-trivial transformation properties of singlet neutrinos under the flavour group, and we will discuss the limits of the EFT approach in this context. In the last part of the thesis, we direct our attention toward new physics search at the LHC, by using EFT approach and giving proposals for how to make manifest the new physics effects on the diboson production channels that get contributions from the

triple gauge boson couplings. More specifically, we will investigate important features of the amplitude, and provide a way to realize the interference between the amplitude of the SM and that of CP-even dimension six operators generating anomalous triple gauge boson couplings. And in the meanwhile we will corroborate our theoretical expectation from the `MadGraph5` simulation. The simple reason of studying the dimension six operators is because they are the less power suppressed non-renormalizable operators relevant for these processes, as mentioned, there is only one dimension five operator allowed by the SM gauge symmetries and it is discussed for the generation of neutrino masses in the first part of the thesis. In the remaining part of this introductory chapter, we will cover some background knowledge of fermion masses in SM and beyond, flavour symmetry approach to understand fermion mass hierarchy and mixing, and a short introduction to SM as an EFT.

1.3 Fermion masses and mixing from flavour symmetry

This section is devoted to a brief introduction to the neutrino mass generation mechanism, a discussion of the fermion mass hierarchy and flavour mixing problem, and a short chronological overview of the prototypical model buildings to explain fermion mass hierarchy and mixing.

1.3.1 Neutrino mass generation mechanism

Neutrinos are strictly massless in the SM, but the oscillation experiments indicate that at least two neutrinos have non-vanishing and all have non-degenerate masses. As known, there is a unique dimension five operator and it does contribute to the neutrino masses, the Weinberg operator [1]

$$\frac{c_{ij}}{2\Lambda}(l_i h)(l_j h), \tag{1.10}$$

where c_{ij} is a dimensionless coefficient and Λ is a mass scale associated to the degrees of freedom integrated out. As usual, we are omitting $SU(2)$ indices and understanding the contraction $l_{ir}\varepsilon_{rs}h_s$. This operator violates individual and total lepton numbers by two units. Moreover, the operator in eq. (1.10) provides a mass term for the neutrino after electroweak symmetry breaking. In fact, once the Higgs boson gets a non-trivial VEV $\langle h\rangle = (0, v)^T$, we will get the Majorana mass term $(1/2)m^{\nu}_{ij}\nu_i\nu_j$, in which the neutrino mass matrix is

$$m^{\nu}_{ij} = v^2 c_{ij}/\Lambda. \tag{1.11}$$

Note that, differently from the charged lepton sector, neutrino masses are suppressed by an additional v/Λ factor, and therefore we can understand the smallness of the neutrino masses in terms of the heaviness of the scale Λ at which the operators is generated and

lepton number is violated. This approach is completely general as long as the new physics accounting for neutrino masses lies above the EW scale (and the lowest order operator in eq. (1.10) indeed dominates).

In the context of a bottom-up approach, let us study whether this unique dimension five operator can be obtained from renormalizable interactions at the tree level. There are two possible ways to connect external legs of the tree level Feynman diagrams by the line of a new particle N, shown as in the figure 1.1.

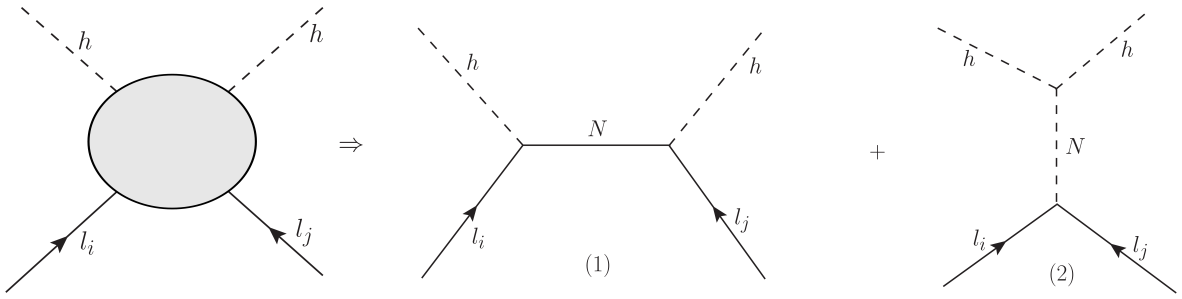

Figure 1.1: Possible mediators to generate Weinberg operator at tree level.

The possibility (1) requires the new heavy degree of freedom N couples to lepton doublet and Higgs field in Lorentz invariant and $G_{\rm SM}$-invariant way. To have Lorentz invariant interaction N must be a fermion. Since l_i and h are transforming as doublets of $SU(2)$, and $2 \times 2 = 1 + 3$, N can be a either singlet or a triplet of $SU(2)$. Obviously N is a colour singlet and has zero hypercharge, so its quantum numbers can be either $(1,1)_0$ or $(1,3)_0$ under $G_{\rm SM}$ in the notation $(SU(3)_{\rm C}, SU(2)_{\rm L})_{\rm Y}$. An insertion of a field in the first kind is called type I seesaw mechanism, which will be discussed in some details below and as we will see in this case N is exactly ν^c; while the second option $(1,3)_0$ for N is called type III seesaw mechanism.

In the possibility (2), first of all, Lorentz invariance requires N to be a scalar. Moreover, it is a colour singlet and has hypercharge $\rm Y = 1$. As far as the $SU(2)$ transformation is concerned, N is in principle either a singlet or a triplet. The possibility of being singlet is excluded because the one of the two vertex has a form $\varepsilon_{rs} h_r h_s N$ which is identically zero. So N must have a quantum number $(1,3)_1$. This is called the seesaw mechanism of type II.

Let us now review in great detail the type I seesaw in the context of EFT. If $G_{\rm SM}$ singlet neutrinos ν_i^c are added to the SM, then Yukawa interactions for the neutrinos are allowed, in the form

$$y_{ij}^N \nu_i^c l_j h + h.c. \,. \tag{1.12}$$

The later generate a neutrino Dirac mass term $m_N = y_N v$ after electroweak symmetry breaking (EWSB). Now, this mass term is proportional to electroweak scale and thus, if it was the only source of neutrino masses, it would be characterized by extremely small couplings. While this is a logical possibility, it is possible to account for the smallness

of neutrino masses by taking into account that in the presence of gauge singlets, we can write an explicit mass term for them

$$\frac{1}{2}M_{ij}\nu_i^c\nu_j^c \subset \mathcal{L}^{\text{mass}}_{\text{SM}+\nu^c} \ . \tag{1.13}$$

This is the only gauge invariant mass term allowed by the SM gauge symmetries and it is not related to the Higgs mechanism and the EWSB scale. Singlet neutrino masses can be arbitrarily large even in the limit $v \to 0$, in which all the other particles' masses vanish. Let us suppose this is the case, $M \gg v$. We can then consider an effective field theory below the scale M, in which the effect of the singlet neutrinos is described by the presence of the non-renormalizable operators. Apart from the kinetic term, the terms in which ν^c appear in the Lagrangian are

$$\frac{1}{2}M_{ij}\nu_i^c\nu_j^c + y^N_{ij}\nu_i^c l_j h + h.c. \subset \mathcal{L}^{\text{ren}}_{\text{SM}+\nu^c} \ . \tag{1.14}$$

The equation of motion from this Lagrangian, up to small correction from the kinetic term, is

$$\frac{\partial \mathcal{L}}{\partial \nu_i^c} = M_{ij}\nu_j^c + y^N_{ij} l_j h = 0, \tag{1.15}$$

leading to $\nu_i^c = -(M^{-1}y^N)_{ij}l_j h$. Plugging this back to the eq. (1.14) we end up with eq. (1.10), where

$$\frac{c_{ij}}{\Lambda} = -(y_N^T M^{-1} y_N)_{ij} \ . \tag{1.16}$$

Combining eq. (1.16) with eq. (1.11) we will get neutrino mass in terms of the Dirac and Majorana mass matrices, m_N and M,

$$m^\nu_{ij} = \frac{c_{ij}}{\Lambda}v^2 = -(m_N^T M^{-1} m_N)_{ij}. \tag{1.17}$$

This result holds at the tree level, and large logs from the computation of radiative corrections may modify it. The proper way to address the problem is to use renormalization group (RG) equation: first calculate c_{ij}/Λ in eq. (1.16) at the high-scale, then use RG equation to run the coefficient down to the electroweak scale, then keep running until m_ν. There we compute neutrino masses by plugging the runned coefficient into eq. (1.17).

The discussion above shows that singlet neutrinos, also called right-handed neutrinos, are the particular example of high energy physics that leads to the operator in eq. (1.10). Note that in the type I seesaw mechanism there could be arbitrary number of gauge singlets ν_i^c, but in order to generate the observed neutrino mass square differences they have to be not less than two, which is necessary to obtain at least two neutrinos with non-vanishing masses.

As it was pointed out before, this is not the only way to achieve Weinberg operator by integrating out the heavy particles at the tree level. Similar procedures can be used to obtain the expressions for the light neutrino masses in the context of the extension of

SM with scalar triplets or fermion triplets.

1.3.2 The SM flavour puzzle

The terminology "flavour" in particle physics was proposed by Harald Fritzsch and Murray Gell-Mann in 1971 when they were trying different flavour of ice-cream in the Baskin-Robbins ice-cream store in Pasadena [2]. Most probably they were inspired by the fact that ice-cream has both colour and flavour and so do quarks, since the terminology was first used in the context of the quark model of hadrons. Of course, leptons also come with different flavours but not with colours, and flavour physics covers the properties of both sets of fermions. Since then both quarks and leptons have been flavoured, and the flavour has commonly used in particle physics community to refer to the copies of fermions which have the same gauge quantum numbers under the SM gauge group. In some occasions it is also interchangeably used as family.

It is apparent from the expression of the SM Lagrangian in eq. (1.5) that, in the absence of flavour part, the Lagrangian possesses a global symmetry $U(3)^5 \times U(1)_H$ acting on the SM matter fields as

$$\begin{aligned} q_i &\to U^q_{ij} q_j, \quad & u^c_i &\to U^{u^c}_{ij} u^c_j, \quad & d^c_i &\to U^{d^c}_{ij} d^c_j\,, \\ l_i &\to U^l_{ij} l_j, \quad & e^c_i &\to U^{e^c}_{ij} e^c_j, \quad & h &\to e^{i\alpha_H} h\,, \end{aligned} \tag{1.18}$$

where $U^q, U^{u^c}, U^{d^c}, U^l, U^{e^c}$ are 3×3 unitary matrices and $\alpha_H \in \mathbb{R}$. These transformations correspond to rotations in the flavour space. Thus, as far as only gauge interactions are concerned, all fermions of a certain type are equivalent. What allows to tell the different family is the Yukawa couplings. In fact, the flavour part of the Lagrangian explicitly breaks $U(3)^5 \times U(1)_H$, and it is straightforward to show that this symmetry is broken to a residual symmetry $U(1)^5$. Of all these $U(1)$ symmetries, one of them turns out to be the one associated to the hypercharge, which is gauged. The others are called accidental symmetries of the SM, which are identified with three individual lepton numbers L_i and a baryon number B. Neutrino masses, if arising from the eq. (1.10), represent a source of breaking of total lepton number. So, the smallness of the neutrino masses is expected to be the associated with the breaking of total lepton number, at high energy, by the five dimensional operator.

Because of the breaking of $U(3)^5 \times U(1)_H$, the flavour degeneracy is lost, and specific pattern of masses and mixing is generated. The peculiar pattern of fermion masses and mixing originated from the breaking of $U(3)^5$ symmetry is one of the long-standing puzzles in the SM. Up to now, it still remains unsolved.

The SM contains thirteen dimensionless flavour parameters, which are nine quark and charged lepton Yukawa couplings, and the three quark mixing angles and one CP-violating phase in the Cabibbo–Kobayashi–Maskawa (CKM) matrix $V_{\rm CKM}$. Once we add neutrino masses to the SM, we would at least have another seven flavour parameters:

three neutrino masses, three mixing angles, one CP-violating phase if neutrinos are Dirac particle or there are three such phases if they are Majorana particle as predicted in our EFT set-up. A full understanding of flavour in the SM therefore requires to unveil the possible origins of at least twenty flavour parameters and of their values.

To illustrate the issue and its importance, let us see flavour part of the SM in more details. According to the Higgs mechanism, all charged fermions acquire masses proportional to their Yukawa couplings and to the Higgs vacuum expectation value (VEV) v, that is $m_f = v y_f$. All the flavour parameters in the quark sector have been measured with very good accuracy, but for the purpose of this introduction it is enough to show their orders of magnitudes as follows [3]

$$\begin{aligned} y_t &\sim 1, \qquad y_c \sim 10^{-3}, \quad y_u \sim 10^{-5}, \\ y_b &\sim 10^{-2}, \quad y_s \sim 10^{-4}, \quad y_d \sim 10^{-5}, \\ y_\tau &\sim 10^{-2}, \quad y_\mu \sim 10^{-4}, \quad y_e \sim 10^{-6}, \\ |V_{us}| &\sim 0.2, \quad |V_{cb}| \sim 0.04, \quad |V_{ub}| \sim 0.004, \quad \delta_{\rm CP} \sim 1. \end{aligned} \tag{1.19}$$

There are only two of these parameters that are of $\mathcal{O}(1)$, one is the top-Yukawa coupling and other is the CP-violating phase. All the other flavour parameters exhibit hierarchies as their values span six orders of magnitudes.

As for the lepton sector, in the past when the SM was built, neutrinos were expected to be massless particles due to the simple fact that right-handed neutrinos do not take part in weak interaction and no experiment observed them; later on, in order to account for the evidence from oscillation experiments, non-zero masses and a mismatch between their flavour eigenstates and mass eigenstates needed to be introduced. Neutrino masses and mixings add new features to the SM flavour puzzle. The accuracy in the determination of flavour parameters in the leptonic sector is getting better with the progress of the big experimental study.

One of the parameters that still needs to be determined has to do with the ordering of the neutrino masses. The first two masses m_1 and m_2 are defined to be the ones with the smallest squared mass difference, with $m_1 < m_2$ by definition. The third mass m_3 either bigger or smaller than m_1, m_2. Correspondingly, if we denote $\Delta m^2_{ij} \equiv m^2_i - m^2_j$, m^2_{31} can have both signs. The sign of $\Delta m^2_{31} = m^2_3 - m^2_1$ has not been fixed yet, although the atmospheric mass square difference $\Delta m^2_{\rm atm} = |\Delta m^2_{31}|$ has been determined by neutrino oscillation data. So there are two possible mass hierarchies: normal hierarchy (or ordering) if $m_3 > m_2 > m_1$ or inverted hierarchy if $m_2 > m_1 > m_3$. Note that there is a possibility of having quasi-degenerate spectrum that occurs when all three neutrino masses are much larger than both solar and atmospheric mass square differences, namely $m^2_i \gg \Delta m^2_\odot \,, \Delta m^2_{\rm atm}$. As we know, neutrino oscillation experiments cannot provide any information about the absolute mass scale of the neutrinos. The neutrino mass scale can be obtained at least in three different ways: from the end point of the beta decay

spectrum, from the neutrinoless double β decay, and from cosmological observations.

The lepton mixing matrix $U_{\rm PMNS}$ is also known as Pontecorvo–Maki–Nakagawa–Sakata matrix (PMNS matrix). In the standard parameterization it is given by

$$\begin{aligned} U_{\rm PMNS} &= R(\theta_{23})R(\theta_{13},\delta_{\rm CP})R(\theta_{12})\,, \\ &= \begin{pmatrix} c_{12}c_{13} & s_{12}c_{13} & s_{13}e^{-i\delta_{\rm CP}} \\ -s_{12}c_{23}-c_{12}s_{23}s_{13}e^{i\delta_{\rm CP}} & c_{12}c_{23}-s_{12}s_{23}s_{13}e^{i\delta_{\rm CP}} & s_{23}c_{13} \\ s_{12}s_{23}-c_{12}c_{23}s_{13}e^{i\delta_{\rm CP}} & -c_{12}s_{23}-s_{12}c_{23}s_{13}e^{i\delta_{\rm CP}} & c_{23}c_{13} \end{pmatrix}, \end{aligned} \tag{1.20}$$

where the part of Majorana phases $\mathrm{Diag}(e^{i\alpha_1}, e^{i\alpha_2}, 1)$ is neglected. The recent experimental data analyses have determined the absolute values of the mixing matrix elements at 3σ level to be in the following ranges [4]

$$|U_{\rm PMNS}| = \begin{pmatrix} 0.800 \to 0.844 & 0.515 \to 0.581 & 0.139 \to 0.155 \\ 0.229 \to 0.516 & 0.438 \to 0.699 & 0.614 \to 0.790 \\ 0.249 \to 0.528 & 0.462 \to 0.715 & 0.595 \to 0.776 \end{pmatrix}. \tag{1.21}$$

The measured absolute values of the PMNS matrix entries appear to be all large with the possible exception of the 13 element, which cannot be larger than 0.16. One of the 21 or 31 elements can be as small as 0.23, whereas all the other elements bound to be larger than 0.43. Note that unitarity prevents the 21 and 31 elements to be both at the lower (or upper) ends of their ranges. The current fits for the Dirac CP-violating phase in leptonic sector prefer nearly-maximal CP-violating values [5], and the sum of neutrino masses has an upper bound of $0.15eV$ at 95% C.L. from the recent cosmological observation [6]. Overall, the pattern of the SM flavour parameters indeed looks peculiar.

While the SM gauge group and field content allow us to determined all gauge interactions just by the three gauge couplings, there is no clear guidance to the form of the Yukawa matrices that describing the SM Yukawa interactions. The conjecture that there is indeed a structure in the flavour parameters is reinforced by considering the values of the four SM parameters other than flavour parameters, namely the three gauge couplings and the Higgs self-coupling at the electroweak scale, which are

$$g_s \simeq 1, \quad g \simeq 0.65, \quad g' \simeq 0.35, \quad \lambda \simeq 0.13\,. \tag{1.22}$$

Evidently, there is no big hierarchy among these parameters, unlike for the parameters in eq (1.19). People often understand small couplings in connection to the small breaking of a symmetry under which they are forced to vanish in the limit in which the symmetry is restored. Many proposals have been put forward already along those lines. In the following sections we will introduce some of them.

1.3.3 A lesson from the quark sector

A pioneering work attempt to explain mass hierarchy and mixing parameters in the quark sector has been done by C. D. Froggatt and H. B. Nielsen [7]. In their approach, all the small dimensionless parameters such as the quark mass ratios and the CKM mixing angles can be interpreted as powers of the breaking parameter of a global $U(1)$ flavour symmetry, without the need to assume widely hierarchical Yukawa couplings. Under this symmetry, a $G_{\rm SM}$-singlet scalar field φ, which is called flavon, has non-zero charge and the SM fermions as well as the Higgs field may also possess non-trivial charges. The flavon field develops a VEV $\langle\varphi\rangle$ and its effect can be parameterized by

$$\epsilon = \frac{\langle\varphi\rangle}{\Lambda} \ll 1\,, \tag{1.23}$$

where Λ is a characteristic energy scale of new physics of flavour. In general, different fermion flavours have different charge assignments. One can assign the flavon field a negative unit of $U(1)$ charge without loss of generality, as it is possible to rescale all the other charges in the unit of the flavon charge. The flavour symmetry is sometimes called horizontal symmetry in contrast to gauge symmetry which is thought as vertical symmetry. The rule is that each term in the Lagrangian including the SM fields and the flavon field should be invariant under the $U(1)_H$ horizontal symmetry. The effective Yukawa couplings then become

$$\begin{aligned} Y^U_{ij} &= y^U_{ij}\epsilon^{|H(q_i)+H(u^c_j)+H(h)|}\,,\\ Y^D_{ij} &= y^D_{ij}\epsilon^{|H(q_i)+H(d^c_j)-H(h)|}\,,\\ Y^E_{ij} &= y^E_{ij}\epsilon^{|H(l_i)+H(e^c_j)-H(h)|}\,, \end{aligned} \tag{1.24}$$

where $H(f)$ is the charge of the field f, and $y^U_{ij}, y^D_{ij}, y^E_{ij}$ are supposed to be of $\mathcal{O}(1)$. For example, if we use following $U(1)_H$ charges for the SM fields

$$\begin{aligned} &H(q_i) = H(u^c_i) = H(e^c_i) = x_i, \quad \boldsymbol{x} = (2,1,0)^T,\\ &H(l_i) = H(d^c_i) = H(h) = 0\,. \end{aligned} \tag{1.25}$$

This results in following parametric suppression of Yukawa couplings

$$\begin{aligned} m_U &\propto \begin{pmatrix} \epsilon^4 & \epsilon^3 & \epsilon^2 \\ \epsilon^3 & \epsilon^2 & \epsilon \\ \epsilon^2 & \epsilon & 1 \end{pmatrix}, \quad m_D \propto \begin{pmatrix} \epsilon^2 & \epsilon & 1 \\ \epsilon^2 & \epsilon & 1 \\ \epsilon^2 & \epsilon & 1 \end{pmatrix},\\ m_E &\propto \begin{pmatrix} \epsilon^2 & \epsilon^2 & \epsilon^2 \\ \epsilon & \epsilon & \epsilon \\ 1 & 1 & 1 \end{pmatrix}. \end{aligned} \tag{1.26}$$

The proportionality holds up to coefficients $y^U_{ij}, y^D_{ij}, y^E_{ij}$ in front of the each matrix elements. The diagonalization of these mass matrices implies the power suppression of up-type quarks, down-type quarks and charged lepton masses according to

$$\begin{aligned} m_t : m_c : m_u &\sim 1 : \epsilon^2 : \epsilon^4 \,, \\ m_b : m_s : m_d &\sim 1 : \epsilon : \epsilon^2 \,, \\ m_\tau : m_\mu : m_e &\sim 1 : \epsilon : \epsilon^2 \,, \\ |V_{us}| \sim \epsilon, \quad |V_{cb}| &\sim \epsilon, \quad |V_{ub}| \sim \epsilon^2, \quad \delta_{\rm CP} \sim 1. \end{aligned} \tag{1.27}$$

An immediate observation at this point is that the chosen set of charges implies that down-type quark and charged lepton mass ratios are the same, while the up-type quark mass ratios approximately square of those. One may think this can explain quantitatively the mass ratios of the up and down types of quarks with all coefficients y_{ij} of their mass matrix, but the charged lepton mass ratios need moderate hierarchies among those couplings. This means that a different choice to the lepton doublet and singlet charges may give better results, as we will see in the next section.

On the other hand, we can get ratios of charged fermion masses and values of quark mixing parameters from the experimentally determined results [3]

$$\begin{aligned} m_t : m_c : m_u &\simeq 1 : 0.007 : 1.3 \times 10^{-5} \,, \\ m_b : m_s : m_d &\simeq 1 : 0.023 : 0.001 \,, \\ m_\tau : m_\mu : m_e &\simeq 1 : 0.06 : 3 \times 10^{-4} \,, \\ |V_{us}| \simeq 0.22, \quad |V_{cb}| &\simeq 0.04, \quad |V_{ub}| \simeq 0.004, \quad \delta_{\rm CP} \simeq 1.2 \,, \end{aligned} \tag{1.28}$$

where the values of u, d and s quark masses are estimated from the $\overline{MS}$ scheme at a renormalization scale of $\mu = 2$ GeV.

By comparing the results from the Eq. (1.27) and Eq. (1.28), one can easily show that for the $\epsilon \sim 0.05$ the mass ratios and mixing parameters from Froggatt - Nielsen mechanism are roughly consistent with mass hierarchy realized in Nature.

There are also other options to reach viable result of quark mass ratios and mixing parameters, for instance, we can choose other set of charges for quarks [8]

$$\begin{aligned} (H(q_1), H(q_2), H(q_3)) &= (3, 2, 0) \,, \\ (H(u^c_1), H(u^c_2), H(u^c_3)) &= (4, 2, 0) \,, \\ (H(d^c_1), H(d^c_2), H(d^c_3)) &= (3, 2, 2) \,, \end{aligned} \tag{1.29}$$

and take value of ϵ equal to the Wolfenstein parameter $\lambda_c = \sin\theta_c = 0.22$. This choice can provide correct order of magnitude of quark mass ratios and of the modules of quark mixing matrix elements.

1.3.4 Flavour symmetry in the lepton sector

We have seen that neutrino masses are extremely small and the leptonic mixing is very different from the mixing in the quark sector. A theory addressing the origin of the flavour parameters must be able to account for such a diversity.

As we have seen, the Froggatt - Nielsen Mechanism discussed in section 1.3.3 can approximately describe quark masses and mixing. This mechanism can be useful for the leptonic sector as well. Let us assume that the neutrino masses originate from the Weinberg operator. The relevant part of the Lagrangian is then

$$y^E_{ij} e^c_i l_j h^c + \frac{c_{ij}}{2\Lambda}(l_i h)(l_j h) + h.c.\ . \tag{1.30}$$

A possible choice of charges is

$$(H(l_1), H(l_2), H(l_3)) = (1,0,0)\,, \quad (H(e^c_1), H(e^c_2), H(e^c_3)) = (3,2,0)\,, \tag{1.31}$$

with the Higgs field invariant in this $U(1)_H$ flavour symmetry. After inserting appropriate powers of flavon field in the terms in eq. (1.30) and replacing Higgs field by its VEV we can read-off the form of charged lepton and neutrino mass matrix

$$m_E = \begin{pmatrix} \epsilon^4 & \epsilon^3 & \epsilon^3 \\ \epsilon^3 & \epsilon^2 & \epsilon^2 \\ \epsilon & 1 & 1 \end{pmatrix}, \quad m_\nu = \begin{pmatrix} \epsilon^2 & \epsilon & \epsilon \\ \epsilon & 1 & 1 \\ \epsilon & 1 & 1 \end{pmatrix}, \tag{1.32}$$

where the coefficients $v y^E_{ij}$ and $v^2 c_{ij}/\Lambda$ in front of the each matrix entries are omitted. Taking $\epsilon = 0.22$, one can approximately reproduce the mass ratios of charged leptons in eq. (1.28). The 23 block of the neutrino mass matrix does not depend on ϵ and it is diagonalized by an $\mathcal{O}(1)$ rotation. And neutrino mass spectrum obtained from the mass matrix in eq.(1.32) has one small mass that is of the order of ϵ^2, and the other two masses are large compared to the first one. The observed value of the neutrino squared mass differences therefore require a mild corrections, making an other two large masses to be accidentally small.

If the Weinberg operator is generated from the type I seesaw mechanism, the above ideas can be applied to high-scale Lagrangian. The relevant Lagrangian is now

$$\mathcal{L}_{\text{flavour}} + y^N_{ij} \nu^c_i l_j h + \frac{1}{2} M_{ij} \nu^c_i \nu^c_j + h.c.\,. \tag{1.33}$$

One can assign following $U(1)_H$ charges to l_i and ν^c_i

$$\begin{aligned} (H(l_1), H(l_2), H(l_3)) &= (1,0,0)\,, \\ (H(\nu^c_1), H(\nu^c_2), H(\nu^c_3)) &= (n_1, n_2, n_3)\,, \end{aligned} \tag{1.34}$$

where $n_1, n_2, n_3 \geq 0$, and impose invariance under the flavour symmetry to write the

neutrino Yukawa matrix and the Majorana mass matrix of right-handed neutrinos in terms of flavons.

Here we choose generic charges n_i for the right-handed neutrino because the result does not depend on that specific case, as discussed below. The invariant neutrino Yukawa and mass matrices are

$$\begin{aligned} Y^N_{ij} &= y^N_{ij}\epsilon^{H(\nu^c_i)+H(l_j)+H(h)}\,, \\ (M_R)_{ij} &= M_{ij}\epsilon^{H(\nu^c_i)+H(\nu^c_j)}\,. \end{aligned} \tag{1.35}$$

Any symmetric matrix M can always be diagonalized by a unitary rotation V

$$M = V^T \,\mathrm{Diag}(M_1, M_2, M_3) V\,, \tag{1.36}$$

with $M_1, M_2, M_3 \geq 0$. Therefore, the effective right-handed neutrino mass matrix can be written as

$$M_R = \mathrm{Diag}(\epsilon^{n_1}, \epsilon^{n_2}, \epsilon^{n_3}) V^T \,\mathrm{Diag}(M_1, M_2, M_3) V \,\mathrm{Diag}(\epsilon^{n_1}, \epsilon^{n_2}, \epsilon^{n_3})\,. \tag{1.37}$$

And Dirac mass matrix reads

$$m_N = Y^N v = \mathrm{Diag}(\epsilon^{n_1}, \epsilon^{n_2}, \epsilon^{n_3}) y^N \,\mathrm{Diag}(\epsilon, 1, 1)\; v\,. \tag{1.38}$$

To obtain the light neutrino mass matrix, we combine the two above matrices in the seesaw formula

$$\begin{aligned} m_\nu &= -m_N^T M_R^{-1} m_N, \\ &= -\,\mathrm{Diag}(\epsilon, 1, 1) y^N V^\dagger \,\mathrm{Diag}(\frac{1}{M_1}, \frac{1}{M_2}, \frac{1}{M_3}) V^* y^N \,\mathrm{Diag}(\epsilon, 1, 1)\; v^2\,, \end{aligned} \tag{1.39}$$

where the charges of right-handed neutrinos disappear. But there is an important caveat to the previous conclusion which is one of the results of this thesis. The low-scale discussion of neutrino masses from the Weinberg operator is not always equivalent to the high-scale discussion within the seesaw mechanism. This will become clear when we study in detail the equivalent condition for the low- and high-scale analysis in chapter 3. Let M be the common scale of the parameters M_1, M_2, M_3, then we get a light neutrino mass matrix

$$m_\nu = \begin{pmatrix} \epsilon^2 & \epsilon & \epsilon \\ \epsilon & 1 & 1 \\ \epsilon & 1 & 1 \end{pmatrix} \frac{v^2}{M}\,. \tag{1.40}$$

The above equation holds up to order one coefficients in front of each entries. This mass matrix requires an order one rotation to diagonalize the 23 block. This, in turn, suggests that if we choose suitable charges of the lepton singlets e^c_i in order to generate the hierarchy of charged lepton masses and also to obtain an appropriate solar mixing

angle, then this mechanism may satisfactorily explain the flavour puzzle in lepton sector.

What we have seen so far are the examples based on the abelian flavour symmetries, but this is not the only possibility. There flavour symmetries have been proposed, such as, an approximate non-abelian continuous flavour symmetries [9–13], non-abelian discrete symmetries such as A_4 [14–33], S_4 [34–46], T' [47–52], A_5 [53–55] and many others [56–61]. Even thought the symmetry approach is nice and popular, it is not the only possible one. There are several examples to explain observed fermion mass hierarchy and mixing through other mechanisms, for instance, without any flavour symmetry [62, 63], fitting the parameters of grand unified theory [64–66], localization of extra-dimension [67] and loop corrections [68].

In the last decade, there has been very active research, driven by the experimental data improvements about neutrino masses and mixing, attempting to find a theoretical explanations for the lepton mass and mixing pattern via discrete flavour symmetries. In this context the implementation of Froggatt - Nielsen mechanism goes along the following line.

- Choose a suitable symmetry group and write their irreducible representations as well as invariants from their tensor products.
- Assign SM leptons, Higgs fields and other extra fields of the model to the representations of the chosen flavour symmetry group.
- Write down all possible lowest order terms allowed by the symmetry. Once the scalars like Higgs and flavons get certain VEVs the charged lepton and neutrino mass matrices will have some specific patterns.
- Diagonalization of the mass matrices may provide hierarchies between the masses and useful informations about mixing parameters. In particular, there could be precise predictions for some of the parameters or for correlations among them.
- Most of the time, symmetry breaking effects are essential to obtain correct mass hierarchies and the exact experimental values of the mixing parameters.
- If the flavour symmetry (with its spontaneous breaking) successfully describes the lepton sector, one can attempt a generalization to the quark sector as well, bearing in mind that the mismatch between the two rotations from up and down type of quark sectors is small, namely $V_u \approx V_d$ so that $V_u V_d^\dagger \sim 1$, whereas the imbalance between two rotations U_e, U_ν from the charged lepton and the neutrino sector is rather large.

Although not directly relevant to this thesis work, in the following we will briefly review the prototypical A_4 model.

1.3.5 An example of discrete flavour symmetry: A_4 model

Discrete non-abelian groups are widely popular due in part to the possibility to obtain precise prediction for some flavour parameters. The determination of the reactor angle indicated that it is non-zero and sizable although small compared to the other two mixing angles. Before $\theta_{13} \neq 0$ was known, the experimental data for the solar and atmospheric mixing angles were matched quite well with so called Tri-Bimaximal Mixing (TBM) ansatz [69–73], which is defined by

$$\theta_{12} = \arcsin(1/\sqrt{3}), \quad \theta_{23} = -\pi/4, \quad \theta_{13} = 0\,, \tag{1.41}$$

or, alternatively, by

$$\begin{aligned} U_{\rm TBM} &= \begin{pmatrix} \sqrt{\frac{2}{3}} & \frac{1}{\sqrt{3}} & 0 \\ -\frac{1}{\sqrt{6}} & \frac{1}{\sqrt{3}} & -\frac{1}{\sqrt{2}} \\ -\frac{1}{\sqrt{6}} & \frac{1}{\sqrt{3}} & \frac{1}{\sqrt{2}} \end{pmatrix} \\ &= \frac{1}{\sqrt{3}} \begin{pmatrix} 1 & 1 & 1 \\ 1 & \omega^2 & \omega \\ 1 & \omega & \omega^2 \end{pmatrix} \begin{pmatrix} 0 & 1 & 0 \\ \frac{1}{\sqrt{2}} & 0 & \frac{-i}{\sqrt{2}} \\ \frac{1}{\sqrt{2}} & 0 & \frac{i}{\sqrt{2}} \end{pmatrix}, \end{aligned} \tag{1.42}$$

where $\omega = e^{2\pi i/3}$. It is easy to see from the structure of this mixing matrix that the elements in the second and the third columns correspond to the tri-maximal and bi-maximal mixing, respectively. In the charged lepton mass basis one can easily find the general form of neutrino mass matrix with eigenvalues $m_1, m_2, m_3 \geq 0$ diagonalized by $U_{\rm TBM}$

$$m_\nu = U_{\rm TBM}\, {\rm Diag}(m_1, m_2, m_3) U_{\rm TBM}^T = \begin{pmatrix} a & b & b \\ b & a+c & b-c \\ b & b-c & a+c \end{pmatrix}, \tag{1.43}$$

where

$$\begin{aligned} a &= \frac{1}{3}(2m_1 + m_2)\,, \\ b &= \frac{1}{3}(m_2 - m_1)\,, \\ c &= \frac{1}{2}(m_3 - m_1)\,. \end{aligned} \tag{1.44}$$

An important observation is that the mass matrix in eq. (1.43) is invariant not only under the 23 permutation P_{23} but also under the unitary rotation

$$\begin{aligned} S_{\rm TBM} &= \frac{1}{3}\begin{pmatrix} -1 & 2 & 2 \\ 2 & -1 & 2 \\ 2 & 2 & -1 \end{pmatrix}, \\ m_\nu &= S_{\rm TBM}^T m_\nu S_{\rm TBM}, \quad m_\nu = P_{23}^T m_\nu P_{23}\,. \end{aligned} \tag{1.45}$$

The two transformations commute with each other, $[P_{23}, S_{\rm TBM}] = 0$, and $S_{\rm TBM}^2 = 1$. The above observations hint towards the existence of some discrete flavour symmetry in lepton sector.

Even though the choice of a discrete group for the explanation of lepton masses and mixing is not unique, the group A_4 became popular for several reasons. First of all, it is the smallest group, thus it is particularly economical, with three dimensional irreducible representation. Moreover, it can explain observed neutrino mixing parameters although not anymore in its simplest form. The group A_4 is a symmetry group of regular tetrahedron and is the even permutation group of four objects, as such it is a subgroup of S_4 as well as a subgroup of the continuous group $SO(3)$. The presentation of A_4 with its two generators S and T is given by

$$A_4 \quad : \quad \langle S, T | S^2 = T^3 = (ST)^3 = e \rangle. \tag{1.46}$$

All of its 12 elements belong to 4 conjugacy classes

$$\begin{aligned} &C_1 : e \\ &C_2 : T, ST, TS, STS \\ &C_3 : T^2, ST^2, T^2S, TST \\ &C_4 : S, T^2ST, TST^2\,. \end{aligned} \tag{1.47}$$

This implies that A_4 contains four inequivalent irreducible representations (irrep) with multiplicity m_1, m_2, m_3 for the representations in each dimensions, and satisfy

$$\begin{aligned} m_1 + 4m_2 + 9m_3 &= 12\,, \\ m_1 + m_2 + m_3 &= 4\,. \end{aligned} \tag{1.48}$$

This equation has a unique set of solutions, $m_1 = 3$, $m_2 = 0$ and $m_3 = 1$, meaning that A_4 has three one-dimensional irreducible representations, 1, $1'$ and $1''$, and one three-dimensional irreducible representation 3. The corresponding matrix representation of the

generators are

$$\begin{aligned} 1: &\quad S=1 \quad T=1 \\ 1': &\quad S=1 \quad T=e^{i2\pi/3} \\ 1'': &\quad S=1 \quad T=e^{i4\pi/3} \\ 3: &\quad S=\begin{pmatrix} 1 & 0 & 0 \\ 0 & -1 & 0 \\ 0 & 0 & -1 \end{pmatrix}, \quad T=\begin{pmatrix} 0 & 1 & 0 \\ 0 & 0 & 1 \\ 1 & 0 & 0 \end{pmatrix}. \end{aligned} \tag{1.49}$$

Note that there is an abuse of notation for S and T. These are, here, referring to the unitary representations of the two generators but not to the generators anymore. From those representations we can further notice that the irreps 1 and 3 are real representations and $1'$, $1''$ are complex conjugated representation of each other. One can see that the three-dimensional representation is written in the basis where the generator S is represented by diagonal matrix but T is not. In principle, one can find infinitely many equivalent representations through basis transformation. Among them there is one interesting basis where the representation of T is diagonal. The basis change is obtained by means of the unitary rotation

$$V=\frac{1}{\sqrt{3}}\begin{pmatrix} 1 & 1 & 1 \\ 1 & \omega^2 & \omega \\ 1 & \omega & \omega^2 \end{pmatrix}, \tag{1.50}$$

where $\omega \equiv e^{i2\pi/3} = (-1+i\sqrt{3})/2$, obviously satisfying the relations $\omega^2 = \omega^*$ and $1+\omega+\omega^2 = 0$. Going to the basis where the representation of T is diagonal has the interesting feature that the representation of S coincides with the $S_{\rm TBM}$ in eq. (1.45), i.e. $VSV^\dagger = S_{\rm TBM}$ and $VTV^\dagger = {\rm Diag}(1,\omega,\omega^2)$. This is a good omen for A_4 to be important candidate of flavour group. As the physical quantities are the same in all equivalent representations, we will continue our discussion in the original basis.

Having the specific representations of the group elements, we can find the tensor product decomposition rules

$$\begin{aligned} &1\times 1' = 1', 1\times 1'' = 1'', \\ &1'\times 1' = 1'', 1'\times 1'' = 1, \\ &1''\times 1'' = 1', \\ &3\times 3 = 1+1'+1''+3_1+3_2\,. \end{aligned} \tag{1.51}$$

The product of two one-dimensional representation is easy to obtain. To see the form of the each component representations in the decomposition of 3×3 consider following two triplets

$$a=(a_1,a_2,a_3), \qquad b=(b_1,b_2,b_3), \tag{1.52}$$

transforming under S and T in eq. (1.49) as $S(a_1, a_2, a_3) = (a_1, -a_2, -a_3)$ and $T(a_1, a_2, a_3) = (a_2, a_3, a_1)$. The irreducible representations obtained from their product (ab) are

$$\begin{aligned} 1 &= a_1b_1 + a_2b_2 + a_3b_3 \\ 1' &= a_1b_1 + \omega^2 a_2b_2 + \omega a_3b_3\,, \\ 1'' &= a_1b_1 + \omega a_2b_2 + \omega^2 a_3b_3\,, \\ 3_1 \equiv (ab)_1 &= (a_2b_3, a_3b_1, a_1b_2)\,, \\ 3_2 \equiv (ab)_2 &= (a_3b_2, a_1b_3, a_2b_1). \end{aligned} \tag{1.53}$$

Let us look at 3_1 as an example. From the transformation properties of the triplets a and b one can easily see that

$$\begin{aligned} S: &\quad (a_2b_3, a_3b_1, a_1b_2) \equiv (x_1, x_2, x_3) \to (a_2b_3, -a_3b_1, -a_1b_2) = (x_1, -x_2, -x_3), \\ T: &\quad (a_2b_3, a_3b_1, a_1b_2) \equiv (x_1, x_2, x_3) \to (a_3b_1, a_1b_2, a_2b_3) = (x_2, x_3, x_1). \end{aligned} \tag{1.54}$$

This is nothing but the transformation of a triplet under S and T. Therefore, (a_2b_3, a_3b_1, a_1b_2) is a triplet under the group representation. Analogously for the representation 3_2.

Having found the group and its representation, now we come to next step of the recipe, which is to assign fields to the different representations and to write down invariant terms under A_4. The following discussions are along the line of the model in [20]. This model contains, on top of the SM leptons, two Higgs doublets h_u, h_d as well as two scalar triplets φ, ϕ and a real scalar singlet ξ of A_4. The scalar fields φ, ϕ and ξ are taken to be singlets of standard model gauge group, they are necessary to the spontaneous breaking of A_4. Field assignments to representations of the flavour group A_4 are as follows

$$l \sim 3, \quad e_i^c \sim 1, 1'', 1', \quad h_u, h_d, \xi \sim 1, \quad \varphi, \phi \sim 3 \tag{1.55}$$

The lowest order Lagrangian includes the following SM gauge invariant and A_4-invariant terms

$$\mathcal{L} \supset \sum_i \frac{y_i}{\Lambda} e_i^c (\varphi l) h_d + \frac{c_1}{\Lambda^2} \xi (l h_u l h_u) + \frac{c_2}{\Lambda^2} \phi (l h_u l h_u) + h.c + \dots\,, \tag{1.56}$$

where the ellipsis refer to higher order terms in the expansion in (VEV/Λ), whose effects are under control and can be made negligibly small. The terms obtained by the exchange of $\varphi \leftrightarrow \phi$ or a missing term in $(l h_u l h_u)$ are prohibited by imposing an additional $\mathbb{Z}_4$ symmetry under which

$$l \to il\,, \quad e_i^c \to -ie_i^c\,, \quad \phi \to -\phi\,, \quad \xi \to -\xi\,, \tag{1.57}$$

all the other fields are invariant under this symmetry.

The two Higgs doublets get VEVs $\langle h_{u,d}\rangle = v_{u,d}$ and the other scalar fields also develop VEVs in the following form

$$\begin{aligned}\langle\varphi\rangle &= (v,v,v)^T\,,\\ \langle\phi\rangle &= (v',0,0)^T\,,\\ \langle\xi\rangle &= u\,.\end{aligned} \tag{1.58}$$

The possible origins of these VEV alignments have been investigated in the context of extra dimension [20, 74] and super symmetry [26], we will not enter in those details here. The charged lepton mass matrix is obtained from the first term in the Lagrangian

$$\begin{aligned}\sum_i \frac{y_i}{\Lambda} e_i^c(\varphi l) h_d = &\frac{y_1}{\Lambda} e_1^c(\varphi_1 l_1 + \varphi_2 l_2 + \varphi_3 l_3) h_d\\ &+ \frac{y_2}{\Lambda} e_2^c(\varphi_1 l_1 + \omega^2\varphi_2 l_2 + \omega\varphi_3 l_3) h_d\\ &+ \frac{y_3}{\Lambda} e_3^c(\varphi_1 l_1 + \omega\varphi_2 l_2 + \omega^2\varphi_3 l_3) h_d.\end{aligned} \tag{1.59}$$

Once the scalar fields get VEVs we will have

$$\begin{aligned}(m_e)_{ij} e_i^c e_j = &\frac{y_1 v v_d}{\Lambda} e_1^c(e_1 + e_2 + e_3)\\ &+ \frac{y_2 v v_d}{\Lambda} e_2^c(e_1 + \omega^2 e_2 + \omega e_3)\\ &+ \frac{y_3 v v_d}{\Lambda} e_3^c(e_1 + \omega e_2 + \omega^2 e_3),\end{aligned} \tag{1.60}$$

from which the charged lepton mass matrix can be read off as

$$m_e = \frac{v v_d}{\Lambda}\begin{pmatrix} y_1 & y_1 & y_1\\ y_2 & \omega^2 y_2 & \omega y_2\\ y_3 & \omega y_3 & \omega^2 y_3\end{pmatrix}. \tag{1.61}$$

Doing a similar exercise for the second and third terms of the Lagrangian in eq. (1.56) we can derive the neutrino mass matrix

$$m_\nu = \begin{pmatrix} a & 0 & 0\\ 0 & a & b\\ 0 & b & a\end{pmatrix}, \tag{1.62}$$

where $a = c_1 u v_u^2/\Lambda^2$ and $b = c_2 v' v_u^2/\Lambda^2$. The charged lepton mass matrices can be diagonalized by following rotations

$$V_{e^c} = \begin{pmatrix} e^{i\alpha_1} & & \\ & e^{i\alpha_2} & \\ & & e^{i\alpha_3}\end{pmatrix}, \quad V_e = \frac{1}{\sqrt{3}}\begin{pmatrix} 1 & 1 & 1\\ 1 & \omega^2 & \omega\\ 1 & \omega & \omega^2\end{pmatrix}, \tag{1.63}$$

where $\alpha_1, \alpha_2, \alpha_3$ are the phases of y_1, y_2, y_3 respectively, in a such way that

$$m_e = \frac{\sqrt{3}vv_d}{\Lambda} V_{e^c}^T \begin{pmatrix} |y_1| & & \\ & |y_2| & \\ & & |y_3| \end{pmatrix} V_e. \tag{1.64}$$

Note that V_e is the first term in the Tri-Bimaximal mixing matrix in eq. (1.42) and that the values of the charged lepton masses are arbitrary, depending on the sizes of the parameters y_i. Thus there is no explanation of the charged lepton mass hierarchy. The charged lepton mass spectrum is

$$(m_e, m_\mu, m_\tau) = \left((\sqrt{3}|y_1|vv_d)/\Lambda, (\sqrt{3}|y_2|vv_d)/\Lambda, (\sqrt{3}|y_3|vv_d)/\Lambda\right), \tag{1.65}$$

if $|y_1| < |y_2| < |y_3|$. The neutrino mass matrix can be diagonalized by the rotation

$$V_\nu = \begin{pmatrix} 0 & \frac{1}{\sqrt{2}} & \frac{1}{\sqrt{2}} \\ 1 & 0 & 0 \\ 0 & \frac{i}{\sqrt{2}} & \frac{-i}{\sqrt{2}} \end{pmatrix} \tag{1.66}$$

up to relative phases of the eigenvalues. This matrix is the Hermitian conjugate of the second term in eq. (1.42), and the neutrino masses are given by

$$m_\nu = V_\nu^T \begin{pmatrix} a+b & & \\ & a & \\ & & -a+b \end{pmatrix} V_\nu. \tag{1.67}$$

The PMNS matrix is

$$\begin{aligned} U_{\text{PMNS}} &= V_e V_\nu^\dagger \\ &= \frac{1}{\sqrt{3}} \begin{pmatrix} 1 & 1 & 1 \\ 1 & \omega^2 & \omega \\ 1 & \omega & \omega^2 \end{pmatrix} \begin{pmatrix} 0 & 1 & 0 \\ \frac{1}{\sqrt{2}} & 0 & \frac{-i}{\sqrt{2}} \\ \frac{1}{\sqrt{2}} & 0 & \frac{i}{\sqrt{2}} \end{pmatrix} \\ &= \begin{pmatrix} \sqrt{\frac{2}{3}} & \frac{1}{\sqrt{3}} & 0 \\ -\frac{1}{\sqrt{6}} & \frac{1}{\sqrt{3}} & -\frac{1}{\sqrt{2}} \\ -\frac{1}{\sqrt{6}} & \frac{1}{\sqrt{3}} & \frac{1}{\sqrt{2}} \end{pmatrix} = U_{\text{TBM}}. \end{aligned} \tag{1.68}$$

The leading order predictions of A_4 flavour symmetry in this model is exactly Tri-Bimaximal mixing. The neutrino masses are predicted to be $m_1 = |a+b|$, $m_2 = |a|$, $m_3 = |-a+b|$ and one can fix these parameters a and b according to the observed solar and atmospheric mass square differences. As it was pointed out before, there is no explanation of the charged lepton mass hierarchy. One can overcome this drawback by introducing an additional flavour symmetry $U(1)_H$ and assigning, as usual, a negative

unit of charge for the flavon field and non-zero charges only for the right-handed fields

$$H(e^c) = 4, \quad H(\mu^c) = 2, \quad H(\tau^c) = 0, \tag{1.69}$$

and we have Yukawa couplings in terms of the flavon parameter ϵ

$$y_e \approx \mathcal{O}(\epsilon^4), \quad y_\mu \approx \mathcal{O}(\epsilon^2), \quad y_\tau \approx \mathcal{O}(1). \tag{1.70}$$

This result rather nicely agrees, if the flavon parameter ϵ has a value of Cabibbo angle, with the observed charged lepton mass ratios. The discussions above have shown the success of the A_4 flavour model in describing observed lepton masses and mixing, but, of course, it is not the only viable model of flavour symmetry. Moreover, possible origins of the lepton masses and mixing from different flavour groups have been studied. To know more about flavour symmetry models, the interested reader is referred to the excellent review articles [75–79].

In this chapter we saw that flavour symmetry seems fruitful way to account for the SM fermion mass hierarchy and mixing. Even thought this kind of symmetry argument is appealing, but there is no solid bases to believe that this is the way that Nature has chosen. As Richard P. Feynman said: "It doesn't matter how beautiful your theory is, it doesn't matter how smart you are. If it doesn't agree with experiment, it's wrong."

1.4 The SM as an effective field theory from TeV scale physics

As we have mentioned before, the EFT Lagrangian can be constructed from the SM Lagrangian by adding non-renormalizable operators. Since the SM Lagrangian is already well known, discussions in this section will be about the non-renormalizable part of the EFT Lagrangian. At the beginning of this section there will be a brief review on the non-renormalizable operators, regarding their classifications in each dimensions and their generic properties related to the conservation/violation of the SM accidental symmetries. Then, at the end, we will particularly focus on the triple gage boson couplings and contributions of the relevant dimension six operators.

Let us now go back to the EFT approach and systematically analyses the possible non-renormalizable operators appearing in the expansion in the Lagrangian. Starting from the lowest order non-renormalizable operators, in the dimension five level there is only one such an operator — Weinberg operator. As we already know, this operator contributes to the neutrino mass generation, that was already discussed in section 1.3. The next order involves dimension six operators which are suppressed by the second power of new physics scale. In contrast to the only one dimension five operator, they emerge in quite big number and give rise to very reach physical consequences. As we saw in the section 1.3, the dimension five operator violates the lepton numbers, whereas the baryon

number is still preserved. One might expect that dimension six operators may break both B and L_i. This is indeed the case.

We have seen that lepton number violation start to appear from the operator with mass dimension ≥ 5 and baryon number can be violated by the operator with dimension ≥ 6. Now, one may wander " is there any general condition relating the dimensions of the operators to the conservation of both lepton and baryon number?". The answer is yes and is very simple: only the even dimensional operators can conserve both lepton and baryon numbers [80]. Namely, having an even dimension is the necessary (but not sufficient) condition to conserve both B and L_i. The proof of the statement also rather easy. Any operator, conserving both L_i and B, must consist of SM fermion pairs, Higgs field, covariant derivative and gauge field strength (in a suitable combinations of these components) listed in table 1.2.

Basic blocks	Lorentz indices	$SU(2)$ doublets	Dimension	Sum
$\psi^c\psi$, h.c.	0	1	3	4
$\psi^\dagger\sigma^\mu\psi$	1	2	3	6
$\psi^c\sigma^\mu\psi^{c\dagger}$	1	0	3	4
$\psi^c\sigma^{\mu\nu}\psi$, h.c.	2	1	3	6
h, h^*	0	1	1	2
D_μ	1	0	1	2
$B_{\mu\nu}$, $G_{\mu\nu}$, $W^a_{\mu\nu}$	2	0	2	4
Effective operator	even	even	D	D+even

Table 1.2: Basic building blocks of the operator conserving both lepton and baryon numbers, ψ collectively denotes a left-handed SM fermions.

Constructing an effective operator from the ingredients in this table requires to have even number of Lorentz indices to make invariants and also even number of $SU(2)$ doublet fields to have either singlet or triplet. Table 1.2 shows that each of these elementary pieces have an even number in the sum of their Lorentz indices, $SU(2)$ doublet fields and their mass dimensions. Any effective operator built by the several copies of these constituents will always end up having an even number in the sum and that is exactly equal to D plus an even number. This means that dimension D of the effective operator must be even too.

In summary, both lepton and baryon number conserving operators can only appear in even dimensions, odd dimensional operators violate either lepton numbers or baryon number or both. Note that this does not mean lepton (or baryon) number violating operator presents only in odd dimensions, it can happen in the even dimensions as well. If one aims at constructing an effective field theory extension of the SM that preserve both lepton and baryon numbers, the Lagrangian in eq. (1.8) is reduced to

$$\mathcal{L}_{\rm EFT} = \mathcal{L}_{\rm SM} + \sum_{d\geq 3}\sum_i \frac{C_i^{(2d)}}{\Lambda^{2d-4}} O_i^{(2d)} \ . \tag{1.71}$$

After getting this general argument, the B and L_i conserving dimension six operators are in the focus of the next discussion. They have been extensively studied in the recent literature [81–88]. There are several types of basis for the dimension six operators, but physics is always basis independent and one can choose prefered basis according to the convenience of addressing the targeted problem. The following discussions will stick to the so called Wasrsaw basis in Ref. [86] which exhaustively classifies all 59 independent dimension six baryon number conserving operators and 4 baryon number violating operators that occur in four fermion interactions. All of these baryon number conserving operators are divided into following 8 classes according to the field contents and number of covariant derivatives

$$\begin{array}{llll} F^3_{\mu\nu}, & H^6, & H^4D^2, & F^2_{\mu\nu}H^2, \\ \bar{\psi}\psi H^3, & \bar{\psi}\psi F_{\mu\nu}H, & \bar{\psi}\psi H^2 D, & (\bar{\psi}\psi)^2, \end{array} \tag{1.72}$$

where $F_{\mu\nu} = G^A_{\mu\nu}, W^I_{\mu\nu}, B_{\mu\nu}$, $A = 1, \ldots 8$, $I = 1, 2, 3$ and H is Higgs doublet. This reference basically updates Ref. [83] by performing detailed rederivation of the independent operators and excluding the redundancies, and provides complete lists of operator basis, with explicit flavour indices p, r, s, t, shown in table 1.3 and table 1.4.

$F^3_{\mu\nu}$	H^6 and H^4D^2	$\bar{\psi}\psi H^3$
$Q_G = f^{ABC}G^{A\nu}_{\mu}G^{B\rho}_{\nu}G^{C\mu}_{\rho}$	$Q_H = (H^\dagger H)^3$	$Q_{eH} = (H^\dagger H)(\bar{l}_p e_r H)$
$Q_{\widetilde{G}} = f^{ABC}\widetilde{G}^{A\nu}_{\mu}G^{B\rho}_{\nu}G^{C\mu}_{\rho}$	$Q_{H\Box} = (H^\dagger H)\Box(H^\dagger H)$	$Q_{uH} = (H^\dagger H)(\bar{q}_p u_r \widetilde{H})$
$Q_W = \epsilon^{IJK}W^{I\nu}_{\mu}W^{J\rho}_{\nu}W^{K\mu}_{\rho}$	$Q_{HD} = \left(H^\dagger D^\mu H\right)^* \left(H^\dagger D_\mu H\right)$	$Q_{dH} = (H^\dagger H)(\bar{q}_p d_r H)$
$Q_{\widetilde{W}} = \epsilon^{IJK}\widetilde{W}^{I\nu}_{\mu}W^{J\rho}_{\nu}W^{K\mu}_{\rho}$		
$F^2_{\mu\nu}H^2$	$\bar{\psi}\psi F_{\mu\nu}H$	$\bar{\psi}\psi H^2 D$
$Q_{HG} = H^\dagger H\, G^A_{\mu\nu}G^{A\mu\nu}$	$Q_{eW} = (\bar{l}_p\sigma^{\mu\nu}e_r)\sigma^I H W^I_{\mu\nu}$	$Q^{(1)}_{Hl} = (H^\dagger i\overleftrightarrow{D}_\mu H)(\bar{l}_p\gamma^\mu l_r)$
$Q_{H\widetilde{G}} = H^\dagger H\, \widetilde{G}^A_{\mu\nu}G^{A\mu\nu}$	$Q_{eB} = (\bar{l}_p\sigma^{\mu\nu}e_r)H B_{\mu\nu}$	$Q^{(3)}_{Hl} = (H^\dagger i\overleftrightarrow{D}^I_\mu H)(\bar{l}_p\sigma^I\gamma^\mu l_r)$
$Q_{HW} = H^\dagger H\, W^I_{\mu\nu}W^{I\mu\nu}$	$Q_{uG} = (\bar{q}_p\sigma^{\mu\nu}T^A u_r)\widetilde{H}\, G^A_{\mu\nu}$	$Q_{He} = (H^\dagger i\overleftrightarrow{D}_\mu H)(\bar{e}_p\gamma^\mu e_r)$
$Q_{H\widetilde{W}} = H^\dagger H\, \widetilde{W}^I_{\mu\nu}W^{I\mu\nu}$	$Q_{uW} = (\bar{q}_p\sigma^{\mu\nu}u_r)\sigma^I\widetilde{H}\, W^I_{\mu\nu}$	$Q^{(1)}_{Hq} = (H^\dagger i\overleftrightarrow{D}_\mu H)(\bar{q}_p\gamma^\mu q_r)$
$Q_{HB} = H^\dagger H\, B_{\mu\nu}B^{\mu\nu}$	$Q_{uB} = (\bar{q}_p\sigma^{\mu\nu}u_r)\widetilde{H}\, B_{\mu\nu}$	$Q^{(3)}_{Hq} = (H^\dagger i\overleftrightarrow{D}^I_\mu H)(\bar{q}_p\sigma^I\gamma^\mu q_r)$
$Q_{H\widetilde{B}} = H^\dagger H\, \widetilde{B}_{\mu\nu}B^{\mu\nu}$	$Q_{dG} = (\bar{q}_p\sigma^{\mu\nu}T^A d_r)H\, G^A_{\mu\nu}$	$Q_{Hu} = (H^\dagger i\overleftrightarrow{D}_\mu H)(\bar{u}_p\gamma^\mu u_r)$
$Q_{HWB} = H^\dagger\tau^I H\, W^I_{\mu\nu}B^{\mu\nu}$	$Q_{dW} = (\bar{q}_p\sigma^{\mu\nu}d_r)\sigma^I H\, W^I_{\mu\nu}$	$Q_{Hd} = (H^\dagger i\overleftrightarrow{D}_\mu H)(\bar{d}_p\gamma^\mu d_r)$
$Q_{H\widetilde{W}B} = H^\dagger\sigma^I H\, \widetilde{W}^I_{\mu\nu}B^{\mu\nu}$	$Q_{dB} = (\bar{q}_p\sigma^{\mu\nu}d_r)H\, B_{\mu\nu}$	$Q_{Hud} = i(\widetilde{H}^\dagger D_\mu H)(\bar{u}_p\gamma^\mu d_r)$

Table 1.3: List of independent dimension six operators, except for four fermion interactions. Here $\widetilde{H} = i\sigma^2 H^*$ and $\widetilde{F}_{\mu\nu} = \frac{1}{2}\epsilon_{\mu\nu\alpha\beta}F^{\alpha\beta}$. Flavour indices are omitted for Q's.

$(\bar{L}L)(\bar{L}L)$	$(\bar{R}R)(\bar{R}R)$	$(\bar{L}L)(\bar{R}R)$
$Q_{ll} = (\bar{l}_p\gamma_\mu l_r)(\bar{l}_s\gamma^\mu l_t)$	$Q_{ee} = (\bar{e}_p\gamma_\mu e_r)(\bar{e}_s\gamma^\mu e_t)$	$Q_{le} = (\bar{l}_p\gamma_\mu l_r)(\bar{e}_s\gamma^\mu e_t)$
$Q_{qq}^{(1)} = (\bar{q}_p\gamma_\mu q_r)(\bar{q}_s\gamma^\mu q_t)$	$Q_{uu} = (\bar{u}_p\gamma_\mu u_r)(\bar{u}_s\gamma^\mu u_t)$	$Q_{lu} = (\bar{l}_p\gamma_\mu l_r)(\bar{u}_s\gamma^\mu u_t)$
$Q_{qq}^{(3)} = (\bar{q}_p\gamma_\mu\tau^I q_r)(\bar{q}_s\gamma^\mu\tau^I q_t)$	$Q_{dd} = (\bar{d}_p\gamma_\mu d_r)(\bar{d}_s\gamma^\mu d_t)$	$Q_{ld} = (\bar{l}_p\gamma_\mu l_r)(\bar{d}_s\gamma^\mu d_t)$
$Q_{lq}^{(1)} = (\bar{l}_p\gamma_\mu l_r)(\bar{q}_s\gamma^\mu q_t)$	$Q_{eu} = (\bar{e}_p\gamma_\mu e_r)(\bar{u}_s\gamma^\mu u_t)$	$Q_{qe} = (\bar{q}_p\gamma_\mu q_r)(\bar{e}_s\gamma^\mu e_t)$
$Q_{lq}^{(3)} = (\bar{l}_p\gamma_\mu\tau^I l_r)(\bar{q}_s\gamma^\mu\tau^I q_t)$	$Q_{ed} = (\bar{e}_p\gamma_\mu e_r)(\bar{d}_s\gamma^\mu d_t)$	$Q_{qu}^{(1)} = (\bar{q}_p\gamma_\mu q_r)(\bar{u}_s\gamma^\mu u_t)$
	$Q_{ud}^{(1)} = (\bar{u}_p\gamma_\mu u_r)(\bar{d}_s\gamma^\mu d_t)$	$Q_{qu}^{(8)} = (\bar{q}_p\gamma_\mu T^A q_r)(\bar{u}_s\gamma^\mu T^A u_t)$
	$Q_{ud}^{(8)} = (\bar{u}_p\gamma_\mu T^A u_r)(\bar{d}_s\gamma^\mu T^A d_t)$	$Q_{qd}^{(1)} = (\bar{q}_p\gamma_\mu q_r)(\bar{d}_s\gamma^\mu d_t)$
		$Q_{qd}^{(8)} = (\bar{q}_p\gamma_\mu T^A q_r)(\bar{d}_s\gamma^\mu T^A d_t)$

$(\bar{L}R)(\bar{R}L)$ and $(\bar{L}R)(\bar{L}R)$	Baryon number violating operators
$Q_{ledq} = (\bar{l}_p^j e_r)(\bar{d}_s q_t^j)$	$Q_{duq} = \epsilon^{\alpha\beta\gamma}\epsilon_{jk}\left[(d_p^\alpha)^T C u_r^\beta\right]\left[(q_s^{\gamma j})^T C l_t^k\right]$
$Q_{quqd}^{(1)} = (\bar{q}_p^j u_r)\epsilon_{jk}(\bar{q}_s^k d_t)$	$Q_{qqu} = \epsilon^{\alpha\beta\gamma}\epsilon_{jk}\left[(q_p^{\alpha j})^T C q_r^{\beta k}\right]\left[(u_s^\gamma)^T C e_t\right]$
$Q_{quqd}^{(8)} = (\bar{q}_p^j T^A u_r)\epsilon_{jk}(\bar{q}_s^k T^A d_t)$	$Q_{qqq} = \epsilon^{\alpha\beta\gamma}\epsilon_{jn}\epsilon_{km}\left[(q_p^{\alpha j})^T C q_r^{\beta k}\right]\left[(q_s^{\gamma m})^T C l_t^n\right]$
$Q_{lequ}^{(1)} = (\bar{l}_p^j e_r)\epsilon_{jk}(\bar{q}_s^k u_t)$	$Q_{duu} = \epsilon^{\alpha\beta\gamma}\left[(d_p^\alpha)^T C u_r^\beta\right]\left[(u_s^\gamma)^T C e_t\right]$
$Q_{lequ}^{(3)} = (\bar{l}_p^j\sigma_{\mu\nu} e_r)\epsilon_{jk}(\bar{q}_s^k\sigma^{\mu\nu} u_t)$	

Table 1.4: List of independent dimension six four fermion operators. Flavour indices of Q's are omitted.

Phenomenology of the dimension six operators have been studied during the past few decades [89–93], bounds on the Wilson coefficients were set by the several experiments [94]. Nowadays, there is a quite big effort made by the LHC to find more accurate bounds on coefficients of these operators [95–97]. In the chapter 4 we will discuss more about the effects of dimension six operators on the SM triple weak gauge boson couplings and give proposals to enhance the interference between the SM amplitude and contribution from these operators.

To go further, a complete list of 20 independent dimension seven operator are presented in Ref. [98], all of these operators violate lepton number and 7 of them violate baryon number as well, as this is the common feature of all odd dimensional operators. Dimension seven operators also have very important phenomenological implications for the new physics searches. For instance, they are very useful to study leptogenesis as well as baryogenesis for understanding of the matter-antimatter asymmetry in the Universe, which is not inside the scope of this thesis, though.

There have been many studies for finding the number of independent higher dimensional operators. For example, dimension eight operators are discussed in Ref. [99], and algorithm for the determination of the contents and non-redundant numbers of any higher dimensional operators for general effective field theories can be found in [100–102]. Since

the higher dimensional operators are more suppressed and have a little effect on low energy physics, in the chapter 4 we will focus only on some of the dimension six operators. In particular, we discuss only about the CP-even dimension six operators that conserve both baryon and lepton numbers. For this reason, we will skip the analysis for all the other operators with dimensions higher than six.

1.4.1 Anomalous triple gauge boson couplings

Due to the non-abelian nature of the SM electroweak (EW) gauge symmetry, it is possible to have three gauge boson interactions. The $\mathcal{L}_{\text{gauge}}$ part of the SM Lagrangian in eq. (1.6) contains following three EW gauge boson interactions

$$\Delta\mathcal{L} = ig\left(W^{+}_{\mu\nu}W^{3\mu}W^{-\nu} - W^{-}_{\mu\nu}W^{3\mu}W^{+\nu} + W^{3}_{\mu\nu}W^{-\mu}W^{+\nu}\right), \tag{1.73}$$

where

$$\begin{aligned} W^{\pm}_{\mu\nu} &= \partial_\mu W^{\pm}_\nu - \partial_\nu W^{\pm}_\mu, \quad W^{\pm}_\mu = \frac{1}{\sqrt{2}}(W^1_\mu \mp iW^2_\mu) \\ W^{3}_{\mu\nu} &= \partial_\mu W^{3}_\nu - \partial_\nu W^{3}_\mu, \qquad W^{3}_\mu = \cos\theta_W Z_\mu + \sin\theta_W A_\mu, \end{aligned} \tag{1.74}$$

in which θ_W is a weak mixing angle. This Lagrangian provides the interaction vertex of two W bosons with a Z or with a photon, i.e. W^+W^-V with $V = Z, \gamma$. In general, the triple gauge coupling (TGC) of W^+W^-V can be obtained from the following effective Lagrangian [103]

$$\begin{aligned} \mathcal{L}_{\text{TGC}}/g_{WWV} \;=\; & ig_1^V\left(W^{+}_{\mu\nu}W^{-\nu}V^{\mu} - W^{-}_{\mu\nu}W^{+\nu}V^{\mu}\right) + i\kappa_V W^{+}_{\nu}W^{-}_{\mu}V^{\mu\nu} + \frac{i\lambda_V}{M_W^2}W^{+}_{\mu\nu}W^{-\nu}_{\rho}V^{\rho\mu} \\ & + g_5^V\varepsilon^{\mu\nu\rho\sigma}\left(W^{+}_{\mu}\overleftrightarrow{\partial}_\rho W^{-}_{\nu}\right)V_\sigma - g_4^V W^{+}_{\mu}W^{-}_{\nu}\left(\partial^\mu V^\nu + \partial^\nu V^\mu\right) \\ & + i\tilde{\kappa}_V W^{+}_{\mu}W^{-}_{\nu}\tilde{V}^{\mu\nu} + \frac{i\tilde{\lambda}_V}{M_W^2}W^{+}_{\rho\mu}W^{-\mu}_{\nu}\tilde{V}^{\nu\rho}\,. \end{aligned} \tag{1.75}$$

Here the SM gauge couplings are $g_{WW\gamma} = g\sin\theta_W = e$ and $g_{WWZ} = g\cos\theta_W$, the field strength is $F_{\mu\nu} = \partial_\mu F_\nu - \partial_\nu F_\mu$ with $F = W^\pm, V$, dual field strength is $\tilde{V}_{\mu\nu} = \frac{1}{2}\varepsilon_{\mu\nu\rho\sigma}V^{\rho\sigma}$ and $W^{+}_{\mu}\overleftrightarrow{\partial}_\rho W^{-}_{\nu} = W^{+}_{\mu}(\partial_\rho W^{-}_{\nu}) - (\partial_\rho W^{+}_{\mu})W^{-}_{\nu}$. There are 14 anomalous triple gauge couplings (aTGCs) in total, among which 6 couplings g_1^V, κ_V and λ_V conserve both parity (P) and charge conjugation (C) while remaining 8 couplings violate either P or C. Comparing two Lagrangians in eq. (1.74) and eq. (1.75) one can easily see that in the SM

$$g_1^V = \kappa_V = 1, \quad \lambda_V = g_4^V = g_5^V = \tilde{\kappa}_V = \tilde{\lambda}_V = 0. \tag{1.76}$$

Invariance under the $U(1)_{\text{EM}}$ gauge symmetry requires $g_1^\gamma = 1$ and $g_4^\gamma = g_5^\gamma = 0$. Since our future discussions related only to the CP-conserving interactions, we are left with

following five aTGCs

$$\delta g_{1,Z}\,, \quad \delta\kappa_\gamma\,, \quad \delta\kappa_Z\,, \quad \lambda_\gamma\,, \quad \lambda_Z\,, \tag{1.77}$$

where $\delta g_{1,Z} \equiv g_{1,Z} - 1$ and $\delta\kappa_{\gamma,Z} \equiv \kappa_{\gamma,Z} - 1$.

If we want to parameterize the triple gauge boson interactions from the EFT Lagrangian that contains the CP-conserving dimension six operators, a convenient basis of the dimension six operators relevant for our future discussions is the SILH basis [85, 104], in which the operators contributing to aTGCs are

$$\begin{aligned}
O_W &= \frac{ic_W\, g}{2M_W^2}\left(H^\dagger\sigma^i \overleftrightarrow{D^\mu} H\right) D^\nu W^i_{\mu\nu}\,,\\
O_{HW} &= \frac{ic_{HW}\, g}{M_W^2}\,(D^\mu H)^\dagger\sigma^i(D^\nu H)W^i_{\mu\nu}\,,\\
O_{HB} &= \frac{ic_{HB}\, g'}{M_W^2}\,(D^\mu H)^\dagger(D^\nu H)B_{\mu\nu}\,,\\
O_{3W} &= \frac{c_{3W}\, g}{6M_W^2}\,\epsilon_{ijk}W^{i\,\nu}_{\mu}W^{j\,\rho}_{\nu}W^{k\,\mu}_{\rho}\,,
\end{aligned} \tag{1.78}$$

where $H^\dagger \overleftrightarrow{D}_\mu H = H^\dagger(D_\mu H) - (D_\mu H^\dagger)H$ and $D_\mu W^a_{\nu\rho} \equiv \partial_\mu W^a_{\nu\rho} + g\varepsilon^{abc}W^b_\mu W^c_{\nu\rho}$. The first operator O_W contributes to oblique parameter S [105, 106], its coefficient c_W is tightly constrained to be around 10^{-5} by EW precision measurements [94, 107–109], we can neglect its effect in the first order approximation. There is following set of relations between the aTGCs in eq. (1.77) and Wilson coefficients of those dimension six operators [84]

$$\begin{aligned}
\delta g_{1,Z} &= c_{HW}/\cos^2\theta_W\,,\\
\delta\kappa_Z &= c_{HW} - \tan^2\theta_W c_{HB}\,,\\
\delta\kappa_\gamma &= c_{HW} + c_{HB}\,,\\
\lambda_Z &= \lambda_\gamma = c_{3W}\,,
\end{aligned} \tag{1.79}$$

from which one can find following relation between $\delta g_{1,Z}$ and $\delta\kappa_{Z,\gamma}$

$$\delta g_{1,Z} = \delta\kappa_Z + \tan^2\theta_W\delta\kappa_\gamma\,. \tag{1.80}$$

So we have only three independent aTGCs conserving both C and P. From above relations between the aTGCs and Wilson coefficients we can always translate experimental bounds on the aTGCs to constraints on the corresponding dimension six operators. More discussions about aTGC will be given in chapter 4.

Chapter 2

Flavour symmetries in the symmetric limit

2.1 Introduction

As discussed, the origin of lepton masses and mixing is one of the open problems in the particle physics. One of the most popular attempts at understanding the SM fermion mass and mixing pattern makes use of flavour symmetry groups [7, 9, 10, 12, 63, 110–119]. The flavour symmetry G is spontaneously broken to a subgroup H (trivial if G is completely broken). And the source of breaking is provided by the vacuum expectation value (vev) of one or more scalar fields ("flavons"), which are singlets under the SM, but transforming non-trivially under G. We write the charged lepton and neutrino mass matrices, m_E and m_ν , as a sum of two components

$$\begin{aligned} m_E &= m_E^{(0)} + m_E^{(1)} \\ m_\nu &= m_\nu^{(0)} + m_\nu^{(1)} \end{aligned} , \tag{2.1}$$

where $m_E^{(0)}$, $m_\nu^{(0)}$ are invariant under G, therefore survive in the limit in which the flavour symmetry is unbroken, while $m_E^{(1)}$, $m_\nu^{(1)}$ are generated after the symmetry breaking, so they are invariant under H but not under G, and vanish in the symmetric limit. The non-vanishing entries in $m_E^{(0)}$, $m_\nu^{(0)}$ are often, and here, assumed to be of the same order, according to the principle that flavour hierarchies should be accounted for by the flavour model itself. The size of the corrections associated to the symmetry breaking effects is assumed to be smaller than the values of $m_E^{(0)}$ and $m_\nu^{(0)}$ (except, of course, the case of these leading order terms vanish).

As the problem required, we have to distinguish two cases whether the leading order pattern of lepton masses and mixings is completely determined by the flavour symmetry alone or the symmetry breaking effects are necessary to be considered. Therefore, our attention will be focused on following two separate scenarios.

1. The symmetric form of the mass matrices, $m_E^{(0)}$ and $m_\nu^{(0)}$, provides an approximate description of lepton flavour observables, in particular of the PMNS matrix; $m_E^{(1)}$ and $m_\nu^{(1)}$ provide the moderate correction necessary for an accurate description. In such a case, we can say that the leading order pattern of lepton masses and mixings is accounted for by the flavour symmetry itself.

2. The symmetry breaking corrections are important even for an approximately correct description of lepton flavour observables. That will appear in two ways: either the size of corrections is turn out to be not smaller than the non-vanishing symmetric terms, this can happen if $m_E^{(0)}$ or $m_\nu^{(0)}$ vanishes, in which case the PMNS matrix is fully undetermined in the symmetric limit; or in the presence of an accidental enhancement of the role of $m_E^{(1)}$, $m_\nu^{(1)}$.[1]

Having made the goal clear, we are going to provide a complete study of the first case and, meanwhile, assessing the need to resort to the second possibility. More specifically, we will obtain a complete characterisation of the flavour symmetry groups G (of any type) and their representations on the SM leptons providing an approximate understanding of lepton masses and mixing in the symmetric limit. Moreover, we will show that the results can be extended to the second case as well, if some (non-trivial) hypotheses hold.

The first case has been extensively considered since the earliest attempts of understanding the pattern of fermion masses and mixings. As charged fermion masses show a clear hierarchical structure, it is natural to account for the lightness of the first two families in terms of small symmetry breaking effects. For instance, the symmetric limit could allow the third family to acquire a mass but not the first two. The symmetric limit is then close to what observed, with the small Yukawas associated to the lighter families approximated by zeros. Considering the quark sector, all the quarks except top and bottom quarks can be massless in the symmetric limit and the CKM matrix is approximated by the identity matrix. The lighter masses and the small CKM mixings are then generated by small perturbations of the symmetric limit associated to the spontaneous breaking of the flavour symmetry.

Does the above scheme apply to neutrino masses and mixings as well? While many models have been proposed in which it does, but, as far as systematic analysis is concerned, the charting all possibilities is missing. Given the large variety of possible cases, it is not a priori obvious that a complete analysis can be carried out in an effective way and would produce results that can be expressed in a concise form. Interestingly, this turns out to be the case: the problem can be studied in full generality, admits a precise mathematical formulation, and a complete and compact solution. While specific implementations of the full solution are well known, the analysis shows that the options we will

[1] This is the case for example if one of the neutrino masses obtained in the symmetric limit is accidentally suppressed and ends up being of the same order of the smaller symmetry breaking corrections. In such a case, the symmetric limit prediction for some of the lepton mixing angles can be drastically modified, and actually determined, by the symmetry breaking effects [120–123].

find are the only possible ones, thus providing a final answer to the above question. The mathematical formulation of the problem, and the definition of "approximate description" will be discussed in section 2.2.

As we will see, while the possibility that lepton flavour can be approximately understood in terms of a symmetry principle alone is aesthetically appealing, future data might disfavour it. In such a case, the symmetry breaking effects become essential for an understanding of lepton flavour. One can then wonder whether the knowledge of the symmetry breaking pattern $G \to H$ can be sufficient, or the intricacies of the flavon spectrum, vevs, and potential should be specified. The knowledge of the breaking patter is sufficient if $m_E^{(0)}$ or $m_\nu^{(0)}$ vanishes in the symmetric limit and the corrections $m_E^{(1)}$, $m_\nu^{(1)}$ are in the most general form allowed by the residual symmetry H, with all their entries of the same order. Under such a (non-trivial) hypothesis, it turns out that the techniques developed to study the symmetric limit can be easily extended to study this case as well, and that the conclusions do not change.

The analysis we perform is fully general in the assumptions that i) the light neutrino masses are in Majorana form and ii) the symmetry arguments can be applied directly to the light neutrino mass matrix (or to the Weinberg operator from which it originates). The second assumption is relevant in the case in which the light neutrino mass matrix arises from physics well above the electroweak scale, the prototypical case being the integration of heavy singlet neutrinos in the context of the seesaw mechanism. In such a case, the heavy degrees of freedom also transform under the flavour symmetry, and a symmetric limit can be defined for their mass matrix as well. One can then wonder whether the "low energy" analysis performed in terms of the light neutrino mass matrix captures the features of the full analysis. This turns out to be true in some cases, but not always, the necessary and sufficient condition of two analysis being equivalent puts some non-trivial conditions on the representations of lepton doublet and singlets, which will be thoroughly study in the next chapter.

The discussions in this chapter goes along the following order. Section 2.2 contains the main result obtained from the general analysis, i.e. the classification of flavour groups and representations leading to an approximate description of lepton masses and mixings. Section 2.3 discusses the case in which either the neutrino or the charged lepton masses all vanish in the symmetric limit, and lepton mixing is determined by symmetry breaking effects. The additional constraints provided by grand-unification will be the subject of section 2.4. Finally, in section 2.5 we draw conclusions of whole chapter.

2.2 Lepton masses and mixings in the symmetric limit

In this section, we aim at providing a full characterisation of the flavour groups G and their representations on the leptons leading to an approximate description of lepton masses and

mixings in the symmetric limit. We will proceed in two steps. First, in section 2.2.1, we will list all representations leading to an approximate description of lepton masses (but not necessarily of lepton mixing). Then, in section 2.2.2, we will select among them the cases in which the PMNS matrix is also approximately realistic in the symmetric limit. Meaning that all the entries, only exception may apply for the 13 element in the first approximation, of the PMNS matrix must be non-vanishing in the symmetric limit, as the magnitudes of all the other entries are in the range of order one and smallness of 13 entry can be generated from a correction.

First of all, we need to define which lepton mass and mixing patterns we consider an approximate description of what observed and to give a precise mathematical formulation of the problem of finding the groups and representations associated to those patterns.

The full list of charged lepton and neutrino mass patterns that we consider to be close to what observed is in table 2.1. Let us illustrate the table by considering a few examples. The case in which the three charged lepton masses are in the form $(A, 0, 0)$ can be considered to be close to what observed because of the smallness of the electron and muon masses compared to the tau mass. Only a small correction to that pattern is required in order to provide an accurate description of the charged lepton spectrum. On the contrary, a pattern such as $(A, A, 0)$, for example, cannot be considered to be close to what observed, as no pair of charged lepton masses are close to be degenerate. The pattern $(A, B, 0)$ is in between. It can be considered close to what observed if A and B are allowed to have different sizes, with $B \ll A$, or vice versa. But not if A and B are assumed to be of the same order of magnitude, unless one entry is accidentally suppressed with respect to the other. In the neutrino sector, a pattern in the form $(a, 0, 0)$ can be considered to be close to what observed, as only a small correction is required to obtain a realistic normal hierarchical spectrum. The pattern $(0, a, a)$ also provides a good approximate description, as a small correction splitting the two degenerate eigenvalues is only required to obtain a realistic inverted hierarchical spectrum. A normal hierarchical spectrum is at present favoured by data [5, 124, 125], but we still retain the inverted spectrum as a viable possibility.

All the entries in table 2.1 are assumed to be positive or zero. The last column of the table corresponds to the possibility that the mass spectrum is fully determined by symmetry breaking effects. Such cases will be considered in section 2.3. Here, we only need to consider the cases in the first two columns. In the first column we list the cases that can be considered as good leading order approximations even when all the non-zero entries are of the same order of magnitude. The cases in the second column, on the contrary, require some degree of hierarchy or degeneracy between the non-zero entries. Such a distinction is more important for charged leptons than neutrinos. The hierarchy among non-zero entries required in the charged lepton cases to account for the hierarchy $m_e \ll m_\mu \ll m_\tau$ is $\mathcal{O}(20)$ in the $(A, B, 0)$ case and $\mathcal{O}(200)$ in the (A, B, C) case. On the other hand, in the neutrino case only milder hierarchies up to $\mathcal{O}(5)$ are required to

	non-zero entries of the same order	hierarchy among non-zero entries	(fully undetermined in the symmetric limit)
charged leptons	$(A,0,0)$	$(A,B,0)$ (A,B,C)	$(0,0,0)$
neutrinos NH	$(a,0,0)$		
neutrinos NH or IH	(a,a,a) (a,b,b)	$(a,b,0)$ (a,b,c)	$(0,0,0)$
neutrinos IH	$(0,a,a)$		

Table 2.1: Charged lepton and neutrino mass patterns in the symmetric limit.

account for $\Delta m^2_{12}/|\Delta m^2_{23}| \ll 1$ in the normal hierarchy case[2]. Such a mild hierarchy is not too far from what can be considered to be of the same order. Therefore, we will only care about the distinction between first and second column in the case of charged leptons. In the case of neutrinos, we distinguish the cases leading (after taking into account small symmetry breaking corrections) to a normal hierarchy (NH), an inverted hierarchy (IH), or to any of the two depending on the sizes of the non-zero entries.

A pedantic remark on the patterns in table 2.1 (which however will play a role in the following) concerns the fact that the pattern $(a,b,0)$, for example, includes the case in which $b=a$, as well as the case in which $b=0$. We define a mass pattern to be "generic" if all the entries that are allowed to be different from each other and non-zero are indeed different from each other and non-zero.

As for the PMNS matrix, we will consider it to be close to what observed in the symmetric limit if either i) none of its elements vanishes or ii) only the 13 element vanishes. Indeed, all of the PMNS entries appear to be of order one, with the exception of the 13 element, $|(U_{\rm PMNS})_{13}| \approx 0.15$. One of the 21 and 31 elements can be as small as about 0.25 if leptonic CP violation will turn out be small, unlike what the present fits seem to suggest [4, 5, 126, 127]. All other elements are bound to be larger than 0.45 (3σ bounds from [4]). As a consequence of the above definition, we will not consider PMNS matrices corresponding to a single 2×2 transformation in the 12, 23, or 13 block, which would require at least four matrix entries to vanish. In the case of PMNS matrices obtained by the combination of two 2×2 transformations in different blocks, the PMNS matrix contains one vanishing entry, which is located in the 13 entry if the two 2×2 rotations are in the 23 and 12 block (in this order).

[2]For inverted hierarchy, a stronger accidental degeneracy is required. For example, in the $(a,b,0)$ case, $a/|b-a| = \mathcal{O}(50)$ is required.

Having specified the mass and mixing patterns that we consider viable in the symmetric limit, we now want to characterise the flavour groups and representations leading to any of those patterns. Let us then give first of all a precise formulation of the problem.

The flavour symmetry group G acts on the SM leptons l_i and e^c_i through unitary representations U_l and U_{e^c} respectively. Here $e^c \sim \overline{e_R}$ denotes the conjugated of the right-handed SM leptons ($\mathrm{SU}(2)_L$ singlets with hypercharge $Y = 1$), and $l = (\nu, e)^T$ denotes the left-handed leptons ($\mathrm{SU}(2)_L$ doublets with hypercharge $Y = -1/2$). With this notation, all the fermion fields are left-handed, which will also turn out to be useful when we will discuss grand-unification in section 2.4. The charged lepton and neutrino mass matrices arise from the Yukawa and Weinberg operators respectively,

$$\lambda^E_{ij} e^c_i l_j h^*, \qquad \frac{c_{ij}}{2\Lambda} l_i l_j h h, \tag{2.2}$$

and are given by

$$m_E = \lambda_E v, \qquad m_\nu = c\, v^2/\Lambda, \tag{2.3}$$

where h is the Higgs field, $v = |\langle h \rangle|$, and Lorentz-invariant contractions of fermion indices are understood. Note the convention in which the singlet leptons appear first in the Yukawa interaction. Note also that the action of G is the same on the two components of l_i, ν_i and e_i, as it is supposed to commute with the SM gauge transformations.

To get a conclusion for the most general case, the group G is assumed to be an arbitrary. It can be continuous or discrete, simple or not, abelian or not, or arbitrary combinations of the above. It is supposed to include all the relevant symmetries, including those possibly used to force specific couplings of the flavons. We denote by U_l and U_{e^c} its representations on the doublet and singlet leptons respectively. From the invariance of the Yukawa and Weinberg operators, one finds that the lepton mass matrices m_E, m_ν are invariant if they satisfy

$$m_E = U^T_{e^c}(g)\, m_E\, U_l\,(g) \qquad m_\nu = U^T_l(g)\, m_\nu\, U_l\ (g) \qquad \forall g \in G. \tag{2.4}$$

In principle, the Higgs doublet h also have a non-trivial transformation property under the flavour symmetry G, but in this minimal setup, considering only the SM particles, we have one family of Higgs field and thus a possible transformation of h under G can be reabsorbed in U_l and U_{e^c}.

We can now formulate the problem we want to address as follows. For each of the $3 \times 6 = 18$ combinations of charged lepton and neutrino mass patterns in table 2.1 (excluding the ones in the third column), we want to determine, or characterise, all groups G and representations U_l, U_{e^c} corresponding to those mass patterns and leading to a viable PMNS matrix. We say that the group and its representation "correspond to" or "force" a given mass pattern if i) the eigenvalues[3] of any pair of invariant matrices m_E, m_ν follow that mass pattern, and if ii) there exists at least a pair of invariant matrices

[3]Here and in the following we use "eigenvalues" to refer to the singular values of m_E, m_ν.

m_E, m_ν such that the eigenvalues not only follow that mass pattern, but are also generic (i.e. with all entries that are allowed to be different and non-zero being different and non-zero). The second requirement is needed, as otherwise we could end up with groups and representations corresponding to a different, more constrained, pattern.

Note that it is important to write the invariance condition for m_E, as in eq. (2.4), and not for $m_E^\dagger m_E$. In the latter case, the important role of U_{e^c} would be lost.

2.2.1 Accounting for lepton masses

In this section we characterise all the groups and representations that force each of the 18 combinations of charged lepton and neutrino mass patterns in the first two columns of table 2.1. It turns out that it is possible to characterise them in terms of their decompositions into irreducible representations ("irreps"), and of the dimensionality, type (complex, real, or pseudoreal), and equivalence of the irreducible components.

We remind that a representation is called "complex" if it is not equivalent to its conjugated representation. A representation that is equivalent to its conjugated is called "real" if it can be represented by real matrices and "pseudoreal" if it cannot. Pseudoreal representations have even dimensions.

The full list of irrep decompositions corresponding to a given mass pattern is shown in tables 2.2, 2.3. The first table only contains the charged lepton mass pattern that does not require hierarchies among the non-zero entries, $(A, 0, 0)$, while the second contains the cases in which a hierarchy is necessary, following the classification in table 2.1. In the rest of this section we will prove and illustrate the results in tables 2.2, 2.3.

In order to prove the results in the tables, we note that there is a close connection between the mass patterns and the irrep decompositions, which we now illustrate. Since the extension is straightforward and useful, let us consider the general case of n lepton families. Let us choose a basis in flavour space in which the charged lepton mass matrix is diagonal, $m_E = \mathrm{Diag}(m_1^E \dots m_n^E)$. In the symmetric limit, the mass eigenvalues are assumed to follow one of the patterns in table 2.1, which means that a certain number of them are assumed to be zero (possibly none) and that groups of non-zero masses may be assumed to be degenerate. In full generality, the mass eigenvalues (for both the charged leptons and neutrinos) can then be written in the form

$$(m_1 \dots m_n) = (\overbrace{0 \dots 0}^{d_0} \quad \overbrace{a_1 \dots a_1}^{d_1} \quad \dots \quad \overbrace{a_N \dots a_N}^{d_N}), \tag{2.5}$$

corresponding to a group of d_0 vanishing masses and N groups of degenerate masses, with multiplicities $d_1 \dots d_N$. In the cases in tables 2.2, 2.3, there is at most one group of degenerate eigenvalues in the neutrino sector, with multiplicity 2 or 3. The values of $a_1 \dots a_N$ can happen to vanish or to be equal to each other. This situation is not generic,

though. In a generic set of mass eigenvalues, $a_1 \dots a_N$ are non-zero and all different from each other.

The results in tables 2.2, 2.3 are obtained using the following facts. Consider a given mass pattern, in which charged lepton and neutrino masses are both in the form eq. (2.5) (with different multiplicities $d_0^E \dots d_{N_E}^E$, $d_0^\nu \dots d_{N_\nu}^\nu$). Then:

- Each subspace in flavour space associated to (zero or non-zero) degenerate charged lepton masses is invariant under both the representations U_l and U_{e^c}. We can then call $U_0^l \dots U_{N_E}^l$ and $U_0^{e^c} \dots U_{N_E}^{e^c}$ the representations on those subspaces.
- The representations corresponding to non-zero charged lepton masses, $U_1^l \dots U_{N_E}^l$ and $U_1^{e^c} \dots U_{N_E}^{e^c}$, are conjugated to each other and irreducible.
- The representations U_0^l and $U_0^{e^c}$ corresponding to the set of vanishing masses can be reducible. None of the irreps on which $U_0^{e^c}$ decomposes is conjugated to any of the irreps on which U_0^l decomposes.

The neutrino mass pattern gives further constraints on U_l:

- Each set of d^ν degenerate non-vanishing neutrino masses must correspond to either a real irrep $r = \bar{r}$ of dimension d^ν; or to a pair of conjugated (Dirac) complex irreps $r + \bar{r}$ of total even dimension d^ν; or to a pair of equivalent pseudoreal irreps $r + r$ with total dimension d^ν multiple of four (case hence not relevant with three neutrinos).
- The remaining irreps in U_l must correspond to the vanishing neutrino masses, and therefore their total dimension should be d_0^ν. Moreover, none of them is real, none of the complex ones is conjugated to any other, and none of the pseudoreal ones is equivalent to any other.

To illustrate how the above remarks lead to the results in tables 2.2, 2.3, let us consider a few examples. Let us first consider the mass pattern (A, B, C) for the charged leptons and (a, b, c) for the neutrinos. As we have three different non-vanishing charged lepton masses, U_l must decompose into 3 one-dimensional irreps and U_{e^c} into the three conjugated ones. As we have three different non-vanishing neutrino masses, the three one-dimensional representations in which U_l decomposes must be real. Depending on whether the three real irreps are equivalent or not, we find the three cases listed in table 2.3. The last case, corresponding to $U_l \sim U_{e^c} \sim 1+1+1$, is trivial. In fact, a real one-dimensional representation can only take the values ± 1. A $1+1+1$ representation can then only be trivial or an overall sign change, thus providing no constraint on m_E, m_ν. A less trivial example is $(A, 0, 0)$ (charged leptons) and (a, b, b) (neutrinos). The charged lepton mass pattern requires U_l to contain a one dimensional irrep corresponding to the non-vanishing mass and a possibly reducible two-dimensional representation corresponding to the two vanishing masses. The neutrino mass pattern requires a one dimensional real irrep, "1",

together with either a two dimensional real irrep, "2", or the sum of a one dimensional complex representation and its conjugated, "$\mathbf{1}+\overline{\mathbf{1}}$". We therefore have either $U_l \sim 1+2$ or $U_l \sim 1+\mathbf{1}+\overline{\mathbf{1}}$. In the first case, the irrep "1" must correspond to the non-zero charged lepton mass (the tau mass) and "2" must correspond to the two zero charged lepton masses (electron and muon masses). The representation U_{e^c} must then be in the form $1+r$, where r is a possibly reducible representation not equivalent to the irrep "2". In the second case, the irrep in U_l corresponding to the tau mass can either be the real one or one of the complex ones ($\mathbf{1}$, without loss of generality). The forms of U_{e^c} shown in table 2.2 follows. As a final example, consider the case in which the three neutrino masses are degenerate. The only possibility is that U_l be a three dimensional real irrep. However, if that was the case, the three charged lepton masses would be forced to be degenerate, which is not a viable mass pattern (unless the masses are all vanishing, a case considered in section 2.3). There are therefore no possible groups and representations realising such a case in the symmetric limit. All the other cases in tables 2.2, 2.3 can be analysed in similar ways.

It is now evident that the results in tables 2.2, 2.3 depend on the flavour group G and on its representations U_l, U_{e^c} on the leptons only through the structure of the decomposition of U_l, U_{e^c} into irreducible components, and more precisely only on i) the dimensions of the irreps (the numbers denoting them in the table), ii) the possible equivalence or conjugation of the different components (conjugation is denoted by a bar over the representation, inequivalent irreps are distinguished by primes), and iii) whether the representation is complex/pseudoreal (boldface) or real (plain). The results show in particular that ($m_E^{(0)} \neq 0$, $m_\nu^{(0)} \neq 0$), i) the patterns with three degenerate non-vanishing neutrinos in the symmetric limit cannot be forced by any flavour group; ii) dimension 3 irreps are not involved in forcing any of the mass patterns we considered; iii) dimension 2 irreps can be contained in U_{e^c} if, in the symmetric limit, $m_e = m_\mu = 0$; in U_l if, in addition to that, $m_{\nu_1} = m_{\nu_2}$; iv) pseudoreal irreps can only play a role in U_{e^c} if, in the symmetric limit, $m_e = m_\mu = 0$; in U_l if, in addition to that, $m_{\nu_1} = m_{\nu_2} = 0$.

2.2.2 Accounting for lepton mixings

We have found so far the possible irrep decompositions leading, in the symmetric limit, to a reasonable approximation for the lepton masses. We now want to select those among them that also lead to a reasonable approximation for the PMNS matrix. As we will see, the form of the PMNS matrix only depends on the structure of the irrep decompositions, and can be determined in terms of the latter with simple rules that do not require the explicit construction of the mass matrices nor their diagonalization. We will present in this section the results and leave the proofs to the appendix A.

lepton masses		decompositions of U_l and U_{e^c}				
$(A00)$	(aaa)	none				
$(A00)$	(abb)	$\mathbf{1}\ \ \overline{\mathbf{1}}\ \ 1$	$1\ \ \mathbf{1}\ \ \overline{\mathbf{1}}$	$1\ \ 2$		
		$\overline{\mathbf{1}}\ \ r \not\supset 1, \mathbf{1}$	$1\ \ r \not\supset \overline{\mathbf{1}}, \mathbf{1}$	$1\ \ r \neq 2$		
$(A00)$	$(0aa)$	$\mathbf{1}\ \ \mathbf{1}'\ \ \overline{\mathbf{1}}$	$\mathbf{1}'\ \ \mathbf{1}\ \ \overline{\mathbf{1}}$	$\mathbf{1}\ \ \mathbf{1}\ \ \overline{\mathbf{1}}$	$\overline{\mathbf{1}}\ \ \mathbf{1}\ \ \mathbf{1}$	$\mathbf{1}\ \ 2$
		$\overline{\mathbf{1}}\ \ r \not\supset \mathbf{1}, \overline{\mathbf{1}'}$	$\overline{\mathbf{1}}'\ \ r \not\supset \mathbf{1}, \overline{\mathbf{1}}$	$\overline{\mathbf{1}}\ \ r \not\supset \mathbf{1}, \overline{\mathbf{1}}$	$\mathbf{1}\ \ r \not\supset \overline{\mathbf{1}}$	$\overline{\mathbf{1}}\ \ r \neq 2$
$(A00)$	$(a00)$	$1\ \ \mathbf{1}\ \ \mathbf{1}'$	$\mathbf{1}\ \ \mathbf{1}'\ \ 1$	$1\ \ \mathbf{1}\ \ \mathbf{1}$	$\mathbf{1}\ \ \mathbf{1}\ \ 1$	$1\ \ \mathbf{2}$
		$1\ \ r \not\supset \overline{\mathbf{1}}, \overline{\mathbf{1}'}$	$\overline{\mathbf{1}}\ \ r \not\supset 1, \overline{\mathbf{1}'}$	$1\ \ r \not\supset \overline{\mathbf{1}}$	$\overline{\mathbf{1}}\ \ r \not\supset 1, \overline{\mathbf{1}}$	$1\ \ r \not\supset \overline{\mathbf{2}}$
$(A00)$	(abc)	$1\ \ 1'\ \ 1''$	$1\ \ 1\ \ 1'$	$1'\ \ 1\ \ 1$	$1\ \ 1\ \ 1$	
		$1\ \ r \not\supset 1', 1''$	$1\ \ r \not\supset 1, 1'$	$1'\ \ r \not\supset 1$	$1\ \ r \not\supset 1$	
$(A00)$	$(ab0)$	$1\ \ 1'\ \ \mathbf{1}$	$\mathbf{1}\ \ 1'\ \ 1$	$\mathbf{1}\ \ 1\ \ 1$	$1\ \ 1\ \ \mathbf{1}$	
		$1\ \ r \not\supset 1', \overline{\mathbf{1}}$	$\overline{\mathbf{1}}\ \ r \not\supset 1, 1'$	$\overline{\mathbf{1}}\ \ r \not\supset 1$	$1\ \ r \not\supset 1, \overline{\mathbf{1}}$	

Table 2.2: Possible decompositions of U_l (above) and U_{e^c} (below) into irreducible components (part I). Each line corresponds to a combination of the charged lepton and neutrino mass patterns in the first two columns of table 2.1. Only the charged lepton pattern $(A00)$, which does not require hierarchies among non-zero entries, is considered here. Irreps are denoted by their dimensions. Boldface fonts denote complex or pseudoreal (if 2-dimensional) representations, regular fonts denote real representations. Primes are used to distinguish inequivalent representations, and in the case of complex representations $\mathbf{1}'$ is supposed to be different from both $\mathbf{1}$ and $\overline{\mathbf{1}}$. "r" denotes a generic, possibly reducible representation, different from or not including the specified irreps, as indicated.

The form of the PMNS matrix $U_{\rm PMNS}$ associated to a given irrep decompositions of U_l and U_{e^c} in the symmetric limit, is

$$U_{\rm PMNS} = H_E P_E V D^{-1} P_\nu^{-1} H_\nu^{-1} \,. \tag{2.6}$$

The contributions to $U_{\rm PMNS}$ on the right hand side have different origins and different physical meanings. Each of them can be obtained without the need of writing explicitly nor diagonalising the lepton mass matrices, with the following rules.

- First, it is useful to order the irreps in such a way that those in U_l, U_{e^c} that are conjugated to each other appear last and in the same position in the list. This way the vanishing charged lepton masses will appear first in the list of eigenvalues. For example, in one of the cases in table 2.3, we could have $U_l = \mathbf{1} + \mathbf{1} + \overline{\mathbf{1}}$, $U_{e^c} = (r \neq \overline{\mathbf{1}}) + \overline{\mathbf{1}} + \mathbf{1}$. Correspondingly, we write a list of generic charged lepton

lepton masses		decompositions of U_l and U_{e^c}			
(ABC)	(aaa)	none			
(ABC)	(abb)	$1\ \ \mathbf{1}\ \ \overline{\mathbf{1}}$			
		$1\ \ \overline{\mathbf{1}}\ \ \mathbf{1}$			
(ABC)	$(0aa)$	$\mathbf{1}\ \ \mathbf{1'}\ \ \overline{\mathbf{1}}$	$\mathbf{1}\ \ \mathbf{1}\ \ \overline{\mathbf{1}}$		
		$\overline{\mathbf{1}}\ \ \overline{\mathbf{1'}}\ \ \mathbf{1}$	$\overline{\mathbf{1}}\ \ \overline{\mathbf{1}}\ \ \mathbf{1}$		
(ABC)	$(a00)$	$1\ \ \mathbf{1}\ \ \mathbf{1'}$	$1\ \ \mathbf{1}\ \ \mathbf{1}$		
		$1\ \ \overline{\mathbf{1}}\ \ \overline{\mathbf{1'}}$	$1\ \ \overline{\mathbf{1}}\ \ \overline{\mathbf{1}}$		
(ABC)	(abc)	$1\ \ 1'\ \ 1''$	$1\ \ 1\ \ 1'$	$1\ \ 1\ \ 1$	
		$1\ \ 1'\ \ 1''$	$1\ \ 1\ \ 1'$	$1\ \ 1\ \ 1$	
(ABC)	$(ab0)$	$1\ \ 1'\ \ \mathbf{1}$	$1\ \ 1\ \ \mathbf{1}$		
		$1\ \ 1'\ \ \overline{\mathbf{1}}$	$1\ \ 1\ \ \overline{\mathbf{1}}$		
$(AB0)$	(aaa)	none			
$(AB0)$	(abb)	$\mathbf{1}\ \ \overline{\mathbf{1}}\ \ 1$	$1\ \ \mathbf{1}\ \ \overline{\mathbf{1}}$		
		$\overline{\mathbf{1}}\ \ \mathbf{1}\ \ r \neq 1$	$1\ \ \overline{\mathbf{1}}\ \ r \neq \mathbf{1}$		
$(AB0)$	$(0aa)$	$\overline{\mathbf{1}}\ \ \mathbf{1}\ \ \mathbf{1'}$	$\mathbf{1}\ \ \mathbf{1'}\ \ \overline{\mathbf{1}}$	$\mathbf{1}\ \ \mathbf{1}\ \ \overline{\mathbf{1}}$	$\overline{\mathbf{1}}\ \ \mathbf{1}\ \ \mathbf{1}$
		$\mathbf{1}\ \ \overline{\mathbf{1}}\ \ r \neq \overline{\mathbf{1'}}$	$\overline{\mathbf{1}}\ \ \overline{\mathbf{1'}}\ \ r \neq \mathbf{1}$	$\overline{\mathbf{1}}\ \ \overline{\mathbf{1}}\ \ r \neq \mathbf{1}$	$\mathbf{1}\ \ \overline{\mathbf{1}}\ \ r \neq \overline{\mathbf{1}}$
$(AB0)$	$(a00)$	$1\ \ \mathbf{1}\ \ \mathbf{1'}$	$\mathbf{1}\ \ \mathbf{1'}\ \ 1$	$1\ \ \mathbf{1}\ \ \mathbf{1}$	$\mathbf{1}\ \ \mathbf{1}\ \ 1$
		$1\ \ \overline{\mathbf{1}}\ \ r \neq \overline{\mathbf{1'}}$	$\overline{\mathbf{1}}\ \ \overline{\mathbf{1'}}\ \ r \neq 1$	$1\ \ \overline{\mathbf{1}}\ \ r \neq \overline{\mathbf{1}}$	$\overline{\mathbf{1}}\ \ \overline{\mathbf{1}}\ \ r \neq 1$
$(AB0)$	(abc)	$1\ \ 1'\ \ 1''$	$1\ \ 1\ \ 1'$	$1'\ \ 1\ \ 1$	$1\ \ 1\ \ 1$
		$1\ \ 1'\ \ r \neq 1''$	$1\ \ 1\ \ r \neq 1'$	$1'\ \ 1\ \ r \neq 1$	$1\ \ 1\ \ r \neq 1$
$(AB0)$	$(ab0)$	$1\ \ 1'\ \ \mathbf{1}$	$1\ \ \mathbf{1}\ \ 1'$	$1\ \ 1\ \ \mathbf{1}$	$\mathbf{1}\ \ 1\ \ 1$
		$1\ \ 1'\ \ r \neq \overline{\mathbf{1}}$	$1\ \ \overline{\mathbf{1}}\ \ r \neq 1'$	$1\ \ 1\ \ r \neq \overline{\mathbf{1}}$	$\overline{\mathbf{1}}\ \ 1\ \ r \neq 1$

Table 2.3: Possible decompositions of U_l (above) and U_{e^c} (below) into irreducible components (part II). Each line corresponds to a combination of the charged lepton and neutrino mass patterns in the first two lines of table 2.1. The charged lepton patterns (ABC) and $(AB0)$ are considered here, which require hierarchies among the non-zero entries. Irreps are denoted by their dimensions. Boldface fonts denote complex representations, regular fonts denote real representations. Primes are used to distinguish inequivalent representations, and in the case of complex representations $\mathbf{1'}$ is supposed to be different from both $\mathbf{1}$ and $\overline{\mathbf{1}}$. "r" denotes a generic, possibly reducible representation, different from or not including the specified irreps, as indicated.

eigenvalues with the non-vanishing eigenvalues corresponding to the conjugated representations. In the example above, the list would be $(0, B, A)$.[4]

- V is a generic unitary transformation commuting with U_l, with $\mathcal{O}(1)$ entries. Its origin is associated to the presence of equivalent copies of the same irrep type in the decomposition of U_l. If all the irrep components are inequivalent, V is trivial. For example, if $U_l = \mathbf{1} + \mathbf{1} + \overline{\mathbf{1}}$, V is a 2×2 unitary transformation in the 12 block.

- D is associated to the possible presence of a Dirac sub-structure in the neutrino mass matrix, and it originates from the presence of complex conjugated irreps within the decomposition of U_l. In the three neutrino case, there are only two possibilities. Either U_l does not contain pairs of complex conjugated irreps, in which case D is trivial, $D_{ij} = \delta_{ij}$. Or there is one pair of one-dimensional complex conjugated representations, in the positions i and j in the list of irreps, in which case D is a maximal 2×2 rotation,

$$D_2 = \frac{1}{\sqrt{2}} \begin{pmatrix} 1 & 1 \\ -i & i \end{pmatrix}, \tag{2.7}$$

  embedded in the ij block. The corresponding mass eigenvalues are degenerate (both positive due to the imaginary unit in D_2, contributing to the Majorana phases). Correspondingly, we write the list of neutrino eigenvalues as follows. If a pair of conjugated irreps is present in U_l in the positions i and j, we have two degenerate non-vanishing eigenvalues in the corresponding positions. We then have a non-vanishing eigenvalue in the position corresponding to each real representation. If the real irrep has dimension $d > 1$, there will be d degenerate eigenvalues. Finally, we have a vanishing eigenvalue corresponding to each unmatched complex representation. In the previous example, with $U_l = \mathbf{1} + \mathbf{1} + \overline{\mathbf{1}}$, we can equivalently choose the two conjugated representations to be the ones in the positions $ij = 23$ or those in the positions $ij = 13$. Such a choice will determine the positions i and j of the corresponding two degenerate neutrino masses in the list of eigenvalues (before the reordering below). So if we choose $ij = 23$, we will have the 2×2 block in eq. (2.7) embedded in the 23 block of the matrix D and the list of neutrino eigenvalues will be in the form $(0aa)$.

- The permutation matrices P_E and P_ν are associated to the possible need of reordering the list of eigenvalues. Indeed, the list of eigenvalues obtained with the above rules is not necessarily in the standard ordering, required for a proper definition of the PMNS matrix. In the example we have considered, the list of charged lepton eigenvalues is $(0, B, A)$. The masses are in standard ordering if $B < A$. On the other hand, if $B > A$, the standard ordering is obtained by switching A and B. Correspondingly, P_E is either the identity or a permutation matrix switching $2 \leftrightarrow 3$. As for the neutrinos, the list of eigenvalues is in the form $(0aa)$. The standard ordering

[4] Note that in the tables, for convenience, the three families appear in inverse order: (3,2,1).

requires the two degenerate eigenvalues to be in the first two positions. Therefore, P_ν is a permutation matrix moving the first entry in the third position.

- Finally, the role of H_e, H_ν is to take into account possible ambiguities in the definition of the PMNS matrix in the symmetric limit. In the real world, all leptons are non-degenerate and the PMNS matrix only has unphysical phase ambiguities, which do not need to be taken into account. When considering the symmetric limit, on the other hand, larger ambiguities can arise due to degenerate, possibly vanishing, masses. In practice, H_E is a generic unitary transformation mixing the massless charged leptons; and H_ν contains a generic unitary transformation mixing the massless neutrinos and a generic orthogonal transformation mixing degenerate massive neutrinos (it turns out, however, that the latter can be ignored if the degeneracy is due to a Dirac structure, in which case it can be reabsorbed into a phase redefinition of V). As discussed in the appendix A, the H_e, H_ν contributions to the PMNS matrix have a different physical nature than the previous ones. They are unphysical, and undetermined, in the symmetric limit. However, they become physical (up to diagonal phases) after symmetry breaking effects split the degenerate mass eigenstates. Depending on the specific form of the symmetry breaking effects, H_e and H_ν can end up being large, small, or zero (unlike the previous contributions, which are determined by the non-zero entries and are large in the absence of accidental correlations [128]).

With the above rules, we can determine the form of the PMNS matrix associated to each irrep pattern in tables 2.2, 2.3 and select the cases leading to a PMNS matrix with no zeros or a zero in the 13 position. The results are illustrated in table 2.4.

As shown, there is a limited number of cases leading, in the symmetric limit, to lepton observables close to what observed. Each case corresponds to a certain decomposition of the flavour representations in terms of real and complex, equivalent and inequivalent representations of given dimension. Each pattern may correspond to different flavour groups and representations, provided that the decomposition of the representation on the leptons follows that pattern. The allowed patterns contain one-dimensional irreps only. Pseudoreal representations do not play a role.

Three out of the six cases in the table are partially trivial. Those are the cases in which $U_l \sim 1+1+1$, for which the representation on the lepton doublets is either the identity representation or an overall sign change. In such a case, the neutrino mass matrix is not constrained at all, and the neutrino masses and PMNS matrix are expected to be completely generic. In particular, the relative smallness of $|(U_{\rm PMNS})_{13}|$ is accidental. We are in the presence of "anarchical" neutrinos [129, 130]. The only constraints that can be obtained are on the charged lepton masses, through the interplay of the trivial U_l with a non-trivial U_{e^c}.

The other three cases provide non-trivial constraints on neutrino masses and mixings. An important result is that they all correspond to inverted neutrino hierarchy, and

irreps	masses	ν hierarchy	H_E P_E V D P_ν H_ν	$U_{\rm PMNS}$	zeros
$1\quad 1\quad 1$ $1\quad r\not\simeq 1$	$(A00)$ (abc)	NH or IH	V	V	none
$\mathbf{1}\quad \mathbf{1}\quad \overline{\mathbf{1}}$ $\overline{\mathbf{1}}\quad r\not\simeq \mathbf{1},\overline{\mathbf{1}}$	$(A00)$ $(0aa)$	IH	H_{12}^E V_{23} D_{12}	$H_{12}^E V_{23} D_{12}^{-1}$	none (**13**)
$1\quad 1\quad 1$ $1\quad 1\quad r\neq 1$	$(AB0)$ (abc)	NH or IH	V	V	none
$\mathbf{1}\quad \mathbf{1}\quad \overline{\mathbf{1}}$ $\overline{\mathbf{1}}\quad \overline{\mathbf{1}}\quad r\neq \mathbf{1}$	$(AB0)$ $(0aa)$	IH	V_{23} D_{12}	$V_{23} D_{12}^{-1}$	**13**
$1\quad 1\quad 1$ $1\quad 1\quad 1$	(ABC) (abc)	NH or IH	V	V	none
$\mathbf{1}\quad \mathbf{1}\quad \overline{\mathbf{1}}$ $\overline{\mathbf{1}}\quad \overline{\mathbf{1}}\quad \mathbf{1}$	(ABC) $(0aa)$	IH	P_E V_{23} D_{12}	$P_E V_{23} D_{12}^{-1}$	**13**, 23, 33

Table 2.4: Irrep decompositions giving rise to a PMNS matrix with no zeros or a single zero possibly in the 13 entry. The first column shows the decomposition of U_l and U_{e^c}, one above the other. Only real and complex irreps appear. The second column shows the corresponding pattern of charged lepton and neutrino masses in the symmetric limit, one above the other, and the third column contains the neutrino hierarchy type, normal (NH) or inverted (IH). The individual contributions to the PMNS matrix are then shown. A matrix with no further specification is generic (e.g. P denotes a generic permutation, V a generic unitary matrix). D_{ij} denotes a $\pi/4$ rotation in the generic form in eq. (2.7) acting in the sector ij. If no information on a certain factor is given, that factor is irrelevant (for example because diagonal or because it can be reabsorbed in another factor). The presence and position of a zero in the PMNS matrix in the symmetric limit is specified in the last column.

specifically to two degenerate and one vanishing neutrino mass in the symmetric limit. Therefore, if the present hint favouring a normal hierarchy were confirmed, we would conclude, within our assumptions, that either the flavour model is not predictive at all in the neutrino sector, or the symmetric limit does not provide an approximate description of lepton masses and mixings. In the latter case, we might have to resort to a caveat in our assumptions (see conclusions) or to the case where all charged lepton or all neutrino masses vanish in the symmetric limit (last column of table 2.1), and symmetry breaking effects are crucial to understand even the basic features of lepton mixing.

Table 2.4 is divided in two parts. In the first part, the hierarchy of the charged lepton masses is naturally accommodated by the vanishing of the two lighter masses in the symmetric limit, in agreement with the principle that hierarchies should be explained by the flavour model. In the second part, hierarchies not accounted for by the flavour theory have to be invoked among the non-zero entries in order to account for the structure of charged lepton masses. The second case in the first part of the table is special, as the

size of the 13 element of the PMNS matrix is determined by the rotation H_{12}^E, which is not physical in the symmetric limit, and will be fixed by the symmetry breaking effects generating the muon mass. Depending on the structure of those effects, the size of $(U_{\rm PMNS})_{13}$ can end up being large, small, or zero. Finally, note that since the parameters entering all the mixing matrices in table 2.4 except D are generic, a specific value of a mixing angle can be obtained only when the matrix D is involved. As the table shows, D can only play a role in the 12 mixing, in agreement with earlier specific results [20].

In the next subsection, we shortly illustrate a few examples of specific flavour groups and representations corresponding to the patterns in table 2.4.

2.2.3 Examples

The results above have been obtained without the need to specify the form of the lepton mass matrices, as they directly followed from the structure of the irrep decompositions. Moreover, there was no need to specify a flavour group or its representation on leptons, as the results hold for any group, of any type, as long as the decompositions of its representations have the structure shown in the tables. In the following, for completeness and as proofs of existence, we will provide examples, in some cases well known, of explicit realisations of the three cases in table 2.4 leading to a PMNS matrix with a (possible) zero in the 13 position in the symmetric limit. All of them require a continuous or discrete symmetry group G with a complex one-dimensional representation $\mathbf{1}$, and a representation on the lepton doublets decomposing as $U_l = \mathbf{1} + \mathbf{1} + \overline{\mathbf{1}}$.

$U_l = \mathbf{1} + \mathbf{1} + \overline{\mathbf{1}}$, $U_{e^c} = \overline{\mathbf{1}} + (r \not\supseteq \mathbf{1}, \overline{\mathbf{1}})$

In this case, corresponding to the second row in table 2.4, the representation on the lepton singlets decomposes into a copy of $\overline{\mathbf{1}}$ and a (possibly reducible) two dimensional representation r whose only requirement is not to contain either $\mathbf{1}$ or $\overline{\mathbf{1}}$ (r could be for example the trivial representation). In the symmetric limit, two charged leptons are forced to be massless, which explains the suppression of the electron and muon mass compared to the tau mass, and the neutrino spectrum turns out to be inverted hierarchical, with $m_3 = 0$ and $m_1 = m_2$. With the notations used in table 2.4, we thus have

$$(m_\tau, m_\mu, m_e) = (A, 0, 0), \qquad (m_{\nu_3}, m_{\nu_2}, m_{\nu_1}) = (0, a, a). \tag{2.8}$$

A non-vanishing value of m_e, m_μ must then be generated by the symmetry breaking effects, which will also give $m_3 \ll m_1 \approx m_2$.

The PMNS matrix does not necessarily have a zero, as it is obtained from the combination of 3 rotations: V_{23}, the $\mathcal{O}(1)$ rotation in the 23 sector commuting with U_l; a maximal 12 rotation D_{12} associated with the Dirac substructure in m_ν forced by U_l; and a rotation H_{12}^E in the 12 sector, associated to the degeneracy of the first two charged leptons and not determined in the symmetric limit. The latter is fixed by the symmetry

breaking effects generating the muon and electron masses. If the H_{12}^E is large, the PMNS matrix is expected not to have any small entry. On the other hand, in the light of the hierarchy $m_e \ll m_\mu$, one can expect H_{12}^E, and consequently $(U_{\rm PMNS})_{13}$, to be relatively small [131–142]. The PMNS matrix thus reads

$$U_{\rm PMNS} = H_{12}^E V_{23} D_{12}^{-1} = \begin{pmatrix} X & X & ? \\ X & X & X \\ X & X & X \end{pmatrix}, \tag{2.9}$$

where X denotes a non-zero entry, not further constrained, and the size of the 13 entry depends on H_{12}^E, as discussed. The form of lepton mass matrices in the symmetric limit is

$$m_E = \begin{pmatrix} & & \\ & & \\ & X & X \end{pmatrix}, \qquad m_\nu = \begin{pmatrix} & X & X \\ X & & \\ X & & \end{pmatrix}. \tag{2.10}$$

It is easy to exhibit an example of a group G and representations U_l, U_{e^c} with a decomposition in irreps as above. An easy choice is $G = U(1)$, with $\omega \in U(1)$ represented by

$$U_l(\omega) = \begin{pmatrix} \omega^* & & \\ & \omega & \\ & & \omega \end{pmatrix}, \quad U_{e^c}(\omega) = \begin{pmatrix} \omega^q & & \\ & \omega^p & \\ & & \omega^* \end{pmatrix}, \tag{2.11}$$

where $p, q \neq \pm 1$. For example, one can choose $p = q = 0$ (trivial representation). A minimal possibility involving a discrete group is $G = \mathbf{Z}_3$, with the same representation of $\omega \in \mathbf{Z}_3$ and $p = q = 0$ as the only possible choice. Any other discrete subgroup of $U(1)$, different from $\mathbf{Z}_2$ would of course also work. It is also possible to realize this case by using the one dimensional representations of non-abelian discrete groups, such as A_4 for example.

$U_l = \mathbf{1} + \mathbf{1} + \overline{\mathbf{1}}$, $U_{e^c} = \overline{\mathbf{1}} + \overline{\mathbf{1}} + (r \neq \mathbf{1})$

In this case, corresponding to the fourth row in table 2.4, the representation on the lepton singlets decomposes into two copies of $\overline{\mathbf{1}}$ and a one dimensional representation r inequivalent to $\mathbf{1}$. In the symmetric limit, one charged lepton is forced to be massless, which explains the suppression of the electron mass compared to the muon and tau masses, but not the hierarchy $m_\mu \ll m_\tau$, and the neutrino spectrum turns out to be inverted hierarchical as before,

$$(m_\tau, m_\mu, m_e) = (A, B, 0), \qquad (m_{\nu_3}, m_{\nu_2}, m_{\nu_1}) = (0, a, a). \tag{2.12}$$

The PMNS matrix contains a zero, unambiguously positioned in the 13 entry. It is obtained from the combination of 2 rotations: V_{23}, the $\mathcal{O}(1)$ rotation in the 23 sector commuting with U_l, and a maximal 12 rotation D_{12}. Unlike the previous case, the form

of the PMNS matrix is determined in the symmetric limit up to phase ambiguities only. The forms of the PMNS matrix and of the lepton mass matrices in the symmetric limit are given by

$$\begin{aligned} U_{\rm PMNS} &= V_{23} D_{12}^{-1} = \begin{pmatrix} X & X & 0 \\ X & X & X \\ X & X & X \end{pmatrix}, \\ m_E &= \begin{pmatrix} & & \\ & X & X \\ & X & X \end{pmatrix}, \quad m_\nu = \begin{pmatrix} & X & X \\ X & & \\ X & & \end{pmatrix}. \end{aligned} \tag{2.13}$$

A simple implementation of this case can be obtained from the previous one by modifying the way the group acts on μ^c. For $G = U(1)$, we can in fact represent $\omega \in U(1)$ by

$$U_l(\omega) = \begin{pmatrix} \omega^* & & \\ & \omega & \\ & & \omega \end{pmatrix}, \quad U_{e^c}(\omega) = \begin{pmatrix} \omega^q & & \\ & \omega^* & \\ & & \omega^* \end{pmatrix}, \tag{2.14}$$

where $q \neq 1$, for example $q = 0$. As before, abelian or non-abelian discrete groups can also be used. For example, for the group $G = \mathbf{Z}_3$, $q = 0$ and $q = 2$ are the only possible choices, and $G = A_4$ also works with its one dimensional representations.

$U_l = \mathbf{1} + \mathbf{1} + \overline{\mathbf{1}}$, $U_{e^c} = \overline{\mathbf{1}} + \overline{\mathbf{1}} + \mathbf{1}$

This case, corresponding to the sixth row in table 2.4, has a particularly well known implementation: $G = U(1)$ acting on leptons according to their $L_\tau + L_\mu - L_e$ charge [143–148]. The disadvantage of this case is that, whatever is the implementation, none of the charged lepton hierarchies, $m_e \ll m_\mu \ll m_\tau$, is explained by the model. The neutrino spectrum is inverted hierarchical, as before, and with the notations used in table 2.4 we have

$$(m_\tau, m_\mu, m_e) = (A, B, C), \qquad (m_{\nu_3}, m_{\nu_2}, m_{\nu_1}) = (0, a, a). \tag{2.15}$$

Another disadvantage is that the PMNS matrix does contain a zero, but the model does not explain why it appears in the 13 entry, as in principle it could also appear in the 23 or 33 entry. This is because the permutation P_E in eq. (2.6), sorting the charged leptons in the standard order, is generic in this case. In other words, the symmetry does force the eigenvalue positioned where the electron should be to be the lightest, and a viable symmetric limit for the PMNS matrix is obtained only in that case, i.e. when the smallest eigenvalue happens to correspond to the lepton transforming as $\overline{\mathbf{1}}$ under U_l. In such a case, the PMNS matrix and the lepton mass matrices in the symmetric limit are

in the form

$$
\begin{aligned}
U_{\rm PMNS} &= P_E V_{23} D_{12}^{-1} = \begin{pmatrix} X & X & 0 \\ X & X & X \\ X & X & X \end{pmatrix}, \\
m_E &= \begin{pmatrix} X & & \\ & X & X \\ & X & X \end{pmatrix}, \quad m_\nu = \begin{pmatrix} & X & X \\ X & & \\ X & & \end{pmatrix}.
\end{aligned}
\tag{2.16}
$$

Examples of the viable flavour symmetries can easily be achieved by the similar way as in the two cases discussed above.

In all of those three cases, U_l is decomposed into three one-dimensional representations and U_{e^c} is not allowed to have a three-dimensional representation, but it can contain a two dimensional representation when two lightest charged leptons are massless in the symmetric limit. In fact, the very role of the two-dimensional representation is to forbid the masses of first two charged leptons through its interplay with the inequivalent representation on the lepton doublets.

We can also consider other cases in which the PMNS matrix has no zero entry in the symmetric limit and the relative smallness of the 13 element is accidental. In such cases, the only purpose of the flavour symmetry might be to enforce the smallness of the electron and possibly the muon mass, while allowing the form of PMNS matrix is arbitrary (in these cases any 3×3 unitary matrix is allowed PMNS). As was shown in table 2.4, these cases require three lepton doublets to be transformed under the same real one-dimensional representation. So there are only two possibilities: either all the lepton doublets are invariant under G, or they transform with a $\mathbf{Z}_2$ changing sign to all of them. The tau lepton mass is always non-vanishing, other charged leptons (electron or muon) have masses in the symmetric limit if lepton singlets transform in the same way as the corresponding lepton doublets, they are massless when lepton singlets and doublets transform differently.

2.3 Lepton mixing from symmetry breaking effects

We will now consider the cases in which all neutrinos or all charged lepton masses vanish in the symmetric limit ($m_E^{(0)} = 0$ or $m_\nu^{(0)} = 0$ in eq. (2.1)), i.e. the cases associated to the last column in table 2.1. In such cases, the sole knowledge of the flavour group and its representation is not sufficient to account for any of the features of lepton mixing, as the PMNS matrix is completely undetermined (unphysical) in the symmetric limit, with its final form fully depending on the symmetry breaking effects.

As symmetry breaking effects are now central, let us consider not only the flavour group G and its representations on the leptons, here denoted by U_l^G and $U_{e^c}^G$, but also the residual group H to which G is spontaneously broken, and its representations on

leptons U_l^H and $U_{e^c}^H$, which are simply the restriction to H of U_l^G and $U_{e^c}^G$. If G is fully broken, the residual group H only contains the identity, and its representations are trivial. Symmetry breaking can take place in more than one step, $G \to H_1 \to \ldots \to H_n$, associated to different scales. In such a case, our results will correspond to the first step of the breaking chain, $H = H_1$, and the corresponding breaking effects will only provide a leading order prediction for the lepton observables, as the contribution of the subsequent steps may be needed to precisely fit them.

We want to characterise the forms of U_l^G and $U_{e^c}^G$ and U_l^H and $U_{e^c}^H$ leading, once G is broken (but H is not), to a pattern of lepton masses and mixing not far from what observed.

Such a problem does not admit a general answer as simple as the one obtained in the previous section. The reason is that the final pattern of lepton observables does not only depend on G, H, U^G, U^H, but it also depends on the specific spectrum of flavons and their vevs (and the scalar potentials determining the vevs). On the other hand, it turns out that a simple answer can be obtained if the following (non-trivial) hypothesis holds: the symmetry breaking corrections, $m_E^{(1)}$, $m_\nu^{(1)}$ in eq. (2.1), have the most general form allowed by the residual symmetry H, with all non-vanishing entries of the same order. Needless to say, neither neutrino nor charged lepton masses should identically vanish after symmetry breaking. In such a case, it turns out that the formalism developed and the results obtained in the previous sections on the possible structures of U^G can be simply reinterpreted in terms of the possible structures of U^H, as we will see below.

The hypothesis we introduced is non-trivial. It amounts at assuming that the lepton observables only depend on the symmetry breaking pattern $G \to H$ and not on the specific breaking mechanism used. This is not the case in most models found in the literature, in which the flavour structure is rather associated to the specific choice of the flavon spectrum, to their coupling to the leptons, and to the form of their vevs. This is the case for example in models where the residual symmetry H is different in the neutrino and charged lepton sectors; and even in the case of U(1) models, in which $H = \{1\}$, all entries are allowed by H, but they typically turn out to be of different sizes, depending on how many powers of the flavons are needed to generated them. Still, the results we will get under the above hypothesis are useful for a complete assessment of the importance of a detailed knowledge of the symmetry breaking mechanism.

Let us motivate the result mentioned above. Suppose, as we do, that G is spontaneously broken to H, that either the charged lepton or the neutrino masses (not both) vanish in the G-symmetric limit, and that, after spontaneous breaking, we obtain a mass pattern close to what observed, i.e. in one of the forms listed in the first two columns of table 2.1. The knowledge of the mass pattern after symmetry breaking allows us to constrain U^H. The possible structures of the irrep decomposition of the representation U^H are in fact listed, for each mass pattern, in tables 2.2, 2.3, where U_l and U_{e^c} should now be interpreted as U_l^H and $U_{e^c}^H$. The group G plays no role at this point. A further constraint comes from the requirement that the PMNS be also close to what observed

after symmetry breaking. In order to find the form of the PMNS matrix associated to a given breaking pattern, we can proceed as in the appendix. We then find that the form of the PMNS matrix again depends on U^H only, and its structure is still given by eq. (2.6), with the form of each factor dictated by the same rules given in that section, where U_l and U_{e^c} should now be interpreted as U_l^H and $U_{e^c}^H$. The group G again plays no role.[5] We conclude that the structure of the irrep decomposition of U^H must be one of those in table 2.4, where once again U_l and U_{e^c} should be interpreted as U_l^H and $U_{e^c}^H$, and the mass pattern and PMNS matrix after symmetry breaking can only be in the forms shown in that table.

The presence of an unbroken, G-symmetric phase played no role in constraining the form of U^H, nor in determining the form of the PMNS matrix. On the other hand, it can play a useful role in providing hierarchies among lepton masses, in particular within the more hierarchical charged lepton masses. We have in fact now two scales available in the sector, let us say the charged lepton one for definiteness, where the masses do not vanish in the symmetric limit: the scale of the non-vanishing entries in $m_E^{(0)}$, allowed by G; and the lower scale of the non-vanishing entries in $m_E^{(1)}$, allowed by H but not by G. We can then use the ratio between those two scales to account for the hierarchy between the tau and muon masses. Therefore, while in section 2.2.2 we focused only on the first two lines in table 2.4, as in the other part of the table the needed hierarchies were not accounted for, now all the first four lines are on the same footing. The hierarchy needed between A and B in the cases in which the charged lepton masses are in the form $(A, B, 0)$ can in fact be provided by the two scales above. On the other hand, the last two lines, corresponding to the (A, B, C) pattern, are still not on the same footing, as they require two hierarchies to be explained.

Let us discuss in greater detail how the available hierarchy can enter the results in table 2.4. Let us first explicitly list the possible mass patterns in the G-symmetric limit. There are two cases. Either the neutrino masses all vanish, in which case the charged lepton masses are in the form $(A, 0, 0)$ (we discard $(A, B, 0)$ and (A, B, C) at this level as in the symmetric limit there is only one scale); or the charged lepton masses all vanish, in which cases neutrino masses are in one of the forms (a, a, a), (a, b, b), (a, b, c), $(0, a, a)$, $(a, b, 0)$, $(a, 0, 0)$. Let us now switch on the symmetry breaking effects. The charged and neutral lepton masses will then get additional contributions from $m_E^{(1)}$, $m_\nu^{(1)}$, which we can denote as proportional to a parameter ϵ. In the sector in which $m^{(0)} \neq 0$, the ϵ parameter

[5] The only possible role of G is in the determination of V_e, V_ν in eq. (A.11), obtained by the diagonalisation of $m_{E,r}$, $m_{\nu,r}$ in eqs. (A.6,A.7,A.8), which now include symmetry breaking effects. In one of the two matrices, say $m_{E,r}$ for definiteness, two scales now enter, the scale of $m_E^{(0)}$ and the scale of $m_\nu^{(1)}$ (while in the neutrino sector $m_\nu^{(0)} = 0$ and only one scale appears). In such a case $V_{e,r}$ may not be a generic matrix with $\mathcal{O}(1)$ entries, it could for example contain small mixing angles. On the other hand, only one scale, that of $m_\nu^{(1)}$, enters $m_{\nu,r}$, so that $V_{\nu,r}$ is still a generic matrix with $\mathcal{O}(1)$ entries. As V is the combination of V_e, and V_ν, V will be also a generic matrix with $\mathcal{O}(1)$ entries, whatever is the form of V_e.

represents the ratio of the two scales, $m^{(1)}$ and $m^{(0)}$.[6] In table 2.5 we show the lepton mass patterns that can be obtained, together with a viable PMNS matrix, taking into account the presence of the two scales. We discard the (A, B, C) charged lepton pattern (last two lines in table 2.4) as it requires at least one unaccounted hierarchy. In table 2.5, the lepton mass pattern in the G-symmetric limit can be obtained by setting $\epsilon = 0$. The corresponding irrep decompositions of U^G are shown, as well as the irrep decomposition of U^H shaping the symmetry breaking corrections. We have checked that for each pair of irrep decompositions of U^G and U^H in the table corresponding to the same mass pattern there exists concrete examples of the groups G and H and of the representations of G, U_l^G and $U_{e^c}^G$, such that the decomposition of the latter under H reproduces the chosen irrep decomposition of U^H.

2.4 Constraints from unification

A theory of flavour should account for both lepton and quark masses. The results we obtained provide constraints on the flavour group following from the observed pattern of lepton masses and mixings. The quark sector can of course provide additional constraints.

In the context of unified theories, the two problems cannot be considered separately, as quarks and leptons are unified in single irreps of the unified gauge group. For example, in SU(5) theories, the lepton doublets l_i are unified with the down quark singlets d_i^c in anti-fundamental representations of SU(5), and the remaining fermions are unified into antisymmetric representations of SU(5). If the action of the flavour group commutes with SU(5), all fermions in the same SU(5) irrep should transform in the same way under the flavour group, $U_{d^c} = U_l$ and $U_{u^c} = U_q = U_{e^c}$. This provides an unavoidable further constraint on the flavour group and its representation. The constraint is even stronger if all the fermions of a single family are unified into a spinorial representation of SO(10). In this section we discuss the effect of such constraints on the previous results.

Let us first assume that the flavour group commutes with SU(5) and call $U_{\bar{5}}$, U_{10} its representations on the SU(5) fermion multiplets. As we have seen, the requirement that the prediction for lepton masses and mixings in the symmetric limit is close to what observed restricts the possible choices of $U_{\bar{5}} = U_l$ and $U_{10} = U_{e^c}$. Table 2.4 summarises the 6 possible forms of their decompositions. Let us now require that the quark masses and mixings are also close what observed in the symmetric limit. By that we mean a quark mass pattern in the form $(A, 0, 0)$ or $(A, B, 0)$ or (A, B, C) in both the up and down quark sector, with the $(A, 0, 0)$ pattern preferred, as the others require hierarchies among the non-vanishing entries. As for the CKM matrix, let us first remind that the CKM angles are all measured to be small, with the only possible exception of the Cabibbo angle, corresponding to the 12 block of the CKM matrix. We then only consider the cases

[6] In principle the correction to the masses could be proportional to higher powers of ϵ, but it turns out that this it not the case, under our hypotheses.

masses	hierarchy	G irreps	H irreps	U_{PMNS}	zeros
$(\epsilon A\,0\,0)$ $(a\;\;b\;\;c)$	NH or IH	$1\;\;1\;\;1$ $r \not\supseteq 1$	$1\;\;1\;\;1$ $1\;\;r \not\supseteq 1$	V	none
$(\epsilon A\,0\,0)$ $(a\;\;b\;\;\epsilon c)$	NH or IH	$1\;\;1\;\;\mathbf{1}$ $r \not\supseteq 1, \overline{\mathbf{1}}$	$1\;\;1\;\;1$ $1\;\;r \not\supseteq 1$	V	none
$(\epsilon A\,0\,0)$ $(a\;\;\epsilon b\;\epsilon c)$	NH	$1\;\;\mathbf{1}\;\;\mathbf{1}$ $\quad$ $1\;\;\mathbf{1}\;\;\mathbf{1'}$ $\quad$ $1\;\;\mathbf{2}$ $r \not\supseteq 1, \overline{\mathbf{1}}$ $\quad$ $r \not\supseteq 1, \overline{\mathbf{1}}, \overline{\mathbf{1'}}$ $\quad$ $r \not\supseteq 1, \overline{\mathbf{2}}$	$1\;\;1\;\;1$ $1\;\;r \not\supseteq 1$	V	none
$(A\,0\,0)$ $(\epsilon a\;\epsilon b\;\epsilon c)$	NH or IH	$\mathbf{1}\;\;\mathbf{1}\;\;\mathbf{1}$ $\quad$ $\mathbf{1}\;\;\mathbf{1}\;\;\mathbf{1'}$ $\quad$ $\mathbf{1'}\;\;\mathbf{1}\;\;\mathbf{1}$ $\overline{\mathbf{1}}\;\;r \not\supseteq \overline{\mathbf{1}}$ $\quad$ $\overline{\mathbf{1}}\;\;r \not\supseteq \overline{\mathbf{1}}, \overline{\mathbf{1'}}$ $\quad$ $\overline{\mathbf{1'}}\;\;r \not\supseteq \overline{\mathbf{1}}$ $\mathbf{1}\;\;\mathbf{1'}\;\;\mathbf{1''}$ $\quad$ $\mathbf{1}\;\;\mathbf{2}$ $\overline{\mathbf{1}}\;\;r \not\supseteq \overline{\mathbf{1'}}, \overline{\mathbf{1''}}$ $\quad$ $\overline{\mathbf{1}}\;\;r \neq \overline{\mathbf{2}}$	$1\;\;1\;\;1$ $1\;\;r \not\supseteq 1$	V	none
$(A\,0\,0)$ $(0\;\epsilon a\;\epsilon a)$	IH	$\mathbf{1}\;\;\mathbf{1}\;\;\mathbf{1'}$ $\quad$ $\mathbf{1}\;\;\mathbf{1'}\;\;\mathbf{1''}$ $\quad$ $\mathbf{1}\;\;\mathbf{2}$ $\overline{\mathbf{1}}\;\;r \not\supseteq \overline{\mathbf{1}}, \overline{\mathbf{1'}}$ $\quad$ $\overline{\mathbf{1}}\;\;r \not\supseteq \overline{\mathbf{1'}}, \overline{\mathbf{1''}}$ $\quad$ $\overline{\mathbf{1}}\;\;r \neq \overline{\mathbf{2}}$	$\mathbf{1}\;\;\mathbf{1}\;\;\overline{\mathbf{1}}$ $\overline{\mathbf{1}}\;\;r \not\supseteq \mathbf{1}, \overline{\mathbf{1}}$	$H_{12}^E V_{23} D_{12}^{-1}$	none (**13**)
$(\epsilon A\,0\,0)$ $(0\;\;a\;\;a)$	IH	$\mathbf{1}\;\;\mathbf{1}\;\;\overline{\mathbf{1}}$ $\quad$ $\mathbf{1'}\;\;\mathbf{1}\;\;\overline{\mathbf{1}}$ $\quad$ $\mathbf{1}\;\;2$ $r \not\supseteq \mathbf{1}, \overline{\mathbf{1}}$ $\quad$ $r \not\supseteq \mathbf{1}, \overline{\mathbf{1}}, \overline{\mathbf{1'}}$ $\quad$ $r \not\supseteq \overline{\mathbf{1}}, 2$	$\mathbf{1}\;\;\mathbf{1}\;\;\overline{\mathbf{1}}$ $\overline{\mathbf{1}}\;\;r \not\supseteq \mathbf{1}, \overline{\mathbf{1}}$	$H_{12}^E V_{23} D_{12}^{-1}$	none (**13**)
$(A\;\epsilon B\;0)$ $(\epsilon a\;\epsilon b\;\epsilon c)$	NH or IH	$\mathbf{1}\;\;\mathbf{1}\;\;\mathbf{1}$ $\quad$ $\mathbf{1}\;\;\mathbf{1}\;\;\mathbf{1'}$ $\quad$ $\mathbf{1'}\;\;\mathbf{1}\;\;\mathbf{1}$ $\overline{\mathbf{1}}\;\;r \not\supseteq \overline{\mathbf{1}}$ $\quad$ $\overline{\mathbf{1}}\;\;r \not\supseteq \overline{\mathbf{1}}, \overline{\mathbf{1'}}$ $\quad$ $\overline{\mathbf{1'}}\;\;r \not\supseteq \overline{\mathbf{1}}$ $\mathbf{1}\;\;\mathbf{1'}\;\;\mathbf{1''}$ $\quad$ $\mathbf{1}\;\;\mathbf{2}$ $\overline{\mathbf{1}}\;\;r \not\supseteq \overline{\mathbf{1'}}, \overline{\mathbf{1''}}$ $\quad$ $\overline{\mathbf{1}}\;\;r \neq \overline{\mathbf{2}}$	$1\;\;1\;\;1$ $1\;\;1\;\;r \neq 1$	V	none
$(A\;\epsilon B\;0)$ $(0\;\epsilon a\;\;\epsilon a)$	IH	$\mathbf{1}\;\;\mathbf{1}\;\;\mathbf{1'}$ $\quad$ $\mathbf{1}\;\;\mathbf{1'}\;\;\mathbf{1''}$ $\quad$ $\mathbf{1}\;\;\mathbf{2}$ $\overline{\mathbf{1}}\;\;r \not\supseteq \overline{\mathbf{1}}, \overline{\mathbf{1'}}$ $\quad$ $\overline{\mathbf{1}}\;\;r \not\supseteq \overline{\mathbf{1'}}, \overline{\mathbf{1''}}$ $\quad$ $\overline{\mathbf{1}}\;\;r \neq \overline{\mathbf{2}}$	$\mathbf{1}\;\;\mathbf{1}\;\;\overline{\mathbf{1}}$ $\overline{\mathbf{1}}\;\;\overline{\mathbf{1}}\;\;r \neq \mathbf{1}$	$V_{23} D_{12}^{-1}$	**13**

Table 2.5: Lepton mass patterns that can be obtained starting from a symmetric limit ($\epsilon = 0$) in which either the neutrino or the charged lepton masses (but not both) vanish. The corrections proportional to ϵ are induced by the spontaneous symmetry breaking $G \to H$, under the hypothesis introduced in section 2.3. The corresponding irrep decompositions of U_l^G, $U_{e^c}^G$ and of U_l^H, $U_{e^c}^H$ leading to a viable form of the PMNS matrix are also shown. As usual, boldface fonts denote complex or pseudoreal (if 2-dimensional) irreps, primes are used to distinguish inequivalent representations, and in the case of complex representations $\mathbf{1'}$ is supposed to be different from both $\mathbf{1}$ and $\overline{\mathbf{1}}$. The representations of G and H are of course different even if represented by the same symbol. If ϵ is reabsorbed into the parameter it multiplies, the mass pattern correspond to the ones in the first four lines of table 2.4 and the irrep decompositions of U_l^H, $U_{e^c}^H$ coincide with those shown in that table.

leading to a CKM matrix which is either diagonal or containing at most a non-trivial 12 block in the symmetric limit. It turns out that the only possible irrep decomposition is $U_{\bar{5}} = 1 + 1 + 1$, $U_{10} = 1 + r \not\supseteq 1$. This uniquely identifies the form of the lepton spectrum in the symmetric limit, with vanishing electron and muon masses, $(A, 0, 0)$, and anarchical neutrino masses, (a, b, c), with a generic PMNS matrix. The structure of the quark masses and mixings in the symmetric limit instead depends on the specific choice of U_{10}. This is shown in table 2.6, where the viable forms of U_{10} and the corresponding mass and mixing patterns are listed. The down quark masses are in the same form as (and are actually equal to) the charged lepton ones in the symmetric limit, as dictated by SU(5). The CKM matrix has the form

$$V_{\rm CKM} = H_U P_U V P_D^{-1} H_D^{-1} \,. \tag{2.17}$$

The contributions to $V_{\rm CKM}$ have similar origins as the corresponding ones in eq. (2.6). As in the case of the PMNS matrix, each of them can be obtained without the need of writing explicitly nor diagonalising the quark mass matrices, with analogous rules. The form of the CKM matrix in terms of those contributions is also indicated in table 2.6. Note the constant presence of an undetermined transformation in the 12 block, H_{12}^D, associated to the vanishing of the two lighter down quark masses in the symmetric limit. As discussed, such undetermined transformations are fixed, up to diagonal phases, by symmetry breaking effects, and they can end up contributing to the Cabibbo angle with a zero, small, or large mixing angle. The patterns shown in the table are viable provided that the permutations P_U, P_D do not modify the position of the heavy eigenvalue. The Cabibbo angle is expected to be large (with the measured value accidentally smallish) in the last case in table 2.6, where a physical V_{12} rotation appears, which will survive symmetry breaking. In all the other cases, the Cabibbo angle can end up being large or small, depending on the symmetry breaking effects. If the two light eigenvalues are permuted, the Cabibbo angle receives a $\pi/2$ contribution, which needs to be (partially) cancelled by other contributions.

If all the fermions of a single family are unified into a dimension 16 spinorial representation of SO(10) commuting with the flavour group, the constraints on the flavour group representation are even stronger, and no solution can be found. In such a case we would have in fact $U_{16} \equiv U_{\bar{5}} = U_{10}$. The symmetric limit is a good approximation in the lepton sector only if U_{16} is trivial. Such a possibility however leads to a generic CKM matrix with $\mathcal{O}(1)$ angles, which we do not consider a viable leading order approximation in the symmetric limit.

$(U_{\bar{5}} = 1 \quad 1 \quad 1)$	masses	$V_{\rm CKM}$	$U_{\rm PMNS}$
$U_{10} = 1 \quad \mathbf{1} \quad \mathbf{1}$ $U_{10} = 1 \quad \mathbf{1} \quad \mathbf{1}'$ $U_{10} = 1 \quad \mathbf{2}$	$(A\,0\,0)_D \quad (A\,0\,0)_E$ $(D\,0\,0)_U \quad (a\;b\;c)_\nu$	$H^U_{12} H^{D\,-1}_{12}$	V
$U_{10} = 1 \quad 1' \quad \mathbf{1}$	$(A\,0\,0)_D \quad (A\,0\,0)_E$ $(DE\,0)_U \quad (a\;b\;c)_\nu$	$P^U_{2\leftrightarrow 3} H^{D\,-1}_{12}$	V
$U_{10} = 1 \quad \mathbf{1} \quad \overline{\mathbf{1}}$	$(A\,0\,0)_D \quad (A\,0\,0)_E$ $(DEF)_U \quad (a\;b\;c)_\nu$	$P_U H^{D\,-1}_{12}$	V
$U_{10} = 1 \quad 1' \quad 1''$	$(A\,0\,0)_D \quad (A\,0\,0)_E$ $(DEF)_U \quad (a\;b\;c)_\nu$	$P_U H^{D\,-1}_{12}$	V
$U_{10} = 1 \quad 1' \quad 1'$	$(A\,0\,0)_D \quad (A\,0\,0)_E$ $(DEF)_U \quad (a\;b\;c)_\nu$	$P_U V_{12} H^{D\,-1}_{12}$	V

Table 2.6: Possible forms of SU(5) unified flavour representations. $U_{\bar{5}}$ is trivial in all cases. The form of fermion masses and of the CKM and PMNS matrices, in the notations of eq. (2.17), corresponding to viable choices are shown. The lepton mass pattern and PMNS matrix are all in the same form, as they all correspond to the case in the first line of table 2.4. $P_{2\leftrightarrow 3}$ is either the identity permutation or the switch of 2 and 3.

2.5 Conclusions

We provided a complete answer to the following general question: what are the flavour groups, of any type, and representations providing, in the symmetric limit, an approximate description of lepton (fermion) masses and mixings?

The assumption we made is quite general: the light neutrinos are of Majorana type, and the symmetry arguments can be applied directly to their mass matrix. Despite the generality of the problem, the complete answer is simple and has an important corollary: either the flavour symmetry does not constrain at all the neutrino mass matrix (anarchy), or the neutrinos have an inverted hierarchical spectrum. Therefore, if the present hint of a normal hierarchical spectrum were confirmed, we would conclude that, under the above assumption, flavour models leading to an approximate description of lepton masses and mixings in the symmetric limit are not able to account for any of the neutrino flavour observables, and symmetry breaking effects must play a primary role in their understanding. Such a conclusion is further strengthened in the case in which the representation of the flavour group commutes with the standard representation of a SU(5) grand unified gauge group. In the latter case, not even the options leading to an inverted hierarchical spectrum are available, and the only option is anarchy. In the case of SO(10), there are no solutions.

The main caveat to the previous conclusion is the assumption that the light neutrinos are of Majorana type, and that the symmetry arguments can be applied directly to their mass matrix. The origin of Majorana neutrino masses most likely resides at high scales, where additional relevant degrees of freedom (singlet neutrinos for example) might live. In such a case, the flavour symmetry acts on the high-scale degrees of freedom as well. The low-energy analysis turns out to be often equivalent to the high-scale analysis, but not always. Such a caveat will be studied in the next chapter.

The possibility to provide a simple systematic answer to the above general question is based on the following result: the structure of lepton masses and mixings only depends on the flavour group and representations through the structure of their decomposition in irreducible components, and in particular only through the dimension, type (complex or real or pseudoreal), and equivalence of those components. We found that there are only six viable structures, listed in table 2.4. All of them contain only one-dimensional real or complex representations.

In passing, we developed a simple technique to determine the form of the lepton masses and mixings directly from the structure of the decomposition in irreducible representations, without the need to specify, nor to diagonalise, the lepton mass matrices. We also noted that it is important to write the invariance condition in terms of the charged lepton mass matrix m_E and not of $m_E^\dagger m_E$, otherwise the important role of the flavour representation on singlet leptons would be lost.

As our results and assumptions imply that an understanding of the flavour observables of normal hierarchical neutrinos must rely on symmetry breaking effects, we also consider the possibility that the neutrino or the charged lepton mass matrix vanishes in the symmetric limit. With a simple extension of the previous techniques, we proved that the sole knowledge of the symmetry breaking pattern, i.e. of the residual unbroken group, is not sufficient to get a better understanding of the flavour observables: the sources of flavour breaking and of their vacuum expectation values need to be specified.

Chapter 3

Flavour symmetries in the context of the seesaw mechanism

In chapter 2 we have studied neutrino masses and mixing by assuming that the neutrinos are Majorana particles and that the flavour symmetries directly put constrains on their mass matrix originated from the Weinberg operator. In this chapter we will consider the possibility that the Weinberg operator originates from a type I seesaw mechanism, and we address two issues. These are the constraints on lepton mixing one obtains (in the symmetric limit) in terms of the Weinberg operator equivalent to those one obtains in terms of the corresponding seesaw Lagrangian. As it will turn out that the two analyses, in terms of the Weinberg operator and seesaw Lagrangian, are not equivalent, we will extend analysis in chapter 2 to the case of a seesaw Lagrangian.

3.1 Introduction

In this chapter we will assume that the Weinberg operator originates, at a tree level, from the type I seesaw mechanism. We will show that discussing the neutrino masses and mixings from the high-scale origin of type I seesaw mechanism is not always equivalent to the low-scale results that we got in in the previous chapter. So there are two inequivalent flavour symmetry discussions of neutrino masses and mixing depending on whether the flavour symmetry is assumed to act on the Lagrangian with Weinberg operator or on the corresponding seesaw Lagrangian. Hereafter we call them as low- and high-scale analyses, respectively. Now that there are two different analyses, it is important to study under which condition they become inequivalent, since equivalent case reproduces the results we already know in previous chapter. As we will see, inequivalence happen in two cases depending on whether or not the singlet neutrino mass matrix is singular in the symmetric limit. If the singlet neutrino mass matrix is non-singular, there is a condition of the flavour group representations on lepton doublets and neutrino singlets that if this condition holds then the high-scale analysis reproduces the low-scale results,

otherwise we may get different results in the high-scale analysis. If the singlet neutrino mass matrix is singular in the symmetric limit, the flavour symmetry G forces some of the singlet neutrinos to have a vanishing mass in this limit and we cannot apply the seesaw formula in the symmetric limit, so symmetry breaking effects are needed to produce non-zero masses for them. We suppose that masses from the symmetry breaking effects are smaller than the non-zero masses in the symmetric limit but they are much bigger than EW scale.

Let us suppose that flavour symmetry G is spontaneously broken to the subgroup H. In the G-symmetric limit the mass matrix of the singlet neutrino is $M^{(0)}$ and that of the light neutrinos is $m_\nu^{(0)}$. They will get corrections $M^{(1)}$ and $m_\nu^{(1)}$ after G is broken to H. At the same time, Dirac mass matrix $m_N^{(0)}$ in the symmetric limit also gets a correction $m_N^{(1)}$ after the symmetry breaking. Therefore, the neutrino mass matrices after the symmetry breaking become

$$\begin{aligned} M &= M^{(0)} + M^{(1)}, \\ m_N &= m_N^{(0)} + m_N^{(1)}, \\ m_\nu &= m_\nu^{(0)} + m_\nu^{(1)}, \end{aligned} \tag{3.1}$$

where $M^{(0)}$, $m_N^{(0)}$ and $m_\nu^{(0)}$ are invariant under G, while $M^{(1)}$, $m_N^{(1)}$ and $m_\nu^{(1)}$ are invariant under H but not under G so they must vanish in the symmetric limit. As was in the low-scale analysis, we assume that mass matrix entries in the G-symmetric limit have the same orders of magnitude due to the requirement that flavour symmetry model itself must generate the mass hierarchy without imposing it by hand. The corrections obtained after the symmetry breaking are assumed to be smaller than the ones surviving in the symmetric limit, and their relative sizes are related to the two flavour symmetry scales of G and H.

An interesting feature of discussing the case in which the singlet neutrino mass matrix is forced to be singular by the flavour symmetry is that the light neutrino mass hierarchy can be generated in this way. For instance, let us say one of the singlet neutrino has vanishing mass in the G-symmetric limit, then one may expect that one of the light neutrino has a large mass compared to the other two in this limit. So the flavour symmetry predicts light neutrino masses are in the normal hierarchy. In one of the our forthcoming discussions we will see that this is indeed the case. This is nothing but right-handed neutrino dominance scheme [149–154]. An important feature here compared to the right-handed neutrino dominance is that the dominant contribution of the singlet neutrino arises naturally from the symmetry breaking effect without need to make such an assumption.

The work in this chapter is organized as follows: in section 3.2 we classify flavour group representations in both low- and high-scale analyses and find conditions to high-scale analysis provide same/different neutrino mass and mixing patterns compared to the low-scale discussion. Section 3.3 contains discussions for the case in which some of the singlet neutrinos have vanishing masses in the symmetric limit. Then, the complete

results captured by high-scale analysis, for the case of singlet neutrino mass matrix is non-singular, will be presented in section 3.4. After that, in section 3.5 there will be an investigation for the fermion masses and mixing from the GUT constraints on top of the conditions of flavour symmetry. Finally, section 3.6 contains our conclusions for this chapter.

3.2 Flavour symmetries in the low- and high-scale analyses

3.2.1 Flavour group representations and lepton mass matrices

Before staring to identify flavour groups and their representations for the viable patterns of neutrino masses in the context of the type I seesaw mechanism, it is important to give precise definitions for the two kinds of flavour symmetry approaches describing neutrino masses and mixing. We already called them as low- and high-scale analyses. The former refers to the description of the neutrino masses in the EW scale without considering the contribution from the heavy singlet neutrinos, while the latter takes into account the effect of these heavy degrees of freedom appearing in seesaw Lagrangian. The low-scale analysis is basically the way used in Ref. [155], in which we have assumed that neutrino masses are described by means of the SM effective Lagrangian and that only the lowest dimensional operator (the Weinberg operator) is relevant. The EW scale description of lepton flavour is then provided by the following Lagrangian:

$$-\mathcal{L}_L = y^E_{ij} e^c_i l_j h^* + \frac{c_{ij}}{2\Lambda} l_i l_j h h + \text{h.c.}\,, \tag{3.2}$$

where we used a Weyl spinor notation, $l_i = (\nu_i, e_i)^T$ denotes the lepton doublets of $\mathrm{SU(2)_L}$, e^c_i are the charged lepton singlets of $\mathrm{SU(2)_L}$, h is the SM Higgs doublet, and the Yukawa interactions are written in the right-left convention. The splitting of the coefficient of the Weinberg operator into the dimensionless numbers c_{ij} and a new physics scale Λ with the constant factor 2 is of course arbitrary. The flavour index runs over 3 families of l_i and e^c_i, $i = 1, 2, 3$, but we can generalize to the case of n lepton families. The charged lepton and light neutrino mass matrices obtained from eq. (3.2) are

$$m_E = y_E v, \qquad m_\nu = c\, v^2/\Lambda, \tag{3.3}$$

where $v = |\langle h \rangle| \approx 174\,\mathrm{GeV}$.

We will consider the low-scale (EW scale) representations U_L of a generic flavour group G, commuting with the SM gauge transformations, acts on the lepton doublet and singlet fields in following way

$$g \in G : \begin{cases} l_i \to U^l_L(g)_{ij} l_j \\ e^c_i \to U^e_L(g)_{ij} e^c_j \end{cases}. \tag{3.4}$$

The Higgs field could in principle also transform under the U_L, but its transformation can, without loss of generality, be reabsorbed in the transformations of l_i and e^c_i.

Apparently, the low-scale Lagrangian $\mathcal{L}_L$ in eq. (3.2) is invariant under U_L if and only if the coefficients of each terms are invariant under the flavour group representations

$$\begin{aligned} y_E &= U^e_L(g)^T y_E\, U^l_L(g), \\ \frac{c}{\Lambda} &= U^l_L(g)^T \frac{c}{\Lambda}\, U^l_L(g), \qquad \forall g \in G\ , \end{aligned} \tag{3.5}$$

or equivalently iff charged lepton and neutrino mass matrices are invariant under the flavour symmetry

$$\begin{aligned} m_E &= U^e_L(g)^T m_E\, U^l_L(g), \\ m_\nu &= U^l_L(g)^T m_\nu\, U^l_L(g), \qquad \forall g \in G\ . \end{aligned} \tag{3.6}$$

This means that the low-scale invariance of the Lagrangian implies the existence of invariant charged lepton and neutrino mass matrix under the flavour symmetry, or vice versa. So one can study the structure of the lepton mass matrix by imposing the flavour symmetry to this low-scale Lagrangian. But in general the flavour symmetry is spontaneously broken through the vacuum expectation value of one or more scalar fields — flavons. Then lepton mass matrices will get contributions from the symmetry breaking effects. Therefore, discussions for the flavour symmetry contains both effects from the symmetric limit and symmetry breaking mechanism.

For the high-scale description, as a specific example of high-scale origin of the effective Lagrangian in eq. (3.2), we will consider a type I seesaw Lagrangian with n singlet neutrinos ν^c_a, $a = 1 \ldots n$. The high-scale analysis of lepton flavour is then provided by the following Lagrangian:

$$-\mathcal{L}_H = \lambda^E_{ij} e^c_i l_j h^* + \lambda^N_{aj} \nu^c_a l_j h + \frac{M_{ab}}{2} \nu^c_a \nu^c_b + \text{h.c.}\ , \tag{3.7}$$

where the eigenvalues[1] of M are all supposed to be much heavier than the EW scale (and in particular non-vanishing). The charged lepton and light neutrino mass matrices obtained from eq. (3.7) are

$$m_E = \lambda_E v\ , \qquad m_\nu = -(\lambda_N v)^T M^{-1} (\lambda_N v) = -m_N^T\, M^{-1} m_N\ , \tag{3.8}$$

where we denoted Dirac mass matrix as $m_N \equiv v\lambda_N$.

We will say that $\mathcal{L}_L$ is the low-scale limit of $\mathcal{L}_H$ if $\mathcal{L}_L$ is obtained at the tree level from $\mathcal{L}_H$ by integrating out the singlet neutrinos, i.e.

$$y_E = \lambda_E \tag{3.9}$$

[1] Here and below we will use "eigenvalues" to refer to singular values.

and

$$\frac{c}{\Lambda} = -\lambda_N^T M^{-1} \lambda_N \ , \tag{3.10}$$

or equivalently if they give rise to the same charged lepton and light neutrino mass matrices.

The high-scale representations U_H of G on the full set of lepton fields, including the singlet neutrinos, are considered to be commuting with the SM gauge transformations and they transform lepton fields as

$$g \in G : \begin{cases} l_i \to U_H^l(g)_{ij} l_j \\ e_i^c \to U_H^e(g)_{ij} e_j^c \\ \nu_a^c \to U_H^\nu(g)_{ab} \nu_b^c \end{cases} . \tag{3.11}$$

As in the case of low-scale analysis, in this case we are considering only one family of Higgs doublet so under the flavour group representation U_H the Higgs field at most gets a sign change or a phase shift, which can be reabsorbed into the transformations of l_i, e_i^c, and ν_a^c, without loss of generality. The representation U_H of G on l_i, e_i^c, ν_a^c trivially corresponds to a representation U_L on l_i, e_i^c ($U_L^l = U_H^l$, $U_L^e = U_H^e$), which we call the "low-scale limit" of high-scale representation U_H.

Imposing the flavour symmetry on the high-scale Lagrangian $\mathcal{L}_H$ requires that its invariant under the representation U_H if and only if following conditions hold

$$\begin{aligned} \lambda_E &= U_H^e(g)^T \lambda_E \, U_H^l(g), \\ \lambda_N &= U_H^\nu(g)^T \lambda_N \, U_H^l(g), \\ M &= U_H^\nu(g)^T M \, U_H^\nu(g), \qquad \forall g \in G \ , \end{aligned} \tag{3.12}$$

or equivalently it is a necessary and sufficient to have invariant mass matrices

$$\begin{aligned} m_E &= U_H^e(g)^T m_E \, U_H^l(g), \\ m_N &= U_H^\nu(g)^T m_N \, U_H^l(g), \\ M &= U_H^\nu(g)^T M \, U_H^\nu(g), \qquad \forall g \in G \ . \end{aligned} \tag{3.13}$$

So the flavour symmetry shapes the form of all those mass matrices in the symmetric limit. Once the flavour symmetry is spontaneously broken, all the mass matrices above will get contributions from the symmetry breaking effect. And full mass matrix become a sum of two components from the symmetric limit and the symmetry breaking effect.

To give a concise definition of equivalence in the symmetric limit of the high-scale flavour symmetry and its low-scale limit in the next section, and also for later purposes, we will separate any unitary and finite dimensional representation U of the group G into two parts (with a possibility that one of them can be empty): a vectorlike part and a fully chiral part. The vectorlike part of U refers to the set of irreducible representations (irreps) that consists of either real or pairs of complex conjugated irreps or of equivalent

pseudoreal irreps; the fully chiral part of U is a set of irreps that does not contain, by definition, any real irreps, nor pairs of complex conjugated irreps, nor pairs of equivalent pseudoreal irreps. From the definition above one can easily find that vectorlike part U_0 of the representation U is equivalent to its complex conjugated representation U_0^*. Meaning that U_0 and U_0^* are related by a unitary similarity transformation, and it contains an even number (e.g. zero) of pseudoreal irreps of each dimension appearing inside the irrep decomposition; while in the fully chiral part, say U_1, of U none of its sub-representations is equivalent to their conjugate, except possibly a single pseudoreal irrep of each type.

Let us see these two parts of the representation from the example of following two irrep decompositions: $U = 1 + \mathbf{1} + \mathbf{1}$ and $U = \mathbf{1} + \mathbf{1} + \bar{\mathbf{1}}$, where 1 and $\mathbf{1}$ stand for any real and complex one dimensional representation respectively, and having a bar means conjugated representation. According to our definition, vectorlike part of the first example is 1 and fully chiral part of it is $\mathbf{1} + \mathbf{1}$, the second example contains vectorlike part $\mathbf{1} + \bar{\mathbf{1}}$ and fully chiral part $\mathbf{1}$. In a similar way, one can separate an irrep decomposition of any n dimensional representation into these two parts (in some cases it is possible to have one of the two parts empty).

After having decomposition of U into vectorlike and fully chiral representations, $U = U_0 + U_1$, we will have following important relations between the irrep decomposition and Weyl fermion mass matrix m (which is complex and symmetric) invariant under U, i.e. $m = U^T(g)\, m\, U(g)$ for $\forall g \in G$:

- U is vectorlike if and only if there exists a non-singular invariant mass matrix for those fermions.
- U is fully chiral if and only if an invariant mass matrix for those fermions necessarily vanishes.
- In case there are both vectorlike and fully chiral parts of U, we can redefine fermions through a unitary transformation (if necessary) and choose the decomposition of U in irreps in such a way that each irrep acts on a separate subset of fermions. Then U_0 and U_1 can be chosen in such a way that each of them groups together the set of those irreps. In this way one can split mass matrix m into the non-singular block corresponding to U_0 and zero blocks for the rest of the representation.

The first two properties are very easy to verify, so we will skip to explain them and say some words about the last one. When U has both non-empty vectorlike part U_0 and fully chiral part U_1 there are two possible situations can occur: either none of the irreps in U_1 is contained in U_0 or some of the irreps in U_1 are also contained in U_0. In the first case the mass matrix is automatically a direct some of the non-singular block corresponding to U_0 and the zero block corresponding to U_1. If there are same types of irreps in U_0 and U_1, the decomposition is not unique anymore, but the number of equivalent irreps of each given type contained in U_0 and U_1 does not depend on the decomposition. So the total number of irreps in U_0 and in U_1 does not change. This situation appears only

for the complex and pseudoreal irreps, as all real irreps are belong to U_0. Each types of overlapped irreps between U_0 and U_1 with their complex conjugates (or a equivalent counterparts in case of pseudoreal irreps) restricts the corresponding part of the mass matrix in a rectangular block. The rectangular block can be brought into upper or lower triangular block by unitary rotations, commuting with these irreps, among the several copies of the same type of representations. Once we are done this for the all rectangular blocks and redefine fields accordingly, the mass matrix ends up being the direct some of non-singular square blocks and all the rest is zero. According to which copies of the same type of irreps correspond to non-singular block or zero block we can easily separate those repeated irreps into vectorlike part or fully chiral part of the representation. Since in this case there is at least one row or one column of the whole mass matrix is zero so it has a zero determinant and thus it is a singular matrix.

We can illustrate this argument by looking at our previous example, $U = \mathbf{1} + \mathbf{1} + \bar{\mathbf{1}}$. In this example there is a common $\mathbf{1}$ in both vectorlike and fully chiral parts of the representation. It is not priory obvious to choose which one of the $\mathbf{1}$ is in the vectorlike part and other in the fully chiral part, but it is for sure that each of these two parts must contain one of the two $\mathbf{1}$. The Weyl fermion mass matrix m invariant under this representation has a rectangular block $(x\ y\ 0)$ in the third row (and its transpose in the third column). We can rotate the first two neutrinos transforming under $\mathbf{1}$ in order to set $x = 0$, without spoiling their transformations under $\mathbf{1}$. Note that any 12 block rotation clearly commutes with the corresponding $\mathbf{1}+\mathbf{1}$ irrep part of U. Once we are done with this rotation, the mass matrix becomes 23 block matrix with the same non-zero off diagonal entries in this block. Given that the 23 block is non-singular, we will choose last two irreps $\mathbf{1} + \bar{\mathbf{1}}$, corresponding to this block, into the vectorlike part and remaining $\mathbf{1}$ belongs to fully chiral part.

Having a relation between the two parts of the irrep decompositions and form of the mass matrix, we can conclude that necessary and sufficient condition to have invariant non-singular Majorana mass matrix is that the flavour representation U does not contain fully chiral part in its irrep decompositions. So the invariant Majorana mass matrix being non-singular indicates there is vectorlike representation U and vice versa.

3.2.2 Equivalence of two analyses in the symmetric limit

We would like to discuss whether the low- and high-scale studies of flavour symmetries in the symmetric limit are equivalent; i.e. whether, in the light of the fact that flavour observables only depend on the low-scale effective Lagrangian, the low-scale analysis captures all the possibilities covered by the one at high-scale. As we will see, in the symmetric limit, the low-scale analysis is covered by the low-scale limit of high-scale analysis, but not all high-scale results are captured by the low-scale analysis.

First of all, we have to note an important caveat. In order for the effective theory description to work, what need to be heavier than the EW scale are the heavy singlet

neutrino masses after the symmetry breaking effects are taken into account. As was pointed out before, the singlet neutrino mass matrix $M = M^{(0)} + M^{(1)}$ in which $M^{(0)}$ is the part invariant under G, satisfying eq. (3.13), and $M^{(1)}$ accounts for the symmetry breaking effects. It is conceivable that one or more heavy singlet neutrino masses vanish in the symmetric limit and they are generated after the symmetry breaking is taken into account. In such a case, $M^{(0)}$ is singular, but M is not. Note that while the masses generated by symmetry breaking effects are small compared to the other heavy masses, they can still be much heavier than the EW scale, so that all the eigenvalues of M can be much heavier than the EW scale. Suppose that this is indeed the case, then the effective theory description given by eq. (3.10) still holds once the symmetry breaking effects are considered; but it does not hold in the symmetric limit, in which $M^{(0)}$ becomes singular. In order for the low-scale description of the flavour theory to have a chance to be equivalent to the high-scale one in the symmetric limit, the heavy singlet neutrino mass matrix must then be allowed to be non-singular in the symmetric limit. So the singlet neutrino mass matrix being non-singular is a necessary condition to the low- and high-scale analyses become equivalent.

On the other hand, as it will be shown below, even if singlet neutrino mass matrix is non-singular in the symmetric limit, the low-scale analysis still is not always equivalent to the high-scale analysis, unless the further condition on the representations is satisfied.

With what above in mind, and in order to formulate the problem we aim at addressing in a precise way, we define the equivalence in the symmetric limit of a high-scale flavour symmetries and their low-scale limits as follows. Let us suppose that U_H and U_L are high- and low-scale representations, respectively, of the flavour group G, and U_L is the low-scale limit of U_H. We say that U_H and U_L are equivalent in the symmetric limit if following two conditions are simultaneously satisfied.

1. U_H^ν is vectorlike, i.e. there exists a non-singular U_H^ν-invariant singlet neutrino mass matrix M (otherwise the second equation in eq. (3.8) can never be written).

2. For each m_ν invariant under U_L, there exist a m_N and a non-singular M invariant under U_H such that $m_\nu = -m_N^T M^{-1} m_N$.

Note that the converse of the second point is always true: given m_E, m_N and M (non-singular) invariant under U_H (thus satisfy conditions in eq. (3.13)), the matrices m_E and $m_\nu = -m_N^T M^{-1} m_N$ are always invariant under U_L that is a low-scale limit of U_H.

After having definition of the equivalence between U_H and U_L, the problem of the equivalence of the high- and low-scale discussions of flavour symmetries in the symmetric limit can then be formulated as follows:

- Is the low-scale limit U_L of a high-scale representation U_H always equivalent to U_H in the symmetric limit?

- Does an equivalent high-scale representation U_H of a flavour group G always exist for any given low-scale representations U_L as a low-scale limit?

The second question has a positive answer: for a given low-scale representation U_L there is always a equivalent high-scale representation U_H such that U_L is a low-scale limit of U_H. However, the low-scale representations do not cover all the possibilities arising at high-scale, i.e. there exist high-scale representations whose low-scale limit is not equivalent to high-scale representation U_H in the symmetric limit. The necessary and sufficient condition for the low-scale limit U_L of U_H to be equivalent in the symmetric limit to U_H is the following: i) U_H^ν is vectorlike and ii) U_H^ν contains vectorlike part of U_L^l. The proof of this statement is given in appendix B. Clearly, the first condition requires non-singular singlet neutrino mass matrix and the second one puts further constraints on the irrep patterns.

As an example of a high-scale flavour symmetry is not equivalent to its low-scale limit in the symmetric limit, let us consider the case in which $G = U(1)$ and the high-scale representation is defined by the following lepton charges: $(1, 0, 0)$ for the l_i, $(1, -1, 0)$ for the ν_i^c and $(1, 1, 0)$ for the e_i^c [156]. The high-scale flavour symmetry constrains m_E, m_N, M to be in the following form

$$m_E = \begin{pmatrix} 0 & 0 & 0 \\ 0 & 0 & 0 \\ 0 & X & X \end{pmatrix}, \quad m_N = \begin{pmatrix} 0 & 0 & 0 \\ X & 0 & 0 \\ 0 & X & X \end{pmatrix}, \quad M = \begin{pmatrix} 0 & X & 0 \\ X & 0 & 0 \\ 0 & 0 & X \end{pmatrix}, \tag{3.14}$$

where no special relation is enforced among the non-vanishing entries denoted by X (except $M_{12} = M_{21}$). The neutrino mass matrix from high-scale analysis is in the form of

$$m_\nu = -m_N^T M^{-1} m_N = \begin{pmatrix} 0 & 0 & 0 \\ 0 & a_2 b_2 & a_2 b_3 \\ 0 & a_3 b_2 & a_3 b_3 \end{pmatrix}. \tag{3.15}$$

It is rank one matrix so there is only one neutrino has non-zero mass. On the other hand, the low-scale symmetry, acting only on l_i and e_i^c, constrains m_E and m_ν to be in the form

$$m_E = \begin{pmatrix} 0 & 0 & 0 \\ 0 & 0 & 0 \\ 0 & X & X \end{pmatrix}, \quad m_\nu = \begin{pmatrix} 0 & 0 & 0 \\ 0 & X & X \\ 0 & X & X \end{pmatrix}, \tag{3.16}$$

here also no special relation (such as an accidental vanishing of 23 block determinant) is imposed among the non-vanishing entries of m_ν, denoted by X, except $m_{12}^\nu = m_{21}^\nu$. Therefore, m_ν is allowed to have rank 2, in which case it cannot be obtained within the high-scale theory. This implies that high- and low-scale versions of the flavour symmetry arguments are not equivalent. This happened due to the fact that the vectorlike part of U^l is not contained in U^ν. In this example irrep decompositions of the high-scale representations are $U_H^l = \mathbf{1} + 1 + 1$, $U_H^\nu = \mathbf{1} + \bar{\mathbf{1}} + 1$ and $U_H^e = \mathbf{1} + \mathbf{1} + 1$. The vectorlike part of U^l is in fact the ones acting trivially on l_2 and l_3, which have charge zero, and

that are not entirely contained in U^ν, as only one trivial (charge zero) representation has contained in U^ν.

If, on the other hand, U^ν_H is vectorlike and contains U^l_{L0}, then low-scale discussion does capture the results of the high-scale analysis in the symmetric limit. So there are two important cases in which the low-scale discussion of a flavour symmetry does not reproduce the results obtained at high-scale, not even in the symmetric limit: a) when U^ν_H is not vectorlike, b) when U^ν_H does not contain vectorlike part of U^l_L.

3.2.3 The high-scale flavour symmetry forcing a given pattern of lepton masses and mixing

In chapter 2 we have considered the problem of finding all possible flavour groups and their representations leading to an approximate description of lepton masses and mixings in the symmetric limit. We have found a complete solution of the problem based on a low-scale analysis. We can now use the results in section 3.2.2 to extend the analysis to a high-scale theory, more precisely for a type I see-saw theory. Our study will include two cases, the high- and low-scale analyses are equivalent or inequivalent. We will be interested more in the latter case where high-scale study is not equivalent to the low-scale limit, as the equivalent case just reproduces the results we already had in chapter 2. The possible low-scale flavour groups and their representations forcing each of the mass patterns in table 2.1 together with a viable form of PMNS in eq. (3.17) are given in table 2.4. All of these representations are characterized in terms of the structures of the decompositions of U^l_L and U^e_L in irrep components, only differences now in the high-scale analysis will be the singlet neutrino representations, containing the vectorlike part of the lepton doublet representations, are taken into account.

As a reminder for the our setup, the lepton flavour pattern providing (according to our subjective definition) an approximate description of the measured flavour observables are those in which the charged lepton and light neutrino masses are in one of the forms in the first two columns of table 2.1 and in which the PMNS matrix has one of the following two forms

$$U_{\rm PMNS} = \begin{pmatrix} X & X & 0 \\ X & X & X \\ X & X & X \end{pmatrix} \quad \text{or} \quad U_{\rm PMNS} = \begin{pmatrix} X & X & X \\ X & X & X \\ X & X & X \end{pmatrix} , \tag{3.17}$$

where X denotes a generic non-zero entry, for at least one choice of the mass eigenstates. This specification is necessary when two or more masses are degenerate in the approximate description.

We have said that the low-scale representation U_L of the flavour group G forces the flavour pattern associated to one of the mass patterns in table 2.1 if following two conditions hold: i) for each $\mathcal{L}_L$ as in eq. (3.2), invariant under U_L, the lepton masses are in the form specified by that mass pattern; and the PMNS matrix is in one of the two forms

in eq. (3.17) for at least one choice of the mass eigenstates.[2] ii) There exists a $\mathcal{L}_L$ as in eq. (3.2), invariant under U_L, such that the lepton masses are in the form specified by the mass pattern; and the PMNS matrix is in one of the two forms in eq. (3.17) for at least one choice of the mass eigenstates.

We call the lepton mass and mixing patterns are generic iff all the masses allowed to be different from each other and non-zero are indeed different from each other and non-zero; and all entries of PMNS matrix allowed to be non-zero are indeed non-zero.

In the previous chapter we have done full characterization of all possible flavour symmetry and their representations in the low-scale analysis. Now we are going to solve the same problem in the case of a flavour symmetry constraining the high-scale theory in eq. (3.7). In other words, we would like to find all possible high-scale flavour groups and their representations forcing each of the charged lepton and neutrino mass patterns in the first two columns of table 2.1 and the form of PMNS matrix in eq. (3.17). During the work of finding irrep decompositions of flavour groups, we use the results in section 3.2.2 to reduce the high-scale problem to the low-scale problem when they are equivalent, and to find the full list of cases not captured by the low-scale analysis when they are not equivalent.

In order to give a definition of the problem in high-scale theory, it is better to start with defining when a high-scale representation U_H is said to force a certain flavour pattern in the symmetric limit. Here again we encounter the same caveat discussed in section 3.2.2, though: one or more of the heavy singlet masses might vanish in the symmetric limit and be generated only once symmetry breaking is taken into account. So we need to treat such a case, in which M is singular in the symmetric limit, separately. There will be detailed discussions for that case in section 3.3. For the time being, let us only consider the cases of high-scale representations for which M is allowed to be non-singular in the symmetric limit. We can then introduce the following definition. We say that the high-scale representation U_H of the flavour group G forces the flavour pattern associated to one of the mass patterns in table 2.1 if:

- U_H is vectorlike so that a non-singular invariant mass term exists for the heavy singlet neutrinos.
- For each $\mathcal{L}_H$ as in eq. (3.7), invariant under U_H, with non-singular M, the light lepton masses are in the form specified by that mass pattern; and the PMNS matrix is in one of the two forms in eq. (3.17) for at least one choice of the mass eigenstates.
- There exists a $\mathcal{L}_H$ as in eq. (3.7), invariant under U_H, such that M is non-singular; the light lepton masses are in the form specified by the mass pattern and generic; and there is a viable form of PMNS matrix, for at least one choice of mass pattern, as in eq. (3.17) and all of its non-zero entries are generic.

[2] The second requirement is trivial here, as every PMNS matrix is in the second form in eq. (3.17).

As emphasized before, we aim at a complete classification of the flavour groups G and their high-scale representations U_H leading, in the symmetric limit, to a given flavour pattern. Since the flavour observables only depend on the low-scale effective Lagrangian, we first of all wonder whether the low-scale analysis might capture all the possibilities covered by the high-scale analysis, at least in the case in which M is allowed to be non-singular in the symmetric limit. If that was the case, we could use the results obtained for the low-scale representations to characterize the high-scale ones: the high-scale representations forcing a given pattern would be those whose low-scale limit is given in table 2.4. This turns out to be possible when the low- and high-scale representations are equivalent in the symmetric limit, but not when they are inequivalent. The interesting cases will appear either U_H^ν does not contain the vectorlike part of U_H^l or M is singular in the symmetric limit due to U_H^ν not being vectorlike.

The equivalent conditions for the low- and high-scale analyses forcing the same pattern is analogous to the conditions for the representations in two analyses being equivalent. Given a certain flavour pattern, there is always exists a high-scale representation U_H forcing the same pattern for every low-scale representation U_L forcing that pattern. And the necessary and sufficient condition to high-scale representation and its low-scale limit force same patterns is U_H^ν have to be vectorlike and it contains the vectorlike part of the U_H^l. The proof of this statement can be found in appendix B.

We then conclude that there are two important cases in which the low-scale analysis fails in characterizing the high-scale flavour symmetries forcing a certain flavour patter in the symmetric limit:

1. When U_H^ν is not vectorlike.

2. When U_H^ν does not contain the vectorlike part of U_H^l.

We will discuss above two cases in sections 3.3 and 3.4, respectively.

3.3 Analysis for M is singular in the symmetric limit

Let us now focus on the case in which M is singular in the symmetric limit. This is the case iff U_H^ν is not vectorlike, i.e. iff in the decomposition of U_H^ν into a vectorlike and fully chiral part, $U_H^\nu = (U_H^\nu)_0 + (U_H^\nu)_1$, the fully chiral part $(U_H^\nu)_1$ is not empty.

We would like to provide a complete classification of the flavour groups G and their high-scale representations U_H leading, in the symmetric limit, to a given flavour pattern. However, the flavour pattern is not even defined now in the symmetric limit, as M is singular and the effective theory approach leading to eqs. (3.8, 3.10) does not apply in the symmetric limit. In the realistic limit in which symmetry breaking effects are present, all singlet neutrino masses are non-vanishing by hypothesis, and much larger than the

EW scale, so that the effective theory approach can be applied. But not in the symmetric limit, when the symmetry breaking effects are switched off.

In order to obtain an intuition of how a flavour pattern in the symmetric limit can be defined even when some of the singlet neutrino masses vanish, let us start from the case in which singlet neutrino mass matrix becomes non-singular after the symmetry breaking effects are considered. The light neutrino masses are inversely proportional to the singlet neutrino masses. Therefore, we expect some of the light neutrino masses to grow and diverge when we take the symmetric limit.[3] In comparison, the mass of the neutrinos whose mass does not diverge in the symmetric limit is hierarchically smaller, with the ratio of masses set by the size of symmetry breaking effects. In the symmetric limit we can then consider the latter masses to vanish and only those that formally diverge to be non-zero. The non-zero masses (if more than one) could be hierarchical, as their relative size depends on the detailed structure of symmetry breaking effects.

The main points in this section are the following: we will consider the same neutrino mass patterns that we have discussed before, i.e. those in the first two columns of table 2.1, but now i) the non-vanishing entries are supposed to correspond to light neutrino masses diverging in the symmetric limit, and the zero entries are supposed to correspond to light neutrino masses that are finite or vanishing in the symmetric limit and ii) hierarchies among the non-zero entries are allowed (and determined by symmetry breaking effects).

We said above that we expect some of the light neutrino masses to grow and diverge when we take the symmetric limit. Whether some of the light neutrino masses indeed diverge in the symmetric limit, and how many, actually depends on the interplay between the singlet neutrino mass matrix and the Dirac neutrino mass matrix. In order to see how, let us recover an expression for the potentially divergent part of the light neutrino mass matrix.

Let us denote by $M^{(0)}$ the singlet neutrino mass matrix in the symmetric limit and by $M^{(1)}$ the symmetry breaking corrections, so that the full singlet neutrino mass matrix is $M = M^{(0)} + M^{(1)}$. Analogously, let $m_N = m_N^{(0)} + m_N^{(1)}$ be the corresponding decomposition of the Dirac neutrino mass matrix into the symmetric ($m_N^{(0)}$) and symmetry breaking ($m_N^{(1)}$) components.

Without loss of generality, we can order the singlet neutrino irreps in such a way that the first n_0 neutrinos form the vectorlike component $(U_H^\nu)_0$ of the singlet neutrino representation and the remaining $n_1 = n - n_0$ neutrinos form the fully chiral component

[3] Actually, no divergence ever arise. When the symmetry breaking effects are gradually switched off, and the singlet neutrino mass vanishing in the symmetric limit decreases. At some point, it approaches, and crosses, the EW scale threshold. When the singlet neutrino mass becomes comparable to the Dirac mass induced by EWSB through its neutrino Yukawa coupling, the effective approach, and the see-saw formula, do not apply anymore. The Dirac mass contribution eventually dominates and the singlet neutrino forms a Dirac neutrino pair with the active neutrino paired by the Dirac mass term.

$(U_H^\nu)_1$. The singlet mass matrices then have a corresponding block decomposition

$$M = \left(\begin{array}{c|c} M_{00} & M_{01} \\ \hline M_{10} & M_{11} \end{array}\right), \quad M^{(0)} = \left(\begin{array}{c|c} M_{00}^{(0)} & 0 \\ \hline 0 & 0 \end{array}\right), \quad M^{(1)} = \left(\begin{array}{c|c} M_{00}^{(1)} & M_{01}^{(1)} \\ \hline M_{10}^{(1)} & M_{11}^{(1)} \end{array}\right). \tag{3.18}$$

Correspondingly, the Dirac mass matrices have a decomposition into a $n_0 \times n$ block of m_{N0} and a $n_1 \times n$ block of m_{N1},

$$m_N = \left(\begin{array}{c} m_{N0} \\ \hline m_{N1} \end{array}\right), \quad m_N^{(0)} = \left(\begin{array}{c} m_{N0}^{(0)} \\ \hline m_{N1}^{(0)} \end{array}\right), \quad m_N^{(1)} = \left(\begin{array}{c} m_{N0}^{(1)} \\ \hline m_{N1}^{(1)} \end{array}\right). \tag{3.19}$$

Because of the presence of vanishing blocks in $M^{(0)}$, the light neutrino mass matrix is potentially dominated by the exchange of the last n_1 singlet neutrinos. A perturbative expression for the light neutrino mass matrix, in the small $M^{(1)}$ approximation can be obtained by means of effective field theory by integrating out the singlet neutrinos in two steps: the first n_0 heavier ones first and subsequently the remaining n_1 lighter ones. We then get

$$-m_\nu \approx [\tilde{m}_{N1}]^T [\tilde{M}_{11}]^{-1} [\tilde{m}_{N1}] + m_{N0}^T \left[M_{00}^{(0)}\right]^{-1} m_{N0}, \tag{3.20}$$

where

$$\tilde{m}_{N1} = m_{N1} - M_{10}^{(1)} {M_{00}^{(0)}}^{-1} m_{N0}\,, \qquad \tilde{M}_{11} = M_{11}^{(1)} - M_{10}^{(1)} {M_{00}^{(0)}}^{-1} M_{01}^{(1)}\,. \tag{3.21}$$

The first term in eq. (3.20) contains the part that is potentially divergent in the limit in which symmetry breaking effects vanish, while the second term is certainly finite. As the maximum rank of $\tilde{m}_{N1}$ is n_1, we can have at most n_1 divergent light neutrino masses.

We can now ask the question: is the exact number of divergent light neutrino masses independent of the symmetry breaking effects? The answer depends on the structure of the flavour representations U_ν^H and U_l^H. In order to see that, let us further split the first term in eq. (3.20) in two parts:

$$-[\tilde{m}_{N1}]^T [\tilde{M}_{11}]^{-1} [\tilde{m}_{N1}] = m_\nu^\infty + m_\nu^{\rm ind}\,, \tag{3.22}$$

where $m_\nu^\infty = -[m_{N1}^{(0)}]^T [\tilde{M}_{11}]^{-1} [m_{N1}^{(0)}]$. Let $r \leq n_1$ be the rank of $m_{N1}^{(0)}$. In the symmetric limit, the first term, m_ν^∞, gives rise to r divergent light masses and $n - r$ vanishing light masses. If the rank of $m_{N1}^{(0)}$ is maximal, $r = n_1$, then the number of divergent light masses is n_1 and does not depend on symmetry breaking effects. Moreover, m_ν^∞ gives the leading order approximation of m_ν in the symmetric limit. If on the other hand the rank of $m_{N1}^{(0)}$ is less than maximal, $r < n_1$, r light masses will diverge. Whether the

remaining $n_0 - r$ potentially divergent masses do indeed diverge depends however on the interplay of the symmetry breaking effects in $m_\nu^{\rm ind}$. The number of divergent light masses then depends on symmetry breaking effects. We can conclude that the condition for the number of divergent light neutrino masses not to depend on symmetry breaking effects is that the rank of $m_{N1}^{(0)}$ is maximal. It is easy to see that this is the case if and only if the representation on the singlet neutrinos associated to $m_{N1}^{(0)}$, i.e. the fully chiral part of the singlet neutrino representation $(U_\nu^H)_1$, is contained in the complex conjugate of the representation on lepton doublets: $(U_\nu^H)_1^* \subseteq U_l^H$.

All in all, when the singlet neutrino mass matrix M is singular we have two cases: all light neutrino masses corresponding to the chiral part of the singlet neutrino representations divergent if $(U_\nu^H)_1^* \subseteq U_l^H$, otherwise the light neutrino mass are partially divergent (or not divergent at all) in the symmetric limit. We will study these cases in the following two sections.

3.3.1 M is singular in the symmetric limit and $(U_\nu^H)_1^* \nsubseteq U_l^H$

In such a case, the mass pattern depends on symmetry breaking effects, as a number of potentially divergent masses rely on how many irreps in chiral part of U_ν^H are contained in the complex conjugate of U_l^H and also on the specific way of symmetry breaking. For this reason, we do not investigate it further.

3.3.2 M is singular in the symmetric limit and $(U_\nu^H)_1^* \subseteq U_l^H$

When all the complex conjugated irreps of the chiral part of U_ν^H are included in U_l^H, the mass pattern is independent of the structure of symmetry breaking effects (as long as the non-zero entries are allowed to be hierarchical). The neutrino mass pattern contains as many non-zero masses as the dimension of the fully chiral part of the singlet neutrino representation $(U_\nu^H)_1$. The matrix m_ν^∞ in eq. (3.22) gives the leading order approximation of m_ν in the symmetric limit:

$$m_\nu = m_\nu^\infty + \text{subleading corrections.} \tag{3.23}$$

Without loss of generality, we can choose a basis for the lepton doublets such that the last n_1 leptons are invariant under U_l^H and they transform with the conjugated representation $(U_\nu^H)_1^*$.

Let us now discuss whether a definite prediction for the structure of the PMNS matrix in the symmetric limit is possible and, in such a case, provide a complete classification of the flavour groups and high-scale representations leading to a viable flavour pattern in the symmetric limit.

By using the results in [155], it is possible to show that the $n_1 \times n$ matrix $m_{N1}^{(0)}$ can be brought in a block form by means of a unitary $n \times n$ transformation V_ν commuting with

U_l^H:

$$m_{N1}^{(0)} = \left(\begin{array}{c|c} 0 & \tilde{m}_{N1}^{(0)} \end{array} \right) V_\nu \,, \tag{3.24}$$

where $\tilde{m}_{N1}^{(0)}$ is a $n_1 \times n_1$ G-invariant matrix. The matrix V_ν is generic, meaning that any unitary matrix V_ν can be obtained from eq. (3.24) for an appropriate invariant $m_{N1}^{(0)}$. We then have

$$m_\nu^\infty = V_\nu^T \left(\begin{array}{c|c} 0 & 0 \\ \hline 0 & -[\tilde{m}_{N1}^{(0)}]^T \tilde{M}_{11}^{-1} [\tilde{m}_{N1}^{(0)}] \end{array} \right) V_\nu = (H_\nu V_\nu)^T \left(\begin{array}{c|c} 0 & 0 \\ \hline 0 & \begin{array}{ccc} a_1 & & \\ & \ddots & \\ & & a_{n_1} \end{array} \end{array} \right) (H_\nu V_\nu) \,, \tag{3.25}$$

where

$$H_\nu = \left(\begin{array}{c|c} \mathbf{1} & 0 \\ \hline 0 & \tilde{H}_\nu \end{array} \right) \quad \text{and} \quad -[\tilde{m}_{N1}^{(0)}]^T \tilde{M}_{11}^{-1} [\tilde{m}_{N1}^{(0)}] = \tilde{H}_\nu^T \begin{pmatrix} a_1 & & \\ & \ddots & \\ & & a_{n_1} \end{pmatrix} \tilde{H}_\nu \,, \tag{3.26}$$

with $\tilde{H}_\nu$ unitary matrix.

Eq. (3.25) leads to a full diagonalization of the neutrino mass matrix (m_ν^∞) in the symmetric limit in terms of the unitary matrix $H_\nu V_\nu$. In order to identify the neutrino contribution to the PMNS matrix, we still need to identify further ingredients. First, we should take into account a possible permutation P_ν needed to take the neutrino masses in standard ordering. Then, we should note that the mass eigenstates associated to the first n_0 neutrinos are undefined in the limit in which eq. (3.25) holds. The mass eigenstates are determined by the corrections to eq. (3.25) splitting the values of the first n_0 neutrino masses. While in the low-scale analysis such corrections are determined by symmetry breaking effects, here the corrections are provided by the second term in eq. (3.20), which does not depend on symmetry breaking. The diagonalization of the upper $n_0 \times n_0$ block of the neutrino mass matrix will then provide an additional component U_0 to the neutrino contribution to the PMNS matrix acting only on the first n_0 neutrino. The determination of the structure of such a contribution follows the rules described in the section 3.4.2.

Now let us apply this general discussion for the case of singlet neutrino mass matrix has one vanishing eigenvalue. According to the relation between the mass matrix and the irrep pattern we know that the singlet neutrino representation has one-dimensional fully chiral part and two-dimensional vectorlike part. Obviously, the one-dimensional fully chiral part is nothing but a one-dimensional complex representation, so the structure of the representation is $U_H^\nu = r + \mathbf{1}$, where r is vectorlike part, possibly reducible, and has

a form in one of the following options:

$$2, \quad 1+1, \quad 1+1', \quad \mathbf{1}'+\overline{\mathbf{1}'}, \quad \mathbf{1}+\bar{\mathbf{1}}. \tag{3.27}$$

In order to have one divergent light neutrino mass in the symmetric limit, lepton doublet representation U_H^l must contain $\bar{\mathbf{1}}$. So it has a from $U_H^l = \bar{\mathbf{1}} + s$, where the representation s can be reducible and no any constraints on it. Concerning the components of $U_{\rm PMNS}$, we can read V_ν in eq. eq. (3.24) from the condition that it commutes with U_H^ν, or it is equivalently fixed by number of $\bar{\mathbf{1}}$ in U_H^ν. If we neglect the symmetric limit correction to light neutrino masses then first two masses are zero thus H_ν is always a 12 block unitary rotation. The irrep decompositions for the viable patterns of masses and mixings are listed in table 3.1, results are shown in a way of comparing the low- and high-scale analysis. The light neutrino mass spectrum in high-scale analysis is in the normal ordering, since one of the neutrino mass from symmetry breaking is much larger than other two. Non-zero charged lepton masses depend on the number of conjugated irrep pairs between the U_l and U_{e^c}. In the high-scale analysis, results in the first three rows are analogous to each other, this is because the irrep decompositions of U_{e^c} are similar, possible irrep patterns of U_H^ν is the same and the way of irrep conjugation between the U_H^l and $U_H^{e^c}$ is also the same. So the high-scale analysis for the one row can simply be extended to the other two. But, notice that, the results in these three rows from the low-scale analysis are different. More precisely, there are different forms of the $U_{\rm PMNS}$ such as, apart from being viable, the 33 element is forced to be zero or the $U_{\rm PMNS}$ is just a 2×2 block matrix. In the high-scale analysis, structures of the PMNS matrix in all cases contains a unitary rotation H_{12}^ν due to the block of two zero neutrino masses, which will be fixed by the symmetric limit. To have viable mixing matrix in this case, the H_{12}^ν must be a large rotation, where as the H_{12}^E, if it appears, requires to be a small rotation in order to have a small 13 element. One may notice that the H_{12}^E and H_{12}^ν are now, in the high-scale analysis, determined by the symmetric limit not by the symmetry breaking effect, which is in contrast to the determination of these two components in the low-scale analysis. In case the H_{12}^E component becomes a big rotation, then the smallness of 13 element turns out to be accidental. In the last row of the table, the only advantage of the high-scale analysis compared to the low-scale version is that the neutrino mass spectrum is predicted to be in the normal hierarchy, although the form of PMNS is undetermined as in the case of low-scale result.

One can go further to the next step by discussing the singlet neutrinos are forced to have two vanishing masses in the symmetric limit. The results for this case are given in the table 3.2. There is no prediction for the neutrino mass hierarchy, as the relative size of two non-zero masses are not determined. The PMNS matrix in the high-scale analysis can have a small 13 element if H_{12}^E is a small rotation and neutrino masses are in the inverted hierarchy, otherwise there is no guarantee to have a small 13 entry. Allowed forms of the PMNS matrix in the low-scale results are arbitrary due to the vanishing

neutrino masses in the symmetric limit.

The last case with three zero singlet neutrino masses in the symmetric limit is less interesting, that is because of the fact that both heavy and light neutrino masses are determined by symmetry breaking effects and there is no prediction for the light neutrino mass hierarchy.

3.4 Analysis for M is non-singular in the symmetric limit

The work in this section covers a complete characterization of the flavour group representations for two cases depending on the low- and high-scale analyses are equivalent or not. In the following we will discuss each of them in turn.

3.4.1 M is non-singular and $(U_H^l)_0 \subseteq U_H^\nu$ in the symmetric limit

As we already know from the equivalence of two analyses, the results of previous chapter can provide a complete classification of the flavour groups G and their high-scale representations U_H (when M is non-singular in the symmetric limit and U_H^ν contains the vectorlike part of U_H^l) leading, in the symmetric limit, to a given flavour pattern. In other words, we know that the flavour pattern forced by U_H is the same as the flavour pattern forced by its low-scale limit U_L. Therefore, we can use the results obtained in [155] for the high-scale representations forcing a given flavour pattern. We concluded that U_H forces the flavour pattern associated to a given mass pattern in table 2.1 iff the irrep decomposition of U_H^l and U_H^e appears in table 2.4 corresponding to that mass pattern. Regarding the irrep patterns of the singlet neutrino representation U_H^ν, it is required to be vectorlike and must contain the vectorlike part of U_H^l. According to the irrep patterns of U_H^l in this table, we can easily see that conditions on U_H^ν can uniquely determine its irrep decomposition. For example, from the irrep decomposition of $U_H^l = 1 + 1 + 1$, we know that the singlet neutrino irrep pattern is $U_H^\nu = 1 + 1 + 1$. In the high-scale result light neutrino mass hierarchy is not determined, which is the same as what we get in the low-scale analysis. In the case of $U_H^l = \mathbf{1} + \mathbf{1} + \overline{\mathbf{1}}$, singlet neutrino representation must have the form $U_H^\nu = 1 + \mathbf{1} + \overline{\mathbf{1}}$. This results in the inverted hierarchy of light neutrino masses in the high-scale analysis, that is also the same in the low-scale limit. When these two analysis become equivalent, all possible irrep decompositions of the high scale analysis, providing viable patterns of lepton masses and mixing, are shown in the table 3.3. Due to the equivalence, discussions in the low-scale analysis can also apply to the high-scale results.

U_H^ν	U_H^l	U_{e^c}	m_E	high-scale analysis						low-scale analysis							
				m_H^ν	H_E	P_E	V	H_ν	$U_{\rm PMNS}$	m_L^ν	H_E	P_E	V	D	P_ν	H_ν	$U_{\rm PMNS}$
$r+\bar{\mathbf{1}}$	$1+\mathbf{1}+\mathbf{1}$	$s \not\supset 1, \bar{\mathbf{1}} + \bar{\mathbf{1}}$	$(0\ 0\ A)$	$(0\ 0\ \alpha)$	H_{12}^E		V_{23}	H_{12}^ν	none (13)	$(0\ 0\ a)$	H_{12}^E		V_{23}		$P_{1\to3}^\nu$		33
		$s \neq 1 + \bar{\mathbf{1}} + \bar{\mathbf{1}}$	$(0\ B\ A)$	$(0\ 0\ \alpha)$			V_{23}	H_{12}^ν	13	$(0\ 0\ a)$			V_{23}		$P_{1\to3}^\nu$		2×2
		$1 + \bar{\mathbf{1}} + \bar{\mathbf{1}}$	$(C\ B\ A)$	$(0\ 0\ \alpha)$		P_E	V_{23}	H_{12}^ν	$13, 23, 33$	$(0\ 0\ a)$		P_E	V_{23}		$P_{1\to3}^\nu$		2×2
$r+\bar{\mathbf{1}}$	$\bar{\mathbf{1}}+\mathbf{1}+\mathbf{1}$	$s \not\supset \mathbf{1}, \bar{\mathbf{1}} + \bar{\mathbf{1}}$	$(0\ 0\ A)$	$(0\ 0\ \alpha)$	H_{12}^E		V_{23}	H_{12}^ν	none (13)	$(a\ a\ 0)$	H_{12}^E		V_{23}	D_{12}			none (13)
		$s \neq \mathbf{1} + \bar{\mathbf{1}} + \bar{\mathbf{1}}$	$(0\ B\ A)$	$(0\ 0\ \alpha)$			V_{23}	H_{12}^ν	13	$(a\ a\ 0)$			V_{23}	D_{12}			13
		$\mathbf{1} + \bar{\mathbf{1}} + \bar{\mathbf{1}}$	$(C\ B\ A)$	$(0\ 0\ \alpha)$		P_E	V_{23}	H_{12}^ν	$13, 23, 33$	$(a\ a\ 0)$		P_E	V_{23}	D_{12}			$13, 23, 33$
$r+\bar{\mathbf{1}}$	$\mathbf{1'}+\mathbf{1}+\mathbf{1}$	$s \not\supset \bar{\mathbf{1}}, \overline{\mathbf{1'}} + \bar{\mathbf{1}}$	$(0\ 0\ A)$	$(0\ 0\ \alpha)$	H_{12}^E		V_{23}	H_{12}^ν	none (13)	$(0\ 0\ 0)$			V				V
		$s \neq \overline{\mathbf{1'}} + \bar{\mathbf{1}} + \bar{\mathbf{1}}$	$(0\ B\ A)$	$(0\ 0\ \alpha)$			V_{23}	H_{12}^ν	13	$(0\ 0\ 0)$			V				V
		$\overline{\mathbf{1'}} + \bar{\mathbf{1}} + \bar{\mathbf{1}}$	$(C\ B\ A)$	$(0\ 0\ \alpha)$		P_E	V_{23}	H_{12}^ν	$13, 23, 33$	$(0\ 0\ 0)$			V				V
$r+\bar{\mathbf{1}}$	$\mathbf{1}+\mathbf{1}+\mathbf{1}$	$s \not\supset \bar{\mathbf{1}} + \bar{\mathbf{1}}$	$(0\ 0\ A)$	$(0\ 0\ \alpha)$			$V_{3\times3}$		$U_{3\times3}$	$(0\ 0\ 0)$			V				V
		$s \neq \bar{\mathbf{1}} + \bar{\mathbf{1}} + \bar{\mathbf{1}}$	$(0\ B\ A)$	$(0\ 0\ \alpha)$			$V_{3\times3}$		$U_{3\times3}$	$(0\ 0\ 0)$			V				V
		$\bar{\mathbf{1}} + \bar{\mathbf{1}} + \bar{\mathbf{1}}$	$(C\ B\ A)$	$(0\ 0\ \alpha)$			$V_{3\times3}$		$U_{3\times3}$	$(0\ 0\ 0)$			V				V

Table 3.1: Summary of the results from the case in which one singlet neutrino having a vanishing mass in the symmetric limit. Representation r is vectorlike and possibly reducible, and $V = V_e V_\nu^\dagger$. $P_{i\to j}$ denotes any permutation such that $\sigma(i) = j$, while $P_{i\leftrightarrow j}$ denotes the switch of i and j or the identity permutation. P_E is a generic permutation.

U_H^ν	U_H^l	U_{e^c}	m_E	high-scale analysis							low-scale analysis							
				m_H^ν	H_E	P_E	V	H_ν	P_ν	$U_{\rm PMNS}$	m_L^ν	H_E	P_E	V	D	P_ν	H_ν	$U_{\rm PMNS}$
$1+\bar{\mathbf{1}}+\overline{\mathbf{1}'}$	$\mathbf{1}+\mathbf{1}+\mathbf{1}'$	$\bar{\mathbf{1}}+r\not\supseteq\bar{\mathbf{1}},\overline{\mathbf{1}'}$	$(0\ 0\ A)$	$(0\ \beta\ \alpha)$	H_{12}^E		V_{23}	H_{12}^ν	$P_{3\to1}^\nu$ if NH **id** if IH	$U_{3\times3}$	$(0\ 0\ 0)$			V				V
		$\bar{\mathbf{1}}+\bar{\mathbf{1}}+r\neq\overline{\mathbf{1}'}$	$(0\ B\ A)$	$(0\ \beta\ \alpha)$			V_{23}	H_{12}^ν	**id** if IH	13	$(0\ 0\ 0)$			V				V
		$\bar{\mathbf{1}}+\bar{\mathbf{1}}+\overline{\mathbf{1}'}$	$(C\ B\ A)$	$(0\ \beta\ \alpha)$		P_E	V_{23}	H_{12}^ν	**id** if IH	$i3$ (13)	$(0\ 0\ 0)$			V				V
$1+\bar{\mathbf{1}}+\bar{\mathbf{1}}$	$\mathbf{1}+\mathbf{1}+\mathbf{1}$	$r\not\supseteq\bar{\mathbf{1}}\ +\bar{\mathbf{1}}$	$(0\ 0\ A)$	$(0\ \beta\ \alpha)$			$V_{3\times3}$			$V_{3\times3}$	$(0\ 0\ 0)$			V				V
		$r\neq\bar{\mathbf{1}}\ +\bar{\mathbf{1}}+\bar{\mathbf{1}}$	$(0\ B\ A)$	$(0\ \beta\ \alpha)$			$V_{3\times3}$			$V_{3\times3}$	$(0\ 0\ 0)$			V				V
		$\bar{\mathbf{1}}+\bar{\mathbf{1}}+\bar{\mathbf{1}}$	$(C\ B\ A)$	$(0\ \beta\ \alpha)$			$V_{3\times3}$			$V_{3\times3}$	$(0\ 0\ 0)$			V				V

Table 3.2: Summary of the results from the case in which two singlet neutrinos having vanishing masses in the symmetric limit. Here we suppose $\alpha > \beta > 0$, and **id** stands for the identity matrix. The V includes both contributions from the charged lepton and the neutrino sector, and $P_{i\to j}$ denotes any permutation such that $\sigma(i) = j$, while $P_{i\leftrightarrow j}$ denotes the switch of i and j or the identity permutation. P_E is a generic permutation.

irreps	masses	ν hierarchy	U_{PMNS}	zeros
$1 \quad 1 \quad 1$ $1 \quad r \not\supseteq 1$ $1 \quad 1 \quad 1$	$(A00)$ (abc)	NH or IH	V	none
$\mathbf{1} \quad \mathbf{1} \quad \overline{\mathbf{1}}$ $\overline{\mathbf{1}} \quad r \not\supseteq \mathbf{1}, \overline{\mathbf{1}}$ $1 \quad \overline{\mathbf{1}} \quad \mathbf{1}$	$(A00)$ $(0aa)$	IH	$H_{12}^{E} V_{23} D_{12}^{-1}$	none $(\mathbf{13})$
$1 \quad 1 \quad 1$ $1 \quad 1 \quad r \neq 1$ $1 \quad 1 \quad 1$	$(AB0)$ (abc)	NH or IH	V	none
$\mathbf{1} \quad \mathbf{1} \quad \overline{\mathbf{1}}$ $\overline{\mathbf{1}} \quad \overline{\mathbf{1}} \quad r \neq \mathbf{1}$ $1 \quad \overline{\mathbf{1}} \quad \mathbf{1}$	$(AB0)$ $(0aa)$	IH	$V_{23} D_{12}^{-1}$	$\mathbf{13}$
$1 \quad 1 \quad 1$ $1 \quad 1 \quad 1$ $1 \quad 1 \quad 1$	(ABC) (abc)	NH or IH	V	none
$\mathbf{1} \quad \mathbf{1} \quad \overline{\mathbf{1}}$ $\overline{\mathbf{1}} \quad \overline{\mathbf{1}} \quad \mathbf{1}$ $1 \quad \overline{\mathbf{1}} \quad \mathbf{1}$	(ABC) $(0aa)$	IH	$P_E V_{23} D_{12}^{-1}$	$\mathbf{13}, 23, 33$

Table 3.3: Possible high-scale irrep decompositions giving rise to viable masses and mixing patterns when M is non-singular and low- and high-scale analyses are equivalent. The first column shows the decomposition of U_H^l, U_H^e and U_H^ν, in this order from above to below. Irreps are denoted by their dimensions. Boldface fonts denote complex representations, regular fonts denote real representations. Primes are used to distinguish inequivalent representations, and in the case of complex representations $\mathbf{1}'$ is supposed to be different from both $\mathbf{1}$ and $\overline{\mathbf{1}}$. "r" denotes a generic, possibly reducible representation, different from or not including the specified irreps, as indicated. No pseudoreal irreps appear. The second column shows the corresponding pattern of charged lepton and neutrino masses in the symmetric limit, one above the other, and the third is the neutrino hierarchy type, normal (NH) or inverted (IH). The structure of the PMNS matrix is then shown. A matrix with no further specification is generic (e.g. P denotes a generic permutation, V a generic unitary matrix). D_{ij} denotes a $\pi/4$ rotation acting in the sector ij. The presence and position of a zero in the PMNS matrix in the symmetric limit is specified in the last column.

3.4.2 M is non-singular and $(U_H^l)_0 \nsubseteq U_H^\nu$ in the symmetric limit

Now we will work out the case where the singlet neutrino mass matrix is non-singular in the symmetric limit and the high-scale analysis is not equivalent to its low-scale limit. The results from the inequivalent cases are listed in the table 3.4, which is organized in a way of comparing the mass spectrum and mixing matrix from two different analyses. In all of these cases both neutrino mass spectrum and mixing patterns are different compared to the low-scale analysis, while charged lepton mass spectrum is the same in both analyses. The former is because of the condition $(U_H^l)_0 \nsubseteq U_H^\nu$, and that is expected from our discussions in previous section. The latter is due to the same choice of irrep

patterns for the U_l and U_e in both analysis. It deserves to emphasis that all masses and mixing patterns can be obtained without knowing the explicit form of mass matrices. The irrep patterns are enough to provide mass spectrum and components of the PMNS matrix from the following simple rules: V commutes with doublet representation, D takes care of Dirac sub-structure, non-trivial H_ν and H_E arise from the degenerate neutrino masses and two vanishing charged lepton masses respectively, and the permutations $P_{\nu,E}$ bring the neutrino and charged lepton masses into the standard ordering. The number of non-zero masses in the light neutrino mass spectrum depends on the rank of the Dirac mass matrix, as the singlet neutrino Majorana mass matrix has a full rank. In addition, the number of non-vanishing neutrino masses is same as the number of irreps in U_H^ν conjugated (equivalent) to the irreps in U_H^l, unless there is an accidental cancellation in the determinant of the non-zero block.

One can see that, from the first two irrep decompositions in table 3.4, neutrino masses are predicted to be in the normal hierarchy, all of the PMNS matrix elements are non-zero and smallness of the 13 element depends on the symmetry breaking effects. Namely, in order to have a form of the PMNS matrix close to the observed pattern, first of all, H_{12}^ν must be a large rotation. Then, the situation depends on the form of H_{12}^E determined from the symmetry breaking: if it becomes a small rotation then there will be a zero in 13 position, otherwise the smallness of the 13 element is not guaranteed. While in the low-scale analysis, the neutrino mass hierarchy is not fixed in the symmetric limit since it depends on the relative sizes of the non-vanishing masses, and PMNS matrix is not in the viable form. In both analyses only the tau lepton has a non-vanishing mass and electron and muon masses are zero in the symmetric limit, so the symmetry breaking effects must be needed to generate masses for the two light charged leptons and also provide mass hierarchy among them.

In the fifth and the sixth irrep decompositions, the flavour symmetry in the high-scale analysis predicts normal hierarchy of the light neutrino mass and also unambiguously fixes a zero in the 13 element of the PMNS matrix in the symmetric limit. In order for the other PMNS matrix elements agree with the experimental data, the large H_{12}^ν rotation must be obtained from the symmetry breaking effects. While in the low-scale results there is no definite hierarchy of neutrino masses, as a consequence of the differences between the non-zero masses are not fixed by the flavour symmetry. Furthermore, there is no explanation for the smallness of the muon mass compared to the tau mass, and form of the PMNS matrix is just a 2×2 block rotation in the symmetric limit which is far from being viable.

The ninth and the tenth irrep decompositions for the high-scale analysis provide normal hierarchy of the neutrino masses, but the charged lepton mass hierarchy is not predicted by the symmetry. And it is not obvious to have a zero fixed for the 13 element of the PMNS matrix, as the position of the zero elements depends on the permutation of charged lepton masses. The results from the low-scale analysis are not so appealing, that is because not only the charged lepton and neutrino mass hierarchies are not predicted

at all but also the PMNS is a 2×2 unitary block rotation which is obviously not close to the observed pattern.

Finally, all the remaining irrep decompositions do not constrain the form of the PMNS matrix in both high- and low-scale analyses, that is mainly because the diagonalization of charged lepton mass matrix requires a generic 3×3 unitary matrix, although there are some cases provide normal hierarchy of the neutrino masses or explain the smallness of electron and muon masses compared to tau lepton mass.

In short, the nice result we can get from this table is that cases with PMNS matrix having a viable form in the high-scale analysis but not in the low-scale analysis predict normal hierarchy of the neutrino mass, which is being preferred by current oscillation data around 3σ level [5].

3.5 The high-scale flavour symmetry in GUT

Our discussions so far have focused only on flavour symmetry of the lepton sector. But there is no reason to prevent flavour symmetry acting on the quark sector as well. A complete and successful flavour theory must take both leptons and quarks into consideration, and give an acceptable solution for the puzzle of observed fermion masses and mixing patterns. As we know, the SM gauge symmetry is an intra-family symmetry, in the sense that it treats the corresponding fermions of different families in a same way and does not mix the fermions in different families. While the flavour symmetry is an inter family symmetry, it does transform non-trivially the leptons (or quarks) of different families and can combine them into a single multiplet. If we imagine every SM fermion with two indices — the fist is family index and the second is gauge group index — then five different types of fermions in the SM can be described solely by their quantum numbers under the flavour symmetry and gauge symmetry regardless of which family they belong to. In this case the flavour symmetry acts horizontally on the row index while gauge symmetry acts vertically on the column index.

More interesting situation will appear when we discuss the problem in the context of the Grand Unified Theories (GUTs) together with a flavour symmetry, as there is a complementary role of the gauge symmetry, unifying the fermions of same family but with different flavours, and flavour symmetry, acting on the different fermion families. For instance, in the context of $SU(5)$ GUT and flavour group G, we have three fermion multiplets of $SU(5)$ gauge group (d_i^c and l_i are in anti-fundamental representation $\bar{5}$; u_i^c, q_i and e_i^c are in the anti-symmetric decuplet representation 10; and ν_i^c are in the singlet) and each of them can transform in the different representations of G. We assume that actions of the gauge and the flavour group representations can commute each other and that fermions in each $SU(5)$ multiplets belong to the same representation of the group G. Further more, when we discuss flavour symmetry in the context of $SO(10)$ GUT, there will be more constraints on the representations of the flavour group. This is because, in

high-scale				low-scale		
irreps	masses	U_{PMNS}	zeros	masses	U_{PMNS}	zeros
$1 \quad 1 \quad 1'$ $1 \quad r \not\supseteq 1, 1'$ $1 \quad s \not\supseteq 1, 1'$	$(A00)$ $(a00)$	$H_{12}^E V_{23} H_{12}^{\nu\,-1}$	none (**13**)	$(A00)$ (abc)	$H_{12}^E V_{23} P_\nu^{-1}$	31, 32, 33
$1 \quad 1 \quad \mathbf{1}$ $1 \quad r \not\supseteq 1, \overline{\mathbf{1}}$ $1 \quad s \not\supseteq 1$	$(A00)$ $(a00)$	$H_{12}^E V_{23} H_{12}^{\nu\,-1}$	none (**13**)	$(A00)$ $(ab0)$	$H_{12}^E V_{23} P_{1\leftrightarrow 3}^{\nu\,-1}$	31, 33
$1 \quad 1 \quad 1$ $1 \quad r \not\supseteq 1$ $1 \quad s \not\supseteq 1$	$(A00)$ $(a00)$	V	none	$(A00)$ (abc)	V	none
$1 \quad 1 \quad 1$ $1 \quad r \not\supseteq 1$ $1 \quad 1 \quad s \neq 1$	$(A00)$ $(ab0)$	V	none	$(A00)$ (abc)	V	none
$1 \quad 1 \quad 1'$ $1 \quad 1 \quad r \neq 1'$ $1 \quad s \not\supseteq 1, 1'$	$(AB0)$ $(a00)$	$V_{23} H_{12}^{\nu\,-1}$	**13**	$(AB0)$ (abc)	$V_{23} P_\nu^{-1}$	4 zeros
$1 \quad 1 \quad \mathbf{1}$ $1 \quad 1 \quad r \neq \overline{\mathbf{1}}$ $1 \quad s \not\supseteq 1$	$(AB0)$ $(a00)$	$V_{23} H_{12}^{\nu\,-1}$	**13**	$(AB0)$ $(ab0)$	$V_{23} P_{1\leftrightarrow 3}^{\nu\,-1}$	4 zeros
$1 \quad 1 \quad 1$ $1 \quad 1 \quad r \neq 1$ $1 \quad s \not\supseteq 1$	$(AB0)$ $(a00)$	V	none	$(AB0)$ (abc)	V	none
$1 \quad 1 \quad 1$ $1 \quad 1 \quad r \neq 1$ $1 \quad 1 \quad s \neq 1$	$(AB0)$ $(ab0)$	V	none	$(AB0)$ (abc)	V	none
$1 \quad 1 \quad 1'$ $1 \quad 1 \quad 1'$ $1 \quad s \not\supseteq 1, 1'$	(ABC) $(a00)$	$P_E V_{23} H_{12}^{\nu\,-1}$	**13**, 23, 33	(ABC) (abc)	$P_E V_{23} P_\nu^{-1}$	4 zeros
$\mathbf{1} \quad 1 \quad 1$ $\overline{\mathbf{1}} \quad 1 \quad 1$ $1 \quad s \not\supseteq 1$	(ABC) $(a00)$	$P_E V_{23} H_{12}^{\nu\,-1}$	**13**, 23, 33	(ABC) $(ab0)$	$P_E V_{23} P_{1\leftrightarrow 3}^{\nu\,-1}$	4 zeros
$1 \quad 1 \quad 1$ $1 \quad 1 \quad 1$ $1 \quad s \not\supseteq 1$	(ABC) $(a00)$	V	none	(ABC) (abc)	V	none
$1 \quad 1 \quad 1$ $1 \quad 1 \quad 1$ $1 \quad 1 \quad 1'$	(ABC) $(ab0)$	V	none	(ABC) (abc)	V	none

Table 3.4: Summary table for the case in which M is non-singular and low- and high-scale analyses are not equivalent. In the first column irrep patterns of U_H^l, U_H^e and U_H^ν are in the successive order of one below the other. The sub-representations r and s can be reducible, and the representation s is required to be vectorlike. $P_{i\leftrightarrow j}$ denotes the transposition of i and j or the identity permutation. Matrix with no further specification is generic (e.g. P_E and P_ν imply generic permutations, and V is a generic 3×3 unitary matrix).

this case, the fermions in each family are unified into a single multiplet of dimension 16 spinorial representation of the gauge group $SO(10)$ and all fermions in this multiplet are considered to transform under the same representation of the flavour group G. In a word, in these flavour symmetric GUT scenarios fermion masses and mixing get more stringent constraints than the ones discussing the flavour and gauge symmetries separately.

When we put GUT constraints on the flavour group representations obtained in the previous sections, there may be some flavour group irrep decompositions accounting for the viable mass and mixing patterns in both lepton and quark sectors. It will be interesting if we can explain the observed lepton and quark masses and mixing simultaneously in the context of GUT flavour symmetry. Before discussing the flavour symmetries of the quark sector we need to remind what are the definitions of the viable quark mass and mixing patterns. As was pointed out in section 2.4, we say both up- and down-type quark mass patterns are viable iff they belong to one of theses three forms $(A, 0, 0)$, $(A, B, 0)$, (A, B, C) and no degenerate non-zero masses are allowed. As for the viable form of CKM matrix, only the diagonal form or at most 12 block rotations are considered to be viable, since all the other quark mixing angles are smaller than 3° except Cabibbo angle which is as big as 13°. Each components of the CKM matrix is given by eq. (2.17), they have similar origins as the components of the PMNS matrix.

In what follows, we will start discussing the $SU(5)$ GUT flavour symmetry. As stated before, all fermions in the same $SU(5)$ multiplets are supposed to transform under the same representation of the flavour group, i.e $U_{\bar{5}} = U_{d^c} = U_l$, $U_{10} = U_{u^c} = U_q = U_{e^c}$ and $U_1 = U_\nu$. Given that we have already found the irrep decompositions for the viable lepton mass patterns and mixings, it is easy to sort out the irrep decompositions of $U_{\bar{5}}$, U_{10} and U_1 from the known forms of U_l, U_{e^c} and U_ν. Imposing the further constraints of viable quark mass and mixing patterns in the symmetric limit selects the results in table 3.5 for the case where M has one vanishing eigenvalue, and table 3.6 summarizes the results for the case in which M has two vanishing eigenvalues. The results in table 3.7 are obtained from the case where the singlet neutrino mass matrix M is non-singular and the low- and high-scale analyses become equivalent. Moreover, tables 3.8 and 3.9 show the results for the case of M is non-singular and the low- and high-scale analyses are inequivalent.

In table 3.5 all of the neutrino mass patterns are in the normal hierarchy, which is the consequence of singlet neutrino mass matrix having one vanishing eigenvalue in the symmetric limit. The charged lepton and down quark mass patterns are always the same, and it is the common feature also in all the other tables. This comes from the fact that both l_i and d_i^c transform under $U_{\bar{5}}$ and both q_i and e_i^c transform under U_{10}. Having such a relation between the representations of leptons and quarks, forms of the invariant mass matrices m_E and m_D are transpose of each other. This, in turn, implies that those two mass matrices have same rank in general, so the number of non-zero eigenvalues are always the same. Furthermore, as we can see, all the mass patterns appeared in down-type quark sector are constrained by the interplay between the representations $U_{\bar{5}}$ and U_{10}, while the up-type quark mass patterns are determined by U_{10} only. The first three rows in table 3.5

provide analogous results for the fermion mass patterns and forms of the CKM and PMNS matrices, this is due to the fact that not only the structure of irrep patterns are similar but also the derivations of the mass and mixing patterns are the same. The CKM matrix associate to the all irrep patterns has two main forms depending on whether or not it contains V_{12}. If there is no V_{12}, form of the $V_{\rm CKM}$ is determined by the permutation ordering the non-vanishing masses of the up-type quarks and by the H_{12}^D from symmetry breaking effect. Only when the combination of these two components provides a diagonal matrix or a small 12 block rotation, then the CKM matrix can accommodate observed quark mixing parameters in the leading order approximation. If, on the other hand, there is a V_{12} contribution, which will remain as it is even after the symmetry breaking, in order to have a realistic mixing matrix we expect V_{12} to be close to the rotation of the Cabibbo angle. In case this expectation is realized, the viable form of $V_{\rm CKM}$ can be obtained when the permutations play trivial role and symmetry breaking fixes $H_{U,D}$ to be diagonal matrix. As for the form of $U_{\rm PMNS}$, there are two possible cases, either all of its entries are non-zero or there is a zero in the 13 position depending on the $H_{E,\nu}$ in the symmetric limit. It is possible to have a viable pattern of the $U_{\rm PMNS}$ and a zero in its 13 element if H_ν becomes a big rotation whereas H_E becomes a small rotation in the symmetric limit. Otherwise, the smallness of the 13 elements is accidental.

Analysis of the results in table 3.6 is basically similar to that in table 3.5, main differences in table 3.6 can be seen from the following two points: there is no definite hierarchy of the neutrino masses, and smallness of $(U_{\rm PMNS})_{13}$ is accidental in all the irrep decompositions.

The results in table 3.7 coincide with the table 2.6, since the low- and high-scale analyses are equivalent. As the discussions of mass patterns and mixings are same as in table 2.6, we will not repeat them here.

Tables 3.8 and 3.9 provide irrep decompositions, mass patterns and form of the mixing matrices when M is non-singular and the low- and high-scale analyses are not equivalent. Both types of hierarchies for the neutrino masses are allowed, and all possible mass patterns appeared in the charged fermion mass spectrum. As a general feature, all the charged lepton and down-type quark mass patterns are always the same, because of the reason stated before. Quark mixing matrix has two kinds of forms with and without V_{12}. If these is no V_{12} in the $V_{\rm CKM}$, then quark mixing pattern depends on the symmetry breaking effects up to the permutation matrix of non-zero masses, while the forms of the $V_{\rm CKM}$ with V_{12} require that V_{12} is close to the rotation of Cabibbo angle. As for the $U_{\rm PMNS}$, the first two irrep decompositions in table 3.8 can contain small 13 element if the rotation H_{12}^E, corresponding to vanishing masses of electron and muon, is small whereas the rotation H_{12}^ν is big, otherwise it is not obvious to have a small 13 element. Irrep decompositions in the next-to-last row of table 3.9 unambiguously fixes the 13 element of PMNS matrix to be zero while the last row of the table shows that $U_{\rm PMNS}$ has a zero in any position of its third column, depending on the permutation for the charged lepton masses.

U_1	$U_{\bar{5}}$	U_{10}	Masses				$V_{\rm CKM}$	$U_{\rm PMNS}$
			m_D	m_U	m_E	m_ν		
$r+\bar{\mathbf{1}}$	$1+\mathbf{1}+\mathbf{1}$	$1'+\mathbf{1}+\bar{\mathbf{1}}$	$(0\ 0\ d)$	$(D\ E\ F)$	$(0\ 0\ A)$	$(0\ 0\ a)$	$P_U H_{12}^{D^{-1}}$	none (13)
		$\mathbf{1}'+\mathbf{1}+\bar{\mathbf{1}}$	$(0\ 0\ d)$	$(0\ D\ E)$	$(0\ 0\ A)$	$(0\ 0\ a)$	$P_{2\leftrightarrow3}^U H_{12}^{D^{-1}}$	none (13)
		$\mathbf{1}+\mathbf{1}+\bar{\mathbf{1}}$	$(0\ 0\ d)$	$(0\ D\ E)$	$(0\ 0\ A)$	$(0\ 0\ a)$	$P_{2\leftrightarrow3}^U V_{12} H_{12}^{D^{-1}}$	none (13)
		$1+\bar{\mathbf{1}}+\bar{\mathbf{1}}$	$(d\ e\ f)$	$(0\ 0\ D)$	$(A\ B\ C)$	$(0\ 0\ a)$	$H_{12}^U V_{12} P_D^{-1}$	$13, 23, 33$
$r+\bar{\mathbf{1}}$	$\bar{\mathbf{1}}+\mathbf{1}+\mathbf{1}$	$1+\mathbf{1}+\bar{\mathbf{1}}$	$(0\ 0\ d)$	$(D\ E\ F)$	$(0\ 0\ A)$	$(0\ 0\ a)$	$P_U H_{12}^{D^{-1}}$	none (13)
		$\mathbf{1}'+\mathbf{1}+\bar{\mathbf{1}}$	$(0\ 0\ d)$	$(0\ D\ E)$	$(0\ 0\ A)$	$(0\ 0\ a)$	$P_{2\leftrightarrow3}^U H_{12}^{D^{-1}}$	none (13)
		$\mathbf{1}+\mathbf{1}+\bar{\mathbf{1}}$	$(0\ 0\ d)$	$(0\ D\ E)$	$(0\ 0\ A)$	$(0\ 0\ a)$	$P_{2\leftrightarrow3}^U V_{12} H_{12}^{D^{-1}}$	none (13)
		$\mathbf{1}+\bar{\mathbf{1}}+\bar{\mathbf{1}}$	$(d\ e\ f)$	$(0\ D\ E)$	$(A\ B\ C)$	$(0\ 0\ a)$	$P_{2\leftrightarrow3}^U V_{12} P_D^{-1}$	$13, 23, 33$
$r+\bar{\mathbf{1}}$	$\mathbf{1}'+\mathbf{1}+\mathbf{1}$	$1+\mathbf{1}+\bar{\mathbf{1}}$	$(0\ 0\ d)$	$(D\ E\ F)$	$(0\ 0\ A)$	$(0\ 0\ a)$	$P_U H_{12}^{D^{-1}}$	none (13)
		$\mathbf{1}'+\mathbf{1}+\bar{\mathbf{1}}$	$(0\ 0\ d)$	$(0\ D\ E)$	$(0\ 0\ A)$	$(0\ 0\ a)$	$P_{2\leftrightarrow3}^U H_{12}^{D^{-1}}$	
		$\mathbf{1}''+\mathbf{1}+\bar{\mathbf{1}}$	$(0\ 0\ d)$	$(0\ D\ E)$	$(0\ 0\ A)$	$(0\ 0\ a)$	$P_{2\leftrightarrow3}^U H_{12}^{D^{-1}}$	
		$\mathbf{1}+\mathbf{1}+\bar{\mathbf{1}}$	$(0\ 0\ d)$	$(0\ D\ E)$	$(0\ 0\ A)$	$(0\ 0\ a)$	$P_{2\leftrightarrow3}^U V_{12} H_{12}^{D^{-1}}$	
$r+\bar{\mathbf{1}}$	$\mathbf{1}+\mathbf{1}+\mathbf{1}$	$1+\mathbf{1}+\bar{\mathbf{1}}$	$(0\ 0\ d)$	$(D\ E\ F)$	$(0\ 0\ A)$	$(0\ 0\ a)$	$P_U H_{12}^{D^{-1}}$	$V_{3\times3}$
		$\mathbf{1}'+\mathbf{1}+\bar{\mathbf{1}}$	$(0\ 0\ d)$	$(0\ D\ E)$	$(0\ 0\ A)$	$(0\ 0\ a)$	$P_{2\leftrightarrow3}^U H_{12}^{D^{-1}}$	$V_{3\times3}$
		$\mathbf{1}+\mathbf{1}+\bar{\mathbf{1}}$	$(0\ 0\ d)$	$(0\ D\ E)$	$(0\ 0\ A)$	$(0\ 0\ a)$	$P_{2\leftrightarrow3}^U V_{12} H_{12}^{D^{-1}}$	$V_{3\times3}$

Table 3.5: Possible forms of SU(5) unified flavour representations for the case of one singlet neutrino having a vanishing mass in the symmetric limit. Representation r is vectorlike and possibly reducible. Form of the fermion masses and of the CKM and PMNS matrices corresponding to viable choices are shown. Neutrino mass pattern and PMNS matrix are obtained from the high-scale results. $P_{2\leftrightarrow3}$ is either the identity permutation or the switch of 2 and 3.

If we discuss flavour symmetry in the context of $SO(10)$ GUT, flavour group representations are very strongly constrained. There is no any flavour group for the description of viable fermion mass and mixing patterns in the symmetric limit. The reason behind this conclusion is that there is no irrep patterns to satisfy $U_{16} \equiv U_1 = U_{\bar{5}} = U_{10}$ and lead to the viable structures of the CKM and PMNS matrices in either case, where the low- and high-scale analyses are equivalent or inequivalent.

3.6 Conclusions and remarks

The main goal of our work in this chapter is to give complete and precise answers to the following two important questions: i) Are the low- and high-scale analyses always equivalent? If not, what are the conditions to be so? ii) Can high-scale flavour symmetry provide approximate description of lepton masses and mixings in the symmetric limit?

U_1	$U_{\bar{5}}$	U_{10}	Masses				$V_{\rm CKM}$	$U_{\rm PMNS}$
			m_D	m_U	m_E	m_ν		
$1+\bar{\mathbf{1}}+\overline{\mathbf{1}'}$	$\mathbf{1}+\mathbf{1}+\mathbf{1}'$	$1+\mathbf{1}+\bar{\mathbf{1}}$	$(0\ 0\ d)$	$(D\ E\ F)$	$(0\ 0\ A)$	$(0\ a\ b)$	$P_U H_{12}^{D\,-1}$	none
		$\mathbf{1}'+\mathbf{1}+\bar{\mathbf{1}}$	$(0\ 0\ d)$	$(0\ D\ E)$	$(0\ 0\ A)$	$(0\ a\ b)$	$P_{2\leftrightarrow3}^U H_{12}^{D\,-1}$	
		$\mathbf{1}''+\mathbf{1}+\bar{\mathbf{1}}$	$(0\ 0\ d)$	$(0\ D\ E)$	$(0\ 0\ A)$	$(0\ a\ b)$	$P_{2\leftrightarrow3}^U H_{12}^{D\,-1}$	
		$\mathbf{1}+\mathbf{1}+\bar{\mathbf{1}}$	$(0\ 0\ d)$	$(0\ D\ E)$	$(0\ 0\ A)$	$(0\ a\ b)$	$P_{2\leftrightarrow3}^U V_{12} H_{12}^{D\,-1}$	
$1+\bar{\mathbf{1}}+\bar{\mathbf{1}}$	$\mathbf{1}+\mathbf{1}+\mathbf{1}$	$1+\mathbf{1}+\bar{\mathbf{1}}$	$(0\ 0\ d)$	$(D\ E\ F)$	$(0\ 0\ A)$	$(0\ a\ b)$	$P_U H_{12}^{D\,-1}$	$V_{3\times3}$
		$\mathbf{1}'+\mathbf{1}+\bar{\mathbf{1}}$	$(0\ 0\ d)$	$(0\ D\ E)$	$(0\ 0\ A)$	$(0\ a\ b)$	$P_{2\leftrightarrow3}^U H_{12}^{D\,-1}$	
		$\mathbf{1}+\mathbf{1}+\bar{\mathbf{1}}$	$(0\ 0\ d)$	$(0\ D\ E)$	$(0\ 0\ A)$	$(0\ a\ b)$	$P_{2\leftrightarrow3}^U V_{12} H_{12}^{D\,-1}$	

Table 3.6: Possible forms of SU(5) unified flavour representations for the case of two singlet neutrinos having vanishing masses in the symmetric limit. Form of the fermion masses and of the CKM and PMNS matrices corresponding to viable choices are shown. Neutrino mass pattern and PMNS matrix are obtained from the high-scale results. $P_{2\leftrightarrow3}$ is either the identity permutation or the switch of 2 and 3.

U_1 and $U_{\bar{5}}$	U_{10}	Masses				$V_{\rm CKM}$	$U_{\rm PMNS}$
		m_D	m_U	m_E	m_ν		
$1+1+1$	$1+\mathbf{1}+\bar{\mathbf{1}}$	$(0\ 0\ d)$	$(D\ E\ F)$	$(0\ 0\ A)$	$(a\ b\ c)$	$P_U H_{12}^{D\,-1}$	$V_{3\times3}$
	$1+1'+1''$	$(0\ 0\ d)$	$(D\ E\ F)$	$(0\ 0\ A)$	$(a\ b\ c)$	$P_U H_{12}^{D\,-1}$	
	$1+1'+1'$	$(0\ 0\ d)$	$(D\ E\ F)$	$(0\ 0\ A)$	$(a\ b\ c)$	$P_U V_{12} H_{12}^{D\,-1}$	
	$1+1'+\mathbf{1}$	$(0\ 0\ d)$	$(0\ D\ E)$	$(0\ 0\ A)$	$(a\ b\ c)$	$P_{2\leftrightarrow3}^U H_{12}^{D\,-1}$	
	$1+\mathbf{2}$	$(0\ 0\ d)$	$(0\ 0\ D)$	$(0\ 0\ A)$	$(a\ b\ c)$	$H_{12}^U H_{12}^{D\,-1}$	
	$1+\mathbf{1}+\mathbf{1}'$	$(0\ 0\ d)$	$(0\ 0\ D)$	$(0\ 0\ A)$	$(a\ b\ c)$	$H_{12}^U H_{12}^{D\,-1}$	
	$1+\mathbf{1}+\mathbf{1}$	$(0\ 0\ d)$	$(0\ 0\ D)$	$(0\ 0\ A)$	$(a\ b\ c)$	$H_{12}^U H_{12}^{D\,-1}$	

Table 3.7: Possible forms of SU(5) unified flavour representations for the case where the singlet neutrino mass matrix is non-singular in the symmetric limit as well as low- and high-scale analyses are equivalent. Form of the fermion masses and of the CKM and PMNS matrices corresponding to viable choices are shown. Neutrino mass pattern and PMNS matrix are obtained from the high-scale results. $P_{2\leftrightarrow3}$ is either the identity permutation or the switch of 2 and 3.

U_1	$U_{\bar{5}}$	U_{10}	Masses				$V_{\rm CKM}$	$U_{\rm PMNS}$
			m_D	m_U	m_E	m_ν		
$1+r\not\supseteq 1,1'$	$1+1+1'$	$1+\mathbf{1}+\bar{\mathbf{1}}$	$(0\ 0\ d)$	$(D\ E\ F)$	$(0\ 0\ A)$	$(0\ 0\ a)$	$P_U H_{12}^{D^{-1}}$	none (13)
		$1+1''+1'''$	$(0\ 0\ d)$	$(D\ E\ F)$	$(0\ 0\ A)$	$(0\ 0\ a)$	$P_U H_{12}^{D^{-1}}$	
		$1+1''+1''$	$(0\ 0\ d)$	$(D\ E\ F)$	$(0\ 0\ A)$	$(0\ 0\ a)$	$P_U V_{12} H_{12}^{D^{-1}}$	
		$1+1''+\mathbf{1}$	$(0\ 0\ d)$	$(0\ D\ E)$	$(0\ 0\ A)$	$(0\ 0\ a)$	$P^U_{2\leftrightarrow 3} H_{12}^{D^{-1}}$	
		$1+\mathbf{2}$	$(0\ 0\ d)$	$(0\ 0\ D)$	$(0\ 0\ A)$	$(0\ 0\ a)$	$H_{12}^U H_{12}^{D^{-1}}$	
		$1+\mathbf{1}+\mathbf{1}'$	$(0\ 0\ d)$	$(0\ 0\ D)$	$(0\ 0\ A)$	$(0\ 0\ a)$	$H_{12}^U H_{12}^{D^{-1}}$	
		$1+\mathbf{1}+\mathbf{1}$	$(0\ 0\ d)$	$(0\ 0\ D)$	$(0\ 0\ A)$	$(0\ 0\ a)$	$H_{12}^U H_{12}^{D^{-1}}$	
$1+r\not\supseteq 1$	$1+1+\mathbf{1}$	$1+\mathbf{1}'+\overline{\mathbf{1}'}$	$(0\ 0\ d)$	$(D\ E\ F)$	$(0\ 0\ A)$	$(0\ 0\ a)$	$P_U H_{12}^{D^{-1}}$	none (13)
		$1+1'+1''$	$(0\ 0\ d)$	$(D\ E\ F)$	$(0\ 0\ A)$	$(0\ 0\ a)$	$P_U H_{12}^{D^{-1}}$	
		$1+1'+1'$	$(0\ 0\ d)$	$(D\ E\ F)$	$(0\ 0\ A)$	$(0\ 0\ a)$	$P_U V_{12} H_{12}^{D^{-1}}$	
		$1+1'+\mathbf{1}$	$(0\ 0\ d)$	$(0\ D\ E)$	$(0\ 0\ A)$	$(0\ 0\ a)$	$P^U_{2\leftrightarrow 3} H_{12}^{D^{-1}}$	
		$1+1'+\mathbf{1}'$	$(0\ 0\ d)$	$(0\ D\ E)$	$(0\ 0\ A)$	$(0\ 0\ a)$	$P^U_{2\leftrightarrow 3} H_{12}^{D^{-1}}$	
		$1+\mathbf{2}$	$(0\ 0\ d)$	$(0\ 0\ D)$	$(0\ 0\ A)$	$(0\ 0\ a)$	$H_{12}^U H_{12}^{D^{-1}}$	
		$1+\mathbf{1}+\mathbf{1}'$	$(0\ 0\ d)$	$(0\ 0\ D)$	$(0\ 0\ A)$	$(0\ 0\ a)$	$H_{12}^U H_{12}^{D^{-1}}$	
		$1+\mathbf{1}+\mathbf{1}$	$(0\ 0\ d)$	$(0\ 0\ D)$	$(0\ 0\ A)$	$(0\ 0\ a)$	$H_{12}^U H_{12}^{D^{-1}}$	
		$1+\mathbf{1}'+\mathbf{1}''$	$(0\ 0\ d)$	$(0\ 0\ D)$	$(0\ 0\ A)$	$(0\ 0\ a)$	$H_{12}^U H_{12}^{D^{-1}}$	
		$1+\mathbf{1}'+\mathbf{1}'$	$(0\ 0\ d)$	$(0\ 0\ D)$	$(0\ 0\ A)$	$(0\ 0\ a)$	$H_{12}^U H_{12}^{D^{-1}}$	
$1+r\not\supseteq 1$	$1+1+1$	$1+\mathbf{1}+\bar{\mathbf{1}}$	$(0\ 0\ d)$	$(D\ E\ F)$	$(0\ 0\ A)$	$(0\ 0\ a)$	$P_U H_{12}^{D^{-1}}$	$V_{3\times 3}$
		$1+1'+1''$	$(0\ 0\ d)$	$(D\ E\ F)$	$(0\ 0\ A)$	$(0\ 0\ a)$	$P_U H_{12}^{D^{-1}}$	
		$1+1'+1'$	$(0\ 0\ d)$	$(D\ E\ F)$	$(0\ 0\ A)$	$(0\ 0\ a)$	$P_U V_{12} H_{12}^{D^{-1}}$	
		$1+1'+\mathbf{1}$	$(0\ 0\ d)$	$(0\ D\ E)$	$(0\ 0\ A)$	$(0\ 0\ a)$	$P^U_{2\leftrightarrow 3} H_{12}^{D^{-1}}$	
		$1+\mathbf{2}$	$(0\ 0\ d)$	$(0\ 0\ D)$	$(0\ 0\ A)$	$(0\ 0\ a)$	$H_{12}^U H_{12}^{D^{-1}}$	
		$1+\mathbf{1}+\mathbf{1}'$	$(0\ 0\ d)$	$(0\ 0\ D)$	$(0\ 0\ A)$	$(0\ 0\ a)$	$H_{12}^U H_{12}^{D^{-1}}$	
		$1+\mathbf{1}+\mathbf{1}$	$(0\ 0\ d)$	$(0\ 0\ D)$	$(0\ 0\ A)$	$(0\ 0\ a)$	$H_{12}^U H_{12}^{D^{-1}}$	

Table 3.8: (Part 1) Possible forms of SU(5) unified flavour representations for the case in which singlet neutrino mass matrix is non-singular in the symmetric limit (as well as low- and high-scale analyses are not equivalent). Representation r is vectorlike and possibly reducible. Form of the fermion masses and of the CKM and PMNS matrices corresponding to viable choices are shown. Neutrino mass pattern and PMNS matrix are obtained from the high-scale results. $P_{2\leftrightarrow 3}$ is either the identity permutation or the switch of 2 and 3.

U_1	$U_{\bar{5}}$	U_{10}	Masses				$V_{\rm CKM}$	$U_{\rm PMNS}$
			m_D	m_U	m_E	m_ν		
$1+1+r\neq 1$	$1+1+1$	$1+\mathbf{1}+\bar{\mathbf{1}}$	$(0\ 0\ d)$	$(D\ E\ F)$	$(0\ 0\ A)$	$(0\ a\ b)$	$P_U H_{12}^{D^{-1}}$	$V_{3\times 3}$
		$1+1'+1''$	$(0\ 0\ d)$	$(D\ E\ F)$	$(0\ 0\ A)$	$(0\ a\ b)$	$P_U H_{12}^{D^{-1}}$	
		$1+1'+1'$	$(0\ 0\ d)$	$(D\ E\ F)$	$(0\ 0\ A)$	$(0\ a\ b)$	$P_U V_{12} H_{12}^{D^{-1}}$	
		$1+1'+\mathbf{1}$	$(0\ 0\ d)$	$(0\ D\ E)$	$(0\ 0\ A)$	$(0\ a\ b)$	$P^U_{2\leftrightarrow 3} H_{12}^{D^{-1}}$	
		$1+\mathbf{2}$	$(0\ 0\ d)$	$(0\ 0\ D)$	$(0\ 0\ A)$	$(0\ a\ b)$	$H_{12}^U H_{12}^{D^{-1}}$	
		$1+\mathbf{1}+\mathbf{1}'$	$(0\ 0\ d)$	$(0\ 0\ D)$	$(0\ 0\ A)$	$(0\ a\ b)$	$H_{12}^U H_{12}^{D^{-1}}$	
		$1+\mathbf{1}+\mathbf{1}$	$(0\ 0\ d)$	$(0\ 0\ D)$	$(0\ 0\ A)$	$(0\ a\ b)$	$H_{12}^U H_{12}^{D^{-1}}$	
$1+r\not\supseteq 1,1'$	$1+1+1'$	$1+1+1''$	$(0\ d\ e)$	$(D\ E\ F)$	$(0\ A\ B)$	$(0\ 0\ a)$	$P_U V_{12} P^{D^{-1}}$	13
$1+r\not\supseteq 1,1'$	$1+1+1'$	$1+1+1'$	$(d\ e\ f)$	$(D\ E\ F)$	$(A\ B\ C)$	$(0\ 0\ a)$	$P_U V_{12} P^{D^{-1}}$	$13, 23, 33$

Table 3.9: (Part 2) Possible forms of SU(5) unified flavour representations for the case in which singlet neutrino mass matrix is non-singular in the symmetric limit (as well as low- and high-scale analyses are not equivalent). Representation r is vectorlike and possibly reducible. Form of the fermion masses and of the CKM and PMNS matrices corresponding to viable choices are shown. Neutrino mass pattern and PMNS matrix are obtained from the high-scale results. $P_{2\leftrightarrow 3}$ is either the identity permutation or the switch of 2 and 3.

The answer to the first question is no, these two analyses are not equivalent. Although for a given mass and mixing pattern forced by a low-scale analysis there is always a high-scale analysis exist to provide same mass and mixing patters, the low-scale analysis cannot cover all the possibilities in the high-scale discussion. A necessary and sufficient condition to these two analyses become equivalent is that the singlet neutrino representation must be vectorlike and it contains vectorlike part of the lepton doublet representation. The answer to the second question is yes, present hint for the normal hierarchy of the neutrino masses can be account for by the high-scale analysis when it is not equivalent to low-scale study. As we know already from the previous chapter, the low-scale result describes neutrino masses either in the inverted hierarchy or in the anarchical (unconstrained) pattern in the symmetric limit, this description can also appear in the high-scale analysis when it become equivalent to the low-scale analysis.

The answers of those questions are based on a very general assumption of the flavour group, a specific mechanism to the neutrino mass generation and our definitions of the viable masses and mixing patterns. There is no restriction on the flavour symmetry, they can be any type. We simply extend SM by considering the singlet neutrinos, and assume that neutrino masses are generated from the type I seesaw mechanism. Our definition for the viable lepton masses and mixings are given in table 2.1 and in eq. (3.17). From these three basic assumptions, we provide thorough identification of the all possible irrep decompositions on lepton doublet, lepton singlet and neutrino singlet. Regarding the

flavour groups, if all the irreps, that can account for the viable mass and mixing patterns, are contained in the possible irreps of a certain group representation then that group can be considered as applicable flavour symmetry group.

To obtain those conclusive answers, we have started our discussion by defining the low- and high-scale analyses of flavour observables according to the two different descriptions of the neutrino masses, either from the Weinberg operator or from the type I seesaw mechanism. Then we provide equivalence condition of these two analyses for the general case of n family. The equivalence condition states that two analyses provide same mass and mixing patterns if and only if i) the representation of the singlet neutrinos is vectorlike and ii) it contains the vectorlike part of the lepton doublet representation. Since we already have had complete classifications of the low-scale analysis in chapter 2, our main interest in this chapter is to find full characterization of flavour group representations for the inequivalent scenarios. Inequivalence happens in two cases, when the singlet neutrino mass matrix is singular or non-singular in the symmetric limit. Both case are discussed separately and results are given by the relations between the irrep patterns and forms of the lepton masses and mixings in the symmetric limit, without knowing the explicit form of the mass matrices.

The results for the cases in which the singlet neutrino mass matrix has one or two vanishing eigenvalues are give in table 3.1 and table 3.2, respectively. In the former case light neutrino masses are predicted to be in the normal hierarchy, while the latter case allows both hierarchies to appear. Comparing the results from the high- and the low-scale discussions, there are two main features deserve to emphasize. Firstly, in the viable cases of the low-scale analysis neutrino masses are allowed either in inverted hierarchy or forced to be all vanishing, while in the high-scale analysis all the mass patterns are in the normal hierarchy, which is slightly preferred by the current oscillation data. Secondly, some cases where the forms of the PMNS matrix were not viable or undetermined in the low-scale analysis now turn out to have a viable mixing patterns in the high-scale result. This means that there are more possibilities of the flavour group representations to provide approximate description of the lepton masses and mixings in the high-scale analysis than the low-scale limit.

The table 3.4 summarizes the inequivalent results when all the singlet neutrino masses are non-zero in the symmetric limit. Here, two interesting outcomes catch our attention, first one is related to the neutrino mass spectrum and other one is about the form of the PMNS matrix. In the high-scale analysis there is no anarchical neutrino mass spectrum which appeared in the low-scale analysis. Structures of the PMNS matrix in the low-scale analysis with a zero in the third row or with 4 zero entries now become viable in the high-scale analysis; moreover, the 13 element is fixed to be zero (or that can be obtained from the trivial permutation of charged lepton masses) in the symmetric limit, or a symmetry breaking effect can explain the smallness of the 13 element.

In the last part of the work we investigate the possibilities of explaining both lepton and quark flavour observables in the context of grand unified theories such as $SU(5)$ and

$SO(10)$. Imposing the non-trivial assumption that the flavour and the gauge group representations commute each other and that the fermions in a same gauge group multiplet transform under the same representation of the flavour symmetry, we have obtained inequivalent results of the high-scale analysis shown in tables 3.5, 3.6, 3.8, 3.9 for the $SU(5)$ GUT; and there is no solution in the context of the $SO(10)$ GUT. Clearly, there are more possibilities to achieve viable fermion masses and mixing in the high-scale analysis in the context of GUT compared to that in the low-scale analysis. Notice that all of the mixing patterns in those viable cases rely on the specific structures of the permutation matrices, $H_{12}^{U,D}$ and V_{12}, some of which are determined by the symmetry breaking effects.

Even though the high-scale analysis can provide a possibility to approximate description of fermion masses and mixings in the symmetric limit, the symmetry breaking effect cannot be absent for the accurate description of SM flavour observables. So it is important to study the problem by considering cumulative contributions from the symmetric limit as well as the symmetry breaking effects that depend not only on the breaking source but also on the chosen way of symmetry breaking.

Chapter 4

Novel measurements of anomalous triple gauge couplings for the LHC

4.1 Introduction

The Standard Model (SM) of particle physics is our best model describing the innermost layer of matter. It has been verified in uncountable experiments spanning a wide range of energies. The Higgs discovery [157, 158] was the icing on the cake of more than forty decades of experiments confirming every testable prediction of the SM. Now, the most important goal of the LHC is the quest for new physics, either in the form of deviations from the SM predictions or as new degrees of freedom in direct searches.

ATLAS and CMS have performed many dedicated searches of Beyond the Standard Model (BSM) theories [159]. All such investigations have led to null results. Before the run of these experiments it was widely acknowledged that the confirmation of the SM and nothing more is a logical possibility. At the same time though there are many theoretically appealing BSM extensions that seem to make sense. Thus, *why nature is not making use of them?* is a very pressing question that should have an answer. In order to make progress towards answering this question we can envision two possible strategies: more clever model building – which may require a paradigm change with respect to conventional views; or to understand in detail the real pressure that the LHC is imposing on the BSMs. This work deals with a particular example in the second direction.

The experimental results suggest that there is at least a moderate mass gap between the electroweak scale m_W and the new physics scale Λ. Given this situation it is very convenient to parametrize possible deviations from the SM in an EFT approach. This consists in viewing the SM as the leading interactions of an effective Lagrangian and incorporate BSM deviations in a perturbative expansion in powers of SM fields or derivatives D_μ over the proper power of Λ,

$$\mathcal{L}_{\text{eff}} = \mathcal{L}_{\text{SM}} + \mathcal{L}_6 + \cdots , \tag{4.1}$$

where ellipses denote terms of order $1/\Lambda^3$ and higher. Given the uncertainty of the current situation we will take a skeptical point of view on the particular UV physics leading to (4.1) and thus only assume the SM gauge symmetries. Then, up to the dimension five Weinberg operator $\sim \Psi_L \Psi_L H H$, the leading deviation from the SM consists in operators of dimension six,

$$\mathcal{L}_6 = \sum_i \frac{c_i O_i}{\Lambda^2} \,. \tag{4.2}$$

The dimensionless coefficients c_i are the Wilson coefficients, which we assume to be perturbative but otherwise arbitrary. The operators appearing in (4.2) were exhaustively listed in chapter 1, see also [83, 86]. The advent of the LHC, especially after the Higgs discovery, has triggered an abundant number of works on interpreting the LHC searches as limits on effective field theory deformations of the SM. It is very interesting to find better ways to measure the SM EFT. This is in fact the purpose of this chapter, which focuses on diboson production WZ/WW at the LHC and how it can be used to constrain the deformations from the SM due to the triple gauge couplings (TGCs) in $\mathcal{L}_6$.

In the SM the TGCs are fixed by the gauge symmetry and included in the gauge kinetic term,

$$ig\left(W^{+\,\mu\nu}W^-_\mu W^3_\nu - W^{-\,\mu\nu}W^+_\mu W^3_\nu + W^{3\,\mu\nu}W^+_\mu W^-_\nu\right) \,, \tag{4.3}$$

where $W^3_\nu = c_\theta\, Z_\nu + s_\theta\, A_\nu$ is a linear combination of the Z and photon vector bosons, and θ is the Weinberg angle. The interaction in (4.3) is written in the unitary gauge, so that the vector boson fields describe both longitudinal and transverse polarizations. There are only two types of CP-even anomalous triple gauge couplings (aTGCs) deviating from (4.3). The first one consists in deforming (4.3) away from the SM point

$$\mathcal{L}^{1st}_{aTGC} = ig\, c_\theta\, \delta g_{1,Z}\, Z_\nu W^{+\,\mu\nu}W^-_\mu + h.c. + ig\,(c_\theta\, \delta\kappa_Z\, Z^{\mu\nu} + s_\theta\, \delta\kappa_\gamma\, A^{\mu\nu})W^+_\mu W^-_\nu \,. \tag{4.4}$$

Modifications of the coupling $W^{+\,\mu\nu}W^-_\mu A_\nu$ is forbidden by electromagnetic gauge invariance and the relation $\delta\kappa_Z = \delta g_{1,Z} - \tan^2\theta\delta\kappa_\gamma$ is satisfied if only dimension six operators are considered. The other type of deformations are obtained by adding extra derivatives on (4.3). This translates into higher powers of momentum in the amplitudes. In an expansion in powers of momentum, the leading such deformation is

$$\mathcal{L}^{2nd}_{aTGC} = \lambda_Z \frac{ig}{m_W^2} W^{+\,\mu_2}_{\mu_1} W^{-\,\mu_3}_{\mu_2} W^{3\,\mu_1}_{\mu_3} \,. \tag{4.5}$$

The study of the triplet of deformations $\{\delta g_{1,Z}, \delta\kappa_Z, \lambda_Z\}$ is a classic test of the SM with a long history starting with the works [103, 160] and continued by [84, 161–163]. [1] Famously, the interactions in (4.4, 4.5) were bounded with percent level accuracy at the LEP-2

[1] See for example [93, 164–171] for recent TGC and EFT analyses.

experiment [94]:

$$\lambda_Z \in [-0.059, 0.017] \ , \quad \delta g_{1,Z} \in [-0.054, 0.021] \ , \quad \delta\kappa_Z \in [-0.074, 0.051] \ , \tag{4.6}$$

at 95% confidence level.

At the LHC, we would like to exploit the energy growth of (4.4, 4.5) to put stronger bounds on TGCs. However it is well known that some of the TGC contributions have an additional suppression factor at high energy. In particular the leading energy contribution coming from the λ_Z TGC does not interfere with SM for any $2 \to 2$ process, which makes its measurements difficult at LHC. This is consequence of helicity selection rules [89, 164, 172], and the result is valid at leading order (LO). The main point of our work in this chapter is to find ways to overcome this suppression. We propose two measurements that enhance the interference of the λ_Z-BSM amplitude with the SM contribution. Our ideas will lead to a better measurement of aTGC at LHC.

This chapter is organized as follows: in section 4.2 we review the basic physics associated to the TGC. Then, in section 4.3 we propose two new variables to improve the accuracy. In section 4.4 we discuss the challenges of the EFT measurements at the LHC. Then in sections 4.5 and 4.6 we discuss our methodology and the results. We conclude and comment on future directions in section 4.7.

4.2 Features of TGC mediated amplitudes

In this section we review simple facts of the diboson production at the LHC. This will allow us to spot measurements that have not been exploited yet and will lead to better sensitivity on the TGCs.

Diboson production at the LHC is dominated by the $2 \to 2$ process $q\bar{q} \to WW/WZ$. To neatly expose the leading energy growth of this probability amplitudes we use the Goldstone equivalence theorem. Namely, we work with the parametrization where the transverse gauge-bosons are massless and the would-be Goldstone bosons in the Higgs doublet describe the longitudinal components of the $W^\pm/Z$ gauge bosons. For definiteness of the notation,

$$\mathcal{L}_{\rm SM} = (D_\mu H)^\dagger D^\mu H + \mathcal{L}_{\rm gauge} + \mathcal{L}_\psi + V(H) \, , \tag{4.7}$$

where the $D_\mu H = (\partial_\mu - ig' Y B_\mu - igT^a W^a_\mu)H$, with T the $SU(2)_L$ generators, $Y = 1/2$ and $H^T = (\sqrt{2}i\, G^+, v + h + iG_0)/\sqrt{2}$. As usual, the pure gauge sector is given by the field strengths $\mathcal{L}_{\rm gauge} = -\frac{1}{4} W^a_{\mu\nu} W_a^{\mu\nu} - \frac{1}{4} B_{\mu\nu} B^{\mu\nu} - \frac{1}{4} G_{A\mu\nu} G^{A\mu\nu}$, the piece $\mathcal{L}_\psi$ involves the Kinetic terms for the fermions and the Yukawa interactions, and $V(H) = -m^2|H|^2 + \lambda|H|^4$. We recall that Goldstone's equivalence theorem,

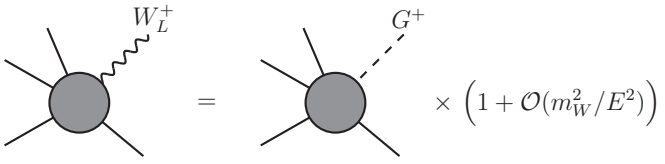

states that to get the leading large energy behavior of the amplitudes with massive gauge bosons in the final state, we can identify in (4.7) the transverse and longitudinal components of the physical gauge bosons as

$$\{W_L^+,\, W_T^+\} \;=\; \{G^+,\, (W^1 - iW^2)/\sqrt{2}\}\;, \tag{4.8}$$

$$\{Z_L,\, Z_T\} \;=\; \{G_0/\sqrt{2},\, \cos\theta_w W_3 - \sin\theta_w\, B\}\,, \tag{4.9}$$

where $\cos\theta_w = g/\sqrt{g'^2 + g^2}$ is the cosine of the Weinberg angle. With this basic result in mind, we proceed to discuss the energy growth of diboson production.

4.2.1 Energy growth

With the parametrization in (4.7) and the identifications in eqs. (4.8, 4.9), the SM triple gauge couplings arise from

$$\mathrm{tr} W_{\mu\nu} W^{\mu\nu} \;\supset\; \partial V_T V_T V_T\,, \tag{4.10}$$

$$(D_\mu H)^\dagger D^\mu H \;\supset\; \partial V_L V_T V_L + v V_T V_T V_L\,, \tag{4.11}$$

where we have neglected SM coupling constants as well as $\mathcal{O}(1)$ numerical factors. In eqs. (4.10, 4.11) we have also suppressed the Lorentz index contractions and denoted by V either the W or Z vector boson. A one line calculation shows that the above TGC lead to s-channel amplitudes with the leading energy growth

$$\begin{aligned} &\mathcal{M}\left(q\bar{q} \to V_T W_T^+\right) \sim E^0\,, \\ &\mathcal{M}\left(q\bar{q} \to V_L W_L^+\right) \sim E^0\,, \\ &\mathcal{M}\left(q\bar{q} \to V_T W_L^+ / V_L W_T^+\right) \sim \frac{v}{E}\,, \end{aligned} \tag{4.12}$$

where E is the center of mass energy of the diboson system. The same asymptotic behavior is found for W^-Z final states. In (4.12) we are working in the limit of massless light quarks, so that these only couple to the transverse gauge bosons, and we neglected subleading $\log(E)$ terms from loop corrections. The process $q\bar{q} \to V_T W_T$ is also mediated by t,u-channel diagrams that have the same energy growth as the s-channel in (4.12).

Next we discuss the energy growth of tree-level amplitudes involving one insertion of the anomalous TGCs $\{\delta g_{1,Z}, \delta\kappa_Z, \lambda_Z\}$, defined in (4.4, 4.5). For this purpose, it is

convenient to parametrize them in terms of the following dimension six operators,

$$\begin{aligned} O_{HB} &= ig'(D^\mu H)^\dagger D^\nu H B_{\mu\nu}\,, \\ O_{HW} &= ig(D^\mu H)^\dagger \sigma^a D^\nu H W^a_{\mu\nu}\,, \\ O_{3W} &= \frac{g}{3!}\epsilon_{abc} W^{a\,\nu}_{\mu} W^{b\,\rho}_{\nu} W^{c\,\mu}_{\rho}\,, \end{aligned} \tag{4.13}$$

which map onto the triplet $\{\delta g_{1,Z},\, \delta\kappa_Z\,, \lambda_Z\}$ as follows

$$\lambda_Z = \frac{m_W^2}{\Lambda^2} c_{3W}\,, \quad \delta g_{1,Z} = \frac{m_Z^2}{\Lambda^2} c_{HW}\,, \quad \delta\kappa_Z = \frac{m_W^2}{\Lambda^2}\left(c_{HW} - \tan^2\theta c_{HB}\right)\,. \tag{4.14}$$

In principle one could use other sets of operators to parametrize deviations in the physics of $q\bar{q} \to WW/WZ$ production. However, it is important to realize that after taking into account the constraints from LEP-1, the main possible deviations in diboson production are due to modifications on the SM triple gauge vertices [173, 174]. [2] See also [93] where this result is studied using different bases of dimension six operators.

The operators in (4.13) include the following TGCs

$$O_{HB} \supset \partial W_L \partial Z_T \partial W_L + v W_T \partial Z_T \partial W_L + v^2 W_T \partial Z_T W_T + \dots\,, \tag{4.15}$$

$$O_{HW} \supset \partial V_L \partial V_T \partial V_L + v V_T \partial V_T \partial V_L + v^2 V_T \partial V_T V_T + \dots\,, \tag{4.16}$$

$$O_{3W} \supset \partial V_T \partial V_T \partial V_T + \dots\,, \tag{4.17}$$

where ellipses denote interactions that either involve a photon or are not of the triple gauge type. Note that in (4.15)-(4.17) we have neglected SM couplings as well as numerical $\mathcal{O}(1)$ factors. At large energies the leading processes mediated by the interactions in (4.15)-(4.17) are

$$\begin{aligned} \mathcal{M}\left(q\bar{q} \to W_L^- W_L^+\right) &\sim E^2/\Lambda^2\; c_{HB} + E^2/\Lambda^2\; c_{HW} \\ &\sim E^2/m_W^2\; \delta g_{1,Z} + E^2/m_W^2\; \delta\kappa_Z\,, \end{aligned} \tag{4.18}$$

$$\mathcal{M}\left(q\bar{q} \to Z_L W_L^+\right) \sim E^2/\Lambda^2\; c_{HW} = E^2/m_Z^2\; \delta g_{1,Z}\,, \tag{4.19}$$

$$\mathcal{M}\left(q\bar{q} \to V_T W_T^+\right) \sim E^2/\Lambda^2\; c_{3W} = E^2/m_W^2\; \lambda_Z\,, \tag{4.20}$$

where we used (4.14) and omitted constant factors in front of the TGCs. The same leading energy growth is found by replacing $W^- \leftrightarrow W^+$ in the final state of (4.19). Interestingly, $\delta\kappa_Z/c_{HB}$ contributes at the order of E^2 only to the process (4.18). The leading contribution of $\delta\kappa_Z$ to $q\bar{q} \to WZ$ appears for the polarizations $\mathcal{M}\left(q\bar{q} \to Z_T W_L^+\right)$

[2] Note that the commonly used SILH basis, apart from the operators of (4.13), also includes a further operator contributing to the aTGC: $O_W = D^\mu W_\mu{}^\nu H D_\nu H + h.c.$. For our purposes though, it is enough to use (4.13) in order to capture the high energy behavior. Our results will be presented in terms of $\{\delta g_{1,Z},\, \delta\kappa_Z\,, \lambda_Z\}$, which can be mapped into any other basis.

and scales as $\sim vE/\Lambda^2$. This follows from the fact that at leading order in energy only the transverse polarization of the Z boson enters in O_{HB}.

Next we discuss the generic properties of the production cross sections in the presence of these BSM amplitudes.

4.2.2 Accuracy obstruction

In general, the $2 \to 2$ scattering cross section in the presence of irrelevant operators scales as

$$\sigma(q\bar{q} \to VV) \sim \frac{g_{\rm SM}^4}{E^2}\left[1 + \overbrace{c_i \frac{E^2}{\Lambda^2}}^{\rm BSM_6 \times SM} + \overbrace{c_i^2 \frac{E^4}{\Lambda^4}}^{{\rm BSM_6}^2} + \dots\right], \tag{4.21}$$

where the first factor $g_{\rm SM}^4/E^2$ accounts for the energy flux of the initial quarks, and we have omitted numerical factors. In (4.21) we explicitly indicated dimension six squared and SM-dimension six interference terms, and ellipses stand for higher order corrections from operators of dimensions ≥ 8. [3] However, the operator O_{3W} (i.e. the λ_Z deformation) is special because the interference between the SM amplitude $\mathcal{M}\left(q\bar{q} \to V_T W_T^+\right) \sim E^0$ in (4.12) and $\mathcal{M}\left(q\bar{q} \to V_T W_T^+\right) \sim c_{3W} E^2$ in (4.20) is suppressed and the scaling of the BSM$_6$ $\times$ SM piece is softer. This is a consequence of the helicity selection rules [172] as we will now review. [4]

The non-interference of the diboson production amplitude through O_{3W} and the SM can be understood by first taking the limit where the masses of the electroweak gauge bosons are zero, namely we focus on transverse polarizations only. In this limit the amplitude of tree-level SM process $q\bar{q} \to VV$ is only non-zero if the transverse helicities of the vector boson are opposite $(\pm, \mp)$. [5] At the same time though, the operator O_{3W} in (4.13) leads to a triple gauge vertex where all three gauge bosons have the same helicity, so the amplitude of the process $q\bar{q} \to VV$ containing O_{3W} vertex is non-zero only if the transverse helicities of the vector boson are same $(\pm, \pm)$. Therefore, there is no interference between two amplitudes, as either SM or O_{3W} amplitude is vanishing for a given pair of transverse helicities of final state vector bosons. One way to understand this result is to look at the helicity structure of three point vertices of the SM and O_{3W}. The Lorentz symmetry, dimensional analysis and special kinematics of the three particle interaction completely fix the structure of three-point amplitude and provide relation

[3] Note that operators of dimension 7 necessarily violate either baryon or lepton number. We assume the scale of such symmetry violation to be very large and therefore irrelevant for diboson physics at the LHC.

[4] See [89] for a pioneering discussion of this effect in the context of QCD.

[5] More generally, this follows from the Maximally Helicity Violation (MHV) helicity selection rules, see for instance [175].

between the modulus of total helicity and dimension of the coupling g,

$$|\sum_{i=1}^{3} h_i| = 1 - [g] \tag{4.22}$$

where $[g]$ denotes mass dimension of the coupling of the three point interactions. The SM triple gauge coupling is dimensionless so the total helicity is ± 1, this means two gauge boson has opposite helicity with respect to the third one. While coefficient of the operator O_{3W} has mass dimension -2, thus total helicity of the amplitude is ± 3. This, in turn, implies that all three gauge bosons have same helicity. When we compute the amplitudes of the process $q\bar{q} \to VV$, non-zero SM amplitudes contain two final state gauge bosons with opposite helicities, while in the O_{3W} amplitudes all final state gauge bosons have same helicity. Another quick way to check this result is to write the field strength in terms of spinor indices $W_{\alpha\dot{\alpha}\beta\dot{\beta}} = W_{\mu\nu}\sigma^{\mu}_{\alpha\dot{\alpha}}\sigma^{\nu}_{\beta\dot{\beta}} = w_{\alpha\beta}\bar{\epsilon}_{\dot{\alpha}\dot{\beta}} + \bar{w}_{\dot{\alpha}\dot{\beta}}\epsilon_{\alpha\beta}$, where as usual the tensors ϵ and $\bar{\epsilon}$ are used to raise α and $\dot{\alpha}$ indices, respectively. O_{3W} in (4.13) can be written terms of the $w/\bar{w}$ fields is given as

$$O_{3W} \propto w_{\alpha}{}^{\beta} w_{\beta}{}^{\gamma} w_{\gamma}{}^{\alpha} + \bar{w}_{\dot{\alpha}}{}^{\dot{\beta}} \bar{w}_{\dot{\beta}}{}^{\dot{\gamma}} \bar{w}_{\dot{\gamma}}{}^{\dot{\alpha}} \,. \tag{4.23}$$

Each antisymmetric tensor field w and $\bar{w}$ are the self-dual and anti-self-dual parts of the field strength, they can create a massless particle carrying helicity $+1$ and -1 respectively, and, therefore, diboson production through (4.23) leads to vector bosons with helicity $(\pm, \pm)$. Thus, at tree level we have that

$$q\bar{q} \longrightarrow V_{T_\pm} V_{T_\mp} \quad \text{(in the SM)}\,, \tag{4.24}$$

$$q\bar{q} \longrightarrow V_{T_\pm} V_{T_\pm} \quad \text{(with } O_{3W} \text{ insertion)}\,. \tag{4.25}$$

Since the final diboson states in (4.24, 4.25) are different, there is no interference between both amplitudes. This statement is exactly true in the massless limit. However, two mass insertions $m_W \partial_\mu G^+ W^{-\mu}$, $m_Z \partial_\mu G^0 Z^\mu$ can be used to flip the helicity of the final states, leading to a non-zero interference between (4.24, 4.25). Flipping the helicity costs a factor m_W^2/E^2. Then, the leading cross section for diboson production in the limit $E \gg m_W$ is given by,

$$\sigma(q\bar{q} \to V_T V_T) \sim \frac{g^4_{\rm SM}}{E^2}\left[1 + c_{3W}\frac{m_V^2}{\Lambda^2} + c_{3W}^2 \frac{E^4}{\Lambda^4}\right]. \tag{4.26}$$

The important point to notice is that the second term of (4.26) has a suppressed energy scaling with respect to the general expectation in (4.21).

This behavior makes EFT consistent measurements of the c_{3W} difficult. Indeed, at the level of the dimension six operators the signal from the O_{3W} will be subdominant compared to the contributions of the other TGCs, which will require further disentanglement of the transverse and longitudinal final state polarizations. But even more, assuming an

ideal separation of the longitudinal polarizations we need to remain in the EFT validity range, namely in the parameter space where the contributions from the dimension eight operators can be safely ignored. For the process $q\bar{q} \to V_T V_T$ the dimension eight contribution to the cross section can be schematically written as

$$\Delta\sigma_{\text{dim=8}}(q\bar{q} \to V_T V_T) \sim \frac{g_{\text{SM}}^4}{E^2}\left[\overbrace{c_8 \frac{E^4}{\Lambda^4}}^{\text{BSM}_8\times\text{SM}} + \overbrace{c_8^2 \frac{E^8}{\Lambda^8}}^{\text{BSM}_8{}^2} + \dots \right]. \tag{4.27}$$

Note that the $\text{BSM}_8 \times \text{SM}$ piece scales as the BSM_6^2 contribution, E^4/Λ^4. Where we have assumed that there is a interference between the SM and the new physics contributions at the level of the dimension eight operators. For the process $q\bar{q} \to V_T V_T$ this is indeed the case, consider for instance

$$gD^\nu W^{\sigma\tau} W_{\nu\tau} D^\mu W_{\mu\sigma} \sim D^{\dot{\alpha}\alpha}\omega_{\alpha\beta}\bar{\omega}_{\dot{\alpha}\dot{\gamma}} D^{\dot{\gamma}\sigma}\omega_\sigma^\beta - D^\alpha_{\dot{\gamma}}\bar{\omega}^{\dot{\beta}\dot{\gamma}}\omega_{\alpha\gamma} D^\sigma_{\dot{\beta}}\omega_\sigma^\gamma + D^\alpha_{\dot{\gamma}}\omega^{\beta\gamma}\omega_{\alpha\gamma} D^{\dot{\sigma}}_{\dot{\beta}}\bar{\omega}^{\dot{\gamma}}_{\dot{\sigma}} + \dots , \tag{4.28}$$

where ellipses denote terms with helicity configurations other than $\sim \omega\omega\bar{\omega}$; or the operator

$$g^2\,(\bar{q}\gamma^\rho q) W_{\rho\nu} D^\mu W_\mu^\nu \sim q^\alpha \bar{q}_{\dot{\beta}} w_\alpha{}^\beta D_\beta{}^{\dot{\alpha}} \bar{w}_{\dot{\alpha}}{}^{\dot{\beta}} + \dots , \tag{4.29}$$

written in terms of spinor indices. The latter operator is a contact interaction contributing to $q\bar{q} \to VZ$ while (4.28) is a modification of the TGC – of the second type according to the discussion around (4.4 - 4.5). Note that both of them lead to final state bosons of helicities $(\pm, \mp)$, like in the SM.

Then the truncation at the dimension six level (4.26) is valid if only [6]

$$\max\left(c_{3W}\frac{m_V^2}{\Lambda^2}, c_{3W}^2\frac{E^4}{\Lambda^4}\right) > \max\left(c_8\frac{E^4}{\Lambda^4}, c_8^2\frac{E^8}{\Lambda^8}\right). \tag{4.30}$$

Suppose we will be able get rid of the interference suppression, then this condition is replaced by

$$\max\left(c_{3W}\frac{E^2}{\Lambda^2}, c_{3W}^2\frac{E^4}{\Lambda^4}\right) > \max\left(c_8\frac{E^4}{\Lambda^4}, c_8^2\frac{E^8}{\Lambda^8}\right), \tag{4.31}$$

which is less restrictive if $c_{3W}E^2/\Lambda^2 < 1$ (given that at LHC $E > m_V$).

Another advantage of having a large interference term is that it leads to the better measurement of the sign of the Wilson coefficient, otherwise very weakly constrained. The importance of the improvement in (4.31) depends on the actual values of the Wilson coefficients or in other words on the UV completions of the given EFT. To make this discussion more concrete we present a few examples in the next subsection.

[6] We are assuming that contributions of operators of dimension higher than eight are even smaller.

4.2.3 Power-counting examples

The strength of the Wilson couplings can be estimated by a given set of power-counting rules characterizing a possible UV completion. Power-counting schemes are useful to incorporate particular biases towards the kind of BSM physics we would like to prove. This is a perfectly legitimate strategy and very much the point of using an Effective Field Theory approach, allowing to parametrize altogether broad classes of models. Particular examples are weakly coupled renormalizable UV completions, Minimal Flavour Violation (MFV) [176], the Strongly Interacting Light Higgs (SILH) [85], flavour universal BSM physics (see e.g. [177]), etc. The power-counting schemes commonly used are imposed through arguments based on the symmetries or dynamics of the Action, such that possible radiative corrections violating the assumed power-counting scheme are kept small or understood.

For example, we may assume that the UV completion is a renormalizable and weakly coupled QFT. Then, the power-counting consist in classifying those operators that are loop generated v.s. those that are generated at tree-level [173, 178]. The latter are expected to be bigger because the former are suppressed by $1/(16\pi^2)$ factors. Then, for example if we have heavy vector-like fermions, we expect

$$c_{3W} \sim \mathcal{O}(1) \times g^2/(4\pi)^2 \,, \quad c_{(4.28)} \sim \mathcal{O}(1) \times g^2/(4\pi)^2 \,, \tag{4.32}$$

where $c_{(4.28)}$ refers to the Wilson coefficient of the dimension eight operator in (4.28); the contribution to $c_{(4.29)}$ has a stronger loop suppression. This setup is somewhat pessimistic since the extra loop suppression makes it hard to prove c_{3W} with the LHC sensitivity. In any case, improvement from (4.30) to (4.31) is

$$E^2 < \Lambda m_W \;\longrightarrow\; E < \Lambda \,. \tag{4.33}$$

As an other power-counting instance, one may envision a scheme where for each extra-field strength that we add to the dimension four SM Lagrangian we pay a factor $g_* \lesssim 4\pi$. With this power-counting we obtain

$$c_{3W} \sim g_*/g \,, \quad c_{(4.28)} \sim g_*/g \,, \quad c_{(4.29)} \sim g_* g/(16\pi^2) \,, \tag{4.34}$$

where the $1/g$ factor is due to the normalization of O_{3W} in (4.13). This power counting, called *pure Remedios*, was introduced in [179]. [7] This power-counting is more optimistic regarding possible LHC signals since g_* can be naturally large. However, in this scenario

[7] In a nutshell, the construction is based on the following observation. Consider the SM effective Lagrangian $\mathcal{L}_{EFT} = \mathcal{L}_{\rm Higgs} + \mathcal{L}_\psi + \frac{\Lambda^4}{g_*^2} L(\hat{F}_{\mu\nu}/\Lambda^2, \partial_\mu/\Lambda)$, where the gauge-field strengths $\hat{F}_{\mu\nu}$ are not canonically normalized and we view L as a functional that we expand in inverse powers of Λ. Then, it is technically natural to set $g_* \gg g$ in $\mathcal{L}_{EFT}$ because as $g \to 0$ the $SU(2)_L$ gauge symmetry acting on $\mathcal{L}_{\rm EFT}$ is deformed into $SU(2)_L^{\rm global} \rtimes U(1)^3_{\rm gauge}$ – we refer to [179] for details.

there is no improvement from (4.30) to (4.31), and in both cases we find

$$E < \Lambda\,. \tag{4.35}$$

Lastly we will discuss one scale one coupling power-counting [85], which predicts

$$c_{3W} \sim c_{(4.28)} \lesssim \frac{g_*}{g}, \quad c_{(4.29)} \lesssim \frac{g_*^2}{g^2}. \tag{4.36}$$

In this case the improvement from (4.30) to (4.31) would be

$$E < \left(\frac{g\Lambda^2 m_W^2}{g_*}\right)^{1/4} \longrightarrow E < \Lambda\sqrt{\frac{g}{g_*}}\,. \tag{4.37}$$

To conclude this subsection we would like to remind the reader that EFT validity discussion needs some assumptions on power-counting (see for a recent discussion [180]). In the rest of this chapter though, we do not commit to any of the aforementioned power-counting rules. We only assume perturbative, but otherwise arbitrary, Wilson coefficients.

4.2.4 Numerical cross-check

In figure 4.1 we show the results of a `MadGraph5` [181] simulation, using the `EWdim6` [80] model [8] , for the process $pp \to VW$. The parametric dependence of the cross section on the TGCs is given by

$$\sigma_{q\bar{q}\to VW} = \sigma_{\rm SM} + \delta\,\sigma_{\rm int} + \delta^2\,\sigma_{\rm BSM^2}\ , \quad \text{with} \quad \delta = \{\delta g_{1,Z},\, \delta\kappa_Z,\, \lambda_Z\}\,, \tag{4.38}$$

In figure 4.1 we plot $\sigma_{\rm int}/\sigma_{\rm SM}$ (top) and $\sigma_{\rm BSM^2}/\sigma_{\rm SM}$ (bottom) for different anomalous TGCs as a function of the invariant mass m_{VW} of the VW final state system. Note that in this ratios the $g_{\rm SM}^4/E^4$ factor in (4.21) cancels and we can read the scaling as a function of the energy from (4.12) and (4.18 – 4.20).

The top plot of figure 4.1 shows the energy scaling of $\sigma_{\rm int}/\sigma_{\rm SM}$. The red and purple lines confirm the quadratic growth expected from the $\delta g_{1,Z}$ and $\delta\kappa_Z$ contribution in (4.18) for the process $q\bar{q} \to W_L^- W_L^+$. The dashed green line depicts an energy dependence of the cross section ratio $\sigma_{\rm int}/\sigma_{\rm SM}$ when only the aTGC $\delta\kappa_Z$ is switch on, the curve shows no growth as a function of the energy, this confirms the discussion of (4.12) and (4.19). Namely, that for the final state ZW, the leading energy growth is only mediated by $\delta g_{1,Z}$ (blue line) but not by $\delta\kappa_Z$ (dashed green line). Lastly, on the same plot we show that $\sigma_{\rm int}/\sigma_{\rm SM}$ mediated by λ_Z has no energy growth, as there is no interference with SM, confirming (4.26). This later measurement comes from WW production, but a similar result for λ_Z is obtained for WZ production.

[8] Note that our definition in (4.13) differs from the one of [80].

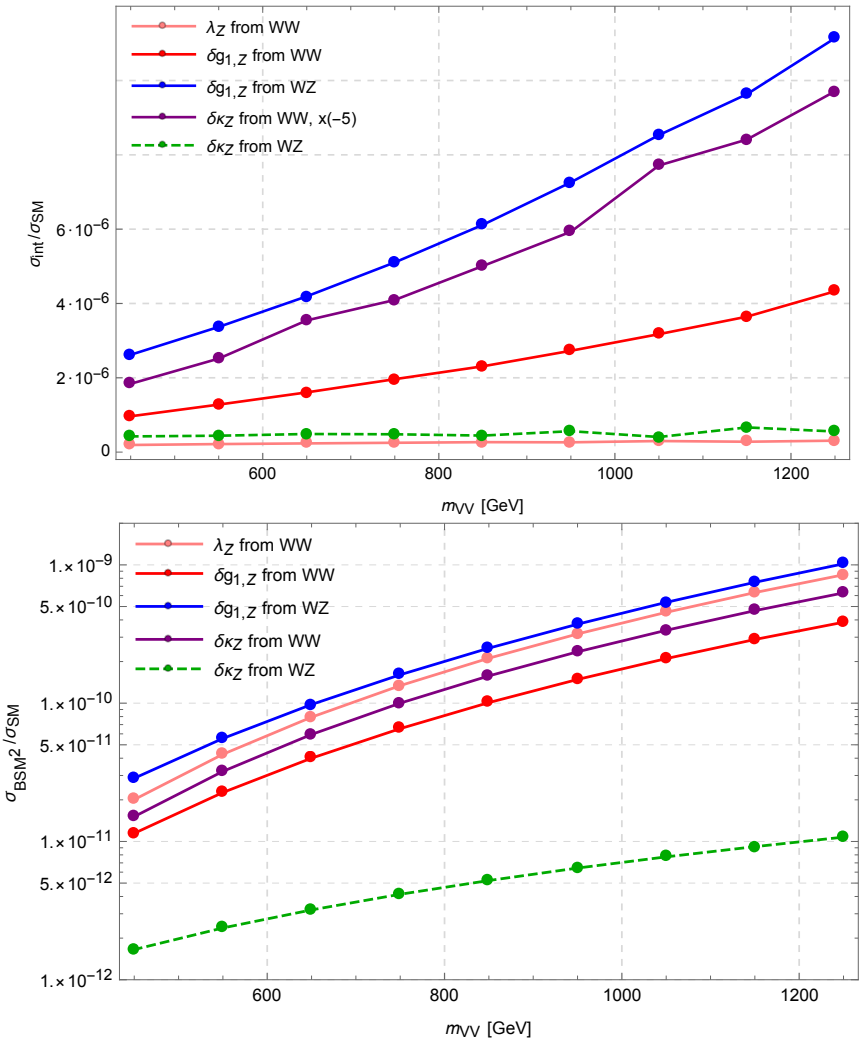

Figure 4.1: Results from a `MadGraph5` simulation of the $pp \to VW$ process mediated by anomalous TGCs, see the main text. The error bars of both plots due to statistical errors is within the width of the plotted lines. We multiplied the line $\sigma_{\rm int}/\sigma_{\rm SM}$ of $\delta\kappa_Z$ from WW by $\times(-5)$ for illustrative reasons.

In the bottom panel of figure 4.1, we show the energy dependence of $\sigma_{\rm BSM^2}/\sigma_{\rm SM}$, confirming the theoretical expectations. Namely, we find that for VW production the factor $\sigma_{\rm BSM^2}/\sigma_{\rm SM}$ mediated by λ_Z and $\delta g_{1,Z}$ scale with the same power E^4. Then, regarding $\delta\kappa_Z$ the amplitude grows as E^2 for WZ production while it scales as E^4 for W^+W^- production — this is the expectation from the squared amplitude $|\mathcal{M}\left(q\bar{q} \to Z_T W_L^+ / Z_L W_T^+\right)|^2 \sim v^2 E^2 \delta\kappa_Z^2$, see text after (4.20).

4.3 Solutions to the non-interference obstruction

In the previous section we showed that for the $2 \to 2$ processes the interference between O_{3W} and the SM is suppressed. In this section we will present two ways to overcome this

suppression. For simplicity reasons in the remaining part of this chapter we will consider the case when only λ_Z deformation is present and the other anomalous TGCs are set to zero.

4.3.1 Angular distributions

The first way of enhancing the interference term is by noting that in reality we are not looking at the $2 \to 2$ process but at $2 \to 4$, i.e. vector bosons decay into fermions $q\bar{q} \to VW \to 4\psi$. Let us consider the differential cross section for the production of the polarized particles $W_{T+}l_-\bar{l}_+$ [9], differential cross section for the Z decay process is given by

$$\frac{d\sigma(q\bar{q} \to W_{T_+} l_- \bar{l}_+)}{d\text{LIPS}} = \frac{1}{2s} \frac{\left| \sum_i (\mathcal{M}^{\text{SM}}_{q\bar{q}\to W_{T_+} Z_i} + \mathcal{M}^{\text{BSM}}_{q\bar{q}\to W_{T_+} Z_i}) \mathcal{M}_{Z_i \to l_- \bar{l}_+} \right|^2}{(k_Z^2 - m_Z^2)^2 + m_Z^2 \Gamma_Z^2}, \tag{4.39}$$

where sum runs over intermediate Z polarizations and $d\text{LIPS} \equiv (2\pi)^4 \delta^4(\sum p_i - p_f) \prod_i d^3 p_i / \left(2E_i (2\pi)^3\right)$ is the Lorentz Invariant differential Phase Space (LIPS). We have factored out a Z-boson propagator, inputting the fact that all Z polarizations have the same mass and width. It is well known that at LHC SM process is dominated by the transverse polarizations [163], so for simplicity let us ignore the contributions from the intermediate longitudinal Z_L bosons. Then in the narrow width approximation the leading contribution to the interference, i.e. the cross term SM $\times$ BSM in (4.39) is given by:

$$\frac{\pi}{2s} \frac{\delta(s - m_Z^2)}{\Gamma_Z m_Z} \mathcal{M}^{\text{SM}}_{q\bar{q}\to W_{T_+} Z_{T_-}} \left(\mathcal{M}^{\text{BSM}}_{q\bar{q}\to W_{T_+} Z_{T_+}} \right)^* \mathcal{M}_{Z_{T_-} \to l_- \bar{l}_+} \mathcal{M}^*_{Z_{T_+} \to l_- \bar{l}_+} + h.c.\,. \tag{4.40}$$

The interference cross section in (4.40) scales with the function $\mathcal{M}_{Z_{T_-} \to l_- \bar{l}_+} \mathcal{M}^*_{Z_{T_+} \to l_- \bar{l}_+}$. This in turn is modulated by the azimuthal angle ϕ_Z between the plane defined by the Z decay leptons and the scattering plane (formed by collision axis and $Z(W)$ bosons), see figure 4.2. It is straightforward to compute (4.40), leading to

$$\frac{d\sigma_{\text{int}}(q\bar{q} \to W_+ l_- \bar{l}_+)}{d\phi_Z} \propto \cos(2\phi_Z)\,. \tag{4.41}$$

The derivation of (4.41) is analogous if we consider the decay of the W gauge boson. Therefore, the differential interference term for the process $q\bar{q} \to VW \to 4\psi$ is unsuppressed and modulated as

$$\frac{d\sigma_{\text{int}}(q\bar{q} \to WZ \to 4\psi)}{d\phi_Z\, d\phi_W} \propto \cos(2\phi_Z) + \cos(2\phi_W), \tag{4.42}$$

[9] Similar ideas where proposed recently for the $W\gamma$ final state [182].

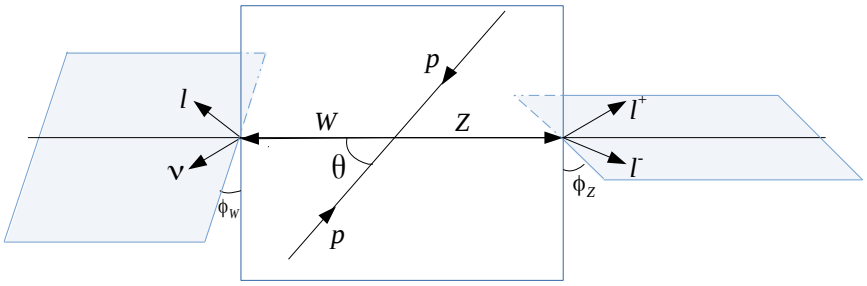

Figure 4.2: Angles for $2 \to 4$ scattering

where $\phi_{W,Z}$ are the corresponding azimuthal angles. Eqs.(4.41, 4.42) are one of our main results. Namely, we would like to take advantage of the modulation of the interference term to prove the anomalous triple gauge coupling λ_Z. Due to the two $2\phi_i$ arguments in (4.42) the asymmetry is not washed out by the ambiguity in the direction of quark-antiquark initial state.

Similarly there is an effect of interference between the intermediate SM amplitude $\mathcal{M}^{\rm SM}_{q\bar{q}\to W_L Z_L}$ of longitudinal vector bosons and the BSM amplitude $\mathcal{M}^{\rm BSM}_{q\bar{q}\to W_T Z_T}$ with transverse vector bosons. The form of the modulation is different from (4.42) and is

$$\frac{d\sigma_{\rm int}(q\bar{q}\to WZ\to 4\psi)}{d\phi_Z\, d\phi_W} \propto \cos\left(\phi_W + \phi_Z\right). \tag{4.43}$$

This later effect of modulation, however, cancels out upon integration on ϕ_W and the direction of quark-antiquark initial states.

Note that, naively, if the vector bosons are produced on-shell one would expect that vector bosons with different helicity contributions should not interfere (or be suppressed by their width) even if we look at the decay products. Namely, one may expect that the interference is further suppressed than the case in which same $2 \to 4$ amplitude was mediated by a $2 \to 2$ sub-process $q\bar{q} \to VW$ that does lead to a cross section containing an interference term. However, this is not true, due to the basic fact that the both helicities have the poles of the propagators at exactly the same energies. Note that in the hypothetical case where the $2 \to 2$ process $\mathcal{M}^{\rm BSM}_{q\bar{q}\to W_+ Z_-} \sim E^2/\Lambda^2$ was not suppressed, we would had gotten an analogous $\Gamma_Z/m_Z \to 0$ limit in (4.40) where the amplitude would be instead controlled by the azimuthal angle of the function $\mathcal{M}_{Z_{T_-}\to l_-\bar{l}_+}\mathcal{M}^*_{Z_{T_-}\to l_-\bar{l}_+}$ (no modulation in ϕ_i in this case), but otherwise the energy growth would be the same.

We have performed a `MadGraph5` numerical simulation to test our theoretical expectations. The results shown in figure 4.3. In the top plot we show the interference differential

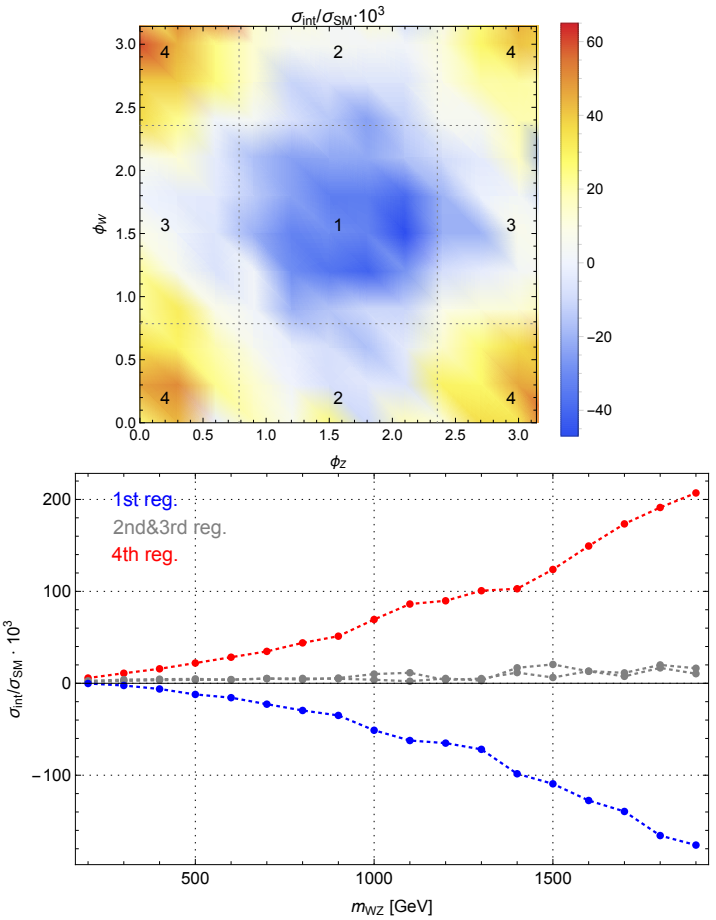

Figure 4.3: Top: Differential interference cross section over SM one as a function of the azimuthal angles $\phi_{W,Z}$ for the events with $W-Z$ invariant mass $m_{WZ} \in [700, 800] GeV$. **Bottom:** same quantity as a function of the m_{WZ} binned according in the four bins defined in the top plot.

cross section over the SM cross section as a function of ϕ_Z and ϕ_W. [10] The shape of the function is as predicted by (4.42). This suggests that we should bin the events into four categories depending on whether $\phi_i \in [\pi/4, 3\pi/4]$. The results are shown on the bottom plot of figure 4.3. The upper red line and the lower blue line correspond to the categories with $\phi_{W,Z} \in [0, \pi/4] \cup [3\pi/4, \pi]$ and $\phi_{W,Z} \in [\pi/4, 3\pi/4]$. We can see that there is a strong cancellation between these two contributions, however individually both of them grow with energy. So binning in azimuthal angles will increase dramatically the sensitivity to the interference.

[10] Note that the SM contribution also has a modulation due to the interference between the amplitudes with different intermediate gauge bosons polarizations. However, this effect is suppressed compared to the constant term.

4.3.2 Going beyond leading order

The non-interference of SM × BSM in diboson production through λ_Z in the $2 \to 2$ process applies at tree-level only. Higher order corrections, either in the form of loops or radiation, overcome the interference suppression and lead to a SM × BSM cross section piece that does grow with energy. This was first noticed in the context of QCD for the gluon operator $\sim G_\mu{}^\nu G_\nu{}^\rho G_\rho{}^\mu$ [89]. Here we apply this idea to the electroweak sector. The corrections from the virtual gluon will introduce the BSM-SM interference, however this effect will be suppressed by $\sim \frac{\alpha_s}{4\pi}$ compared to the angular modulation discussed in the previous section. Another possibility is to consider $2 \to 3$ processes, namely the production of the pair of the electroweak bosons with a hard QCD jet $VV + j$ .Then using Eq. (4.23) the BSM amplitudes have following helicity configuration,

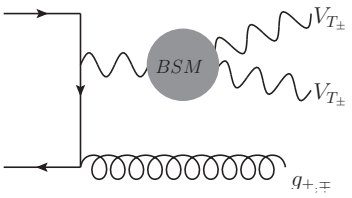

where the gluon g can take any polarization. In the SM the same process has necessarily the helicity configuration

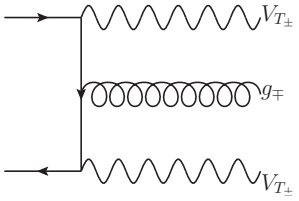

i.e. it can not be of the Maximally Helicity Violating type. Thus, the extra gluon radiation helps in sucking helicity allowing the same final state process as in $VV + j$ mediated by O_{3W}. We find this simple observation interesting, since the requirement of extra radiation qualitatively changes the cross section behavior and provides a better handle on the interference terms. Note also that the solution we are advocating in this section is complementary to the analysis presented in the section 4.3.1, in addition to the binning in the azimuthal angle we just require an extra hard jet.

Remember that the interference effect becomes small both in the soft and collinear jet limits [89]. This is expected since interfering SM amplitudes $A(q\bar{q} \to V_{T_\pm} V_{T_\pm} g_\mp)$ cannot be generated from $A_{SM}(q\bar{q} \to VV)$ by splitting quark(anti-quark) line into $q(\bar{q}) \to q(\bar{q})g$. So there will be no usual soft and collinear singularities corresponding to the poles of the splitting functions, which we have checked by explicit calculation. Then the interference term in these limits, even if growing with energy, will be completely buried inside the SM contribution.

We cross-check the theoretical expectations with a `MadGraph5` simulation. In figure 4.4 we plot the ratio $\sigma_{\rm int}/\sigma_{\rm SM}$ for diboson production as a function of the invariant mass m_{WZ}, making various requirements on the extra gluon. In blue we ask for no extra radiation which corresponds to the non-interference effect discussed in figure 4.1. In red and pink we require a hard gluon which takes a significant fraction of the diboson phase-space, $m_{WZ}/10$ and $m_{WZ}/5$ respectively. Importantly, the simulation shows the expected energy growth of the interference term. On the other hand, the purple curve does not show a steady growth of the energy. This is also expected since that curve is obtained by imposing a fixed lower cut on the jet p^T. As the energy of the diboson is increased the extra jet becomes relatively soft and the energy growth is lost. We find by numerical simulations (see figure 4.4) that we need to require something like $p_j^T \gtrsim \frac{m_{WZ}}{5}$ to have a quadratic growth with energy. Error bars are due to the statistical treatment of the Monte Carlo (MC) simulation – we regard them as small enough to convey our point.

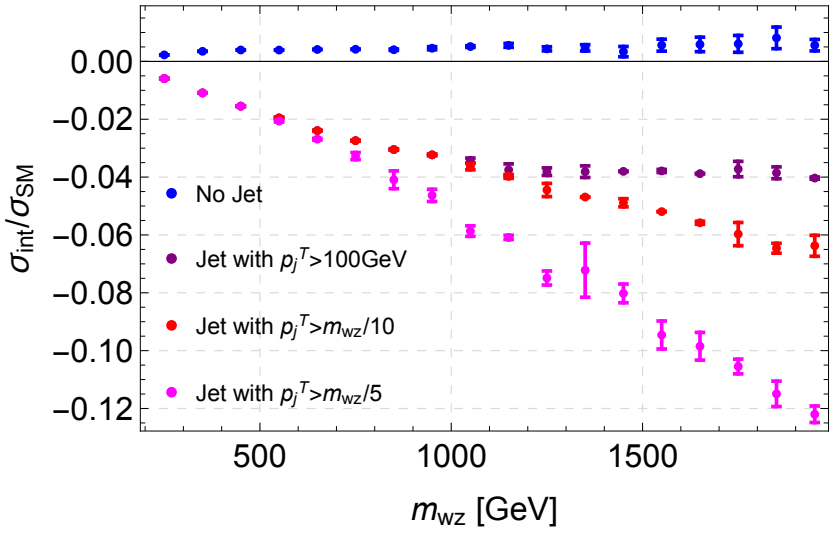

Figure 4.4: $\sigma_{\rm int}/\sigma_{\rm SM}$ as a function of m_{WZ} for the process $pp \to WZ$ (blue) and the process $pp \to VW + j$, with $p_j^T > m_{WZ}/5$ (pink), $p_j^T > m_{WZ}/10$ (red), and $p_j^T > 100$ GeV (purple).

4.4 EFT validity

So far we were presenting the observables particularly sensitive to the SM×BSM interference term. However this is not enough to ensure the validity of the EFT interpretation of diboson production at the LHC. The convergence of the EFT expansion is controlled by the ratio of the invariant mass of the diboson system over the new physics scale and thus $m_{VW}/\Lambda \ll 1$ should be satisfied. However at the LHC it is hard to keep m_{VW}/Λ fixed. First, the precise collision energy is unknown and not fixed, leading to an imprecise knowledge of m_{VW} from event to event. Secondly and more importantly, in many instances experimentalists only reconstruct the visible decay products. Namely, the $W-Z$

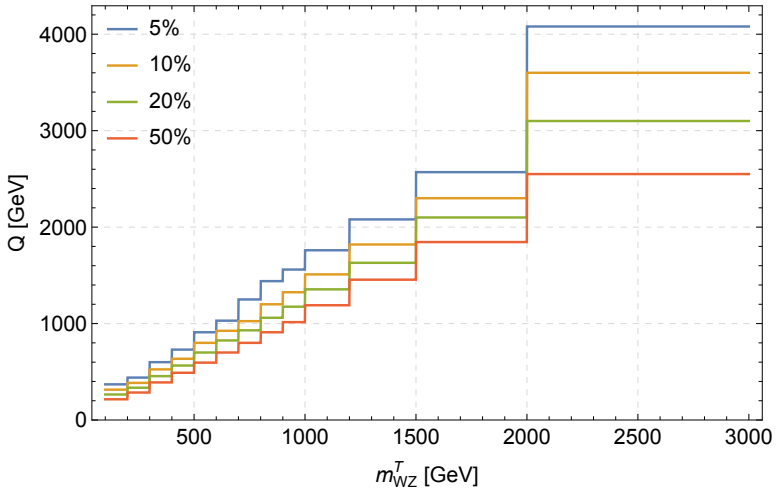

Figure 4.5: We show, for the process $q\bar{q} \to WZ$ with λ_Z turned on, the leakage as a function of m^T_{WZ}, see main text for the definition.

transverse mass

$$m^T_{WZ} = \sqrt{(E^W_T + E^Z_T)^2 - (p^W_x + p^Z_x)^2 - (p^W_y + p^Z_y)^2}\,, \tag{4.44}$$

in the WZ production or the (visible) dilepton invariant mass

$$m_{ll} = \sqrt{(p_{l^-} + p_{l^+})^2}\,, \tag{4.45}$$

of the WW decay products. The invariant mass m_{VW} of the diboson system is always greater or equal the visible invariant masses $m_{VW} \geq m_{ll}, m^T_{WZ}$. This implies that binning and cutting the distributions in terms of variables m_{ll} or m^T_{WZ} does not allow to ensure $m_{VW}/\Lambda \ll 1$. As an illustration of this point, in figure 4.5 we show the *leakage*. This is defined as the percentage of the number of events in a given m^T_{WZ} (or m_{ll}) bin with invariant mass m_{VW} larger than a certain scale Q. In equations,

$$\text{Leakage} = \frac{N_i(m_{VW} > Q)}{N_i} \times 100\%\,, \tag{4.46}$$

where N_i is the total number of events in the given m^T_{WZ} (or m_{ll}) bin. For instance, the red line in the bin $m^T_{WZ} \in [1500, 2000]$ GeV is interpreted as follows. Of all the events in that bin, 50% of them have an invariant mass $m_{WZ} \gtrsim 1800$ GeV. These numbers were calculated using only the σ_{BSM^2} term of the cross section, see (4.38), which is the term giving the largest leakage.

Naively, we can use the information in figure 4.5 to set consistent bounds on the EFT. For example, if we require $\Lambda = 2$ TeV and the precision of the measurement $\lesssim O(1) \times 5\%$ we should keep the transverse mass bins only up to 1.5 TeV. This would work under the assumption that the leakage calculated using the dimension six operator squared provides

a conservative estimate compared to the full UV complete model, namely that we do not have a very large number of events for some value of invariant mass $M_* > 2$ TeV. This assumption is for example spoiled in the presence of the narrow Bright-Wigner resonances and the calculation with dimension six operators underestimates the cross section and leakage by the factor of

$$\frac{\sigma^{full}}{\sigma^{d=6}} \sim \frac{\pi\Lambda^2}{\Gamma^2}, \tag{4.47}$$

which becomes very large for narrow resonances (Λ, Γ are the mass and the width of the resonance). At the same time in the more strongly coupled theories (4.47) is only of order one $O(1)$. Thus, under the assumption $\sigma^{full}/\sigma^{d=6} \lesssim O(1)$, we can use the figure 4.5 to find the correspondence between the transverse and invariant mass cut-offs once the precision of the measurement is specified.

The leakage can be made arbitrarily small by simply assuming a large enough value of Λ in the EFT interpretation. Then there is obviously no danger of narrow Breit-Wigner peaks, since the new particles would be too heavy to be produced at LHC. However, this is somewhat dissatisfying because then LHC sensitivities only allow to prove Wilson coefficients that are on the verge of non-perturbativity, in order to compensate the large value of Λ. For instance in [183] bounds on the TGCs Wilson coefficients are of order $c_i \lesssim [-2.5, 2.5]$ [11], with the cut-off $\Lambda = 1$TeV. This is done by analyzing the whole range of $m^T_{VW} \approx [50, 650]$ GeV, and thus we expect large number of the events to have invariant masses $m_{VW} \gtrsim 1$ TeV. Then for the proper EFT interpretation we should set $\Lambda \gtrsim 2$ TeV, thus implying that the bound gets loosened roughly as $c_i \lesssim [-2.5, 2.5] \longrightarrow c_i \lesssim 4\times[-2.5, 2.5]$, which pushes the EFT even further on the verge of non-perturbativity.

Next we will discuss another possible approach to perform a consistent EFT analysis. It allows to lower the cut-off Λ and hence be sensitive to somewhat less exotic theories, at least when the statistics is enlarged in the upcoming future.

4.4.1 Dealing with the leakage of high invariant mass events

The idea consists in comparing the observed cross section with the new physics expectation only in the constrained phase space satisfying the EFT validity requirements. This approach was originally suggested for the Dark Matter searches at LHC [184] and later applied for the anomalous TGCs measurements [164]. Next we discuss our implementation of these ideas.

In the standard analysis, for every bin say in $m^T_{WZ} \in [m^T_1, m^T_2]$, one would compare the observed number of events $n_{\rm obs}$ with the theory prediction $M_{\rm th}$, which in our case reads

$$M_{\rm th} = n_{\rm SM} + n_1 c_{3W} + n_{\rm BSM^2} c^2_{3W}\,, \tag{4.48}$$

[11] We have rescaled the bounds of [183] to our normalization in (4.13).

where $n_{\rm SM}$ is the SM prediction, and n_1, $n_{\rm BSM^2}$ come from the $\sigma_{\rm int}$ and $\sigma_{\rm BSM^2}$ pieces in (4.38). In practice this comparison can be done by evaluating the likelihood on a given bin by a Poisson distribution $p(n_{\rm obs}|M_{\rm th}) = \frac{1}{n_{\rm obs}!}e^{-M_{\rm th}}M_{\rm th}^{n_{\rm obs}}$. Note however that if we took this procedure we would be comparing $M_{\rm th}$ with $n_{\rm obs}$ for events where the formula $M_{\rm th}$ is not valid unless the new physics scale Λ is very large – see the discussion of figure 4.5.

Instead, what we will do is to compare the observed number of events with the quantity $N_{\rm th}$, which we define as follows:

$$N_{\rm th} = \begin{cases} \widetilde{N}_{\rm th} & \text{if} \quad \widetilde{N}_{\rm th} > n_{\rm SM} \\ n_{\rm SM} & \text{otherwise} \end{cases} , \tag{4.49}$$

where we define $\widetilde{N}_{\rm th} = \tilde{n}_{\rm SM} + \tilde{n}_1 c_{3W} + \tilde{n}_{\rm BSM^2} c_{3W}^2$ with $\tilde{n}_i$ is defined as $n_i|_{m_{inv}<\Lambda_{\rm MC}}$, i.e. we restrict the expected number of events in the EFT to have invariant mass m_{WZ} (or m_{WW}) below certain fixed cut-off scale $\Lambda_{\rm MC}$. [12] Thus, in practice the likelihood is modeled by $p(n_{\rm obs}|N_{\rm th}) = \frac{1}{n_{\rm obs}!}e^{-N_{\rm th}}N_{\rm th}^{n_{\rm obs}}$.

The key question is whether the bounds obtained using (4.49) lead to more conservative estimates than the ones which could come from the knowledge of full theory. The number of events in the full theory is

$$N_{\text{full theory}} = \widetilde{N}_{\rm th} + [N_{\text{full theory}}]_{m_{inv}>\Lambda_{MC}} , \tag{4.50}$$

where we approximated the theory below Λ_{MC} by the EFT expansion. Note that both terms in (4.50) are positive. Then, the bounds from (4.49) are conservative only if

$$|n_{SM} - N_{\rm th}| \leq |n_{SM} - N_{\text{full theory}}| , \tag{4.51}$$

condition that is always fulfilled with our definition of $N_{\rm th}$ in (4.49).

Finally, let us note that in Ref. [164] the choice of the theory is $N_{\rm th} = n_{\rm SM} + \tilde{n}_1 c_{3W} + \tilde{n}_{\rm BSM^2} c_{3W}^2$, instead of (4.49). This amounts to modifying the BSM amplitudes by the "form factor"

$$\mathcal{M}_{BSM} \to \mathcal{M}_{BSM} \times \theta(\Lambda_{\rm MC} - m_{inv}) , \tag{4.52}$$

where the $\theta(x)$ is the Heaviside step function or any close function behaves like $(1+e^{-\alpha[\Lambda_{\rm MC}-m_{inv}]/m_{inv}})^{-1}$ with $\alpha \gg 1$ [13]. Then, equation (4.51) is fulfilled only if one assumes that the deviations from the SM below and above Λ_{MC} are of the same sign, $\text{sign}(\Delta\sigma_{\rm BSM})|_{m_{inv}>\Lambda_{MC}} = \text{sign}(\Delta\sigma_{\rm BSM})|_{m_{inv}<\Lambda_{MC}}$. Or in terms of the variables in (4.49)

$$\text{sign}(N_{\text{full theory}} - n_{\rm SM} - \tilde{n}_1 c_{3W} - \tilde{n}_{\rm BSM^2} c_{3W}^2) \quad = \quad \text{sign}(\tilde{n}_1 c_{3W} + \tilde{n}_{\rm BSM^2} c_{3W}^2) . \tag{4.53}$$

[12] We are distinguishing the assumed cut-off scale $\Lambda_{\rm MC}$ set in the MC simulation from the true value of Λ in the SM EFT, which is of course an unknown constant of nature. Also note that $\Lambda_{\rm MC}$ is analog to the scale Q introduced in (4.46).

[13] Note though that such function is not analytic in $\Lambda_{\rm MC}^{-1}$.

Note that this condition is trivially satisfied when BSM^2 dominates the cross section, however it is not true once interference term is of the same size [164].

At last we would like to comment about the procedure in the experimental study [96]. There, a different form-factor for the new physics contribution is used

$$\mathcal{M}_{BSM} \to \mathcal{M}_{BSM} \times \frac{1}{\left(1+\frac{m_{inv}^2}{\Lambda_{MC}^2}\right)^2} \,. \tag{4.54}$$

The different form factors would lead to identical results for $\Lambda_{MC} \gg m_{inv}$, but there will be order one differences for the events with invariant mass close to the cut-off Λ_{MC}. Also, note that while the UV assumptions are very clear when using (4.52) they are somewhat more obscure in (4.54). The reason being that the fall-off of the form factor in (4.54) is not steep enough and its validity requires some discussion or assumptions on the leakage along the lines we did at around (4.47).

4.5 Details of the collider simulation and statistical procedure

In this section we explain our procedure for estimating the improvements of the LHC sensitivity due to the differential distributions proposed in the section 4.3. We have decided to look at the cleanest decay channel in the pair production of the vector bosons, namely the process $pp \to W^\pm Z \to lll\nu$. In our analysis we have followed the signal selection procedure presented in the experimental work [96]. For the signal simulation we have used `MadGraph5` [181] with the model `EWdim6` [80] at LO [14]. The results are reported for the 14 TeV LHC collision energy and two benchmark luminosities, 300 and 3000 fb^{-1}.

We have checked that our partonic level simulation reproduces the acceptance at the particle level $A_{WZ} = 0.39$, for the experimental analysis at 8 TeV [96]; it is defined as the ratio of the fiducial to the total cross section

$$\sigma^{tot}_{W^\pm Z} = \frac{\sigma^{fid}_{W^\pm Z \to l'\nu ll}}{B_W B_Z A_{WZ}} \,. \tag{4.55}$$

The fiducial cross section is defined as

$$\sigma^{fid}_{W^\pm Z \to l'\nu ll} = \frac{N_{data} - N_{bkg}}{\mathcal{L}\, C_{WZ}} \times \left(1 - \frac{N_\tau}{N_{all}}\right) \,, \tag{4.56}$$

[14] One can perform the complete NLO study of the anomalous TGC using the model `EWdim6NLO` by C. Degrande. In our study however we have decided to ignore the effects of the virtual gluon, which we believe to be phenomenologically less important (see discussion in section 4.3.2). For other QCD advances in SM and BSM calculations of the weak boson pair production see [185–190]

where the factor C_{WZ} simulates the detector efficiency $C_{WZ} = N_{events}^{particle}/N_{events}^{detector} \approx 0.6$ [96], and we approximate it to be flavour universal. In eq. (4.55) B_i denote the corresponding branching fractions; while the factor N_τ/N_{total} in eq. (4.56) is the contribution of the leptons from τ decays which [96] estimated to be of $\sim 4\%$ and thus we will ignore it. $\mathcal{L}$ is the integrated Luminosity, below we report results for $\mathcal{L} = 300$ fb^{-1} and 3 ab^{-1}.

We bin all the events according to their transverse mass m_{WZ}^T, and transverse momentum of the jet p_j^T. In particular p_j^T is binned as

$$p_j^T = [0, 100],\ [100, 300],\ [300, 500],\ [500, \infty]\ \text{GeV}\,. \tag{4.57}$$

For the events with $p_j^T < 100$ GeV we also bin the azimuthal angle ϕ_Z into two categories

$$\phi_Z \in [\pi/4, 3/4\pi] \quad \text{and} \quad \phi_Z \in [0, \pi/4] \cup [3\pi/4, \pi]\,. \tag{4.58}$$

The azimuthal angle ϕ_Z is defined here as an angle between the plane spanned by Z boson decay leptons and the plane formed by the collision axis and the Z boson. For the higher p_j^T bins we have checked that the binning in azimuthal angle results in little improvement of the bounds. The reason being that the modulation effect becomes subdominant compared to energy growth due to additional hard jet.

For each bin defined above we calculate the cross section in the presence of the c_{3W} deformation according to the formulas (4.48) and (4.49). The coefficients n_{SM}, n_{BSM^2} are calculated by switching off BSM and SM contributions respectively. For the interference term n_1 this is not possible, since as it is shown in our analysis there are phase space regions where this contribution has the opposite signs. So in order to avoid any issues with the negative values of cross section we have fitted it while keeping both SM and BSM contributions. This procedure generically can lead to large errors on the determination of the n_1 coefficient. These errors were kept under control by performing a large enough number of simulations and iteratively choosing for the fit the values of c_{3W} maximizing the interference term.

We have performed the analysis for for three values of the invariant mass cut-off

$$\Lambda_{\text{MC}} = 1,\ 1.5,\ 2\ \text{TeV}\ . \tag{4.59}$$

These are reasonable choices in view of the current direct exclusion bounds.

In order to reduce the fitting time we have used partonic level simulation to determine the coefficients in the eqs. (4.48, 4.49). For the bin $p_j^T \in [0, 100]$ GeV we sum partonic level simulations with 0 jet and 1 jet with $p_j^T \in [20, 100]$ GeV. We have checked that for the SM input this approximation agrees well with the results obtained with `Madgraph/Pythia` [191] interface with showering and jet matching. One may worry whether emission of a QCD jet can spoil the azimuthal angle modulation, however we have checked that even for relatively hard jets $p_j^T \lesssim 100$ GeV angular modulation remains an important effect. This makes our partonic simulation results robust.

For the backgrounds we have followed closely the results in [96], where it was shown that the dominant background for the anomalous TGCs is the SM W, Z boson production. The second most important background comes from the misidentified leptons $\sim 12\%$ and ZZ final state $\sim 7\%$ and the contribution of the $t\bar{t}$ is at percent level. Since most of these backgrounds come from the $q\bar{q}$ initial state (except for $t\bar{t}$ which is small) at 14 TeV we expect a very similar situation. In our study we have decided to consider only the SM weak boson production as a background, the other contributions will provide an additional increase of the background by $\sim 20\%$ and the relaxations of the bounds by $\sim 10\%$, which we ignore in our study. For systematic uncertainties we use the results in [96], where it was reported that the dominant errors come from the muon and electron identification efficiencies and it was estimated to be at the level of 2.4%. The statistical analysis is done using the Bayesian approach, where systematic errors are estimated using one nuisance parameter ξ, normally distributed

$$p(N_{\rm th}|n_{\rm obs}) \propto \int d\xi e^{-\xi N_{\rm th}} (\xi N_{\rm th})^{n_{\rm obs}} \exp\left[-\frac{(\xi-1)^2}{2\sigma^2_{syst}}\right] . \tag{4.60}$$

4.6 Results

We present our bounds on c_{3W}/Λ^2 in table 4.1. We report LHC prospects for 300 fb^{-1} as well as for 3 ab^{-1} luminosity (Lumi.) values. Exclusive (Excl.) bounds are obtained according to the method described in section 4.5, binning in ϕ_Z and p_j^T, while inclusive (Incl.) corresponds to no binning in ϕ_Z and $p_j^T \leq 100$ GeV. The total leakage in the various bins of m_{WZ}^T is $\lesssim 5\%$ for each value of Q; such bins are selected using figure 4.5. [15]

The bounds of the rows *Excl./Incl., linear* are obtained by including only the linear terms in c_{3W} in BSM piece of cross section. In the linear analysis, values of the Wilson coefficient $|c_{3W}| \gtrsim 3$ lead to negative number of events. Nevertheless, such values lie outside the credibility intervals of the fit. In order to avoid this issue for arbitrary values of c_{3W} during the scan we have used the following modification of (4.48)

$$M_{th} = (n_{\rm SM} + c_{3W} n_1) \times \theta(n_{\rm SM} + c_{3W} n_1), \tag{4.61}$$

where the θ is the usual step function. Generically, this later procedure is of course inconsistent. However, comparing linear v.s. non-linear gives a sense of how much sensitive are the bounds to the quadratic piece term BSM_6^2 in the cross section (4.21). In this respect, note that the exclusive analysis sensitivity to the linear terms has drastically increased compared to the inclusive one. For instance, the gain from the second to the first row is very mild, implying that the bound is mostly proving the interference term. Instead, the bounds from the third to the fourth row drastically relax implying that the

[15] The scale Q is roughly equal to the Monte-Carlo cut-off Λ_{MC}, but see the discussion of figure 4.5 and table 4.2.

	Lumi. 300 fb^{-1}		Lumi. 3000 fb^{-1}		Q [TeV]
	95% CL	68% CL	95% CL	68% CL	
Excl.	[-1.06,1.11]	[-0.59,0.61]	[-0.44,0.45]	[-0.23,0.23]	1
Excl., linear	[-1.50,1.49]	[-0.76,0.76]	[-0.48,0.48]	[-0.24,0.24]	
Incl.	[-1.29,1.27]	[-0.77,0.76]	[-0.69,0.67]	[-0.40,0.39]	
Incl., linear	[-4.27,4.27]	[-2.17,2.17]	[-1.37,1.37]	[-0.70,0.70]	
Excl.	[-0.69,0.78]	[-0.39,0.45]	[-0.31,0.35]	[-0.17,0.18]	1.5
Excl., linear	[-1.22,1.19]	[-0.61,0.61]	[-0.39,0.39]	[-0.20,0.20]	
Incl.	[-0.79,0.85]	[-0.46,0.52]	[-0.41,0.47]	[-0.24,0.29]	
Incl., linear	[-3.97,3.92]	[-2.01,2.00]	[-1.27,1.26]	[-0.64,0.64]	
Excl.	[-0.47,0.54]	[-0.27,0.31]	[-0.22,0.26]	[-0.12,0.14]	2
Excl., linear	[-1.03,0.99]	[-0.52,0.51]	[-0.33,0.32]	[-0.17,0.17]	
Incl.	[-0.52,0.57]	[-0.30,0.34]	[-0.27,0.31]	[-0.15,0.19]	
Incl., linear	[-3.55,3.41]	[-1.79,1.75]	[-1.12,1.11]	[-0.57,0.57]	

Table 4.1: Exclusive (Excl.) bounds on $c_{3W}/\Lambda^2 \times \text{TeV}^2$ are obtain according to the method described in section 4.5, binning in ϕ_Z and p_j^T. Inclusive (Incl.): no binning and jet veto at $p_j^T \leq 100$ GeV. The bounds of the rows *Excl./Incl., linear* are obtained by including only the linear terms in c_{3W} BSM cross section. The total leakage in the various bins of m_{WZ}^T is $\lesssim 5\%$ for each value of Q.

consistent bound of the third row is giving a lot of power to the quadratic pieces in c_{3W}^2. This comparison illustrates the improvement from the differential distributions versus the inclusive analyses. Of course such a gain is always expected. However, in this case the improvement is dramatic because, as explained in section 4.3, the interference terms of the differential cross section have a qualitatively different behavior, namely they grow with the center of mass diboson energy.

This radical increase towards the sensitivity of the interference term is illustrated in figure 4.6. There, we have injected a signal corresponding to the $c_{3W}/\Lambda^2 = 0.3$ TeV^{-2}. The red and black curves are posterior probabilities with $\Lambda_{MC} = 2$ TeV and corresponding to inclusive and exclusive analysis respectively (by inclusive we mean only binning in m_{WZ}^T and ignoring high p_j^T bins). The curves are obtained by requiring the leakage to be $\lesssim 5\%$ as done in table 4.1, (shaded grey area indicates the 95% credibility intervals for the exclusive analysis). We can clearly see that our variables will be able to access the sign of the c_{3W} Wilson coefficient otherwise hidden from the inclusive searches. Inspired by the figure 4.3 we can see that the following asymmetry variable turns out to be very sensitive to the new physics contribution:

$$R_{\phi_Z} = \frac{N_{\phi_Z \in [\pi/4, 3\pi/4]} - N_{\phi_Z \in [0,\pi/4] \cup [3\pi/4,\pi]}}{N_{\phi_Z \in [\pi/4, 3\pi/4]} + N_{\phi_Z \in [0,\pi/4] \cup [3\pi/4,\pi]}} \,. \tag{4.62}$$

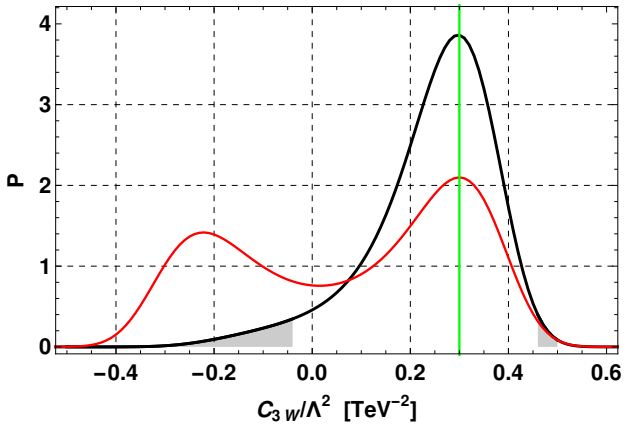

Figure 4.6: Posterior probability for the inclusive and exclusive analysis after 3 ab^{-1} at LHC, see details in the main text.

Indeed, we have checked that the SM contribution partially cancels, making R_{ϕ_Z} particularly sensitive to new physics contributions.

We would like to comment for what kind of theories our bounds are relevant. We can see that at most we are getting towards the constraint $c_{3W}/\Lambda^2 \lesssim 0.2/\text{TeV}^2$. Weakly coupled renormalizable theories lead to the Wilson coefficients which are at least order of magnitude smaller (4.32), unless we are dealing with abnormally large multiplicities of new electroweak states just above the LHC reach. At the same time more strongly coupled theories can lead to the larger values of Wilson coefficients in the ball park of the LHC precision.

Table 4.1 and figure 4.6 are our main final results. We find that LHC at 3ab^{-1}(300fb^{-1}) will be able to constrain the λ_Z aTGC coupling to be

$$\lambda_Z \in [-0.0014, 0.0016] \quad ([-0.0029, 0.0034]) \tag{4.63}$$

for the 95% posterior probability interval for $\Lambda_{MC} = 2$ TeV. Results for the other values of Λ_{MC} can be trivially deduced from the table 4.1).

For the sake of completeness we also compare in table 4.2 the bounds on the Wilson coefficient obtained using the methods discussed in the section 4.4. We can see that all methods lead to results in the same ball park. Even though, the method of (4.49) does not make any assumption on the nature of UV completion, the sensitivity to the interference term is a bit worse than in the other two methods.

4.7 Conclusions and outlook

We have discussed the prospects of the measurements of the c_{3W} Wilson coefficient (λ_Z TGC) at LHC. This parameter was considered to be particularly difficult to test at hadron

	Lumi. 300 fb^{-1}		Lumi. 3000 fb^{-1}		Q [TeV]
	95% CL	68% CL	95% CL	68% CL	
Same as table 4.1	[-1.06,1.11]	[-0.59,0.61]	[-0.44,0.45]	[-0.23,0.23]	
Use of (4.49)	[-1.59,1.55]	[-1.05,1.01]	[-1.17,1.06]	[-0.72,0.66]	1
Method of [164]	[-0.88,0.88]	[-0.50,0.50]	[-0.41,0.40]	[-0.22,0.22]	
Same as table 4.1	[-0.69,0.78]	[-0.39,0.45]	[-0.31,0.35]	[-0.17,0.18]	
Use of (4.49)	[-0.74,0.79]	[-0.48,0.50]	[-0.51,0.52]	[-0.34,0.30]	1.5
Method of [164]	[-0.55,0.60]	[-0.32,0.35]	[-0.26,0.29]	[-0.15,0.16]	
Same as table 4.1	[-0.47,0.54]	[-0.27,0.31]	[-0.22,0.26]	[-0.12,0.14]	
Use of (4.49)	[-0.49,0.53]	[-0.30,0.34]	[-0.30,0.33]	[-0.20,0.20]	2
Method of [164]	[-0.43,0.47]	[-0.24,0.27]	[-0.20,0.23]	[-0.12,0.13]	

Table 4.2: Comparison of different methods.

colliders due to the suppressed interference effects. In our study we have shown that this suppression is not the case once the differential distributions are considered. In particular we have shown that this suppression can be overcome by studying the angular modulation in azimuthal angles in eq. (4.42). Independently of this modulation we have shown that requiring an additional hard QCD jet leads to the energy growth of the interference between the SM and BSM contributions.

Looking at the cleanest $pp \to WZ \to lll\nu$ channel we have estimated the importance of these observables for the LHC by calculating the prospects on the bounds at 300 fb^{-1}(3 ab^{-1}), at 14 TeV LHC. Our simplified analysis by no means can be considered a complete experimental study, however the most important and robust results are the relative improvements of the measurements due to the angular modulations and the hard QCD jet distributions. We have also discussed the challenges of the consistent EFT analysis for the TGC measurements at LHC.

The improvements in determination of λ_Z due to the differential distributions turn out to be of the order of $15-25\%$ depending on the assumptions on EFT cut-off. Even though this gain in precision does not seem to be very big, the sensitivity to the interference term is significantly increased (factor of $\sim 3-4$), which makes the EFT expansion less model dependent as well as provides a handle on the sign of the Wilson coefficient. Of course it is not a novelty that the differential distributions improve the accuracy of the measurements. However in this case the improvement is particularly significant due to the energy growth of the differential interference term.

In the future it would be interesting to use the differential distributions proposed to perform a global EFT analysis in order to find the best variables to distinguish between not only BSM and SM but also between different BSM contributions. Very similar azimuthal angle modulation will appear every time there are amplitudes with different

polarizations of the intermediate gauge bosons. These ideas will be explored in the future for the measurements of the other aTGCs.

It will be also interesting to study the azimuthal angle modulation for other $2 \to 2$ processes that are otherwise suppressed by the helicity selection rules, like for example $V_T V_T \to V_{L,T} V_{L,T}$. On the collider side, studies of the other decay channels as well as full inclusion of the NLO effects will be very important.

Chapter 5

Summary and conclusions

The work in this thesis consists of two main parts, general analysis of the possible flavour symmetries and their representations accounting for the approximate description of lepton masses and mixing in the symmetric limit and proposals for the better measurements of anomalous triple gauge boson couplings at LHC.

The first part of the thesis provides a complete answer to the general question: what are flavour symmetry group (of any type) and their representations providing approximate description of lepton masses and mixing in the symmetric limit? The answer of this question depends on two different assumptions on the description of neutrino masses, i.e. the neutrino masses are generated from the Weinberg operator or from the type I seesaw mechanism. Despite the generality of the question, the complete answer is rather simple. Under the first assumption we considered neutrinos are of Majorana type, and flavour symmetry constrains directly the form of neutrino mass matrix. In this case, we found six possible irrep decompositions of flavour symmetries (shown in table 2.4) and all of which lead to neutrino mass spectrum either in inverted hierarchy or unconstrained (anarchy) in the symmetric limit. Therefore, if the present hint of normal hierarchy were confirmed, then we conclude that, under our assumption, flavour symmetries leading to the approximate description of lepton masses and mixing in symmetric limit are not able to account for neutrino masses and mixing, and symmetry breaking must play primary role in their understanding. This conclusion is further strengthen in the context of $SU(5)$ and $SO(10)$ grand unified theories, in case their representations commute with the representation of flavour symmetry.

The conclusion above relies on our assumptions that neutrino masses originated from the Weinberg operator in the electroweak scale and symmetry arguments directly apply to neutrino mass matrix. It is also important to take into account the light neutrino mass generation from the physics well above the electroweak scale. The prototypical example of this kind is the seesaw mechanism with heavy singlet neutrinos. In this case the singlet neutrinos can also transform non-trivially under the flavour symmetry and their mass matrix gets constraints as well. So now one natural question arises: does

the low-scale analysis always capture the features of the high-scale analysis or not? We find this is not always the case. The necessary and sufficient condition to they become equivalent is that the singlet neutrino representation must be vectorlike and it contains vectorlike part of the lepton double representation. When these two analysis become equivalent the conclusions in low-scale analysis can also apply to the high scale discussion, otherwise the high-scale analysis provides new outcome. There are two cases where the inequivalence can occur. We have investigated each of them separately base on the fact that if the singlet neutrino mass matrix is singular or not. We have obtained complete set of predictions from the high-scale analysis in the symmetric limit for the inequivalent cases, and found that there are indeed some flavour group representations allow to have normal hierarchy of neutrino masses. Therefore, even if the current hints for the normal hierarchy get confirmed from the future experimental data, the flavour symmetry still can provide approximate description of lepton masses and mixing in the symmetric limit. To conclude, the current status of the neutrino masses and mixing can be approximately described by the high-scale analysis of the flavour symmetry when it is not equivalent to the low-scale limit. Otherwise, the symmetry breaking effects must play a leading role in determining the observed lepton masses and mixing.

In the last part of the thesis, we have proposed two measurements to overcome the suppression of interference between SM amplitude and that of the operator O_{3W} in the EFT extension of SM. The first measurement is an angular modulation property of the interference term with respect to the azimuthal angle of the final state leptons. The theoretical expectation is given in eq.(4.42) and numerical simulation result is shown in figure 4.3. The second measurements is the energy growth of the interference due to an additional hard jet, which is shown in figure 4.4. We provide prospective bounds on the Wilson coefficient of the operator O_{3W} and also on the corresponding anomalous triple gauge coupling, by looking at the cleanest channel $pp \to WZ \to lll\nu$ and using two luminosities 300 fb^{-1} and 3 ab^{-1} at 14 TeV LHC. As a final comment, the important and robust results from our analysis are the relative improvements of the measurements due to the angular modulation and the hard jet distribution, but this does not mean we completed full experimental study. In the future it will be interesting to apply our proposal to perform global EFT analysis in order to distinguish different BSM contributions in a certain process.

Appendix A

Proof of the results in section 2.2

In this appendix, we find the general form of the PMNS matrix associated to a generic decomposition of U_l and U_{e^c} in irreducible components. We consider the general case of n families.

Let us first introduce a few notations. The irreducible components of U_l are of different, possible inequivalent types. A given irrep type "r", of dimension d_r, can appear in the decomposition of U_l more than once. We denote with n_r the number of times it appears. Analogously, n_r^c is the number of times the irrep r appears in the decomposition of U_{e^c}.

Given a lepton doublet l_i, we can then associate three labels to it. We can denote by r the type of irrep to which l_i belongs. As each type of representation may appear more than once in the decomposition of U_l, we can denote by k the occurrence to which l_i belongs ($1 \leq k \leq n_r$). Finally, as the irrep r may have dimension larger than 1, we can denote by a the position of the lepton l_i within its irrep multiplet ($1 \leq a \leq d_r$). All in all, the lepton l_i is identified by its "irrep coordinates" (r, k, a). Such coordinates can be used as an alternative labeling of the lepton doublets l_i (and of its components e_i, ν_i). The generic lepton doublet will in this case be denoted by l_{rka}. Clearly, there is a correspondence between the two possible labeling, the one by $1 \leq i \leq n$ and the one by rka, defined by

$$l_i = l_{rka} \ . \tag{A.1}$$

Analogous coordinates (r, k, a) can be used to identify the lepton singlets e_i^c. The irreps r found in the decomposition of U_{e^c} can be different than the ones found in U_l, and their multiplicities in the decompositions can also be different.

We can, and will, choose a flavour basis for the leptons l_i and e_i^c, and the mappings between the "i" and the "(rka)" indices, as follows.

- Each irrep of type r acts on a set of subsequent leptons $(l_{i_0} \dots l_{i_0+d_r})$, forming a certain occurrence k_0 of the irrep type r, $(l_{i_0} \dots l_{i_0+d_r}) = (l_{rk_01} \dots l_{rk_0d_r})$.

- As stated in section 2.2.1, non-vanishing charged lepton masses correspond to conjugated irreps in the decompositions of U_l and U_{e^c}. Consider then the copies

$k = 1 \dots n_r$ of a certain irrep type r in U_l and the copies $h = 1 \dots n^c_{\bar{r}}$ of the conjugated representation $\bar{r}$ in U_{e^c} ($\bar{r} = r$ if r is real or pseudoreal). Only a number $\min(n_r, n^c_{\bar{r}})$ of them can be paired to get possibly non-vanishing masses, while all the residual unpaired leptons are forced to be massless. We assume that the leptons l_{rka} and $e^c_{\bar{r}ka}$ occupy the same positions in the lists $l_1 \dots l_n$ and $e^c_1 \dots e^c_n$, for all $k \leq \min(n_r, n^c_{\bar{r}})$. Tables 2.2, 2.3 use such a convention.

- All irreps of type r are represented by the same $d_r \times d_r$ unitary matrix U_r on the corresponding leptons: $l_{rka} \to U^r_{ab} l_{rkb}$, $e^c_{rka} \to (U^{\bar{r}}_{ab})^* e^c_{rkb}$.[1] If r is real, the matrix U is real; if r is complex, $U_{\bar{r}} = (U_r)^*$; if r is pseudoreal, $\omega\, U_r = U^*_r\, \omega$, where

$$\omega = \begin{pmatrix} 0 & 1 & & & \\ -1 & 0 & & & \\ & & \ddots & & \\ & & & 0 & 1 \\ & & & -1 & 0 \end{pmatrix}, \tag{A.2}$$

  is a $d_r \times d_r$ antisymmetric block matrix and d_r is even for pseudoreal representations.

Having set up the necessary notations, we are now ready to discuss the structure of the lepton mass matrices in the above basis. A non-zero entry $m^E_{ij} \neq 0$ paring the leptons e^c_i and e_j is allowed only when the irrep to which e^c_i and l_j belong are conjugated, say r and $\bar{r}$ respectively. If r or $\bar{r}$ appear more than once in the decomposition of U_l or U_{e^c}, the non-zero entries form a rectangular block, of size $n^c_{\bar{r}} \times n_r$, whose entries we can denote by $m^{E,r}_{kh}$. If the irrep r has dimension $d_r > 1$, $m^{E,r}_{kh}$ is the common diagonal element for all the leptons in the corresponding multiplet. Such a structure becomes transparent when the mass matrices are written in terms of the irrep coordinates. Indeed, the invariance under G forces the charged lepton mass matrix to be in the form

$$m^E_{rka,shb} = \delta_{\bar{r}s} \delta_{ab}\, m^{E,r}_{kh}. \tag{A.3}$$

Conversely, any charged lepton mass matrix in that form is of course invariant. Analogously, the form of the neutrino mass matrix is

$$m^\nu_{rka,shb} = \begin{cases} \delta_{\bar{r}s}\delta_{ab} m^{\nu,r}_{kh} & \text{if } r,s \text{ both complex} \quad (m^{\nu,r} \text{ generic}) \\ \delta_{rs}\delta_{ab} m^{\nu,r}_{kh} & \text{if } r,s \text{ both real} \quad (m^{\nu,r} \text{ symmetric}) \\ \delta_{rs}\omega_{ab} m^{\nu,r}_{kh} & \text{if } r,s \text{ both pseudoreal} \quad (m^{\nu,r} \text{ antisymmetric}) \\ 0 & \text{if } r,s \text{ of different type} \end{cases} \tag{A.4}$$

[1] In practice: if r is real or complex, it has the same action on lepton doublets and singlets, as $(U^{\bar{r}}_{ab})^* = U^r_{ab}$; if r is pseudoreal, it acts on the singlets in the conjugated (but equivalent) way, as $(U^{\bar{r}}_{ab})^* = (U^r_{ab})^*$.

Note that the entries $m^{\nu,r}_{kh}$ appear in off diagonal positions, unless the representation r is real. This is of course because of the Majorana nature of the neutrino mass matrix. Diagonal entries are allowed in the symmetric limit only when the representation to which the corresponding lepton belongs is real.

Note also that pseudoreal representations are only marginally relevant in the three neutrino case. As the dimension of pseudoreal representations is even, there is room for at most one pseudoreal irrep in that case. Moreover, if one two-dimensional pseudoreal representation appears in U_l, the two rows and columns of the neutrino mass matrix corresponding to that representation vanish, as $m^{\nu,r}$ in eq. (A.4) is a 1×1 antisymmetric matrix, so that $m^{\nu,r} = 0$. Still, we will stick in the following for completeness to the n neutrino case and to the full treatment of the pseudoreal case.

The PMNS matrix arises from the diagonalisation of m^E_{ij} and m^ν_{ij} in eqs. (A.3,A.4). It is made of four types of contributions, each with a different physical origin:

1. A core contribution V associated to the presence of equivalent irreps in the lepton doublet representation U_l.

2. A contribution D associated to the possible presence of Dirac structures in m^ν and providing maximal mixing.

3. Permutations P associated to the requirement that charged lepton and neutrino masses need to be in a standard ordering.

4. "Unphysical" contributions H associated to the arbitrariness in the choice of the basis in flavour space for degenerate leptons.

Let us see how such contributions arise from the diagonalisation of m_E and m_ν.

A.1 V

The first contribution V to the PMNS matrix is a unitary matrix commuting with U_l. Such a unitary matrix V mixes lepton multiplets belonging to identical irreps and is non-trivial only if the decomposition U_l contains more than one copy of the same irrep. All possible forms of V compatible with the previous requirements can be obtained.

In order to show how V arises, we observe that m_ν, m_E can be diagonalised, up to Dirac structures in the neutrino sector (we will see below what this means) by unitary transformations of the charged leptons and neutrinos ν_i, e_i, e^c_i commuting with the action of G,

$$\begin{aligned} \nu'_{rka} &= V^{\nu,r}_{kh} \nu_{rha} \\ e'_{rka} &= V^{e,r}_{kh} e_{rha} \\ e^{c\prime}_{rka} &= V^{e^c,r}_{kh} e^c_{rha}. \end{aligned} \tag{A.5}$$

$V^{\nu,r}$, $V^{e,r}$, $V^{e^c,r}$ are squared matrices and $V^{\nu,r}$, $V^{e,r}$ have the same dimension n_r. They mix full equivalent multiplets (they do not act on the index a) and are non-trivial in the presence of more than one copy of the representation r. The above transformations can be chosen to diagonalise each of the blocks in eqs. (A.3,A.4) as follows.

In the case of charged lepton blocks, we have

$$m_{E,r} = V^T_{e^c,\bar{r}}\, m^{\text{diag}}_{E,r}\, V_{e,r}\ . \tag{A.6}$$

As for the neutrino blocks, we need to treat the pseudoreal case differently. In the case of real or complex representations, we have

$$m_{\nu,r} = V^T_{\nu,\bar{r}}\, m^{\text{diag}}_{\nu,r}\, V_{\nu,r}\ . \tag{A.7}$$

If r is real, $m_{\nu,r}$ is a symmetric complex matrix, and eq. (A.7) gives its diagonalisation in terms of a single unitary transformation $V_{\nu,r}$. If r is complex, the block is in general rectangular, $m_{\nu,\bar{r}} = m^T_{\nu,r}$, and eq. (A.7) gives the diagonalisation of both in terms of two independent complex matrices $V_{\nu,r}$ and $V_{\nu,\bar{r}}$ of dimension n_r and $n_{\bar{r}}$ respectively. When the matrices $m^{\text{diag}}_{E,r}, m^{\text{diag}}_{\nu,r}$ above are rectangular, we conventionally choose the non-vanishing eigenvalues to appear on the diagonal starting from the lower-right corner. For example, if there are more columns than rows

$$m^{\text{diag}} = \begin{pmatrix} 0 & \cdots & 0 & X & & 0 \\ & & & & \ddots & \\ 0 & \cdots & 0 & 0 & & X \end{pmatrix}\ ,$$

where X denotes the position of the eigenvalues. Eqs. (A.6) and (A.7) define $V_{e,r}$ ($V_{\nu,r}$) for each irrep type r found in the decomposition of U_l, provided that $\bar{r}$ is also found in the decomposition of U_{e^c} (U_l), so that the block to be diagonalised exists. If this is not the case, we define $V_{e,r}$ ($V_{\nu,r}$) to be the identity matrix.

Let us now consider the special case of a neutrino block corresponding to a pseudoreal representation r. In such a case, $m_{\nu,r}$ is a square, $n_r \times n_r$ antisymmetric matrix. It can be reduced to the following "pseudo-diagonal" form

$$m_{\nu,r} = V^T_{\nu,r}\, m^{\text{ps-diag}}_{\nu,r}\, V_{\nu,r}\ , \quad (m^{\text{ps-diag}}_{\nu,r})_{kh} = m^{\nu,r}_k \omega_{kh}\ , \quad m^{\nu,r}_{2\kappa} = m^{\nu,r}_{2\kappa-1} \geq 0\ . \tag{A.8}$$

The matrix ω can now have even or odd dimension, depending on the number of copies n_r of the irrep r. If n_r is odd, ω is the restriction to the first n_r rows and columns of a matrix ω of larger even dimension, which means that it is in the form in eq. (A.2), with the addition of one extra vanishing row and column. The matrix $m^{\text{ps-diag}}_{\nu,r}$ is therefore an

antisymmetric block diagonal matrix, with subsequent 2×2 blocks in the form

$$\begin{pmatrix} 0 & m_k^{\nu,r} \\ -m_k^{\nu,r} & 0 \end{pmatrix} ,$$

possibly followed by a singly vanishing diagonal entry if n_r is odd. Therefore, the pseudoreal irreps are now paired in couples (12), (34), ..., $(2\kappa-1, 2\kappa)$, ..., each associated to degenerate masses, with a possibly unpaired last irrep (if the total number is odd) associated to a zero mass.

All in all, we have

$$m_E = V_{e^c}^T \, m_E^{\text{diag}} \, V_e \ , \qquad m_\nu = V_\nu^T \, m_\nu^{\text{s-diag}} \, V_\nu \ , \tag{A.9}$$

where

$$V_{ij}^{\nu} = \delta_{\bar{r}s}\delta_{ab} V_{kh}^{\nu,s} \qquad V_{ij}^{e} = \delta_{\bar{r}s}\delta_{ab} V_{kh}^{e,s} \qquad V_{ij}^{e^c} = \delta_{\bar{r}s}\delta_{ab} V_{kh}^{e^c,s}, \tag{A.10}$$

and $i \leftrightarrow (rka)$ and $j \leftrightarrow (shb)$, as defined by eq. (A.1). Clearly, V_e and V_ν commute with U_l. We can now define

$$V = V_e \, V_\nu^\dagger \ , \tag{A.11}$$

which represents the core contribution to the PMNS matrix and also commutes with U_l.

Eq. (A.9) brings the charged lepton mass matrix in diagonal form,

$$(m_E^{\text{diag}})_{ij} = \delta_{\bar{r}s}\delta_{kh}\delta_{ab} m_h^{E,r} \ . \tag{A.12}$$

The eigenvalues do lie on the diagonal because of the assumptions we made on the ordering of the charged leptons. The leptons e'_{rka} get mass $m_k^{E,r}$ by pairing with $e^{c\prime}_{\bar{r}ka}$. If the multiplet has dimension $d_r > 1$, all the leptons in the multiplets end up being degenerate. As the number of representations of type r acting on the lepton doublets, labeled by $k = 1 \ldots n_r$, and the number of representations of type $\bar{r}$ acting on the lepton singlets, labeled by $k = 1 \ldots n_{\bar{r}}^c$, can be different, only the first $k = 1 \ldots \min(n_r, n_r^c)$ pairs get a possibly non-zero mass, while all residual unpaired charged leptons are forced to be massless.

Eq. (A.9) brings the neutrino mass matrix in a "semi-diagonal" form,

$$(m_\nu^{\text{s-diag}})_{ij} = \begin{cases} \delta_{\bar{r}s}\delta_{kh}\delta_{ab} m_k^{\nu,r} & \text{if neither } r \text{ nor } s \text{ is pseudoreal} \\ \delta_{\bar{r}s}\omega_{kh}\omega_{ab} m_k^{\nu,r} & \text{if both } r \text{ and } s \text{ are pseudoreal} \\ 0 & \text{otherwise} \end{cases} , \tag{A.13}$$

where again $m_{2\kappa-1}^{\nu,r} = m_{2\kappa}^{\nu,r}$ in the pseudoreal case (κ integer).

All neutrinos ν'_{rka} corresponding to real representations r get a diagonal (Majorana) mass term $m_k^{\nu,r}$ by pairing to themselves. If the representation has dimension $d_r > 1$, all neutrinos in the multiplets are degenerate. The neutrinos ν'_{rka} corresponding to complex

representations r get a Dirac mass term $m_k^{\nu,r} = m_k^{\nu,\bar{r}}$ by pairing to the neutrinos in $\nu'_{\bar{r}ka}$ in the conjugated representation $\bar{r}k$. If $d_r > 1$, all the neutrinos in the two conjugated multiplets are degenerate. As the number of representations of type r, labeled by $k = 1 \dots n_r$, and the number of representations of type $\bar{r}$, labeled by $k = 1 \dots n_{\bar{r}}$, can be different, only the first $k = 1 \dots \min(n_r, n_{\bar{r}})$ pairs get a possibly non-zero mass, while all residual unpaired neutrinos are forced to be massless. Finally, in the case of pseudoreal representations, the two pairs of neutrinos $\nu'_{r,2\kappa,2\alpha}$, $\nu'_{r,2\kappa-1,2\alpha-1}$ and $\nu'_{r,2\kappa,2\alpha-1}$, $\nu'_{r,2\kappa-1,2\alpha}$ both get a Dirac mass term, both with mass $m_{2\kappa}^{\nu,r} = m_{2\kappa-1}^{\nu,r}$. If $d_r > 1$, all the neutrinos in the two paired multiplets $k = 2\kappa$ and $k = 2\kappa - 1$ are degenerate. For n_r odd, two spare neutrinos are massless.

To summarize, $m_\nu^{\text{s-diag}}$ is not necessarily diagonal because of the possible presence of Dirac structures associated to paired conjugated and pseudoreal representations, and its non-vanishing entries can be found:

- In all the diagonal positions $m^{\text{s-diag}}_{rka,rka}$ corresponding to real irreps r, providing a Majorana mass term for the neutrino ν'_{rka}.
- In symmetric off-diagonal positions, $m^{\text{s-diag}}_{\bar{r}ka,rka} = m^{\text{s-diag}}_{rka,\bar{r}ka}$, corresponding to complex representations r and $k \leq \min(n_r, n_{\bar{r}})$, providing a Dirac mass term to the conjugated neutrinos ν'_{rka} and $\nu'_{\bar{r}ka}$.
- In symmetric off-diagonal positions $m^{\text{s-diag}}_{r(2\kappa)(2\alpha),r,(2\kappa-1)(2\alpha-1)} = m^{\text{s-diag}}_{r(2\kappa-1)(2\alpha-1),r(2\kappa)(2\alpha)} = -m^{\text{s-diag}}_{r(2\kappa)(2\alpha-1),r(2\kappa-1)(2\alpha)} = -m^{\text{s-diag}}_{r(2\kappa-1)(2\alpha),r(2\kappa)(2\alpha-1)}$, corresponding to pseudoreal representations r and $\kappa = 1 \dots \lfloor n_r/2 \rfloor$, $\alpha = 1 \dots d_r/2$.

A.2 D

In order to complete the diagonalisation of the lepton mass matrices, we need to diagonalise the Dirac structures in $m_\nu^{\text{s-diag}}$. This is how the contribution D to the PMNS matrix, containing a maximal mixing transformation for each Dirac structure, arises.

As discussed in the previous subsection, the semi-diagonal matrix $m_\nu^{\text{s-diag}}$ contains a diagonal block corresponding to the neutrinos ν_{rka} in real irreps r; a 2×2 Dirac block corresponding to neutrinos in paired conjugated complex representations ν_{rka} and $\nu_{\bar{r}ka}$, $k = 1 \dots \min(n_r, n_{\bar{r}})$; a trivially diagonal vanishing block corresponding to neutrinos in unpaired complex representations ν_{rka}, $k > \min(n_r, n_{\bar{r}})$; a trivially diagonal vanishing block corresponding to the neutrinos ν_{rn_ra} in the last copy of the pseudoreal irrep r, if n_r is odd (and in particular if there is only one copy of r); if there are at least two copies of r, a 4×4 Dirac block corresponding to the four neutrinos $\nu'_{r,2\kappa-1,2\alpha-1}$, $\nu'_{r,2\kappa,2\alpha}$, $\nu'_{r,2\kappa-1,2\alpha}$, $\nu'_{r,2\kappa,2\alpha-1}$. The matrix $m_\nu^{\text{s-diag}}$ can then be diagonalised by diagonalising the above Dirac blocks as follows.

As seen, there are two types of Dirac blocks, associated to complex conjugated and to pseudoreal irreps respectively (only the former are relevant to the three neutrino case, as the latter arises only in the presence of at least four neutrinos).

In the case of a Dirac block associated to the neutrinos ν_{rka} and $\nu_{\bar{r}ka}$ in conjugated complex irreps, and for $k = 1 \dots \min(n_r, n_{\bar{r}})$, $a = 1 \dots d_r$, the block has the form

$$\begin{pmatrix} 0 & m_k^{\nu,r} \\ m_k^{\nu,r} & 0 \end{pmatrix} , \tag{A.14}$$

where $m_k^{\nu,r} \geq 0$ ($m_k^{\nu,r} = m_k^{\nu,\bar{r}}$). Its diagonalisation is trivial

$$\begin{pmatrix} 0 & m_k^{\nu,r} \\ m_k^{\nu,r} & 0 \end{pmatrix} = D_2^T \begin{pmatrix} m_k^{\nu,r} & 0 \\ 0 & m_k^{\nu,r} \end{pmatrix} D_2 , \qquad D_2 = \frac{1}{\sqrt{2}} \begin{pmatrix} 1 & 1 \\ -i & i \end{pmatrix} . \tag{A.15}$$

The unitary matrix D_2 corresponds to a maximal rotation by an angle $\pi/4$, together with a phase redefinition by the imaginary unit i, needed to make the diagonal entries positive. Such a Majorana phase is physical, but it plays a negligible role in oscillation experiments. The matrix D_2 is defined up to a phase, meaning that we could have equivalently used the following form of D_2,

$$\frac{1}{\sqrt{2}} \begin{pmatrix} e^{i\theta} & e^{-i\theta} \\ \mp i e^{i\theta} & \pm i e^{-i\theta} \end{pmatrix} . \tag{A.16}$$

The phase θ corresponds to the freedom to perform a O(2) transformation on the two degenerate neutrino mass eigenstates, and can be reabsorbed in a phase redefinition of V_ν. The sign is unphysical.

In the case of a Dirac block associated to the two paired pseudoreal irreps $2\kappa - 1$ and 2κ ($\kappa = 1 \dots \lfloor n_r/2 \rfloor$) and involving the four neutrinos $\nu'_{r,2\kappa-1,2\alpha-1}$, $\nu'_{r,2\kappa,2\alpha}$, $\nu'_{r,2\kappa-1,2\alpha}$, $\nu'_{r,2\kappa,2\alpha-1}$ (rows and columns of the matrix below ordered accordingly), the block has the form

$$\left(\begin{array}{cc|cc} 0 & m_{2k}^{\nu,r} & & \\ m_{2k}^{\nu,r} & 0 & & \\ \hline & & 0 & -m_{2k}^{\nu,r} \\ & & -m_{2k}^{\nu,r} & 0 \end{array}\right) = \left(\begin{array}{cc|cc} D_2 & & & \\ & & & \\ \hline & & & \\ & & & iD_2 \end{array}\right)^T \left(\begin{array}{cc|cc} m_{2k}^{\nu,r} & & & \\ & m_{2k}^{\nu,r} & & \\ \hline & & m_{2k}^{\nu,r} & \\ & & & m_{2k}^{\nu,r} \end{array}\right) \left(\begin{array}{cc|cc} D_2 & & & \\ & & & \\ \hline & & & \\ & & & iD_2 \end{array}\right) , \tag{A.17}$$

where $m_{2\kappa}^{\nu,r} \geq 0$ ($m_{2\kappa}^{\nu,r} = m_{2\kappa-1}^{\nu,r}$).

Based on what above, we can define unitary matrix D to be the product of the (commuting) 2×2 transformations D_2 acting on neutrinos in paired complex or pseudoreal representations. The matrix D will therefore be diagonal in the block corresponding to the neutrinos in real irreps and in the block corresponding to the neutrinos in unpaired complex or pseudoreal representations; it will contain an instance of the matrix D_2 in each

2×2 block corresponding to neutrinos ν_{rka} and $\nu_{\bar{r}ka}$ in paired conjugated complex representations, $k = 1 \ldots \min(n_r, n_{\bar{r}})$; and it will contain an instance of D_2 and iD_2 in each pair of 2×2 blocks corresponding to the neutrinos ($\nu'_{r,2\kappa-1,2\alpha-1}$, $\nu'_{r,2\kappa,2\alpha}$) and ($\nu'_{r,2\kappa-1,2\alpha}$, $\nu'_{r,2\kappa,2\alpha-1}$) respectively, in paired pseudoreal representations, $\kappa = 1 \ldots \lfloor n_r/2 \rfloor$.

As a consequence, the semi-diagonal matrix $m_\nu^{\text{s-diag}}$ is diagonalised as follows

$$m_\nu^{\text{s-diag}} = D^T m_\nu^{\text{diag}} D \,, \tag{A.18}$$

where m_ν^{diag} is diagonal, with degenerate eigenvalues in the positions corresponding to neutrinos in paired complex conjugated or pseudoreal representations.

A.3 P

What above provides a full diagonalisation of the lepton mass matrix in terms of the unitary transformations V_e, V_{e^c} and (DV_ν):

$$m_E = V_{e^c}^T \, m_E^{\text{diag}} \, V_e \,, \qquad m_\nu = (DV_\nu)^T \, m_\nu^{\text{diag}} \, (DV_\nu \,). \tag{A.19}$$

We are therefore close to identifying the PMNS matrix. In order to do that, we should take into account the fact that the order of the rows and columns of the PMNS matrix is defined by a standard ordering of the leptons. In the case of charged leptons, the standard ordering coincides with the mass ordering, $m_{e_1} \leq \ldots \leq m_{e_n}$. In the three neutrino case, the standard ordering for neutrinos defines the mass eigenstates ν_1 and ν_2 to be the two ones closer in terms of squared mass difference, with ν_1 being the lightest of the two. In order to find the PMNS matrix, we should then permute the lepton mass eigenstates in order to have them in the standard ordering. This is achieved by two permutation matrices P_E and P_ν,

$$m_E^{\text{diag}} = P_E^T m_E^{\text{diag,so}} P_E \,, \qquad m_\nu^{\text{diag}} = P_\nu^T m_\nu^{\text{diag,so}} P_\nu \,, \tag{A.20}$$

where "so" stands for "standard ordering".

A few comments are in order. We are considering here the symmetric limit. On the other hand, the standard ordering is defined on the physical masses, which also get contributions from symmetry breaking effects. However, in the assumption we made that symmetry breaking effects are small, the ordering is not affected by symmetry breaking effects.

An exception to the latter argument arises in the presence of degenerate eigenvalues (vanishing or not). Which linear combination of the corresponding leptons will end up being the lighter or heavier crucially depends in this case on the symmetry breaking effects. This type of ambiguity will be taken into account by the H matrix defined in the next subsection, so that no permutation needs to be introduced.

As an example in which a physical permutation is involved is when the charged lepton spectrum ends up being $(m_{e_3}, m_{e_2}, m_{e_1}) = (0, 0, A)$ instead of $(m_{e_3}, m_{e_2}, m_{e_1}) = (A, 0, 0)$. In such a case a permutation $P^E_{1\to 3}$ moving the first lepton in the last position is necessary (such a permutation is defined up to a further permutation of the first two elements, but the latter does not need to be taken into account). In such a case, the permutation only depends on the mass pattern and not on the specific values of the non-zero entries. A physical permutation is also needed when the mass ordering depends on the specific values of the non-zero entries, for example if $(m_{e_3}, m_{e_2}, m_{e_1}) = (A, B, 0)$. In the latter case, no permutation is needed if $B < A$, whereas a $2 \leftrightarrow 3$ permutation is needed when $B > A$. In such a case, the permutation is not defined by the mass pattern alone.

It is possible and useful to choose the ordering of leptons (and of their irreps) to start with in such a way to minimize the permutations needed.

A.4 H

We have now brought the lepton mass matrices in diagonal form, with the leptons in standard ordering

$$m_E = (P_E V_{e^c})^T \, m_E^{\text{diag,so}} \, (P_E V_e \,), \qquad m_\nu = (P_\nu D V_\nu)^T \, m_\nu^{\text{diag,so}} \, (P_\nu \, D V_\nu \,). \tag{A.21}$$

A final point has to be taken into account in order to write the most general form of the PMNS matrix: the latter is not uniquely defined. This is because of the ambiguities associated to the definition of the mass eigenstates. The role of the unitary matrices H is to take into account such ambiguities.

In the real world case in which all the lepton masses are non-degenerate, the ambiguity is only associated to unphysical phases. It is well known, for example, that the most general form of the CKM matrix contains five unphysical phases associated to the possibility to redefine the phases of up and down quarks, without modifying the diagonal form of the mass matrices. In the approximate world described by the symmetric limit, on the other hand, the ambiguity can be non-trivial, owing to the possible presence of degenerate, possibly vanishing, masses. It is then important to take into account such contributions, as they become physical when symmetry breaking effects, removing the degeneracy, are considered.

The ambiguity affecting the definition of the PMNS matrix is associated to the unitary transformations H_ν, H_e, H_{e^c} leaving the diagonal form of the lepton mass matrices invariant, i.e. such that

$$m_E^{\text{diag,so}} = H_{e^c}^T m_E^{\text{diag,so}} H_e \,, \qquad m_\nu^{\text{diag,so}} = H_\nu^T m_\nu^{\text{diag,so}} H_\nu \,. \tag{A.22}$$

As only H_e (and not H_{e^c}) enters the PMNS matrix, we are interested in the most general form of H_e for which a proper H_{e^c} exists satisfying eq. (A.22). This taken into account,

H_e and H_ν are characterised by

$$H_e (m_E^{\text{diag,so}})^2 = (m_E^{\text{diag,so}})^2 H_e, \qquad m_\nu^{\text{diag,so}} = H_\nu^T m_\nu^{\text{diag,so}} H_\nu \,. \tag{A.23}$$

In the previous equation, the eigenvalues in $m_E^{\text{diag,so}}$, $m_\nu^{\text{diag,so}}$ are supposed to be non-generic. We remind that our analysis focuses on a given mass pattern in table 2.1, and that a set of eigenvalues in a certain pattern is generic if all the entries that are allowed to be different and non-zero are indeed different and non-zero. The possible forms of H_e, H_ν then only depend on the mass pattern being considered. Consider for example a mass pattern in which the mass eigenvalues are in the form in eq. (2.5), where the degeneracies are $d_0^E \dots d_{N_E}^E$ for the charged leptons and $d_0^\nu \dots d_{N_\nu}^\nu$ for the neutrinos (the vanishing entries do not necessarily need to appear first, but let us for simplicity assume that this is the case). Then H_e and H_ν have the form

$$H_e = \text{BDiag}(U_0, U_1, \dots U_{N_E}) \,, \qquad H_\nu = \text{BDiag}(U_0', R_1, \dots R_{N_\nu}) \,, \tag{A.24}$$

where $U_i \in U(d_i^E)$, $U_0' \in U(d_0^\nu)$ are unitary matrices and $R_i \in O(d_i^\nu)$ are real orthogonal matrices. In eq. (A.24), BDiag denotes a block diagonal matrix, with the diagonal blocks specified as arguments.

The H_e, H_ν contributions to the PMNS matrix have a different physical nature than the previous ones. The previous contributions are known, once the entries of the mass matrices in the symmetric limit are known. Barring special correlations, they correspond to large mixing if all the non-vanishing entries in the symmetric mass matrices are of the same order. On the contrary, H_e and H_ν are unphysical, and undetermined, in the symmetric limit. However, they become physical (up to diagonal phases) after symmetry breaking effects split the degenerate mass eigenstates. By taking H_e and H_ν into account, we then make sure that the PMNS matrix after symmetry breaking is close to the one described by eq. (2.6) in the symmetric limit, for some values of H_e, H_ν. Depending on the specific form of the symmetry breaking effects, H_e and H_ν can end up being be large, small, or zero.

A.5 The PMNS matrix

By combining everything above, we find that the PMNS matrix is in the form in eq. (2.6). That equation may contain some redundancy. The form of V may have an undetermined component that can be parameterized by H_e or H_ν. This happens for example when V is in principle non-trivial because of the presence of multiple copies of the same irrep, but those irreps correspond to massless leptons. We then choose V to be the identity on the massless leptons and encode the undetermined component in H_e, H_ν. Another redundancy appear in the case of Dirac structures, in which the diagonal neutrino mass matrix ends up having two degenerate eigenvalues. By definition, H_ν then contains a

2×2 orthogonal rotation. However, as discussed in appendix A.2, that rotation can be reabsorbed in a phase redefinition of V. We will therefore not include it in H_ν.

Appendix B

The low- and high-scale analyses equivalence condition

B.1 Conditions for the low- and high-scale representations become equivalent

In this part of the appendix we will provide proofs of the conditions under which the low- and high-scale representations become equivalent.

First of all, let us see the following relation between the low- and high-scale representations of the flavour group. Suppose that we are considering n family of singlet neutrinos and of other leptons. For a given low-scale representation U_L of a flavour group G there exists a high-scale representation U_H of G such that i) U_L is the low-scale limit of U_H and ii) U_H and U_L are equivalent in the symmetric limit.

In order to prove that above statement is correct, we have to show an existence of the high-scale representations U_H for every low-scale representation U_L such that U_L is low-scale limit of U_H and it is equivalent to U_H in the symmetric limit.

As was explained before, we can write the leptons in a basis such that U_L^l decomposed into irreps each acting on a separate set of leptons, and then collect those irreps into the first group forming a vectorlike sub-representation U_{L0}^l of U_L^l and the second group forming a fully chiral sub-representation U_{L1}^l. For convenience, we can order the lepton doublets l_i in such a way that U_{L0}^l acts on the first n_0 of leptons and U_{L1}^l acts on the last $n_1 = n - n_0$ of them. If the first or the second group (corresponding to vectorlike or fully chiral part) is empty, then $n_0 = 0$ or $n_1 = 0$. We can define the high-scale representation a follows: we take $U_H^l = U_L^l$, $U_H^\nu = (U_{L0}^l)^* + \mathbf{id}$, where $\mathbf{id}$ is the trivial representation acting on the singlet neutrinos in the same position as those on which U_{L1}^l acts, and of course we choose $U_H^e = U_L^e$. Clearly, U_L is the low-scale limit of U_H. To complete the proof of the statement above, in the following we will show that U_L is equivalent to U_H.

It is easy to see that the first condition in definition of U_H and U_L to be equivalent holds. As the U^l_{L0} is vectorlike, $(U^l_{L0})^*$ is also vectorlike, and $U^\nu_H = (U^l_{L0})^* + \mathbf{id}$ is a sum of two vectorlike parts thus it is vectorlike.

Now let us prove that the second condition in definition of the U_H and U_L to be equivalent is also satisfied. In other words, for each m_ν invariant under U^l_L, we have to show that there exist m_N, M invariant under U_H, with M non-singular, such that $m_\nu = -m_N^T M^{-1} m_N$. We construct m_N and M in terms of m_ν as follows. First of all, we observe that for a given m_ν we can order the fermions in such a way that not only U^l_{L0} acts on the first n_0 of them, but also m_ν has a block decomposition $m_\nu = \mathrm{BDiag}(\bar{m}, 0)$, where the first block matrix $\bar{m}$ is non-singular and it has dimension $\bar{n} \leq n_0$, and the first group of $\bar{n}$ leptons form a sub-representation of U^l_{L0}. We can then define $m_N = \mathrm{BDiag}(v\mathbf{1}_{\bar{n}}, \mathbf{0}_{n-\bar{n}})$ and $M = -\mathrm{BDiag}(v^2\bar{m}^{-1}, \overline{M}\mathbf{1}_{n-\bar{n}})$, where v is the electroweak scale, a constant $\overline{M} \gg v$, and $\mathbf{1}_{n-\bar{n}}$ is an identity matrix. By this way we can make all the eigenvalues of M much heavier than the EW scale, since all the eigenvalues of m_ν are much smaller than v. Moreover, M is apparently non-singular because $\bar{m}$ is non-singular and $\overline{M} \neq 0$. It is easy to see that M and m_N are invariant under the U_H defined above and that $-m_N^T M^{-1} m_N = m_\nu$. This verifies the second condition and also concludes the proof of whole statement: all the low-scale representations U_L of a flavour group G are the low-scale limit of an equivalent (in the symmetric limit) high-scale representation U_H.

As we know from the example in section 3.2.2 that low-scale discussion of the flavour symmetry does not capture all possible results obtained from the high-scale. Then, under which conditions low-scale limit U_L of a high-scale representation U_H is always equivalent to U_H in the symmetric limit? The answer of this question is as follows: the low-scale limit U_L is equivalent to U_H if and only if U^ν_H is vectorlike and U^ν_H contains vectorlike part of U^l_L.

In order to prove this is indeed a necessary and sufficient condition for general case of n family, let us suppose that U_H is a high-scale representation of G and U_L is a low-scale limit, and $U^l_L = U^l_{L0} + U^l_{L1}$ is a splitting of U^l_L into a vectorlike and fully chiral part. Then we will prove following two statements separately:

1. if U_L is equivalent to U_H, then U^ν_H is vectorlike and U^ν_H contains U^l_{L0}.

2. if U^ν_H is vectorlike and U^ν_H contains U^l_{L0}, then U_L is equivalent to U_H.

Let us start with the proof of first statement. If U_L is equivalent to U_H, then U^ν_H is vectorlike (from the their equivalence condition). So we just need to prove U^ν_H contains U^l_{L0}. If U^l_{L0} is empty, the statement is true, as in such a case U^ν_H trivially contains U^l_{L0}. If U^l_{L0} is not empty, we can choose a basis for the lepton doublets in which U^l_{L0} acts on the first $n_0 \geq 1$ doublets and U^l_{L1} on the subsequent $n_1 = n - n_0$ doublets. As U^l_{L0} is vectorlike, there exists a dimension n_0 non-singular matrix m_0 invariant under U^l_{L0}. The matrix $m_\nu = \mathrm{BDiag}(m_0, \mathbf{0}_{n_1})$ is then invariant under U^l_L. Given that U_L is equivalent to U_H, there exist m_N, M invariant under U_H, with M non-singular, such that

$m_\nu = -m_N^T M^{-1} m_N$. Considering the $n \times n_0$ submatrix $\hat{m}_N$ made of the first n_0 columns of m_N, we have $m_0 = -\hat{m}_N^T M^{-1} \hat{m}_N$. Since m_0 is non-singular, $\hat{m}_N$ must have rank n_0. It is then possible to choose a basis for the singlet neutrinos ν_i such that $\hat{m}_N$ is in the upper triangular form, with non-vanishing diagonal entries. It is now straightforward to show that the singlet neutrinos facing lepton doublets in a given irrep component of U_{L0}^l transform in the conjugated irrep. It then follows that the restriction of U_H^ν on the first n_0 singlet neutrinos is precisely $(U_{L0}^l)^* \sim U_{L0}^l$. Therefore, U_H^ν contains U_{L0}^l.

The proof of the second statement requires to show U_L is equivalent to U_H, by using the fact that U_H^ν is vectorlike and that U_H^ν contains U_{L0}^l. Since U_H^ν being vectorlike is already given, we only need to prove that for each m_ν invariant under U_L there exist a m_N and a non-singular M invariant under U_H such that $m_\nu = -m_N^T M^{-1} m_N$.

For the invariant mass matrix m_ν under U_L, we can choose a basis for the lepton doublets such that: U_L^l decomposes into irreps each acting on a separate set of leptons; a first (possibly empty) group of irrep, which will be associated to the non-singular part of m_ν, corresponds to the first $\bar{n}$ doublets and also to the sub-representation $\bar{U}_L^l$; a second (possibly empty) group of irreps corresponds to the next $\bar{\bar{n}}$ doublets and to the sub-representation $\bar{\bar{U}}_L^l$. Putting together these two groups of irrep forms the representation $U_{L0}^l = \bar{U}_L^l + \bar{\bar{U}}_L^l$ acting on the first $n_0 = \bar{n} + \bar{\bar{n}}$ leptons, which is vectorlike while the restriction U_{L1}^l of U_L^l to the remaining $n_1 = n - n_0$ leptons is instead fully chiral. Therefore, the form of the mass matrix is $m_\nu = \mathrm{BDiag}(\bar{m}, \mathbf{0}_{\bar{\bar{n}}}, \mathbf{0}_{n_1})$, with $\bar{m}$ non-singular. Note that $\bar{U}_L^l$ is vectorlike, as $\bar{m}$ is invariant and non-singular. Then $\bar{\bar{U}}_L^l$ is also vectorlike, as both U_{L0}^l and $\bar{U}_L^l$ are. For the reason that U_H^ν contains U_{L0}^l by hypothesis, we can choose a basis for the neutrino singlets such that the first n_0 singlet neutrinos transform with $(U_{L0}^l)^* \sim U_{L0}^l$. The remaining $n - n_0$ singlets will transform with the restriction U_{H1}^ν of U_H^ν to them (under which they are invariant). Note that U_{H1}^ν is vectorlike, as $(U_{L0}^l)^*$ is vectorlike and $U_H^\nu = (U_{L0}^l)^* + U_{H1}^\nu$ is also vectorlike.

We can now construct m_N and M as follows. As U_{H1}^ν is vectorlike, there exists a non-singular $n_1 \times n_1$ symmetric matrix M_1 invariant under U_{H1}^ν. We can choose the latter in such a way that all its eigenvalues are much heavier than the EW scale. Since $\bar{\bar{U}}_L^l$ is vectorlike, there exists a non-singular symmetric matrix $\bar{\bar{m}}$ invariant under $\bar{\bar{U}}_L^l$. We can find a non-singular $\bar{\bar{m}}$ in such a way that all of its eigenvalues are much smaller than the EW scale. After that, we define $M = \mathrm{BDiag}(v^2 \bar{m}^{-1}, v^2 \bar{\bar{m}}^{-1}, M_1)$. Finally, we define $m_N = \mathrm{BDiag}(v \mathbf{1}_{\bar{n}}, \mathbf{0}_{\bar{\bar{n}}}, \mathbf{0}_{n_1})$.

It is now straightforward to show that: all the eigenvalues of M are much heavier than the EW scale, M is invariant under U_H^ν, m_N is invariant under U_H and $m_\nu = -m_N^T M^{-1} m_N$.

B.2 The low- and high-scale analyses forcing the same flavour pattern

In this section we will find general condition for the n family case of the low- and high-scale analyses forcing the same pattern in the symmetric limit.

To begin with, let us see that for a certain flavour pattern, each low-scale representation U_L forcing that pattern is the low-scale limit of a high-scale representation U_H forcing the same pattern. In order to achieve this purpose, we will consider a given flavour pattern, i.e. a mass pattern in table 2.1 and a PMNS matrix as in eq. (3.17), and a low-scale representation U_L forcing that pattern. Then we will demonstrate that there exists a high-scale representation U_H forcing the same pattern.

From the discussion in section B.1 we know that there always exists a high-scale representation U_H having U_L as low-scale limit and equivalent to U_L in the symmetric limit. So now it is enough to show that U_H forces the same flavour pattern as U_L. To see U_H forces the same pattern as U_L, we need to verify three conditions, in the definition of high-scale representation forcing a given pattern, are satisfied.

The first condition is satisfied because U_H is equivalent to U_L in the symmetric limit and U_H^ν is then vectorlike by the definition of equivalence between the U_H and U_L.

In order to verify the second condition, we should show that for a given $\mathcal{L}_H$ as in eq. (3.7), invariant under U_H, with non-singular M, lepton masses and mixings are in the specified flavour pattern. Our starting point here is that the Lagrangian $\mathcal{L}_H$ is invariant under U_H, with non-singular M, and m_E and m_N, M are the corresponding mass matrices, as given by eq. (3.8). The flavour pattern associated to U_H is nothing but the flavour pattern associated to m_E and $m_\nu = -m_N^T M^{-1} m_N$. On the other hand, m_E and m_ν turn out to be invariant under U_L (see a comment below the definition of U_H and U_L equivalent in chapter 3). The flavour pattern associated to m_E, m_ν is then the given pattern, as U_L by hypothesis forces that pattern.

In order to verify the third condition, we should exhibit that there exists a $\mathcal{L}_H$ as in eq. (3.7), invariant under U_H, with non-singular M, such that the lepton masses and mixings are in the given flavour pattern and generic (i.e. with all masses allowed to be non-zeros and different indeed non-zero and different, and with all the PMNS entries allowed to be non-zero indeed non-zero in at least one flavour basis, except possibly the 13 entry). Let us consider a high-scale representation U_H such that U_L is the low-scale limit of U_H and it is equivalent to U_H in the symmetric limit. The existence of such a representation is guaranteed by the existence of the U_H for every U_L and they are equivalent, which is discussed in beginning of the section B.1. Regarding the m_ν, m_E invariant under U_L and giving masses and mixings in the given pattern, and generic, their existence are guaranteed by the hypothesis that U_L forces the given pattern. Now because of the equivalence of U_H and U_L, there is a m_N and a non-singular M (besides the m_E we already have) invariant under U_H such that $m_\nu = -m_N^T M^{-1} m_N$, and a corresponding

high-scale Lagrangian $\mathcal{L}_H$ invariant under U_H. The lepton masses and mixings associated to $\mathcal{L}_H$, being the one associated to m_E and m_ν, are then indeed in the given flavour pattern and generic. So these arguments conclude whole statement, for a certain flavour pattern each low-scale representation U_L forcing that pattern is the low-scale limit of a high-scale representation U_H forcing the same pattern.

Now we will close this section by discussing the necessary and sufficient condition for low-scale limit U_L forces same pattern as U_H. The low-scale limit U_L forces same pattern as U_H if and only if these two representations are equivalent in the symmetric limit. In order to show this is indeed a necessary and sufficient condition we will prove following two statements one by one:

1. if U_L is equivalent to U_H in the symmetric limit, then U_L forces the same pattern as U_H.

2. if U_L forces the same pattern as U_H, then U_L is equivalent to U_H.

Let us start with the first statement, in order to conclude U_L forces the same pattern as U_H by using the fact that U_L is equivalent to U_H in the symmetric limit, we have to confirm two conditions, which are in the definition of low-scale representations forcing a given flavour pattern, are satisfied. The proofs of these two conditions are given in the following two paragraphs.

In order to verify the first condition, we need to show that for any given low-scale Lagrangian $\mathcal{L}_L$ as in eq. (3.2) invariant under U_L, the lepton masses and mixings induced by $\mathcal{L}_L$ are also in the pattern forced by U_H. As $\mathcal{L}_L$ is invariant under U_L, the corresponding m_ν and m_E are invariant under U_L. So what needs to be proven in the second step is the associated masses and mixing follow the pattern forced by U_H. Knowing that U_L is equivalent to U_H, there exist invariant m_N, M (besides the m_E we already have), with M is non-singular, and a corresponding Lagrangian $\mathcal{L}_H$ is invariant under U_H, such that $m_\nu = -m_N^T\, M^{-1} m_N$. As the high-scale representation U_H forces the given pattern, associated masses and mixings follow that pattern. And those are also the masses and mixings associated to m_E, m_ν, which follow the pattern forced by U_H.

In order to verify the second condition, we need to show that there exists a $\mathcal{L}_L$ as in eq. (3.2), invariant under U_L, such that the lepton masses and mixings are in the pattern forced by U_H, and generic. Since U_H forces the given pattern, there exists a $\mathcal{L}_H$ as in eq. (3.7), invariant under U_H, such that M is non-singular and the lepton masses and mixings are in the given pattern, and generic. If $\mathcal{L}_L$ is a low-scale limit of $\mathcal{L}_H$, then $\mathcal{L}_L$ is invariant under U_L. The lepton masses and mixings induced by $\mathcal{L}_L$ are the same as those induced by $\mathcal{L}_H$ and are, therefore, in the flavour pattern forced by U_H, and generic.

On the other hand, for the proof of the second statement, we will rely on the given condition (U_L forces the same pattern as U_H). In order to conclude that U_L is equivalent to U_H, we will follow a following strategy: we will prove i) U_H^ν is vectorlike and ii) U_H^ν contains the vectorlike part of U_L^l, then using the statement in section B.1 — the

existence of U_H for every U_L as a low-scale limit and they are equivalent — we derive U_L is equivalent to U_H.

It is very easy to get U_H^ν is vectorlike, that just follows from the definition of forcing a pattern at high-scale. Now we have to prove that U_H^ν contains the vectorlike part of U_L^l. Suppose that $\bar{n}$ is the number of neutrino masses allowed to be non-vanishing in the symmetric limit in the chosen pattern, and that n_0 is the dimension of the vectorlike part U_{L0}^l of U_L^l. From the fact that U_{L0}^l acts on the first n_0 fermions in the non-singular block of the mass matrix and that U_L also forces the chosen pattern, we conclude $\bar{n} = n_0$. Let us now choose a m_N and a non-singular M, invariant under U_H, with lepton masses and mixing in a generic pattern. Their existence is guaranteed by the definition of forcing a pattern at high-scale. Then $m_\nu = -m_N^T M^{-1} m_N$ is invariant under U_L^l and has n_0 non-vanishing eigenvalues. According to the relation between structure of the mass matrix and two parts (vectorlike and fully chiral part) of the representation, and taking into account that $\bar{n} = n_0$, we will choose a basis for the lepton doublets such that: U_L^l decomposes into irreps each acting on a separate set of leptons, a first group of irrep forms the representation U_{L0}^l while the remaining ones form U_{L1}^l, so $m_\nu = \mathrm{BDiag}(m_0, \mathbf{0}_{n-n_0})$ with non-singular m_0 block. Now we will proceed as the argument in section B.1. Considering the $n \times n_0$ submatrix $\hat{m}_N$ made of the first n_0 columns of m_N, we have $m_0 = -\hat{m}_N^T M^{-1} \hat{m}_N$. Since m_0 is non-singular, $\hat{m}_N$ must have rank n_0. It is then possible to choose a basis for the singlet neutrinos ν_i such that m_{N0} is in upper triangular form, with non-vanishing diagonal entries. It is now straightforward to show that the singlet neutrinos facing lepton doublets in a given irrep component of U_{L0}^l transform in the conjugated irrep. So it follows that the restriction of U_H^ν on the first n_0 singlet neutrinos is precisely $(U_{L0}^l)^* \sim U_{L0}^l$, therefore U_H^ν contains U_{L0}^l. With this conclusion we have reached to the end of the proof. So the necessary and sufficient condition to the low-scale limit U_L forcing the same flavour pattern as U_H is that these two representations are equivalent in the symmetric limit. From this condition we can say that there are two and only two important cases in which the low-scale analysis fails in characterizing the high-scale flavour symmetries that forcing a certain flavour pattern in the symmetric limit:

- When U_H^ν is not vectorlike.
- When U_H^ν does not contain the vectorlike part of U_H^l.

Detailed discussions of these two inequivalent cases can be found in chapter 3.

Appendix C

Further details of the bounds on c_{3W}

In this appendix we compare the relative importance of the various differential observables on the constraints on c_{3W}/Λ^2. The results for 300(3000) fb^{-1} are presented in the table C.1. The labels *Excl./Incl. linear* have exactly the same meaning as in the table 4.1 . *No* ϕ_Z *binning* stands for binning only p_j^T and *No* p_j^T *binning* stands for using only the information in $p_j^T \in [0, 100]$GeV category and the angular binning. We can see that both binning p_j^T and ϕ_Z lead to the increase of sensitivity of the interference term with the later being stronger. Table C.1 is generated using the leakage $\lesssim 5\%$ for various Q values. The procedure of [164] leads roughly to the same results and the method of eq. (4.49) shows lower sensitivity on the interference term. Bin by bin information about the SM and BSM contributions can be available by request.

	Lumi. 300 fb^{-1}		Lumi. 3000 fb^{-1}		Q [TeV]
	95% CL	68% CL	95% CL	68% CL	
Excl.	[-1.06,1.11]	[-0.59,0.61]	[-0.44,0.45]	[-0.23,0.23]	1
Excl., linear	[-1.50,1.49]	[-0.76,0.76]	[-0.48,0.48]	[-0.24,0.24]	
No ϕ_Z binning	[-1.19,1.20]	[-0.69,0.70]	[-0.57,0.57]	[-0.32,0.31]	
No ϕ_Z binning, linear	[-2.28,2.22]	[-1.15,1.14]	[-0.74,0.73]	[-0.38,0.38]	
No p_j^T binning	[-1.14,1.17]	[-0.64,0.67]	[-0.50,0.51]	[-0.27,0.27]	
No p_j^T binning, linear	[-1.80,1.81]	[-0.91,0.92]	[-0.57,0.57]	[-0.29,0.29]	
Incl.	[-1.29,1.27]	[-0.77,0.76]	[-0.69,0.67]	[-0.40,0.39]	
Incl., linear	[-4.27,4.27]	[-2.17,2.17]	[-1.37,1.37]	[-0.70,0.70]	
Excl.	[-0.69,0.78]	[-0.39,0.45]	[-0.31,0.35]	[-0.17,0.18]	1.5
Excl., linear	[-1.22,1.19]	[-0.61,0.61]	[-0.39,0.39]	[-0.20,0.20]	
No ϕ_Z binning	[-0.75,0.82]	[-0.43,0.49]	[-0.37,0.43]	[-0.21,0.25]	
No ϕ_Z binning, linear	[-2.02,1.95]	[-1.02,1.00]	[-0.65,0.64]	[-0.33,0.33]	
No p_j^T binning	[-0.73,0.80]	[-0.41,0.49]	[-0.34,0.38]	[-0.19,0.20]	
No ϕ_Z binning., linear	[-1.43,1.40]	[-0.72,0.71]	[-0.45,0.45]	[-0.23,0.23]	
Incl.	[-0.79,0.85]	[-0.46,0.52]	[-0.41,0.47]	[-0.24,0.29]	
Incl., linear	[-3.97,3.92]	[-2.01,2.00]	[-1.27,1.26]	[-0.64,0.64]	
Excl.	[-0.47,0.54]	[-0.27,0.31]	[-0.22,0.26]	[-0.12,0.14]	2
Excl., linear	[-1.03,0.99]	[-0.52,0.51]	[-0.33,0.32]	[-0.17,0.17]	
No ϕ_Z binning	[-0.50,0.56]	[-0.28,0.34]	[-0.25,0.30]	[-0.14,0.18]	
No ϕ_Z binning, linear	[-1.84,1.73]	[-0.92,0.89]	[-0.59,0.58]	[-0.30,0.30]	
No p_j^T binning	[-0.49,0.55]	[-0.28,0.32]	[-0.23,0.27]	[-0.13,0.15]	
No p_j^T binning, linear	[-1.18,1.12]	[-0.60,0.58]	[-0.37,0.37]	[-0.19,0.19]	
Incl.	[-0.52,0.57]	[-0.30,0.34]	[-0.27,0.31]	[-0.15,0.19]	
Incl., linear	[-3.55,3.41]	[-1.79,1.75]	[-1.12,1.11]	[-0.57,0.57]	

Table C.1: Bounds on $c_{3W}/\Lambda^2 \times \text{TeV}^2$. The total leakage in the various bins of m_{WZ}^T is $\lesssim 5\%$.

Bibliography

[1] S. Weinberg, *Baryon and Lepton Nonconserving Processes*, *Phys. Rev. Lett.* **43** (1979) 1566.

[2] T. E. Browder, T. Gershon, D. Pirjol, A. Soni and J. Zupan, *New Physics at a Super Flavor Factory*, *Rev. Mod. Phys.* **81** (2009) 1887 [arXiv:0802.3201].

[3] Particle Data Group collaboration, C. Patrignani et al., *Review of Particle Physics*, *Chin. Phys.* **C40** (2016) 100001.

[4] I. Esteban, M. C. Gonzalez-Garcia, M. Maltoni, I. Martinez-Soler and T. Schwetz, *Updated fit to three neutrino mixing: exploring the accelerator-reactor complementarity*, *JHEP* **01** (2017) 087 [arXiv:1611.01514].

[5] F. Capozzi, E. Lisi, A. Marrone and A. Palazzo, *Current unknowns in the three neutrino framework*, *Prog. Part. Nucl. Phys.* **102** (2018) 48 [arXiv:1804.09678].

[6] S. Vagnozzi, E. Giusarma, O. Mena, K. Freese, M. Gerbino, S. Ho et al., *Unveiling ν secrets with cosmological data: neutrino masses and mass hierarchy*, *Phys. Rev.* **D96** (2017) 123503 [arXiv:1701.08172].

[7] C. D. Froggatt and H. B. Nielsen, *Hierarchy of Quark Masses, Cabibbo Angles and CP Violation*, *Nucl. Phys.* **B147** (1979) 277.

[8] F. Feruglio, *Pieces of the Flavour Puzzle*, *Eur. Phys. J.* **C75** (2015) 373 [arXiv:1503.04071].

[9] M. Dine, R. G. Leigh and A. Kagan, *Flavor symmetries and the problem of squark degeneracy*, *Phys. Rev.* **D48** (1993) 4269 [hep-ph/9304299].

[10] R. Barbieri, L. J. Hall, S. Raby and A. Romanino, *Unified theories with $U(2)$ flavor symmetry*, *Nucl. Phys.* **B493** (1997) 3 [hep-ph/9610449].

[11] R. Barbieri and L. J. Hall, *A Grand unified supersymmetric theory of flavor*, *Nuovo Cim.* **A110** (1997) 1 [hep-ph/9605224].

[12] R. Barbieri, L. J. Hall and A. Romanino, *Consequences of a $U(2)$ flavor symmetry*, *Phys. Lett.* **B401** (1997) 47 [hep-ph/9702315].

[13] S. F. King and G. G. Ross, *Fermion masses and mixing angles from $SU(3)$ family symmetry and unification*, *Phys. Lett.* **B574** (2003) 239 [hep-ph/0307190].

[14] E. Ma and G. Rajasekaran, *Softly broken A_4 symmetry for nearly degenerate neutrino masses*, *Phys. Rev.* **D64** (2001) 113012 [hep-ph/0106291].

[15] K. S. Babu, E. Ma and J. W. F. Valle, *Underlying A_4 symmetry for the neutrino mass matrix and the quark mixing matrix*, *Phys. Lett.* **B552** (2003) 207 [hep-ph/0206292].

[16] M. Hirsch, J. C. Romao, S. Skadhauge, J. W. F. Valle and A. Villanova del Moral, *Phenomenological tests of supersymmetric A_4 family symmetry model of neutrino mass*, *Phys. Rev.* **D69** (2004) 093006 [hep-ph/0312265].

[17] E. Ma, *A_4 symmetry and neutrinos with very different masses*, *Phys. Rev.* **D70** (2004) 031901 [hep-ph/0404199].

[18] E. Ma, *Non-Abelian discrete symmetries and neutrino masses: Two examples*, *New J. Phys.* **6** (2004) 104 [hep-ph/0405152].

[19] S.-L. Chen, M. Frigerio and E. Ma, *Hybrid seesaw neutrino masses with A_4 family symmetry*, *Nucl. Phys.* **B724** (2005) 423 [hep-ph/0504181].

[20] G. Altarelli and F. Feruglio, *Tri-bimaximal neutrino mixing from discrete symmetry in extra dimensions*, *Nucl. Phys.* **B720** (2005) 64 [hep-ph/0504165].

[21] E. Ma, *Aspects of the tetrahedral neutrino mass matrix*, *Phys. Rev.* **D72** (2005) 037301 [hep-ph/0505209].

[22] E. Ma, *Tetrahedral family symmetry and the neutrino mixing matrix*, *Mod. Phys. Lett.* **A20** (2005) 2601 [hep-ph/0508099].

[23] A. Zee, *Obtaining the neutrino mixing matrix with the tetrahedral group*, *Phys. Lett.* **B630** (2005) 58 [hep-ph/0508278].

[24] E. Ma, *Tribimaximal neutrino mixing from a supersymmetric model with A_4 family symmetry*, *Phys. Rev.* **D73** (2006) 057304 [hep-ph/0511133].

[25] X.-G. He, Y.-Y. Keum and R. R. Volkas, *A_4 flavor symmetry breaking scheme for understanding quark and neutrino mixing angles*, *JHEP* **04** (2006) 039 [hep-ph/0601001].

[26] G. Altarelli and F. Feruglio, *Tri-bimaximal neutrino mixing, A_4 and the modular symmetry*, *Nucl. Phys.* **B741** (2006) 215 [hep-ph/0512103].

[27] M. Hirsch, A. S. Joshipura, S. Kaneko and J. W. F. Valle, *Predictive flavour symmetries of the neutrino mass matrix*, *Phys. Rev. Lett.* **99** (2007) 151802 [hep-ph/0703046].

[28] F. Bazzocchi, S. Kaneko and S. Morisi, *A SUSY A_4 model for fermion masses and mixings*, *JHEP* **03** (2008) 063 [arXiv:0707.3032].

[29] M. Honda and M. Tanimoto, *Deviation from tri-bimaximal neutrino mixing in A_4 flavor symmetry*, *Prog. Theor. Phys.* **119** (2008) 583 [arXiv:0801.0181].

[30] G. Altarelli, F. Feruglio and C. Hagedorn, *A SUSY SU(5) Grand Unified Model of Tri-Bimaximal Mixing from A_4*, *JHEP* **03** (2008) 052 [arXiv:0802.0090].

[31] Y. Lin, *A Predictive A_4 model, Charged Lepton Hierarchy and Tri-bimaximal Sum Rule*, *Nucl. Phys.* **B813** (2009) 91 [arXiv:0804.2867].

[32] G. Altarelli and D. Meloni, *A Simplest A_4 Model for Tri-Bimaximal Neutrino Mixing*, *J. Phys.* **G36** (2009) 085005 [arXiv:0905.0620].

[33] S. Antusch, S. F. King and M. Spinrath, *Measurable Neutrino Mass Scale in $A_4\times$ SU(5)*, *Phys. Rev.* **D83** (2011) 013005 [arXiv:1005.0708].

[34] C. Hagedorn, M. Lindner and R. N. Mohapatra, *S_4 flavor symmetry and fermion masses: towards a grand unified theory of flavor*, *JHEP* **06** (2006) 042 [hep-ph/0602244].

[35] E. Ma, *Neutrino mass matrix from S_4 symmetry*, *Phys. Lett.* **B632** (2006) 352 [hep-ph/0508231].

[36] Y. Cai and H.-B. Yu, *A $SO(10)$ GUT Model with S_4 Flavor Symmetry*, *Phys. Rev.* **D74** (2006) 115005 [hep-ph/0608022].

[37] H. Zhang, *Flavor $S_4 \otimes Z_2$ symmetry and neutrino mixing*, *Phys. Lett.* **B655** (2007) 132 [hep-ph/0612214].

[38] Y. Koide, *S_4 flavor symmetry embedded into $SU(3)$ and lepton masses and mixing*, *JHEP* **08** (2007) 086 [arXiv:0705.2275].

[39] F. Bazzocchi and S. Morisi, *S_4 as a natural flavor symmetry for lepton mixing*, *Phys. Rev.* **D80** (2009) 096005 [arXiv:0811.0345].

[40] H. Ishimori, Y. Shimizu and M. Tanimoto, *S_4 Flavor Symmetry of Quarks and Leptons in SU(5) GUT*, *Prog. Theor. Phys.* **121** (2009) 769 [arXiv:0812.5031].

[41] W. Grimus, L. Lavoura and P. O. Ludl, *Is S_4 the horizontal symmetry of tri-bimaximal lepton mixing?*, *J. Phys.* **G36** (2009) 115007 [arXiv:0906.2689].

[42] F. Bazzocchi, L. Merlo and S. Morisi, *Fermion Masses and Mixings in a S_4 based Model*, *Nucl. Phys.* **B816** (2009) 204 [arXiv:0901.2086].

[43] G.-J. Ding, *Fermion Masses and Flavor Mixings in a Model with S_4 Flavor Symmetry*, *Nucl. Phys.* **B827** (2010) 82 [arXiv:0909.2210].

[44] S. Morisi and E. Peinado, *An S_4 model for quarks and leptons with maximal atmospheric angle*, *Phys. Rev.* **D81** (2010) 085015 [arXiv:1001.2265].

[45] H. Ishimori, K. Saga, Y. Shimizu and M. Tanimoto, *Tri-bimaximal Mixing and Cabibbo Angle in S_4 Flavor Model with SUSY*, *Phys. Rev.* **D81** (2010) 115009 [arXiv:1004.5004].

[46] J. T. Penedo, S. T. Petcov and A. V. Titov, *Neutrino mixing and leptonic CP violation from S_4 flavour and generalised CP symmetries*, *JHEP* **12** (2017) 022 [arXiv:1705.00309].

[47] P. H. Frampton and T. W. Kephart, *Simple nonAbelian finite flavor groups and fermion masses*, *Int. J. Mod. Phys.* **A10** (1995) 4689 [hep-ph/9409330].

[48] A. Aranda, *Neutrino mixing from the double tetrahedral group T'*, *Phys. Rev.* **D76** (2007) 111301 [arXiv:0707.3661].

[49] P. H. Frampton and T. W. Kephart, *Flavor Symmetry for Quarks and Leptons*, *JHEP* **09** (2007) 110 [arXiv:0706.1186].

[50] P. H. Frampton, T. W. Kephart and S. Matsuzaki, *Simplified Renormalizable T' Model for Tribimaximal Mixing and Cabibbo Angle*, *Phys. Rev.* **D78** (2008) 073004 [arXiv:0807.4713].

[51] P. H. Frampton and S. Matsuzaki, *T' Predictions of PMNS and CKM Angles*, *Phys. Lett.* **B679** (2009) 347 [arXiv:0902.1140].

[52] G.-J. Ding, *Fermion Mass Hierarchies and Flavor Mixing from T' Symmetry*, *Phys. Rev.* **D78** (2008) 036011 [arXiv:0803.2278].

[53] L. L. Everett and A. J. Stuart, *Icosahedral (A_5) Family Symmetry and the Golden Ratio Prediction for Solar Neutrino Mixing*, *Phys. Rev.* **D79** (2009) 085005 [arXiv:0812.1057].

[54] F. Feruglio and A. Paris, *The Golden Ratio Prediction for the Solar Angle from a Natural Model with A_5 Flavour Symmetry*, *JHEP* **03** (2011) 101 [arXiv:1101.0393].

[55] G.-J. Ding, L. L. Everett and A. J. Stuart, *Golden Ratio Neutrino Mixing and A_5 Flavor Symmetry*, *Nucl. Phys.* **B857** (2012) 219 [arXiv:1110.1688].

[56] W. Grimus, A. S. Joshipura, S. Kaneko, L. Lavoura and M. Tanimoto, *Lepton mixing angle $\theta_{13} = 0$ with a horizontal symmetry D_4*, *JHEP* **07** (2004) 078 [hep-ph/0407112].

[57] E. Ma, *Polygonal derivation of the neutrino mass matrix*, *Fizika* **B14** (2005) 35 [hep-ph/0409288].

[58] I. de Medeiros Varzielas, S. F. King and G. G. Ross, *Neutrino tri-bi-maximal mixing from a non-Abelian discrete family symmetry*, *Phys. Lett.* **B648** (2007) 201 [hep-ph/0607045].

[59] R. N. Mohapatra, S. Nasri and H.-B. Yu, *S_3 symmetry and tri-bimaximal mixing*, *Phys. Lett.* **B639** (2006) 318 [hep-ph/0605020].

[60] C. Luhn, S. Nasri and P. Ramond, *The Flavor group $\Delta(3n^2)$*, *J. Math. Phys.* **48** (2007) 073501 [hep-th/0701188].

[61] W. Grimus and L. Lavoura, *A Model for trimaximal lepton mixing*, *JHEP* **09** (2008) 106 [arXiv:0809.0226].

[62] S. M. Barr, *Flavor without flavor symmetry*, *Phys. Rev.* **D65** (2002) 096012 [hep-ph/0106241].

[63] L. Ferretti, S. F. King and A. Romanino, *Flavour from accidental symmetries*, *JHEP* **11** (2006) 078 [hep-ph/0609047].

[64] K. S. Babu and S. M. Barr, *An SO(10) solution to the puzzle of quark and lepton masses*, *Phys. Rev. Lett.* **75** (1995) 2088 [hep-ph/9503215].

[65] C. H. Albright and S. M. Barr, *Construction of a minimal Higgs SO(10) SUSY GUT model*, *Phys. Rev.* **D62** (2000) 093008 [hep-ph/0003251].

[66] G. Altarelli and G. Blankenburg, *Different $SO(10)$ Paths to Fermion Masses and Mixings*, *JHEP* **03** (2011) 133 [arXiv:1012.2697].

[67] N. Arkani-Hamed and M. Schmaltz, *Hierarchies without symmetries from extra dimensions*, *Phys. Rev.* **D61** (2000) 033005 [hep-ph/9903417].

[68] W. Altmannshofer, C. Frugiuele and R. Harnik, *Fermion Hierarchy from Sfermion Anarchy*, *JHEP* **12** (2014) 180 [arXiv:1409.2522].

[69] P. F. Harrison, D. H. Perkins and W. G. Scott, *Tri-bimaximal mixing and the neutrino oscillation data*, *Phys. Lett.* **B530** (2002) 167 [hep-ph/0202074].

[70] P. F. Harrison and W. G. Scott, *Symmetries and generalizations of tri-bimaximal neutrino mixing*, *Phys. Lett.* **B535** (2002) 163 [hep-ph/0203209].

[71] Z.-z. Xing, *Nearly tri-bimaximal neutrino mixing and CP violation*, *Phys. Lett.* **B533** (2002) 85 [hep-ph/0204049].

[72] P. F. Harrison and W. G. Scott, *Permutation symmetry, tri-bimaximal neutrino mixing and the S_3 group characters*, *Phys. Lett.* **B557** (2003) 76 [hep-ph/0302025].

[73] P. F. Harrison and W. G. Scott, *Status of tri-bimaximal neutrino mixing*, in *Proceedings of the 2nd NO-VE International Workshop on Neutrino Oscillations: Venice, December 3-5, 2003*, pp. 435–444, 2004, [hep-ph/0402006].

[74] T. Kobayashi, Y. Omura and K. Yoshioka, *Flavor Symmetry Breaking and Vacuum Alignment on Orbifolds*, *Phys. Rev.* **D78** (2008) 115006 [arXiv:0809.3064].

[75] G. Altarelli and F. Feruglio, *Discrete Flavor Symmetries and Models of Neutrino Mixing*, *Rev. Mod. Phys.* **82** (2010) 2701 [arXiv:1002.0211].

[76] H. Ishimori, T. Kobayashi, H. Ohki, Y. Shimizu, H. Okada and M. Tanimoto, *Non-Abelian Discrete Symmetries in Particle Physics*, *Prog. Theor. Phys. Suppl.* **183** (2010) 1 [arXiv:1003.3552].

[77] W. Grimus and P. O. Ludl, *Finite flavour groups of fermions*, *J. Phys.* **A45** (2012) 233001 [arXiv:1110.6376].

[78] S. F. King and C. Luhn, *Neutrino Mass and Mixing with Discrete Symmetry*, *Rept. Prog. Phys.* **76** (2013) 056201 [arXiv:1301.1340].

[79] D. Meloni, *GUT and flavor models for neutrino masses and mixing*, *Front.in Phys.* **5** (2017) 43 [arXiv:1709.02662].

[80] C. Degrande, N. Greiner, W. Kilian, O. Mattelaer, H. Mebane, T. Stelzer et al., *Effective Field Theory: A Modern Approach to Anomalous Couplings*, *Annals Phys.* **335** (2013) 21 [arXiv:1205.4231].

[81] C. J. C. Burges and H. J. Schnitzer, *Virtual Effects of Excited Quarks as Probes of a Possible New Hadronic Mass Scale*, *Nucl. Phys.* **B228** (1983) 464.

[82] C. N. Leung, S. T. Love and S. Rao, *Low-Energy Manifestations of a New Interaction Scale: Operator Analysis*, *Z. Phys.* **C31** (1986) 433.

[83] W. Buchmuller and D. Wyler, *Effective Lagrangian Analysis of New Interactions and Flavor Conservation*, *Nucl. Phys.* **B268** (1986) 621.

[84] K. Hagiwara, S. Ishihara, R. Szalapski and D. Zeppenfeld, *Low-energy effects of new interactions in the electroweak boson sector*, *Phys. Rev.* **D48** (1993) 2182.

[85] G. F. Giudice, C. Grojean, A. Pomarol and R. Rattazzi, *The Strongly-Interacting Light Higgs*, *JHEP* **06** (2007) 045 [hep-ph/0703164].

[86] B. Grzadkowski, M. Iskrzynski, M. Misiak and J. Rosiek, *Dimension-Six Terms in the Standard Model Lagrangian*, *JHEP* **10** (2010) 085 [arXiv:1008.4884].

[87] R. Alonso, E. E. Jenkins, A. V. Manohar and M. Trott, *Renormalization Group Evolution of the Standard Model Dimension Six Operators III: Gauge Coupling Dependence and Phenomenology*, *JHEP* **04** (2014) 159 [arXiv:1312.2014].

[88] J. Elias-Miró, C. Grojean, R. S. Gupta and D. Marzocca, *Scaling and tuning of EW and Higgs observables*, *JHEP* **05** (2014) 019 [arXiv:1312.2928].

[89] L. J. Dixon and Y. Shadmi, *Testing gluon selfinteractions in three jet events at hadron colliders*, *Nucl. Phys.* **B423** (1994) 3 [hep-ph/9312363].

[90] K. Whisnant, J.-M. Yang, B.-L. Young and X. Zhang, *Dimension-six CP conserving operators of the third family quarks and their effects on collider observables*, *Phys. Rev.* **D56** (1997) 467 [hep-ph/9702305].

[91] A. Pierce, J. Thaler and L.-T. Wang, *Disentangling Dimension Six Operators through Di-Higgs Boson Production*, *JHEP* **05** (2007) 070 [hep-ph/0609049].

[92] A. Crivellin, S. Najjari and J. Rosiek, *Lepton Flavor Violation in the Standard Model with general Dimension-Six Operators*, *JHEP* **04** (2014) 167 [arXiv:1312.0634].

[93] A. Falkowski and F. Riva, *Model-independent precision constraints on dimension-6 operators*, *JHEP* **02** (2015) 039 [arXiv:1411.0669].

[94] DELPHI, OPAL, LEP Electroweak, ALEPH, L3 collaboration, S. Schael et al., *Electroweak Measurements in Electron-Positron Collisions at W-Boson-Pair Energies at LEP*, *Phys. Rept.* **532** (2013) 119 [arXiv:1302.3415].

[95] CMS collaboration, V. Khachatryan et al., *Measurement of the* $\mathrm{W^+W^-}$ *cross section in pp collisions at* $\sqrt{s} = 8$ *TeV and limits on anomalous gauge couplings*, *Eur. Phys. J.* **C76** (2016) 401 [arXiv:1507.03268].

[96] ATLAS collaboration, G. Aad et al., *Measurements of* $W^{\pm}Z$ *production cross sections in pp collisions at* $\sqrt{s} = 8$ *TeV with the ATLAS detector and limits on anomalous gauge boson self-couplings*, *Phys. Rev.* **D93** (2016) 092004 [arXiv:1603.02151].

[97] ATLAS collaboration, A. M. Burger, *Measurement of the diboson production cross section at 8TeV and 13TeV and limits on anomalous triple gauge couplings with the ATLAS detector*, *PoS* **DIS2017** (2018) 155.

[98] L. Lehman, *Extending the Standard Model Effective Field Theory with the Complete Set of Dimension-7 Operators*, *Phys. Rev.* **D90** (2014) 125023 [arXiv:1410.4193].

[99] L. Lehman and A. Martin, *Low-derivative operators of the Standard Model effective field theory via Hilbert series methods*, *JHEP* **02** (2016) 081 [arXiv:1510.00372].

[100] L. Lehman and A. Martin, *Hilbert Series for Constructing Lagrangians: expanding the phenomenologist's toolbox*, *Phys. Rev.* **D91** (2015) 105014 [arXiv:1503.07537].

[101] B. Henning, X. Lu, T. Melia and H. Murayama, *Hilbert series and operator bases with derivatives in effective field theories*, *Commun. Math. Phys.* **347** (2016) 363 [arXiv:1507.07240].

[102] B. Henning, X. Lu, T. Melia and H. Murayama, *2, 84, 30, 993, 560, 15456, 11962, 261485, ...: Higher dimension operators in the SM EFT*, *JHEP* **08** (2017) 016 [arXiv:1512.03433].

[103] K. Hagiwara, R. D. Peccei, D. Zeppenfeld and K. Hikasa, *Probing the Weak Boson Sector in $e^+e^- \to W^+W^-$*, *Nucl. Phys.* **B282** (1987) 253.

[104] R. Contino, M. Ghezzi, C. Grojean, M. Muhlleitner and M. Spira, *Effective Lagrangian for a light Higgs-like scalar*, *JHEP* **07** (2013) 035 [arXiv:1303.3876].

[105] M. E. Peskin and T. Takeuchi, *New constraint on a strongly interacting Higgs sector*, *Phys. Rev. Lett.* **65** (1990) 964.

[106] M. E. Peskin and T. Takeuchi, *Estimation of oblique electroweak corrections*, *Phys. Rev.* **D46** (1992) 381.

[107] J. Ellis, V. Sanz and T. You, *The Effective Standard Model after LHC Run I*, *JHEP* **03** (2015) 157 [arXiv:1410.7703].

[108] L. Bian, J. Shu and Y. Zhang, *Prospects for Triple Gauge Coupling Measurements at Future Lepton Colliders and the 14 TeV LHC*, *JHEP* **09** (2015) 206 [arXiv:1507.02238].

[109] G. Brooijmans et al., *Les Houches 2017: Physics at TeV Colliders New Physics Working Group Report*, in *10th Les Houches Workshop on Physics at TeV Colliders (PhysTeV 2017) Les Houches, France, June 5-23, 2017*, [arXiv:1803.10379].

[110] J. Bijnens and C. Wetterich, *Fermion Masses From Symmetry*, *Nucl. Phys.* **B283** (1987) 237.

[111] M. Leurer, Y. Nir and N. Seiberg, *Mass matrix models*, *Nucl. Phys.* **B398** (1993) 319 [hep-ph/9212278].

[112] L. E. Ibanez and G. G. Ross, *Fermion masses and mixing angles from gauge symmetries*, *Phys. Lett.* **B332** (1994) 100 [hep-ph/9403338].

[113] A. Pomarol and D. Tommasini, *Horizontal symmetries for the supersymmetric flavor problem*, *Nucl. Phys.* **B466** (1996) 3 [hep-ph/9507462].

[114] R. Barbieri, G. R. Dvali and L. J. Hall, *Predictions from a $U(2)$ flavor symmetry in supersymmetric theories*, *Phys. Lett.* **B377** (1996) 76 [hep-ph/9512388].

[115] C. D. Carone, L. J. Hall and H. Murayama, *$(S_3)^3$ flavor symmetry and $p \to K^0 e^+$*, *Phys. Rev.* **D53** (1996) 6282 [hep-ph/9512399].

[116] E. Dudas, C. Grojean, S. Pokorski and C. A. Savoy, *Abelian flavor symmetries in supersymmetric models*, *Nucl. Phys.* **B481** (1996) 85 [hep-ph/9606383].

[117] C. D. Carone and L. J. Hall, *Neutrino physics from a $U(2)$ flavor symmetry*, *Phys. Rev.* **D56** (1997) 4198 [hep-ph/9702430].

[118] N. Irges, S. Lavignac and P. Ramond, *Predictions from an anomalous U(1) model of Yukawa hierarchies*, *Phys. Rev.* **D58** (1998) 035003 [hep-ph/9802334].

[119] J. K. Elwood, N. Irges and P. Ramond, *Family symmetry and neutrino mixing*, *Phys. Rev. Lett.* **81** (1998) 5064 [hep-ph/9807228].

[120] P. Binetruy, S. Lavignac and P. Ramond, *Yukawa textures with an anomalous horizontal Abelian symmetry*, *Nucl. Phys.* **B477** (1996) 353 [hep-ph/9601243].

[121] P. Binetruy, S. Lavignac, S. T. Petcov and P. Ramond, *Quasidegenerate neutrinos from an Abelian family symmetry*, *Nucl. Phys.* **B496** (1997) 3 [hep-ph/9610481].

[122] Y. Grossman, Y. Nir and Y. Shadmi, *Large mixing and large hierarchy between neutrinos with Abelian flavor symmetries*, *JHEP* **10** (1998) 007 [hep-ph/9808355].

[123] G. Altarelli and F. Feruglio, *Theoretical models of neutrino masses and mixings*, *Springer Tracts Mod. Phys.* **190** (2003) 169 [hep-ph/0206077].

[124] F. Simpson, R. Jimenez, C. Pena-Garay and L. Verde, *Strong Bayesian Evidence for the Normal Neutrino Hierarchy*, *JCAP* **1706** (2017) 029 [arXiv:1703.03425].

[125] P. F. de Salas, D. V. Forero, C. A. Ternes, M. Tortola and J. W. F. Valle, *Status of neutrino oscillations 2018: 3σ hint for normal mass ordering and improved CP sensitivity*, *Phys. Lett.* **B782** (2018) 633 [arXiv:1708.01186].

[126] T2K collaboration, K. Abe et al., *Combined Analysis of Neutrino and Antineutrino Oscillations at T2K*, *Phys. Rev. Lett.* **118** (2017) 151801 [arXiv:1701.00432].

[127] F. Capozzi, E. Di Valentino, E. Lisi, A. Marrone, A. Melchiorri and A. Palazzo, *Global constraints on absolute neutrino masses and their ordering*, *Phys. Rev.* **D95** (2017) 096014 [arXiv:1703.04471].

[128] V. Domcke and A. Romanino, *Stable lepton mass matrices*, *JHEP* **06** (2016) 031 [arXiv:1604.08879].

[129] L. J. Hall, H. Murayama and N. Weiner, *Neutrino mass anarchy*, *Phys. Rev. Lett.* **84** (2000) 2572 [hep-ph/9911341].

[130] N. Haba and H. Murayama, *Anarchy and hierarchy*, *Phys. Rev.* **D63** (2001) 053010 [hep-ph/0009174].

[131] P. H. Frampton, S. T. Petcov and W. Rodejohann, *On deviations from bimaximal neutrino mixing*, *Nucl. Phys.* **B687** (2004) 31 [hep-ph/0401206].

[132] A. Romanino, *Charged lepton contributions to the solar neutrino mixing and θ_{13}*, *Phys. Rev.* **D70** (2004) 013003 [hep-ph/0402258].

[133] S. F. King, *Predicting neutrino parameters from $SO(3)$ family symmetry and quark-lepton unification*, *JHEP* **08** (2005) 105 [hep-ph/0506297].

[134] S. Antusch and S. F. King, *Charged lepton corrections to neutrino mixing angles and CP phases revisited*, *Phys. Lett.* **B631** (2005) 42 [hep-ph/0508044].

[135] K. A. Hochmuth, S. T. Petcov and W. Rodejohann, $U_{PMNS} = U_l^\dagger U_\nu$, *Phys. Lett.* **B654** (2007) 177 [arXiv:0706.2975].

[136] P. S. Bhupal Dev, R. N. Mohapatra and M. Severson, *Neutrino Mixings in SO(10) with Type II Seesaw and θ_{13}*, *Phys. Rev.* **D84** (2011) 053005 [arXiv:1107.2378].

[137] S. Dev, S. Gupta and R. Raman Gautam, *Parametrizing the Lepton Mixing Matrix in terms of Charged Lepton Corrections*, *Phys. Lett.* **B704** (2011) 527 [arXiv:1107.1125].

[138] D. Marzocca, S. T. Petcov, A. Romanino and M. Spinrath, *Sizeable θ_{13} from the Charged Lepton Sector in SU(5), (Tri-)Bimaximal Neutrino Mixing and Dirac CP Violation*, *JHEP* **11** (2011) 009 [arXiv:1108.0614].

[139] G. Altarelli, F. Feruglio and L. Merlo, *Tri-Bimaximal Neutrino Mixing and Discrete Flavour Symmetries*, *Fortsch. Phys.* **61** (2013) 507 [arXiv:1205.5133].

[140] D. Marzocca, S. T. Petcov, A. Romanino and M. C. Sevilla, *Nonzero $|U_{e3}|$ from Charged Lepton Corrections and the Atmospheric Neutrino Mixing Angle*, *JHEP* **05** (2013) 073 [arXiv:1302.0423].

[141] S. Gollu, K. N. Deepthi and R. Mohanta, *Charged lepton correction to tribimaximal lepton mixing and its implications to neutrino phenomenology*, *Mod. Phys. Lett.* **A28** (2013) 1350131 [arXiv:1303.3393].

[142] D. Marzocca and A. Romanino, *Stable fermion mass matrices and the charged lepton contribution to neutrino mixing*, *JHEP* **11** (2014) 159 [arXiv:1409.3760].

[143] S. T. Petcov, *On Pseudodirac Neutrinos, Neutrino Oscillations and Neutrinoless Double beta Decay*, *Phys. Lett.* **B110** (1982) 245.

[144] R. Barbieri, L. J. Hall, D. Tucker-Smith, A. Strumia and N. Weiner, *Oscillations of solar and atmospheric neutrinos*, *JHEP* **12** (1998) 017 [hep-ph/9807235].

[145] A. S. Joshipura and S. D. Rindani, *Vacuum solutions of neutrino anomalies through a softly broken U(1) symmetry*, *Eur. Phys. J.* **C14** (2000) 85 [hep-ph/9811252].

[146] R. N. Mohapatra, A. Perez-Lorenzana and C. A. de Sousa Pires, *Type II seesaw and a gauge model for the bimaximal mixing explanation of neutrino puzzles*, *Phys. Lett.* **B474** (2000) 355 [hep-ph/9911395].

[147] S. T. Petcov and W. Rodejohann, *Flavor symmetry $L_e - L_\mu - L_\tau$, atmospheric neutrino mixing and CP violation in the lepton sector*, *Phys. Rev.* **D71** (2005) 073002 [hep-ph/0409135].

[148] G. Altarelli and R. Franceschini, *Neutrino masses with inverse hierarchy from broken $L_e - L_\mu - L_\tau$: A Reappraisal*, *JHEP* **03** (2006) 047 [hep-ph/0512202].

[149] S. F. King, *Atmospheric and solar neutrinos with a heavy singlet*, *Phys. Lett.* **B439** (1998) 350 [hep-ph/9806440].

[150] S. F. King, *Atmospheric and solar neutrinos from single right-handed neutrino dominance and U(1) family symmetry*, *Nucl. Phys.* **B562** (1999) 57 [hep-ph/9904210].

[151] S. F. King, *Large mixing angle MSW and atmospheric neutrinos from single right-handed neutrino dominance and U(1) family symmetry*, *Nucl. Phys.* **B576** (2000) 85 [hep-ph/9912492].

[152] S. F. King, *Constructing the large mixing angle MNS matrix in seesaw models with right-handed neutrino dominance*, *JHEP* **09** (2002) 011 [hep-ph/0204360].

[153] S. Antusch and S. F. King, *Sequential dominance*, *New J. Phys.* **6** (2004) 110 [hep-ph/0405272].

[154] S. Antusch, S. Boudjemaa and S. F. King, *Neutrino Mixing Angles in Sequential Dominance to NLO and NNLO*, *JHEP* **09** (2010) 096 [arXiv:1003.5498].

[155] Y. Reyimuaji and A. Romanino, *Can an unbroken flavour symmetry provide an approximate description of lepton masses and mixing?*, *JHEP* **03** (2018) 067 [arXiv:1801.10530].

[156] G. Altarelli and F. Feruglio, *Models of neutrino masses from oscillations with maximal mixing*, *JHEP* **11** (1998) 021 [hep-ph/9809596].

[157] ATLAS collaboration, G. Aad et al., *Observation of a new particle in the search for the Standard Model Higgs boson with the ATLAS detector at the LHC*, *Phys. Lett.* **B716** (2012) 1 [arXiv:1207.7214].

[158] CMS collaboration, S. Chatrchyan et al., *Observation of a new boson at a mass of 125 GeV with the CMS experiment at the LHC*, *Phys. Lett.* **B716** (2012) 30 [arXiv:1207.7235].

[159] P. Sphicas, *Highlights from EPS 2017*, July 12, 2017. https://indico.cern.ch/event/466934/contributions/2474222/attachments/1492504/2320608/EPS-Highlights-final.pdf.

[160] K. J. F. Gaemers and G. J. Gounaris, *Polarization Amplitudes for $e^+e^- \to W^+W^-$ and $e^+e^- \to ZZ$*, *Z. Phys.* **C1** (1979) 259.

[161] A. De Rujula, M. B. Gavela, P. Hernandez and E. Masso, *The Selfcouplings of vector bosons: Does LEP-1 obviate LEP-2?*, *Nucl. Phys.* **B384** (1992) 3.

[162] U. Baur, T. Han and J. Ohnemus, *WZ production at hadron colliders: Effects of nonstandard WWZ couplings and QCD corrections*, *Phys. Rev.* **D51** (1995) 3381 [hep-ph/9410266].

[163] U. Baur, T. Han and J. Ohnemus, *Amplitude zeros in $W^\pm Z$ production*, *Phys. Rev. Lett.* **72** (1994) 3941 [hep-ph/9403248].

[164] A. Falkowski, M. Gonzalez-Alonso, A. Greljo, D. Marzocca and M. Son, *Anomalous Triple Gauge Couplings in the Effective Field Theory Approach at the LHC*, *JHEP* **02** (2017) 115 [arXiv:1609.06312].

[165] F. Campanario, R. Roth, S. Sapeta and D. Zeppenfeld, *Anomalous couplings in WZ production beyond NLO QCD*, *PoS* **LHCP2016** (2016) 141 [arXiv:1612.03577].

[166] L. Berthier, M. Bjørn and M. Trott, *Incorporating doubly resonant $W^\pm$ data in a global fit of SMEFT parameters to lift flat directions*, *JHEP* **09** (2016) 157 [arXiv:1606.06693].

[167] L. Berthier and M. Trott, *Consistent constraints on the Standard Model Effective Field Theory*, *JHEP* **02** (2016) 069 [arXiv:1508.05060].

[168] A. Butter, O. J. P. Eboli, J. Gonzalez-Fraile, M. C. Gonzalez-Garcia, T. Plehn and M. Rauch, *The Gauge-Higgs Legacy of the LHC Run I*, *JHEP* **07** (2016) 152 [arXiv:1604.03105].

[169] B. Dumont, S. Fichet and G. von Gersdorff, *A Bayesian view of the Higgs sector with higher dimensional operators*, *JHEP* **07** (2013) 065 [arXiv:1304.3369].

[170] J. Ellis, V. Sanz and T. You, *Complete Higgs Sector Constraints on Dimension-6 Operators*, *JHEP* **07** (2014) 036 [arXiv:1404.3667].

[171] B. M. Gavela, E. E. Jenkins, A. V. Manohar and L. Merlo, *Analysis of General Power Counting Rules in Effective Field Theory*, *Eur. Phys. J.* **C76** (2016) 485 [arXiv:1601.07551].

[172] A. Azatov, R. Contino, C. S. Machado and F. Riva, *Helicity selection rules and noninterference for BSM amplitudes*, *Phys. Rev.* **D95** (2017) 065014 [arXiv:1607.05236].

[173] J. Elias-Miro, J. R. Espinosa, E. Masso and A. Pomarol, *Higgs windows to new physics through d=6 operators: constraints and one-loop anomalous dimensions*, *JHEP* **11** (2013) 066 [arXiv:1308.1879].

[174] A. Pomarol and F. Riva, *Towards the Ultimate SM Fit to Close in on Higgs Physics*, *JHEP* **01** (2014) 151 [arXiv:1308.2803].

[175] L. J. Dixon, *Calculating scattering amplitudes efficiently*, in *QCD and beyond. Proceedings, Theoretical Advanced Study Institute in Elementary Particle Physics, TASI-95, Boulder, USA, June 4-30, 1995*, pp. 539–584, 1996, [hep-ph/9601359].

[176] G. D'Ambrosio, G. F. Giudice, G. Isidori and A. Strumia, *Minimal flavor violation: an effective field theory approach*, *Nucl. Phys.* **B645** (2002) 155 [hep-ph/0207036].

[177] R. Barbieri, A. Pomarol, R. Rattazzi and A. Strumia, *Electroweak symmetry breaking after LEP-1 and LEP-2*, *Nucl. Phys.* **B703** (2004) 127 [hep-ph/0405040].

[178] C. Arzt, M. B. Einhorn and J. Wudka, *Patterns of deviation from the standard model*, *Nucl. Phys.* **B433** (1995) 41 [hep-ph/9405214].

[179] D. Liu, A. Pomarol, R. Rattazzi and F. Riva, *Patterns of Strong Coupling for LHC Searches*, *JHEP* **11** (2016) 141 [arXiv:1603.03064].

[180] R. Contino, A. Falkowski, F. Goertz, C. Grojean and F. Riva, *On the Validity of the Effective Field Theory Approach to SM Precision Tests*, *JHEP* **07** (2016) 144 [arXiv:1604.06444].

[181] J. Alwall, R. Frederix, S. Frixione, V. Hirschi, F. Maltoni, O. Mattelaer et al., *The automated computation of tree-level and next-to-leading order differential cross sections, and their matching to parton shower simulations*, *JHEP* **07** (2014) 079 [arXiv:1405.0301].

[182] G. Panico, *Electroweak precision tests at hadron colliders*, January 11, 2017. https://indico.cern.ch/event/587148/contributions/2409109/attachments/1393682/2123873/Panico_EWPT_at_LHC.pdf.

[183] CMS collaboration, A. M. Sirunyan et al., *Search for anomalous couplings in boosted* WW/WZ $\to \ell\nu\mathrm{q}\bar{\mathrm{q}}$ *production in proton-proton collisions at* $\sqrt{s} = 8$ *TeV*, *Phys. Lett.* **B772** (2017) 21 [arXiv:1703.06095].

[184] D. Racco, A. Wulzer and F. Zwirner, *Robust collider limits on heavy-mediator Dark Matter*, *JHEP* **05** (2015) 009 [arXiv:1502.04701].

[185] F. Campanario, M. Rauch and S. Sapeta, W^+W^- *production at high transverse momenta beyond NLO*, *Nucl. Phys.* **B879** (2014) 65 [arXiv:1309.7293].

[186] F. Campanario, M. Rauch and S. Sapeta, *ZZ production at high transverse momenta beyond NLO QCD*, *JHEP* **08** (2015) 070 [arXiv:1504.05588].

[187] F. Campanario and S. Sapeta, *WZ production beyond NLO for high-*p_T *observables*, *Phys. Lett.* **B718** (2012) 100 [arXiv:1209.4595].

[188] M. Grazzini, S. Kallweit, S. Pozzorini, D. Rathlev and M. Wiesemann, W^+W^- *production at the LHC: fiducial cross sections and distributions in NNLO QCD*, *JHEP* **08** (2016) 140 [arXiv:1605.02716].

[189] M. Grazzini, S. Kallweit, D. Rathlev and M. Wiesemann, $W^\pm Z$ *production at hadron colliders in NNLO QCD*, *Phys. Lett.* **B761** (2016) 179 [arXiv:1604.08576].

[190] S. Dawson, I. M. Lewis and M. Zeng, *Threshold resummed and approximate next-to-next-to-leading order results for* W^+W^- *pair production at the LHC*, *Phys. Rev.* **D88** (2013) 054028 [arXiv:1307.3249].

[191] T. Sjostrand, S. Mrenna and P. Z. Skands, *A Brief Introduction to PYTHIA 8.1*, *Comput. Phys. Commun.* **178** (2008) 852 [arXiv:0710.3820].